THE UNIVERSITY OF KANSAS CENTER FOR RESEARCH, INC.
2291 Irving Hill Drive—Campus West
Lawrence, Kansas 66045

Progress Report for

A Research Program to Reduce Interior Noise
in General Aviation Airplanes

NASA Contract NCCI-6

STUDY OF NOISE REDUCTION CHARACTERISTICS OF COMPOSITE FIBER-REINFORCED PANELS, INTERIOR PANEL CONFIGURATIONS, AND THE APPLICATION OF THE TUNED DAMPER CONCEPT

KU-FRL-417-18

Prepared by: Jaap Laméris, Project Manager

Scott Stevenson

Barry Streeter

Approved by: Jan Roskam, Principal Investigator

Flight Research Laboratory

University of Kansas Center for Research, Inc.

Lawrence, Kansas

March 1982

SUMMARY

In this report, the work carried out to investigate the noise reduction characteristics of square, fiber-reinforced, laminated panels and interior panel configurations at the University of Kansas Flight Research Laboratory is presented. In addition, the concept of a tuned damper has been investigated as an application to increase the noise reduction of a panel at its fundamental resonance frequency.

The experimental study was carried out on 20 x 20 inch panels in a frequency range of 20 Hz to 5000 Hz. Tests were conducted under normal sound incidence in the KU-FRL Beranek tube acoustic facility.

The results of the tests with the fiber-reinforced, laminated panels indicate better low frequency noise reduction characteristics for the graphite-epoxy panels than for the Kevlar panels, due to their higher stiffness. Variations in thickness caused by the manufacturing process have prevented the making of decisive conclusions about the influence of the ply orientation.

Various kinds of interior panel configurations have been studied. Sandwich panels consisting of a foam core and fiberglass facings exhibit higher sound attenuation characteristics than most of the single layer panels tested. Doubling the core thickness of these panels has a larger beneficial effect than doubling the thickness of the skin layer. Treatments such as carpet, Royalite, and woolen/leather covering are generally more effective at higher frequencies due to the addition of mass.

Tests with a tuned ring damper have indicated that it is possible to increase the damping and noise reduction in a wide range of fre-

quencies around the fundamental resonance frequency of a panel. Using two viscoelastic damping materials, LD-400 and Aquaplas, a gain of 8-9 dB was measured at a weight penalty of about 9% of the panel mass. However, theoretical analysis of this tuned damper concept did not predict well the experimental results and needs more study. Also some disadvantages of the type of damper used have been discussed.

TABLE OF CONTENTS

TABLE OF CONTENTS, continued

LIST OF FIGURES

LIST OF FIGURES, continued

LIST OF FIGURES, continued

LIST OF TABLES

LIST OF SYMBOLS

Symbol	Definition	Dimension
A	Cross section area of a solid (block) damper	[in]
a	Panel width	[in]
b	Panel height	[in]
Dij	Elements of flexural rigidity matrix	[lb_fin]
d	Deflection	[in]
E	Modulus of elasticity	[lb_f/in^2]
E_{11}	Modulus of elasticity in warp direction	[lb_f/in^2]
E_{22}	Modulus of elasticity in fill direction	[lb_f/in^2]
E_1^*	Complex modulus of panel	[lb_f/in^2]
$E_{2\omega}^*$	Complex modulus of damper	[lb_f/in^2]
F	Equivalent pressure force	[lb_f]
Fr	Fundamental resonance frequency	[Hz]
Gxy	Shear modulus	[lb_f/in^2]
h	Panel thickness	[in]
I	Cross section area moment of damper	[in^4]
I_D	See Equation 4.5.	[-]
I_N	See Equation 4.3.	[-]
j	(-1)	[-]
K2	Damper stiffness	[lb/in]
K'	Equivalent panel stiffness	[lb_f/in]
k1	See Equation 4.1.	[in]
k2	See Equation 4.1.	[in]

LIST OF SYMBOLS, continued

Symbol	Definition	Dimension
k_x k_y k_{xy}	Panel curvatures	$[in^{-1}]$
L	Height of a solid (block) damper	[in]
M	Bending moment	[lb-in]
M'	Equivalent panel mass	$[lb_m]$
M2	Damper mass	$[lb_m]$
$\bar{m}$	Panel mass per unit of area	$[lb_m/in^2]$
m	Modal number	[-]
N	See Equation 4.11.	[-]
n	Modal number	[-]
n	Ratio of damper natural frequency to system natural frequency	[-]
P	Uniform pressure	$[lb_f/in^2]$
Q_{i_j}	Elements of stiffness matrix	$[lb_f/in^2]$
$\overline{Q_{i_j}}$	Elements of transformed stiffness matrix	$[lb_f/in^2]$
R	Ring damper radius	[in]
R_N	See Equation 4.2.	[-]
R_D	See Equation 4.4.	[-]
S	See Equation 4.14.	[-]
T	Transmissibility; see Equation 4.1.	[-]
t	Panel thickness	[in]

LIST OF SYMBOLS (continued)

Symbol	Definition	Dimension
Xi	Displacement element i	[in]
Ui	See Table 2.3.	[lb_f/in^2]

Greek Symbol		
α	Damping factor	[-]
α	Modulus ratio	[-]
α_i	Boundary condition coefficients	[-]
β	See Equation 4.14.	[-]
$\delta_{2E\omega}$	Damping factor	[-]
θ	Angle between main ply direction and X axis of panel	[rad/s]
ζ	Correction factor; see Equation 4.10.	[-]
μ	Mass ratio	[-]
ν	Poison's ratio	[-]
ρ	Panel mass per unit of volume	[lb_m/in^3]
ω	Angular input frequency of system	[rad/s]
ω_o	Angular natural frequency of system	[rad/s]
ω_a	Angular natural frequency of damper	[rad/s]
ω_n	Angular natural frequency of panel	[rad/s]
Ω	Ratio of input frequencies to system natural frequency	[-]

LIST OF SYMBOLS (continued)

Subscript	Definition
i	Integer
m	Modal number
n	Modal number
o	Optimal condition

LIST OF ACRONYMS

Acronym/ Abbreviation	Definition
dB	Decibel
CRINC	(KU) Center for Research, Inc.
FRL	Flight Research Laboratory
Hz	Herz, cycles per second
KU	University of Kansas
NASA	National Aeronautics and Space Administration
NR	Noise reduction

CHAPTER 1

INTRODUCTION

This report is a continuation of the documentation of the research accomplished under continuing NASA Cooperative Agreement NCCI-6. The progress of the research accomplished during the period May 1, 1981, through September 31, 1981, of the current project year (May 1, 1981 through April 30, 1982) was included in the previous report, KU-FRL-417-17 (Reference 1).

The present report covers the period from October 1, 1981, through February 28, 1982. In the beginning of this period, the nine loudspeakers in the noise generation unit of the acoustic facility had to be replaced, and extensive testing took place to recalibrate the system. It was not possible to obtain test data consistent with tests conducted earlier, although the repeatability of tests after the replacement was good. As a result, future tests, including those described in this report, will be compared only with other tests conducted after the replacement.

The application of fiber-reinforced composite materials, such as Graphite-Epoxy and Kevlar, for secondary or primary structures is growing in the commercial airplane industry. This trend is also true in the general aviation industry but at a slower pace. A remarkable exception is the all-composite Learfan. As a response to this development, a composite panel program was initiated during this period. The effects of some of the parameters that affect noise reduction of these panels have been investigated. These are discussed in Chapter 2.

Materials for the internal covering of the fuselage frame vary from a simple sandwich foam panel to a luxurious panel with upholstery or a carpet covering, depending on the function of the airplane. At the request of Beech Aircraft Corporation, samples of possible candidates for internal panel configuration have been tested at the KU-FRL acoustic facility. Results of these tests are described in Chapter 3.

Increasing the damping characteristics of a structural panel will, among other things, reduce the vibration amplitudes at resonance frequencies, with attendant reductions in sound radiation. In general, damping treatments consist of covering the entire panel on the inside with a layer of a viscoelastic damping material. Highly damped panels, according to this method, usually involve penalties of weight and complexity. As an alternative the use of a dynamic absorber (also called a tuned damper) has been proposed (References 2-3). Chapter 4 gives an analysis of the damping mechanism of such a tuned damper and reports some test results for a particular tuned damper configuration.

CHAPTER 2

FIBER-REINFORCED COMPOSITE PANELS

2.1 INTRODUCTION

The use of composite laminated materials, such as graphite-epoxy and Kevlar*, is slowly increasing in the aviation industry. With the noticeable exception of the all-composite (graphite-epoxy) Learfan and some of the smaller, home-built planes, application of these materials has been until now mainly limited to secondary or small primary structures. By virtue of their high strength-to-weight ratio and their directional dependent properties, fiber-reinforced laminates offer the designer the potential to design light-weight, "customized" structures with the main stiffness direction in the most desired direction. However, the composition of the laminate (i.e., the number and ply orientation of the various layers) that would be optimal for a structural design may not be optimal for noise control. Involving both aspects in the early design process of the laminated panel could avoid unnecessary weight penalty, resulting from application of additional or a larger amount of sound absorption material for noise control.

This chapter describes a test program initiated to study the noise reduction characteristics of fiber-reinforced composite panels. The fiber materials and the ply orientation were chosen to be the variables in the test program.

---

*Kevlar is a trade name of Dupont for an aramid fiber material in combination with an epoxy resin.

2.2 DESCRIPTION OF THE PANELS

Table 2.1 summarizes the variables in the tests conducted. Six panels were made from graphite-epoxy, and five from Kevlar. These panels were manufactured by Beech Aircraft Corporation. Details of the manufacturing process as well as the properties of the material are presented in Table 2.2. Each panel has outside dimensions of 20 inches by 20 inches and consists of three layers of the same thickness. Each layer, except one, is made of a woven cloth material with the two main directions of the fibers perpendicular to each other. The only exception is the middle layer of panel 330, which is a unidirectional tape of graphite-epoxy. The ply orientation of each panel is indicated by the angles between the main fiber direction of each layer with the X axis of the panel. A superscript "u" is used as an indication of a unidirectional layer. Three different ply orientations were used: (1) main fiber directions along the X-axis, 0-0-0; (2) top and bottom layers oriented with main direction along diagonal, middle layer along X-axis, 45-0-45; and (3) top and middle layers oriented along X-axis and middle layer along diagonal, 0-45-0. In addition, in one graphite-epoxy panel (#330) with a ply-orientation of 45-0-45, a unidirectional tape was used instead of a woven material for the middle layer. Although the total thickness of each panel was specified as 0.030 inch, variations in the manufacturing process resulted in differences in thickness and in density between the panels. In particular, the graphite-epoxy panels appeared to be most susceptible to differences in quality control. In Table 2.1 the measured average thickness is indicated for each panel.

Table 2.1 DESCRIPTION OF COMPOSITE PANELS

Panel #	Material	Orientation of Layers	Number of Hat Stiffeners	Thickness (in)
330	Graphite-epoxy	45-0^u-45	0	.038
331	"	0-0-0	0	.049
332	"	45-0-45	0	.030
333	"	0-45-0	0	.040
334	"	45-0-45	1	.029
335	"	45-0-45	2	.029
336	Kevlar	0-0-0	0	.028
337	"	45-0-45	0	.028
338	"	0-45-0	0	.030
339	"	45-0-45	1	.029
340	"	45-0-45	2	.029

All layers consist of woven material, except the middle layer of Panel 330, which is a unidirectional tape.

Table 2.2 ESTIMATED MATERIAL PROPERTIES OF GRAPHITE-EPOXY AND KEVLAR LAMINATES

Graphite-Epoxy

material:	HEXCEL W 3T282/F593 (cloth)	
cure:	350°/60'/50 psi	
E_{11}:	9.73×10^6 psi	
E_{22}:	9.10×10^6 psi	estimated from Reference 4a
Gxy:	3.5×10^6 psi	
ν_{12}:	0.3	

material:	USP E788-T300 (unidirectional tape)	
cure:	350°/60'/50 psi	
E_{11}:	18.0×10^6 psi	
E_{22}:	3.6×10^6 psi	estimated from Reference 4b
Gxy:	0.96×10^6 psi	
ν_{12}:	0.3	

Kevlar

material:	USP E719/281 (cloth)	
cure:	250°/60'/40 psi	
E_{11}:	3.87×10^6 psi	
E_{22}:	3.24×10^6 psi	estimated from Reference 4b
Gxy:	1.45×10^6 psi	
ν_{12}:	0.3	

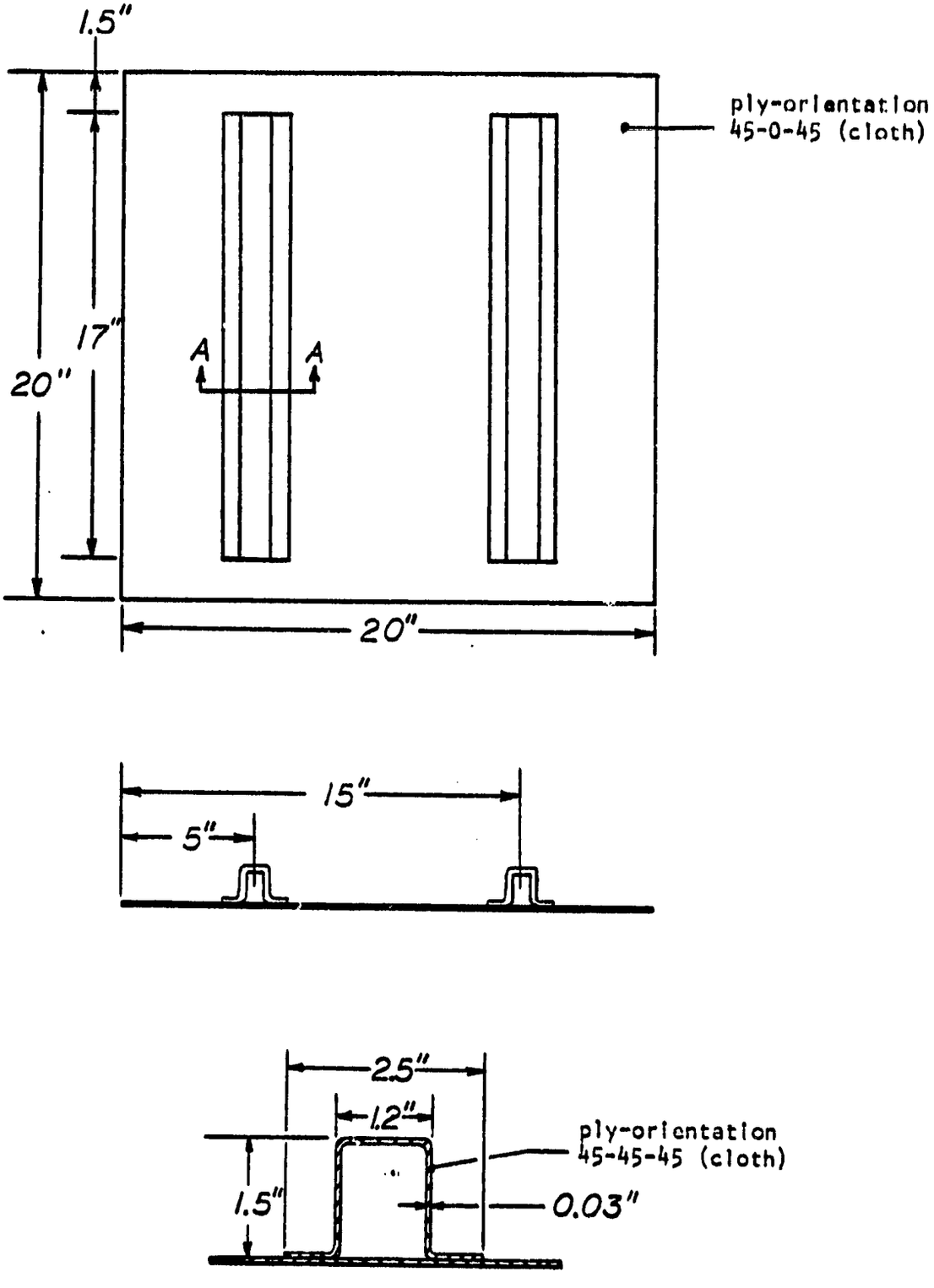

Figure 2.1 Dimensions of Composite Panel with 2 Stiffeners

In addition to the variable ply orientation, two panels of each material were stiffened with one or two stiffeners of the hat type.

Figure 2.1 shows the geometrical properties with a single stiffener. The stiffener is located at the center line of the panel.

During the tests, the stiffened panels were oriented in such a way that the direction of the stiffeners was vertical, i.e. the situation shown in Figure 2.1.

2.3 THEORETICAL ANALYSIS

By varying the ply orientation, it is possible to give the panel its highest stiffness in the direction where it is most needed. The noise reduction characteristics of a panel at low frequencies is mainly dominated by the stiffness of the panel, i.e. the ability of the panel to resist bending moments, introduced by the load perpendicular to the plane of the panel. Also the fundamental resonance frequency will be dependent on the panel's stiffness. This section attempts to relate the low frequency noise reduction characteristics and the natural resonance frequency with the stiffness characteristics of the panel, determined by the geometrical properties of the laminate.

Laminated panels, which are symmetrical about the midplane, do not have a coupling between in-plane loads and bending loads, and the resistance to bending can be expressed in terms of the elements of the "D" matrix in the constitutive equations (Reference 5):

$$\begin{bmatrix} M_x \\ M_y \\ M_{xy} \end{bmatrix} = \begin{bmatrix} D11 & D12 & D16 \\ D12 & D22 & D26 \\ D16 & D26 & D66 \end{bmatrix} \cdot \begin{bmatrix} k_x \\ k_y \\ k_{xy} \end{bmatrix} \qquad (2.1)$$

where M_x, M_y, and M_{xy} = bending moments

D11, D22, D66,

D12, D16, D26 = orthotropic elastic constants

k_x, k_y, k_{xy} = plate curvatures.

Because the equations of specially orthotropic plates (for which D16 and D26 = 0) are less complex than those governing more general laminated plates, laminated panels are often assumed to behave as such specially orthotropic plates. Reference 6 gives the natural frequency of a rectangular plate for various boundary conditions as:

$$f_{m,n} = \frac{1}{2\pi\sqrt{\bar{m}}} \sqrt{D11\left(\frac{\alpha_1}{a}\right)^4 + 2(D12 + 2D66)\frac{\alpha_2}{a^2b^2} + D22\left(\frac{\alpha_3}{b}\right)^4} \qquad (2.2)$$

where:

a, b = dimensions of panel area exposed to sound (18" x 18")

$\bar{m}$ = mass per unit area of the plane

m, n = modal number

Dij = orthotropic elastic constants

α_i = coefficients describing boundary conditions of each side of the panel and modal numbers.

Reference 6 gives the following approximated values for the coefficients α_i at the fundamental resonance frequency:

all sides clamped	all sides simply supported
$\alpha_1 = \alpha_3 = 4.730$	$\alpha_1 = \alpha_3 = \pi$
$\alpha_2 = 151.3$	$\alpha_2 = \pi^4$

Table 2.3 gives the equations used for the determination of the orthotropic elastic constants Dij. Material properties of Kevlar and graphite-epoxy laminates were estimated from structural data provided by References 4a and 4b and presented in Table 2.2. Appendix A presents a listing of the FORTRAN program that was used to compute the elements of the D matrix and the resonance frequencies for a laminated panel

Table 2.3 EQUATIONS USED FOR COMPUTATION OF THE D MATRIX

Stiffness Matrix

$$Q_{11} = E_{11}/(1 - \nu_{12}\nu_{21})$$

$$Q_{22} = E_{22}/(1 - \nu_{12}\nu_{21})$$

$$Q_{12} = \nu_{21}E_{11}/(1 - \nu_{12}\nu_{21}) \qquad \text{Where } \nu_{21}E_{11} = \nu_{21}E_{22}$$

$$Q_{66} = G_{xy}$$

$$Q_{16} = Q_{26} = 0$$

Transformed Stiffness Matrix Q (Material axes rotated about Angle θ)

$$\overline{Q_{11}} = U1 + U2*COS(2\theta) + U3*COS(4\theta)$$

$$\overline{Q_{22}} = U1 - U2*COS(2\theta) + U3*COS(4\theta)$$

$$\overline{Q_{12}} = U4 - U3*COS(4\theta)$$

$$\overline{Q_{66}} = U5 - U3*COS(4\theta)$$

$$\overline{Q_{16}} = -.5*U2*SIN(2\theta) - U3*SIN(4\theta)$$

$$\overline{Q_{26}} = -.5*U2*SIN(2\theta) + U3*SIN(4\theta)$$

where:

$$U1 = 1/8(3Q_{11} + 3Q_{22} + 2Q_{12} + 4Q_{66})$$

$$U2 = 1/2(Q_{11} - Q22)$$

$$U3 = 1/8(Q_{11} + Q_{22} - 2Q_{12} - 4Q_{66})$$

$$U4 = 1/8(Q_{11} + Q_{22} + 6Q_{12} - 4Q_{66})$$

$$U5 = 1/8(Q_{11} + Q_{22} - 2Q_{12} + 4Q_{66})$$

$$Dij = \int_{-h/2}^{h/2} \overline{Q_{ij}} * Z^2 dZ = \frac{1}{3}\overline{Q_{ij}}_b * Z^3 \Big]_{-h/2}^{-h/6} + \frac{1}{3}\overline{Q_{ij}}_m * Z^3 \Big]_{-h/6}^{h/6} + \frac{1}{3}Q_{ij_t} * Z^3 \Big]_{h/6}^{h/6}$$

(Panel consists of 3 equal thickness layers.)

(b, m, and t indicate bottom, middle, and top layer, respectively.)

with three layers of equal thickness. Table 2.4 presents for each (unstiffened) panel the computed values for the elastic constants Dij and the fundamental resonance frequency based on the estimated values of the material properties. Also indicated in parentheses are the values of Dij and $f_{1,1}$ if each panel would have the same thickness of .030" (mass of each panel is proportional to the change in thickness). As can be seen, the agreement between measured and computed values of the resonance frequency is poor, at least not consistent. Although the measured values for the graphite-epoxy panels are within 10 Hz of the calculated values for a panel with all of the edges clamped, measured values of the more flexible Kevlar panels are much higher than the predicted values for a clamped edge condition. The actual boundary conditions of the panel in the KU-Beranek tube are not exactly known. Part of the disagreement may be due to the estimated average values of the material properties, used in the calculations, and/or to the cavity effect of the Beranek tube (Reference 7). This cavity effect will increase the stiffness of the panel and therefore increase the fundamental resonance frequency of the panel. Due to the variations in thickness, effect of ply orientation on the noise reduction cannot be determined directly from the test results. When the orthotropic constants Dij are determined for laminates with equal thickness, .032", variations between them as a result of ply orientation are less pronounced than for the tested panels. (See Table 2.4.)

The higher stiffness characteristics of the graphite-epoxy laminates will result in higher noise reduction characteristics than comparably sized Kevlar panels.

Table 2.4 COMPARISON OF MEASURED AND PREDICTED FUNDAMENTAL RESONANCE FREQUENCIES

MATERIAL	GRAPHITE-EPOXY				KEVLAR		
Panel #	330	331	332	333	336	337	338
Ply-Orientation	45-0[u]-45	0-0-0	45-0-45	0-45-0	0-0-0	45-0-45	0-45-0
Weight (lbs)	.826	1.039	.617	.900	.562	.566	.547
Thickness (in)	0.038	0.049	0.030	0.040	0.028	0.028	0.030
Density (lb/in^2)	.0021 (.00163)*	.0026 (.00161)	.00155 (.00155)	.0023 (.00169)	.00142 (.00152)	.00144 (.00154)	.00141 (.00141)
D11 ($lb_f in$)	47.2 (23.5)	104.7 (23.9)	22.8 (22.8)	56.6 (23.9)	7.6 (9.4)	7.1 (8.8)	9.4 (9.4)
D22	45.2 (22.2)	97.5 (22.4)	22.8 (22.8)	53.0 (22.4)	6.4 (7.9)	7.1 (8.8)	7.9 (7.9)
D12	13.8 (6.9)	29.2 (6.7)	7.0 (7.0)	15.9 (6.7)	1.9 (2.4)	1.9 (2.2)	2.4 (2.4)
D16	-0.8 (-0.4)	0.0 (0.0)	-0.4 (-0.4)	-0.0 (-0.0)	0.0 (0.0)	-0.3 (-0.4)	-0.0 (-0.0)
D26	-0.8 (-0.4)	0.0 (0.0)	-0.4 (-0.4)	-0.0 (-0.0)	0.0 (0.0)	-0.3 (-0.4)	-0.0 (-0.0)
D66	16.2 (8.0)	34.3 (7.9)	8.2 (8.2)	18.7 (7.9)	2.7 (3.3)	2.6 (3.2)	3.3 (3.3)
$f_{1,1}$ (Hz) Simply Supp.	28.0 (22.6)	37.2 (22.7)	22.8 (22.8)	29.2 (22.1)	13.6 (14.5)	13.5 (14.3)	15.1 (15.1)
$f_{1,1}$ (Hz) Clamped	51.0 (41.3)	68.4 (41.6)	41.6 (41.6)	53.6 (40.6)	24.5 (26.4)	24.8 (26.2)	27.5 (27.5)
$f_{1,1}$ (Hz) Measured	50-58	72-65	55-50	72-70	52-52	48-48	36-38

* derived values for laminates with thickness 0.030"

2.4 EXPERIMENTAL RESULTS

Noise reduction curves of each conducted test are presented in Appendix B. Each panel was tested twice in a random sequence. All tests were performed in the KU-FRL Beranek tube. A detailed description of this acoustic test facility is presented in Reference 8, which also shows the general arrangement of the test installation and illustrates in detail the position of the panel in the tube. The tests were performed on 20" by 20" panels with an exposed area of 18" x 18" under normal sound incidence and room termperature. All edges of the panel were clamped with 25 in-lb torque at the clamping points. Figure 2.2 gives an example of a typical noise reduction curve of a general aviation type specimen tested at the KU-FRL facility. The fundamental panel/cavity resonance frequency divides the noise reduction curve into two regions: stiffness controlled and mass controlled. In this report, the noise reduction characteristics of the panels will be interpreted using these two regions. For the interpretation of the noise reduction in the high frequency region (500-5000 Hz), a least-square-average line will be used to indicate the general trend. In the graphical presentation of the results in the next sections, noise reduction values at frequencies of 30 and 3000 Hz are used to represent the low frequencies (i.e. the stiffness-controlled region) and high frequencies (i.e. the mass-controlled region), respectively. The choice of these frequencies is rather arbitrary; and for a complete view of the characteristics over a wide range of frequencies, the original curves presented in Appendix A should be consulted. Table 2.5 also gives some numerical values for certain frequencies of all the tests conducted.

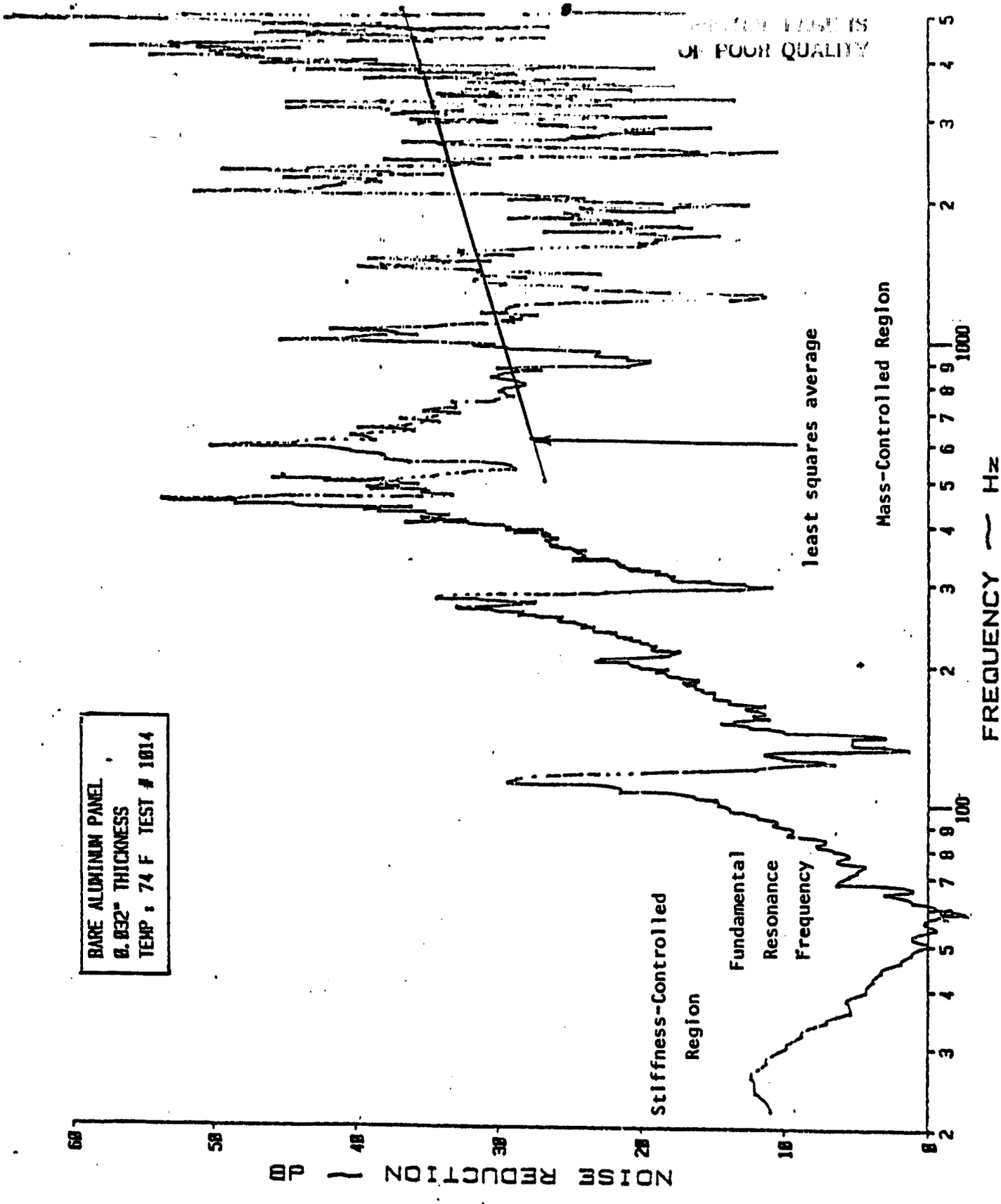

Figure 2.2 Noise Reduction Characteristics of a Typical General Aviation Type Panel

Table 2.5 NUMERICAL VALUES OF FIBER-REINFORCED LAMINATED PANEL TESTS

	GRAPHITE-EPOXY						KEVLAR				
Panel	330	331	332	333	334	335	336	337	338	339	340
Ply-Orientation	45-0$_u$-45	0-0-0	45-0-45	0-45-0	45-0-45	45-0-45	0-0-0	45-0-45	0-45-0	45-0-45	45-0-45
# of Stiffeners	0	0	0	0	1	2	0	0	0	1	2
Noise Reduction at (Hz)											
30	7.4*	9.7	3.6	17.0	15.5	20.0	3.6	3.3	4.3	10.0	17.6
	7.4**	15.0	10.0	15.0	19.0	20.5	8.8	4.2	4.5	8.4	17.8
40	4.0	4.4	-0.5	7.4	10.2	14.4	3.6	1.8	8.4	10.0	12.5
	3.4	7.5	3.0	8.1	7.7	16.2	3.6	4.4	3.4	7.1	12.2
50	-1.2	1.7	-0.6	6.0	8.1	13.4	1.7	.2	4.9	4.8	10.7
	.4	5.4	-0.4	5.7	9.6	13.0	3.1	1.3	5.9	13.6	9.8
100	3.9	8.6	8.4	3.0	.3	-.3	2.9	1.9	2.5	9.9	5.7
	-1.5	7.4	2.8	6.3	.1	0.	-.7	2.8	1.9	1.6	4.8
200	17.7	5.9	14.7	3.3	9.4	1.9	16.8	6.8	11.5	10.8	10.1
	15.1	23.5	13.1	7.2	8.3	5.1	19.3	6.8	11.2	9.3	6.9
400	26.5	30.3	29.2	29.5	28.8	36.6	20.5	20.8	19.6	19.6	24.1
	26.5	27.0	25.0	30.2	28.2	33.3	17.5	21.1	18.8	21.0	17.5
500***	24.4	25.0	23.2	25.2	22.8	21.8	22.7	23.2	22.9	23.8	23.7
	25.7	26.0	22.9	25.9	23.1	22.6	22.9	23.1	22.9	23.8	23.2
3000***	29.1	30.2	27.9	30.3	27.4	26.3	27.3	28.0	27.6	28.7	28.6
	31.0	31.3	27.6	30.0	27.8	27.2	27.7	27.8	27.6	28.7	28.0
5000***	33.0	34.3	31.7	34.5	31.2	29.9	31.0	31.9	31.4	32.6	32.5
	35.2	35.6	31.4	34.1	31.6	30.9	31.4	31.6	31.3	32.6	31.8
Fundamental Resonance Frequency (Hz)	50-58	72-65	55-50	72-70	116-112	92-96	52-52	48-48	36-38	68-92	84-82

NOTES: * Results from first test ** Results from second test *** Determined from least-square-average line

2.4.1 GRAPHITE-EPOXY PANELS

Figure 2.3 shows the noise reduction characteristics of four unstiffened panels with different ply orientations as a function of their (bulk) density. Noise reduction values at frequencies of 30 Hz (notched bars) and at 3000 Hz (open bars) are presented, as well as the variance between the two identical tests. The influence of repeatability was most noticeable in the low frequency domain, where the effect of differences in clamping and testing conditions is the largest.

At 3000 Hz the noise reduction of each panel is about 30 dB, except panel 322 which has a value of 27.5 dB. No noticeable effect of the mass law can be found based on the panel density, but there is an increase in noise reduction with increasing thickness. In the low frequency region, average noise reduction values range from 7 dB for both 45-0-45 panels to 12 dB for the 0-0-0 panel and 16 dB for the panel with the 0-45-0 orientation. Because of the variations in density and thickness, no strong conclusions can be made about the influence of the ply orientation; but both panels, having at least two main directions of the fibers parallel to the edges, have significantly higher noise reduction values than the panels with their main fiber directions along the diagonals.

Figure 2.4 shows the noise reduction characteristics of the graphite-epoxy panels with respectively 0, 1, and 2 stiffeners. Each panel has a 45-0-45 ply orientation with a minimal variance in thickness. The low frequency noise reduction values show clearly the beneficial influence of the stiffeners. At 3000 Hz no influence of

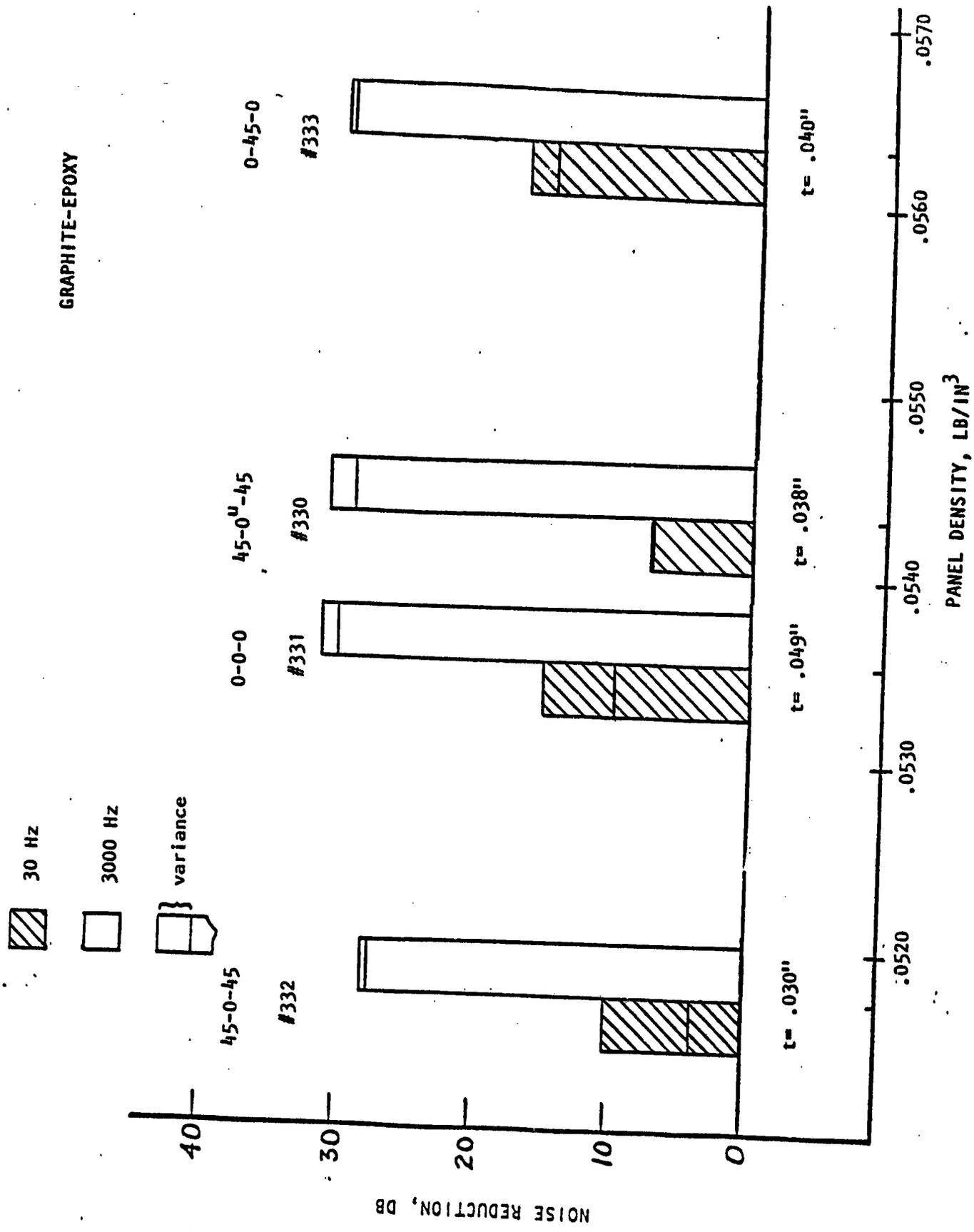

Figure 2.3 Effect of Ply Orientation on Noise Reduction Characteristics of Unstiffened Graphite-Epoxy Panels at Low and High Frequencies

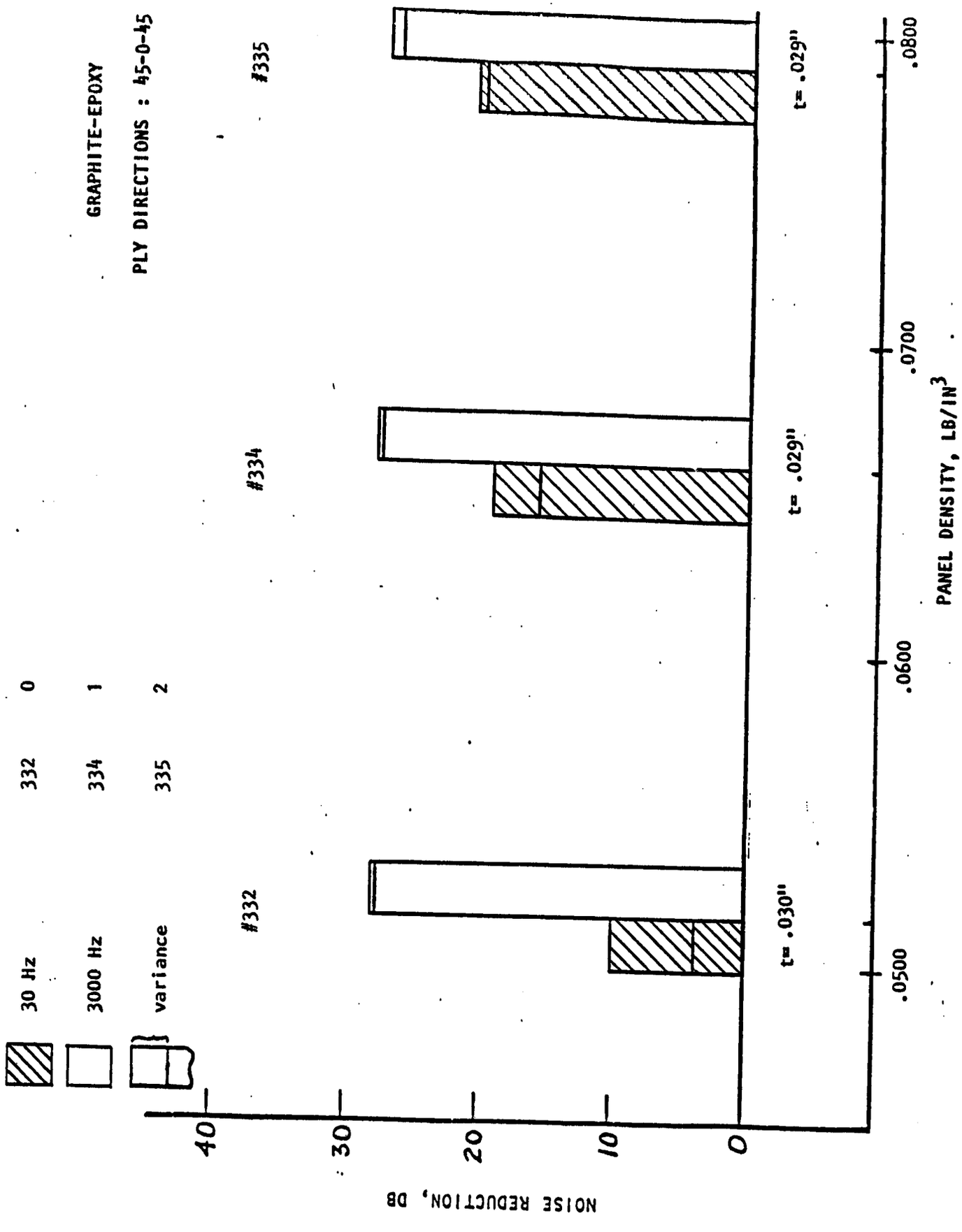

Figure 2.4 Effect of Stiffeners on Noise Reduction Characteristics of Graphite-Epoxy Panels with 45-0-45 Ply Orientation at Low and High Frequencies

the mass can be observed when mass in the form of the stiffeners is added. By comparison, the noise reduction values at 30 and 3000 Hz of an aluminum panel with a comparable thickness of 0.032 inch are 10 and 35 dB. Taking into account the difference in density (.055 vs .080 lb/in^3), graphite-epoxy panels are at least comparable to or better than aluminum panels at low frequencies.

2.4.2 KEVLAR PANELS

Figure 2.5 shows the noise reduction characteristics of the unstiffened Kevlar panels having three different ply orientations. Compared to the graphite-epoxy panels, the low frequency noise reduction values of the Kevlar laminates are lower due to their lower stiffness. Also the repeatability of the tests with Kevlar are relatively better. The results at 30 Hz tend to confirm the trend observed that panels which have more fibers parallel to the edges of the panel have higher noise reduction values than panels with the main fiber direction along the diagonal. However, more tests have to be performed to investigate other factors that could have an effect. Such factors include the influence of the variance in thickness and density, and geometrical properties of the panel (square or rectangular).

Figure 2.6 presents the noise reduction characteristics of the Kevlar panels with 0, 1, and 2 stiffeners, respectively. Again, the beneficial effect of the stiffener is observed at low frequencies. The addition of one or two stiffeners resulted in a gain of 5 or 14

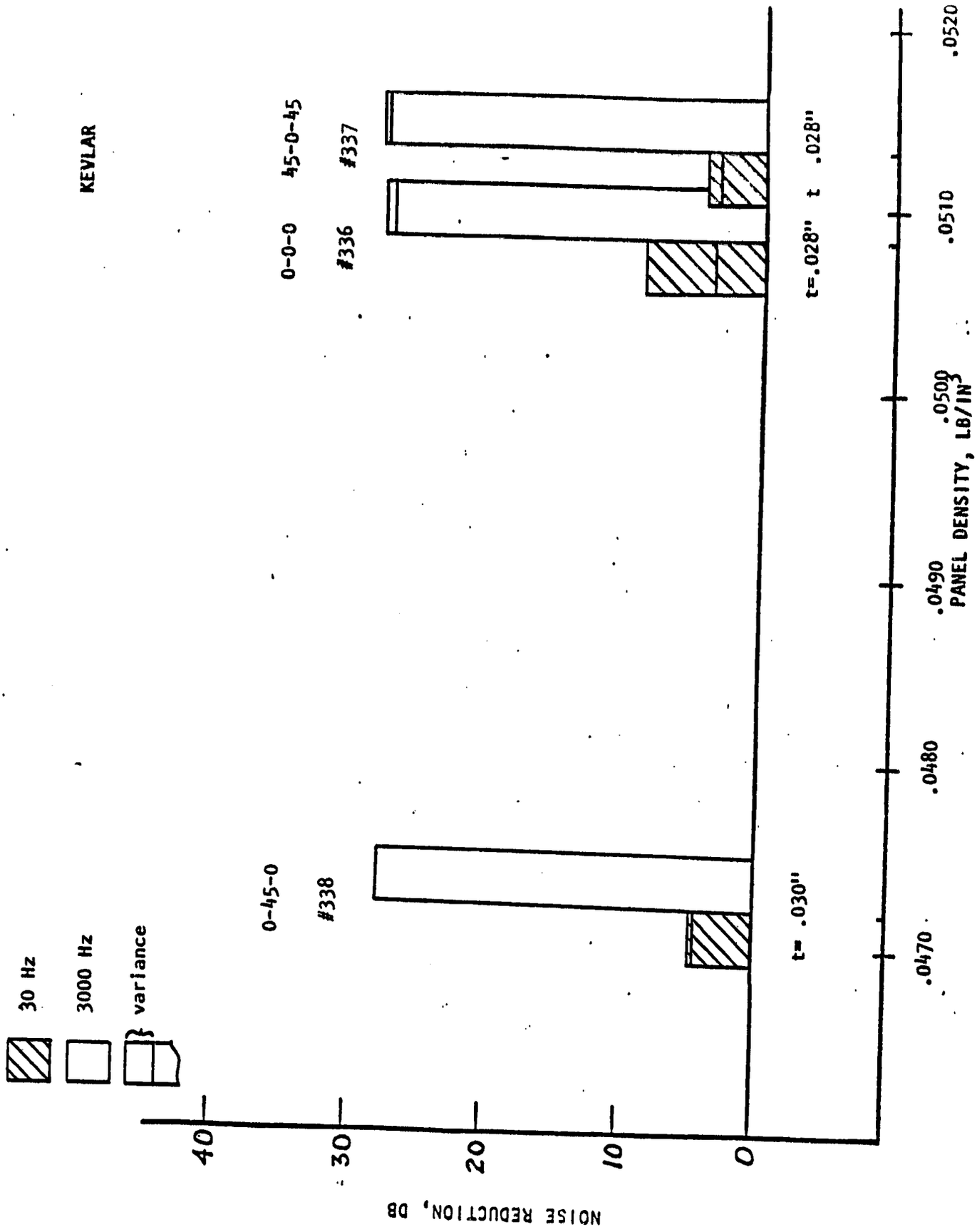

Figure 2.5 Effect of Ply Orientation on Noise Reduction Characteristics of Unstiffened Kevlar Panels at Low and High Frequencies

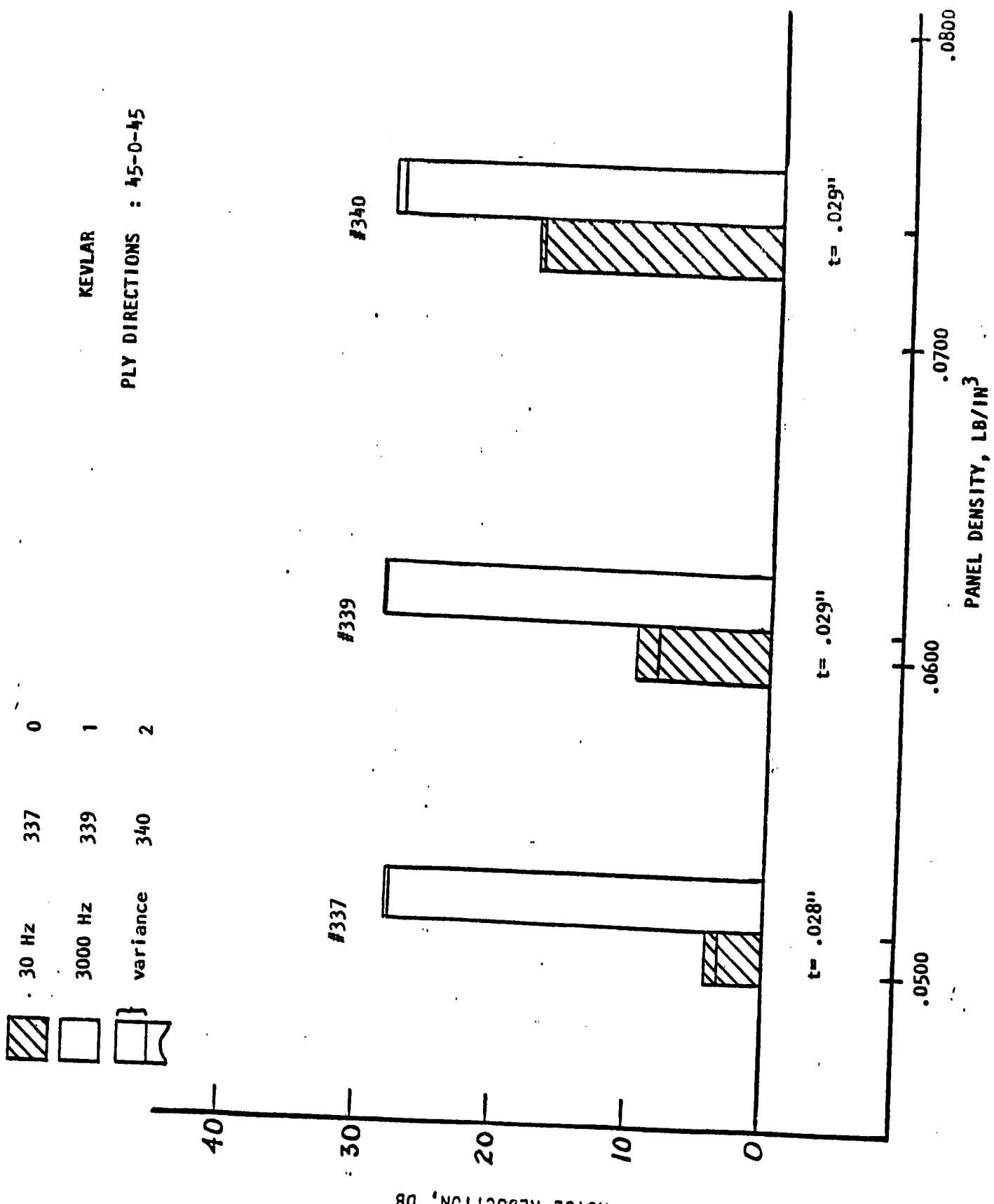

Figure 2.6 Effect of Stiffeners on Noise Reduction Characteristics of Kevlar Panels with 45-0-45 Ply Orientation at Low and High Frequencies

dB, respectively. Addition of one or two stiffeners resulted in a slight increase of the noise reduction at high frequencies.

2.5 CONCLUSIONS AND RECOMMENDATIONS

The conducted tests have indicated the importance of quality control during the manufacturing process of the laminated panels. Variations in thickness and density have prevented the isolation of the influence of the ply orientation on the noise reduction characteristics of laminated panels. Variations in thickness can be caused by differences in the manufacturing of the laminates, but different ply orientations can also result in thickness variations during the lay-up process. The graphite-epoxy panels were more susceptible to variations in thickness and density than the Kevlar panels. The repeatability of the tests was in general better for the Kevlar panels and at higher frequencies.

Graphite-epoxy panels possess higher noise reduction characteristics than Kevlar panels in the low frequency region because of their higher stiffness properties. At high frequencies the noise reduction characteristics of both materials are comparable. Increasing the stiffness of a panel with one or two stiffeners has a beneficial effect on the low frequency noise reduction characteristics of a panel. Addition of the mass of the stiffeners does not increase noticably the noise reduction at higher frequencies for the tested composite panels.

Compared to an aluminum panel with a thickness of 0.032 inch, graphite-epoxy panels have better noise attenuation characteristics at low frequencies, while Kevlar panels have poorer such characteristics. However, for a true comparison between aluminum and composite structures, realistic values of panel thicknesses should be used. Actual laminated panels will generally have a larger number of layers with more variation in ply orientations. It is recommended to extend the study of the influence of ply orientation on a theoretical basis. It is also recommended to study the influence of the sound incidence angle on the noise reduction characteristics and the composite loss factor of these panels. The results of the current tests have indicated that in preparation for future tests, care must be taken during the manufacturing process to produce panels with equal thickness.

CHAPTER 3

INTERIOR PANEL CONFIGURATIONS

3.1 INTRODUCTION

Panel configurations used for covering the fuselage structure on the inside vary in density and type of material, depending upon the function of the airplane. Typically, inexpensive, light-weight materials are used in commercially oriented general aviation airplanes; but more luxurious materials such as carpet are also used in business and executive-type airplanes.

Besides having a function of decoration, the internal wall is often part of a double wall structure and can be used as part of the treatment to reduce externally generated noise. Interior panel configurations consist in general of a base material and a covering. In this chapter the noise reduction characteristics of a number of possible candidate materials and treatments are determined. The panels were provided by the Beech Aircraft Corporation, who also determined the type of materials and treatments to be tested.

3.2 DESCRIPTION OF THE PANELS

Table 3.1 presents a listing of the panels tested. All panels were 20" x 20" in size, and except for the panels treated with carpet each treated panel was completely covered with one or two layers of different material. Panels 313, 319, and 343 had only their exposed area (18" x 18") covered with carpet.

Table 3.1 DESCRIPTION OF INTERIOR PANEL CONFIGURATIONS

Panel	Panel Material	Treatment
	(Group I)	
311	45% open .025" Aluminum	---
312	45% open .025" Aluminum	.5" foam + leather covering
313	45% open .025" Aluminum	carpet
	(Group II)	
315	.25" Klege-Cell type 75 with 1 layer of type A fiberglass both sides	---
316	(same as above)	.125" neoprene + woolen covering
317	.125" Klege-Cell type 75 with 1 layer of type A fiberglass both sides	---
318	(same as above)	.020" Royalite covering
319	(same as above)	carpet
320	(same as above)	.5" foam + leather covering
	(Group III)	
323	.25" Rohacell, grade 51 with 1 layer of 120 phenolic pre-preg skin both sides	---
325	(same as above)	.125" neoprene + woolen covering
347	.25" Rohacell, grade 51 with 2 layers of 120 phenolic pre-preg skin both sides	---
341	.125" Rohacell, grade 51 with 1 layer of 120 phenolic pre-preg skin both sides	---

Table 3.1 DESCRIPTION OF INTERIOR PANEL CONFIGURATIONS, continued

Panel	Panel Material	Treatment
342	.125" Rohacell, grade 51 with 1 layer of 120 phenolic pre-preg skin both sides	---
343	(same as above)	carpet
344	(same as above)	.25" neoprene + leather covering
	(Group IV)	
321	.032" Aluminum	Klege-Flex type 45
322	(same as above)	SJ 2052x1005 damping treatment
345	two .032" Aluminum panels bonded together	2 rectangular cutouts in one sheet
346	(same as above)	4 rectangular cutouts in one sheet
	(Group V)	
314	.090" Lexan	---
326	.25" Orcofilm blanket	---

The first group of panels is composed of a standard aluminum panel, perforated with holes for an amount of 45% of the area, and two different types of treatment. The second group consists of a sandwich panel with four different treatments. The sandwich panel is composed of a Klege-Cell type foam core and fiberglass as the skin material. Two thicknesses were used for the core. The third group consists of sandwich panels composed of a Rohacell type foam core and phenolic pre-preg skin. Two different core thicknesses and four different treatments were used. Also one panel was tested with two layers of skin material on both sides, panel #347. The fourth group consists of a standard aluminum panel with a thickness of 0.032" with, respectively, a sound absorbing material, Klege-Flex type 45, and a damping treatment material, SJ 2052x1005. The last two configurations in this group consist of two .032" aluminum panels bonded together. Panel #345 has two rectangular cutouts, while panel #346 has four rectangular cutouts in one sheet. Figure 3.1 shows the layout of these panels. It can be noted that, unlike the sandwich panels, the bonded aluminum panels are not limited to use in internal wall configurations but are, in practice, normally used as the main skin. Nevertheless, these panels were included in this investigation. The last group consists of 2 panels composed of different kinds of materials: a .09" Lexan panel and a thermal blanket contained in a bag of Orcofilm. Because of the flexibility of the thermal blanket, for the test this material was clamped between two steel frames. The area exposed to the direction of the sound was 16" x 16".

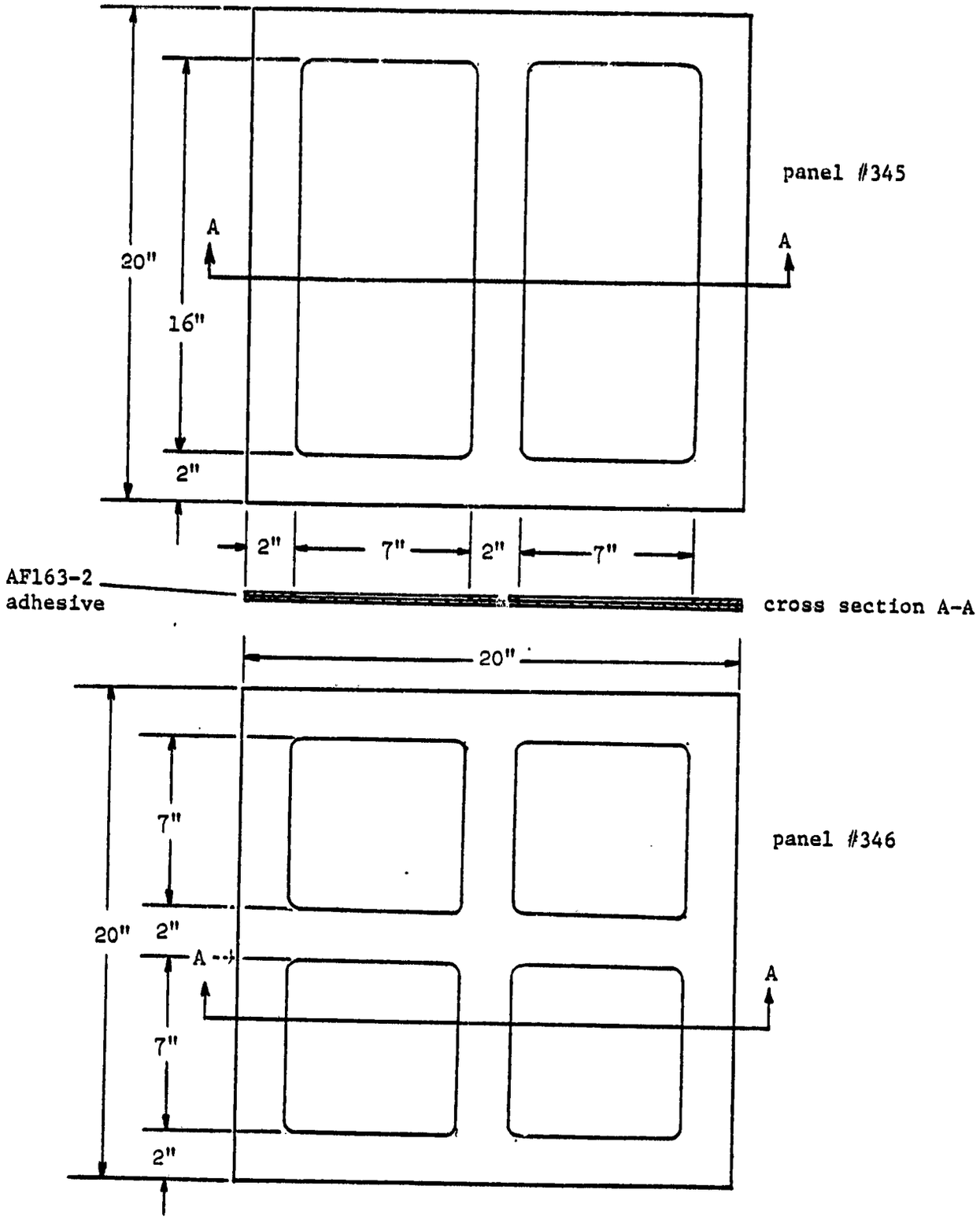

Figure 3.1 Geometric Properties of Panels 345 and 346

3.3 RESULTS

Appendix C presents the noise reduction curves for each panel tested. All of the panels were tested twice within the test period in a random sequence. The repeatability was in general good, especially in the high frequency domain. The variance between two identical tests was within 2 or 3 dB, except for five panels (#312, 323, 343, 344 and 346). Normal test procedures were used, and all the tests were carried out at room temperature.

Bar graphs were made, presenting values of noise reduction at two frequencies. The same comments which were made in Chapter 2 about the choice of the frequencies represented are valid for these tests. Numerical results are presented in Table 3.2 for each panel tested.

Group I: Perforated Panels

Figure 3.2 shows the noise reduction characteristics of a standard perforated aluminum panel with two different treatments. Noise reduction values of frequencies of 30 Hz and 3000 Hz are described, as well as the variance between two identical tests. The values are plotted as a function of the surface density, which is a common parameter used in theoretical analysis of double-wall structures. As expected, the noise reduction of a perforated panel is minimal. When this panel is combined with a half-inch thick covering of foam and leather, noise reduction is increased. Attaching a half-inch thick carpet will increase the surface density of the panel

Table 3.2 NUMERICAL VALUES OF INTERIOR PANEL CONFIGURATIONS

Panel ID	Panel Material	Treatment[2]	Noise Reduction 30 Hz[1]	Noise Reduction 3000 Hz[1]	Fr Hz
Group I					
311	45% open Aluminum	- - - - -	0.5	0.0	102
312	(same as above)	1[2]	7.8	35.8	41
313	(same as above)	2	2.2	18.6	100
Group II					
315	.25" Klege-Cell type 75 + 1 layer fiberglass on both sides	- - - - -	19.3	21.6	16
316	(same as above)	3	20.6	29.9	71
317	.125" Klege-Cell type 75 +1 layer fiberglass on both sides	- - - - -	9.6	22.2	114
318	(same as above)	4	8.7	27.7	71
319	(same as above)	2	8.0	42.1	45
320	(same as above)	1	12.9	34.6	67
Group III					
323	.25" Rohacell + 1 layer of 120 phenolic pre-preg skin on both sides	- - - - -	18.7	19.1	160
325	(same as above)	3	19.5	27.1	120
347	.25" Rohacell + 2 layers of 120 phenolic pre-preg skin on both sides	- - - - -	22.55	23.19	168
341	.125" Rohacell + 1 layer of 120 phenolic pre-preg skin on both sides	- - - - -	8.59	25.16	70-78
342	(same as above)	4	10.42	25.50	77
343	(same as above)	1	9.51	39.97	76-78
344	(same as above)	9	10.63	34.20	72-78
Group IV					
321	.032" Aluminum	5	10.6	34.8	57
322	(same as above)	6	3.7	38.1	40

[1] and [2]: See explanatory footnotes at conclusion of Table 3.2.

Table 3.2 NUMERICAL VALUES OF INTERIOR PANEL CONFIGURATIONS, continued

Panel ID	Panel Material	Treatment[2]	30 Hz[1]	3000 Hz[1]	Fr Hz
345	two .032" Aluminum panels bonded together	7	12.01	34.27	66
346	(same as above)	8	13.87	37.45	62-64
Group V					
314	.090" Lexan	- - - - -	3.9	37.8	42
326	Orcofilm	- - - - -	14.0	9.5	44

[1]average values of 2 tests

[2]1 = carpet

2 = .5" foam + leather covering

3 = .125" neoprene + woolen covering

4 = Royalite

5 = Klege-Flex type 45

6 = SJ 2025x1005 damping material

7 = two rectangular cutouts

8 = four rectangular cutouts

9 = .25" neoprene + leather covering

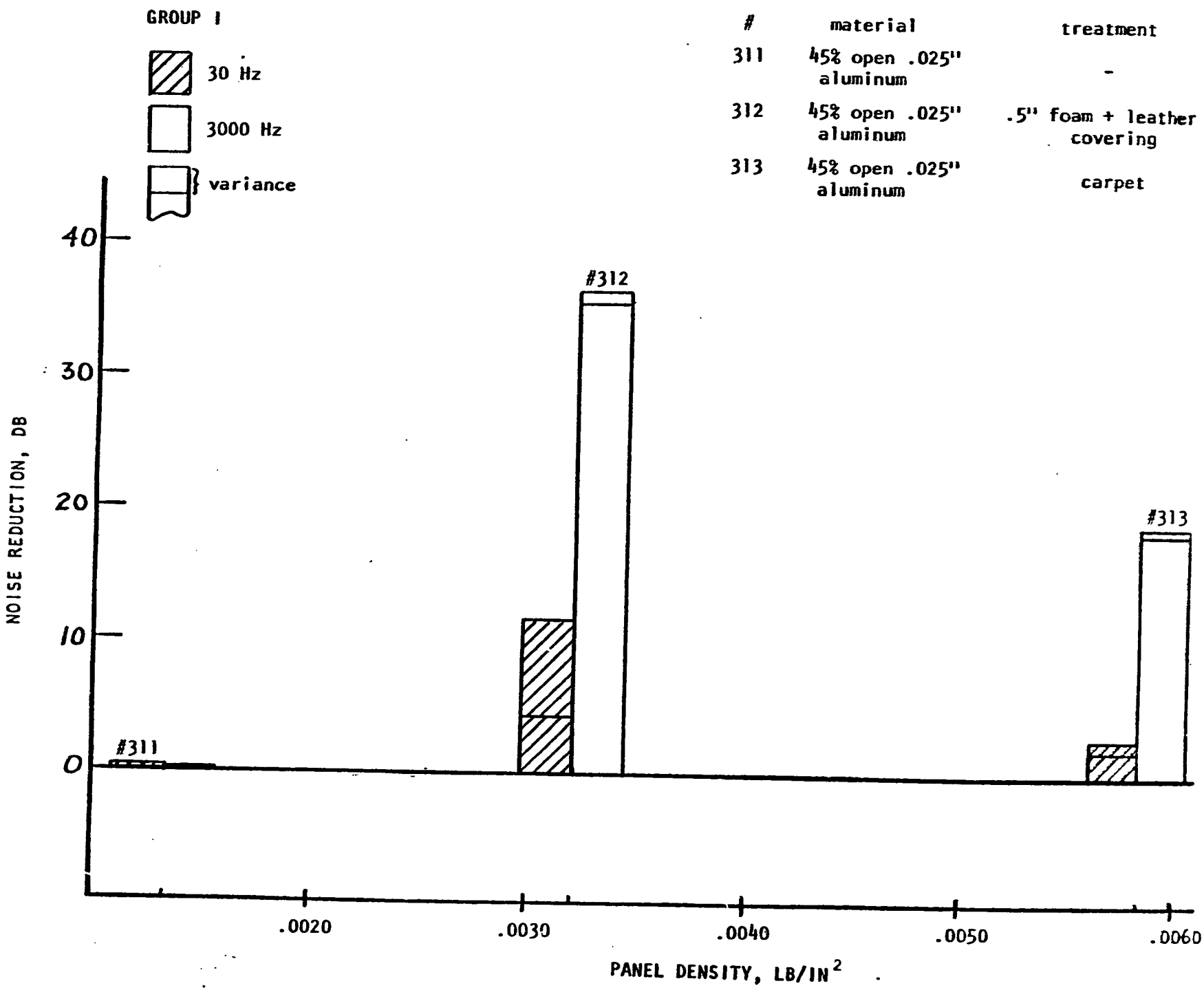

Figure 3.2 Noise Reduction Characteristics of Interior Panel Configurations, Group I

but will decrease the noise reduction characteristics relative to the foam and leather covering. Carpet has an open cell structure resulting in a lower noise reduction than with a more closed structure of leather cover and foam with sound absorbing characteristics.

Group II: Sandwich Panels with a Klege-Cell Core

This group consisted of a sandwich panel made from 2 layers of fiberglass and a core of Klege-Cell type 75 foam. Two core thicknesses were used: a 0.25 inch (panel #315) and a 0.125 inch (panel #317). Results are presented in Figure 3.3. Although panel #3.5 has a higher stiffness and a correspondingly higher noise reduction value of 30 Hz than panel #317 with a core size half the thickness, the increase in mass does not result in a higher noise reduction value at 3000 Hz in the mass-controlled frequency region.

Covering a sandwich panel with a 0.125 inch neoprene and woolen covering (panel #316) increases the high frequency noise reduction at 3000 Hz with about 8 dB, compared to the bare panel (#315), but does not have a noticeable effect on the low frequency noise reduction characteristics (about 1 dB). Treating the base sandwich panel with a Royalite covering (panel #318) or with a carpet (panel #319) does not increase the low frequency noise reduction at 30 Hz; but due to the increased mass, a higher value at 3000 Hz is obtained. When the panel was covered with foam and a leather covering (panel #320), low frequency noise reduction was increased about 3 dB, while at 3000 Hz the noise reduction gain amounted to 12 dB.

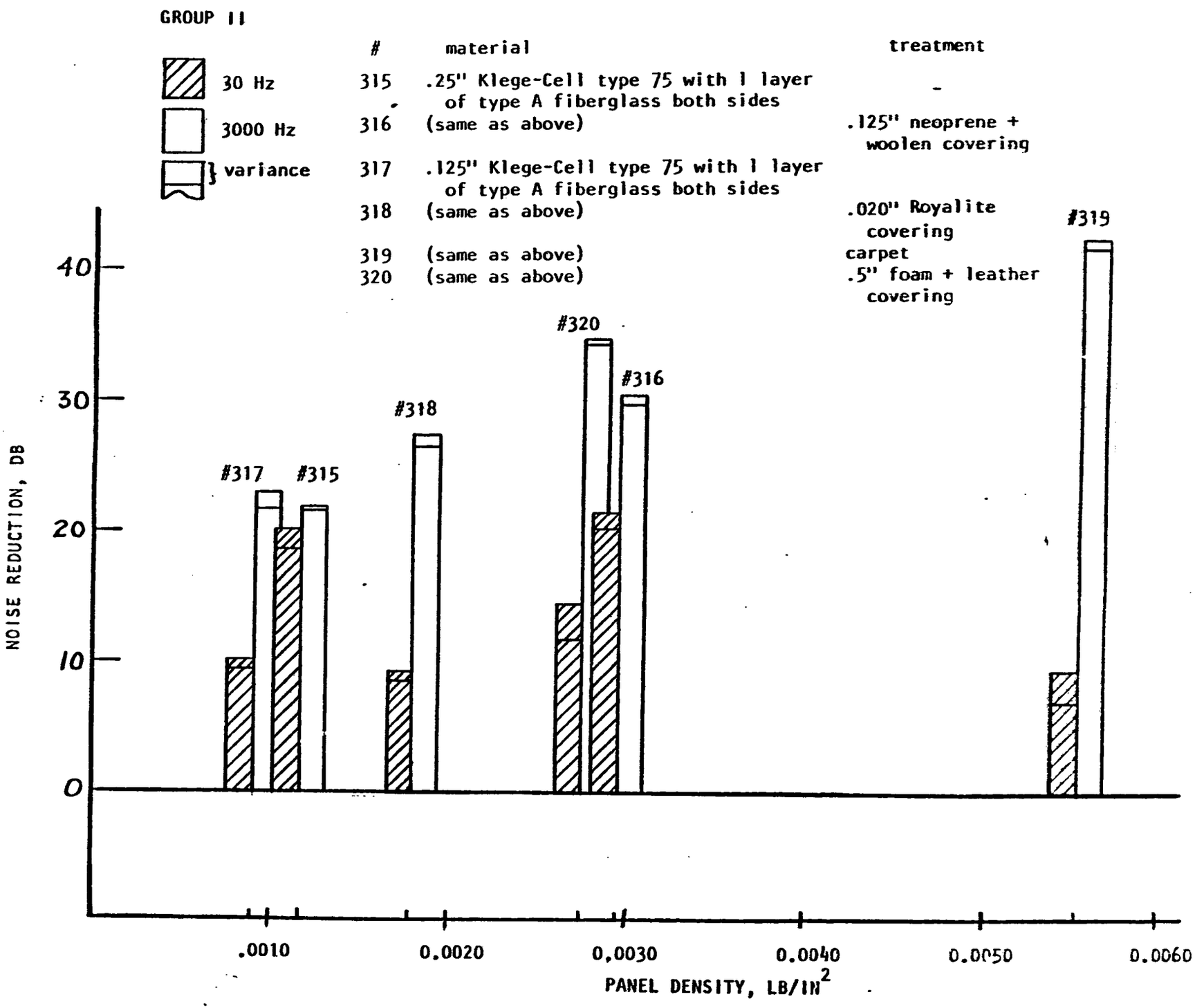

Figure 3.3 Noise Reduction Characteristics of Interior Panel Configurations, Group II

Group III: Sandwich Panels with a Rohacell Core

This group is composed of seven sandwich panels consisting of a Rohacell type core and a phenolic pre-preg skin material. Rohacell is a type of foam with a density of 3.1 lb/ft and is applied in two thicknesses: .125" (panels #341 through #344) and .25" (panels #323, 325 and 347). Figure 3.4 presents the noise reduction values at 30 and 3000 Hz for each panel in this group. Doubling the thickness of the core resulted in an average gain of 10 dB at 30 Hz, while at high frequencies a slight drop in noise reduction was experienced (#323 and #341). When two layers of skin material are applied, as in the case of panel #347, the stiffness of the panel will increase, corresponding with an average increase of about 4 dB in the stiffness-controlled frequency domain. When one-eighth inch neoprene combined with a woolen covering is applied to panel #323 with a .25" core, the average value of noise reduction at 30 Hz is slightly increased (.8 dB), and the high frequency noise reduction at 3000 Hz is increased by about 8 dB (panel #325).

When the basic sandwich panel is treated with Royalite, carpet or a combination of neoprene and a leather covering, a minimal gain in the stiffness-controlled region is measured. At high frequencies in the mass-controlled region, a large increase in noise reduction is observed due to the increase of mass.

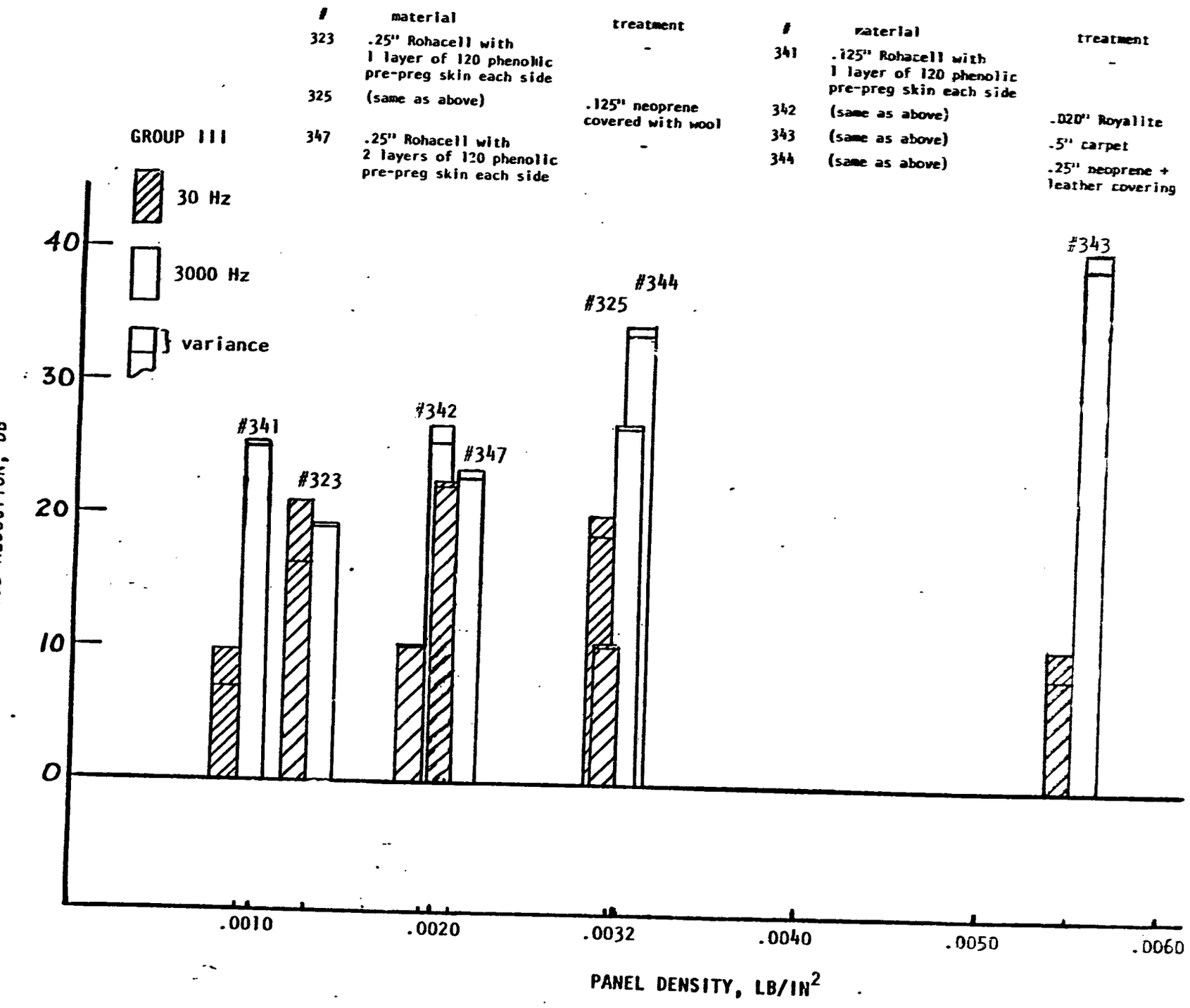

Figure 3.4 Noise Reduction Characteristics of Interior Panel Configurations, Group III

Group IV: Aluminum Panels

Figure 3.5 shows the results of tests with two 0.032 inch aluminum panels, one with a foam material, Klege-Flex type 45 (panel #321) and the other covered with a "constrained" damping material, SJ 2025x1005. The layer density of the panel covered with damping tape results in a higher noise reduction value at 3000 Hz, but there is no influence of a possible stiffening effect of the damping tape on the low frequency noise reduction characteristics. Panels 345 and 346 are composed of two aluminum sheets bonded together with two and four rectangular cutouts in one sheet, respectively. Panel 346 has a larger stiffness in the width direction than the panels with only two cutouts due to the acting doubler in the center of the panel. Figure 3.5 shows that at low frequencies (30 Hz) the resulting average gain in noise reduction amounted to almost 2 dB.

Group IV: Miscellaneous

Figure 3.6 shows the noise reduction characteristics at 30 Hz and at 3000 Hz for two panels of different kinds of materials. Panel 314 is made from 0.090 inch Lexan and has a low stiffness. At 30 Hz, Lexan has a low noise reduction value of about 4 dB, and at 3000 Hz it has a noise reduction of about 38 dB.

Panel #326 consists of fiberglass thermal blanket, 0.5 inch thick, contained in a bag of Orcofilm. The noise reduction values at 30 Hz and 3000 Hz were, respectively, 1.5 dB and 9.5 dB.

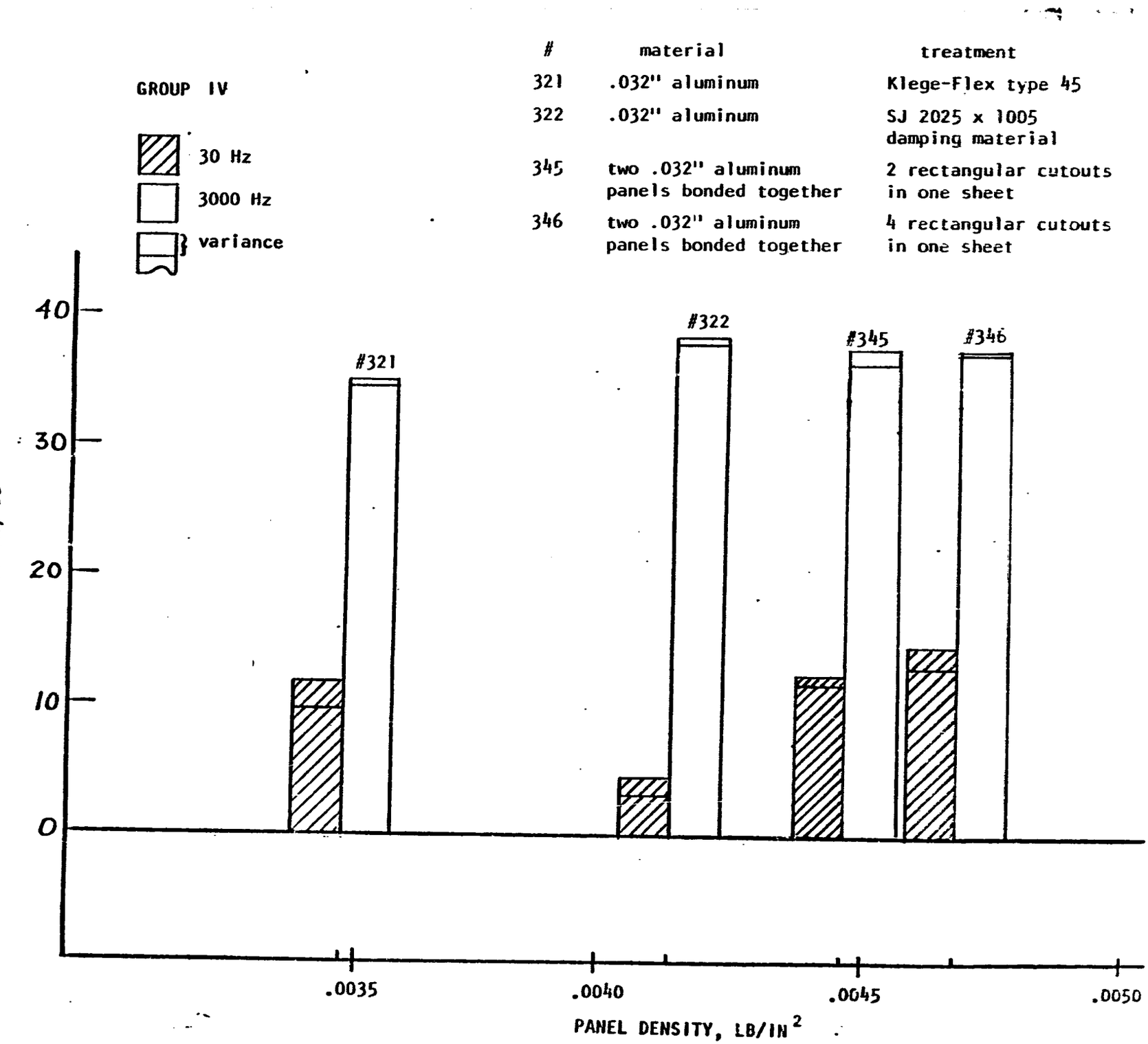

Figure 3.5 Noise Reduction Characteristics of Interior Panel Configurations, Group IV

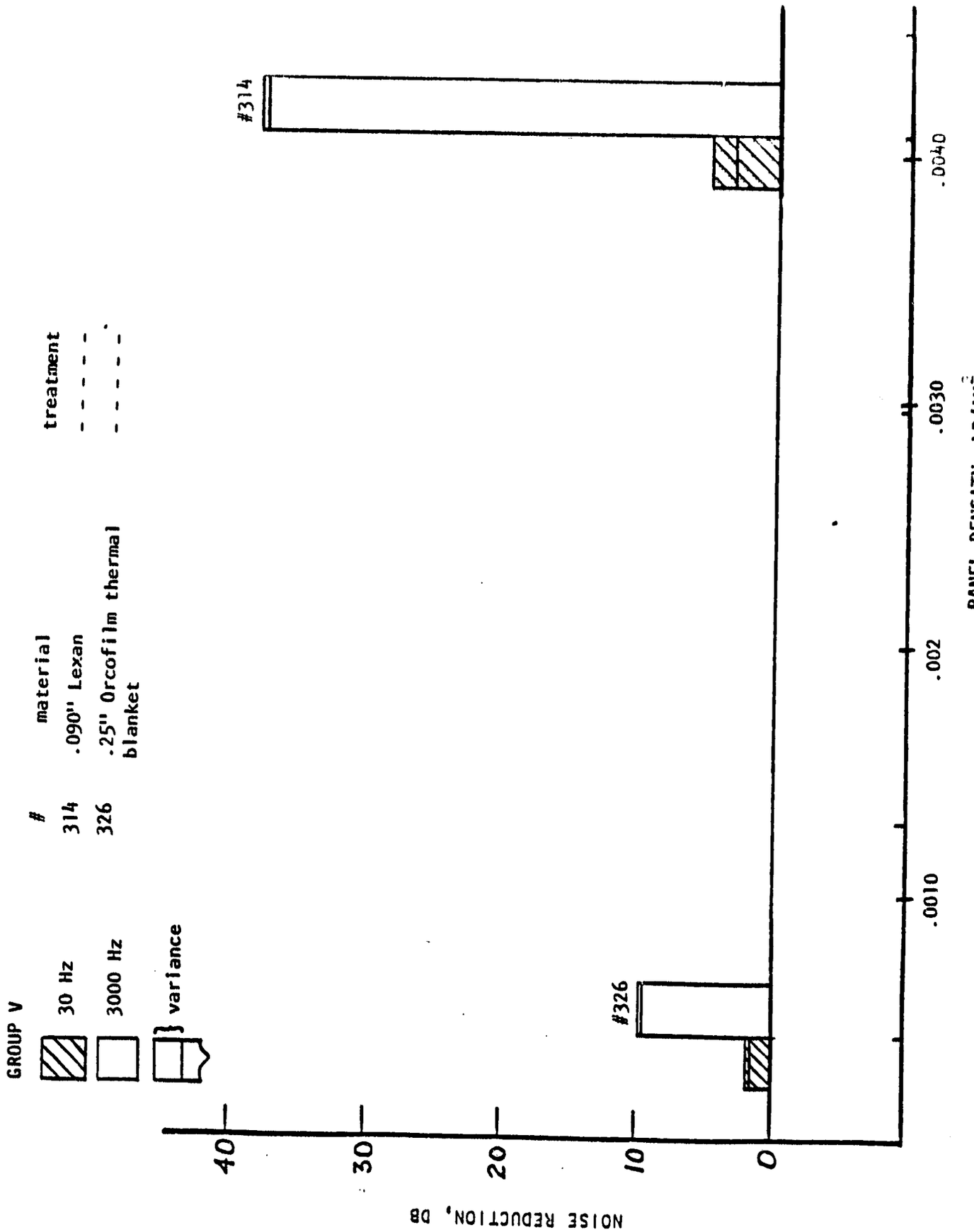

Figure 3.6 Noise Reduction Characteristics of Interior Panel Configurations, Group V

material. Bonding a standard aluminum panel with another sheet with two or four rectangular cutouts increased noise reduction at low and high frequencies. The relatively stiffer panel with four cutouts also resulted in a higher noise reduction at low frequencies.

Due to their low stiffness, the Lexan panel and the Orcofilm thermal blanket appeared to have low noise reduction characteristics in the stiffness-controlled region. The thermal blanket also had low noise reduction characteristics, at higher frequencies.

3.4 CONCLUSIONS

A large number of panels have been tested to study the noise reduction characteristics of various types of materials and treatments for possible use in internal panel configurations. Also some panels composed of aluminum sheets have been included in this test series.

The most effective panels in relation to their noise reduction characteristics were the sandwich panels composed of a foam core and a fiberglass or phenolic type skin material. Doubling the core thickness amounted to a larger gain in noise reduction in the stiffness-controlled region than the gain due to doubling the skin thickness. Treating the panel with Royalite, carpet, or a combination of foam and leather/woolen covering did not noticeably affect low frequency noise reduction characteristics but had a beneficial effect at higher frequencies due to the addition of mass. Comparison of the two types of core material indicated an equal or a little higher noise reduction for the sandwich panels with Klege-Cell as core material than the panels with a Rohacell core.

Perforated aluminum panels have, as expected, minimal sound attenuation characteristics. When they are treated with a foam and leather covering or with carpet, the overall level of noise reduction is raised--in particular in the mass-controlled region.

Covering a standard aluminum panel with a damping material resulted in a noise reduction gain at high frequencies, but the constraining damping layer did not increase noise reduction in the stiffness-controlled region compared to the panel with sound absorbing

CHAPTER 4

THE TUNED DAMPER CONCEPT

4.1 INTRODUCTION

Sound-transmission characteristics of structures are determined by three structural properties, namely: mass, stiffness, and damping. Damping is defined as the conversion of ordered mechanical energy in a structure into thermal energy. Increasing the panel damping will primarily (1) reduce the vibration amplitudes at resonances with attendant reductions in stresses and sound radiation, (2) lead to a more rapid decay of free vibrations and to corresponding reductions of noise generated by repetitive impacts at the panel, (3) increase sound isolation of the panel above its critical frequency, and (4) reduce transmission of vibrational energy (Reference 8). The most widely used way to increase the damping of a panel consists of covering the entire backside with a constrained viscoelastic layer. Unfortunately, highly damped panels usually involve penalties of weight accordingly. Little attention, however, has been paid to partial application of damping material or the use of dynamic absorption as a way to increase the damping properties of the panel (Reference 8). This chapter deals with the application of a viscoelastic, tuned damper to an aircraft panel. This particular damper consists of a mass attached to the panel by a viscoelastic link. The properties of this damper represented by the spring stiffness constant and a damping ratio have been chosen to optimize the damping at the frequency of the panel corresponding to the place of maximum vibration.

A theoretical method of predicting optimum damper properties is given and compared to experimental results.

4.2 THEORETICAL ANALYSIS

4.2.1 INTRODUCTION

The damper-panel system can be modeled as shown in Figure 4.1. The system consists of an effective vibrating panel area with mass M' and complex equivalent panel stiffness E_1^*, and a viscoelastic damper with stiffness $E_{2\omega}^*$ and mass M2. The complex stiffness E* is defined as $E(1 + j\delta_E)$, where E is the Young's Modulus of the material and δ_E is the damping ratio of the material. δ_E is also called the damping or loss factor. In the case of a viscoelastic material, $E_{2\omega}^*$ and the damping ratio $\delta_{2E\omega}$ are dependent on the frequency as indicated by the subscript ω. This frequency dependence is the reason that this system cannot be treated as a simple spring-mass-damper system. In the following analysis, the damping ratio of the panel itself is assumed to be negligible (about 10^{-4} for aluminum, Reference 10).

Transmissibility, T, is used as a measure of the damper effectiveness. Transmissibility is defined as the magnitude of the displacement ratio $\hat{X}_2/\hat{X}_1$ and can be expressed in general form as (Reference 9):

$$T = \left|\frac{\hat{X}_2}{\hat{X}_1}\right| = \left(\frac{R_N^2 + I_N^2}{R_D^2 + I_D^2}\right)^{1/2} \qquad (4.1)$$

where:

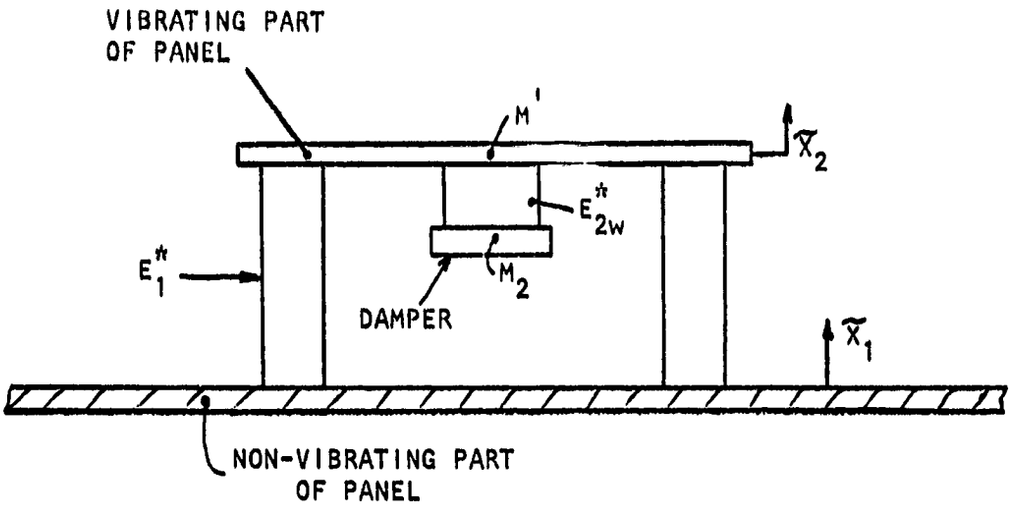

Figure 4.1 Idealized Picture of a Dynamic Absorber

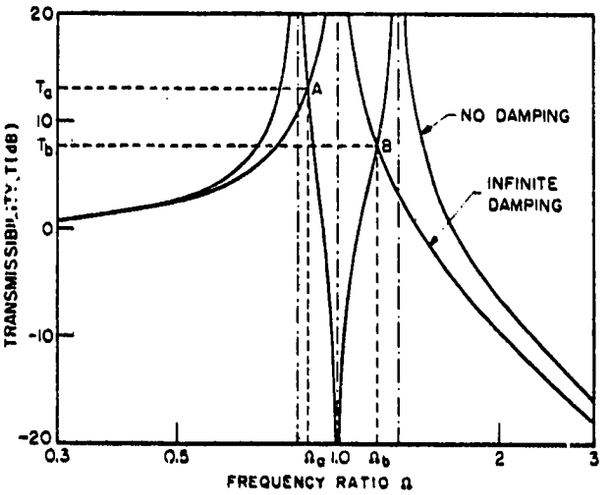

Figure 4.2 Transmissibility of a Dynamic Absorber with Zero and Infinite Absorber Damping, Reference 9

$$R_N = [-\Omega^2(E_{2a}/E_{2\omega}) + n^2] \tag{4.2}$$

$$I_N = n^2\delta_{2E\omega} \tag{4.3}$$

$$R_D = \{\mu\Omega^4(E_{2a}/E_{2\omega}) - \Omega^2[n^2 + (E_{2a}/E_{2\omega})] + n^2\} \tag{4.4}$$

$$I_D = n^2\delta_{2E\omega}(1 - \Omega^2) \tag{4.5}$$

$\delta_{2E\omega}$ = damping ratio of damper at angular frequency ω

$\Omega = \frac{\omega}{\omega_o}$ = ratio of input frequency to system natural frequency

$\omega_o = (\frac{k_1 E_{1o}}{M'+M2})$ = system natural frequency, where E is the modulus value at that frequency

$n = \frac{\omega_a}{\omega_o}$ = ratio of damper natural frequency to system natural frequency

$\omega_a = (\frac{k_2 E_{2a}}{M2})$ = damper natural frequency

$\mu = \frac{M'}{M' + M2}$ = damper mass ratio

k_1, k_2 = constants used to convert the elastic link modulus to an equivalent spring constant for panel and damper, respectively (Reference 11)

The choice of suitable values for ω_a--and therefore for n--and for $\delta_{2E\omega}$ is an important factor in achieving optimum damper performance.

4.2.2 DETERMINATION OF OPTIMUM TUNING AND DAMPING

Expressions for optimum damper tuning and damping may be obtained in closed form from the simplified equation derived from general transmissibility equations (4.1) - (4.5):

$$T^2 = \frac{(-\Omega^2\alpha + n^2)^2 + (n^2\delta_{2E\omega})^2}{\{[\mu\Omega^4\alpha - \Omega^2(\alpha + n^2) + n^2]^2 + (n^2\delta_{2E\omega})^2(1 - \Omega^2)^2\}} \tag{4.6}$$

where:

$$\alpha = E_{2a}/E_{2\omega}$$

When the damping ratio of the damper $\delta_{2E\omega}$ becomes infinitely large, the transmissibility equation (4.6) reduces to the transmissibility of the undamped simple system:

$$T = \pm \frac{1}{1 - \Omega^2} \tag{4.7}$$

When $\delta_{2E\omega}$ is zero, the transmissibility equation simplifies to the form:

$$T = \frac{\pm(-\Omega^2\alpha + n^2)}{[\mu\Omega^4\alpha - \Omega^2(\alpha + n^2) + n^2]} \tag{4.8}$$

These expressions for T vary with the frequency ratio Ω in the manner shown in Figure 4.2. The two curves intersect at values of the frequency ratio equal to Ω_A and Ω_B. The transmissibility of the undamped absorber has a minimum value at the frequency to which the damper is tuned ($\alpha = 1$, and $n = \omega_a/\omega_o = 1$). "Compensating" resonant peaks are introduced on each side of this region of attenuation or trough. For any value of the damping factor $\delta_{2E\omega}$ in the range $0 < \delta_{2E\omega} < \infty$, the transmissibility of the dynamic absorber will lie between the two curves shown in Figure 4.2 and will possess either one maximum within the frequency range Ω_A and Ω_B or two maxima outside this range. At Ω_A and Ω_B the transmissibility becomes independent of the value of $\delta_{2E\omega}$, and every transmissibility curve will pass through the so-called "fixed" points A and B. The tuned damper is

said to be most favorably tuned and damped when the two maximum values of transmissibility outside the frequency range Ω_A and Ω_B are equal, because this common value will be exceeded if the damper is tuned or damped any differently. In the classical theory it is assumed that the maximum values of T actually occur at Ω_A and Ω_B. The parameter n is then chosen in such way that T_A and T_B become equal, and $\delta_{2E\omega}$ is chosen so that the maximum of the transmissibility curve takes the values T_A and T_B. This will occur according to Equation 4.7 when:

$$\Omega_A^2 + \Omega_B^2 = 2 \tag{4.9}$$

Determination of the optimum value of $\delta_{2E\omega}$ is algebraically tedious. Snowdon (Reference 9) derives the following equations for the optimum values of n (n_o) and $\delta_{2E\omega}$, $(\delta_{2E\omega})_o$:

$$n_o = \mu\left[\frac{2(1 + \mu)}{1 + 3\mu}\right]^{1/2} \tag{4.10}$$

$$(\delta_{2E\omega})_o = \frac{N\zeta}{2\sqrt{2}}\left\{\left[1 + \left(\frac{1 + 3\mu}{2\mu}\right)\Omega_A^2\right]^{1/2} + \left[1 + \left(\frac{1 + 3\mu}{2\mu}\right)\Omega_B^2\right]^{1/2}\right\} \tag{4.11}$$

where:

$$N = \left(\frac{1 - \mu}{1 + \mu}\right)^{1/2}$$

$$\zeta = \left(\frac{10.5 - n_o^2}{10}\right)^{1/2}\left(\frac{1 - \Omega_A}{\Omega_B - 1}\right)^{1/4}$$

ζ is a correction factor used by Snowdon to achieve equal values of maximum transmissibility. In the deviation of n_o and $(\delta_{2E\omega})_o$ by Snowdon, it was assumed that the modulus $E_{2\omega}$ varies as:

$$\frac{E_{2a}}{E_{2\omega}} = \frac{\omega_a}{\omega} \tag{4.12}$$

and that the damping ratio δ_{2E} is a constant. The latter assumption of a damping ratio independent on the frequency is not exact, but it is almost true for materials with a high damping ratio in the frequency range of interest.

The values of Ω_A and Ω_B are given by Snowdon as:

$$\Omega_{A,B} = \phi \pm \psi \tag{4.13}$$

where:

$$\phi = [\frac{1 + 3\mu}{2(1+\mu)}]^{1/2}$$

$$\psi = [\frac{1 - \mu}{2(1 + \mu)}]^{1/2}$$

In summary, the optimum damping and tuning factors can be computed as follows.

For a given panel with mass ratio μ, the values of Ω_A and Ω_B may be found from Equation (4.13). The optimum tuning parameters n_o and $(\delta_{2E\omega})_o$ may be found using Equations (4.10) and (4.11), respectively. The optimum damper equivalent stiffness K2 may be found by:

$$K2 = E_{2\omega} \cdot k_2 = \omega_a^2 M2 \tag{4.14}$$

where:

$$\omega_a = n_o \omega_o$$

$$\omega_o^2 = \frac{K'}{M' + M2}$$

k_2 = equivalent damper stiffness = $(\frac{A}{L})(1 + \beta S) = \frac{K2}{E_{2\omega}}$

A, L, β, and S are derived from Reference 11 and are related to the conversion of the damper modulus to an equivalent stiffness constant. ω_o is fixed by the system. The optimum value for the damping ratio by the damper $(\delta_{2E\omega})_o$ is found by Equation (4.11).

Figure 4.3 shows the relationship between mass ratio and optimum values of damping ratio, damper stiffness and transmissibility for a 0.032" aluminum panel with the damper tuned to the fundamental resonance frequency. It can be seen that as the mass ratio decreases (i.e., the damper mass increases), the required optimum value of the damper stiffness will first reach a maximum after which it decreases. To obtain a low value in the transmissibility, a high damping factor of the damper material is desired as a low value of the mass ratio (or a high damper mass).

In practice, the damping factor of the damping material will be the limiting factor. For example, when a damper is made from Aquaplas--a damping material with a damping factor of .43 at room temperature--the corresponding optimum values of μ, K2, and T can be determined by the graphical construction shown in Figure 4.3. Values of the damping factor are temperature and frequency dependent, while damping stiffness and damper mass can be adjusted more easily.

4.2.3 DETERMINATION OF PANEL EQUIVALENT STIFFNESS AND MASS

In the last two sections, the panel equivalent stiffness, K', and panel equivalent mass, M', were mentioned; and they will now be derived. A square panel with length a, thickness h, stiffness E, and clamped edge conditions will be used. According to Reference 10, the deflection at the center of this panel due to uniform pressure P_o is:

$$d_{fix} = 0.013 \frac{P_o a^4}{Eh^3} \tag{4.15}$$

Assuming the equivalent force to be

$$F_p = P_o a^2, \tag{4.16}$$

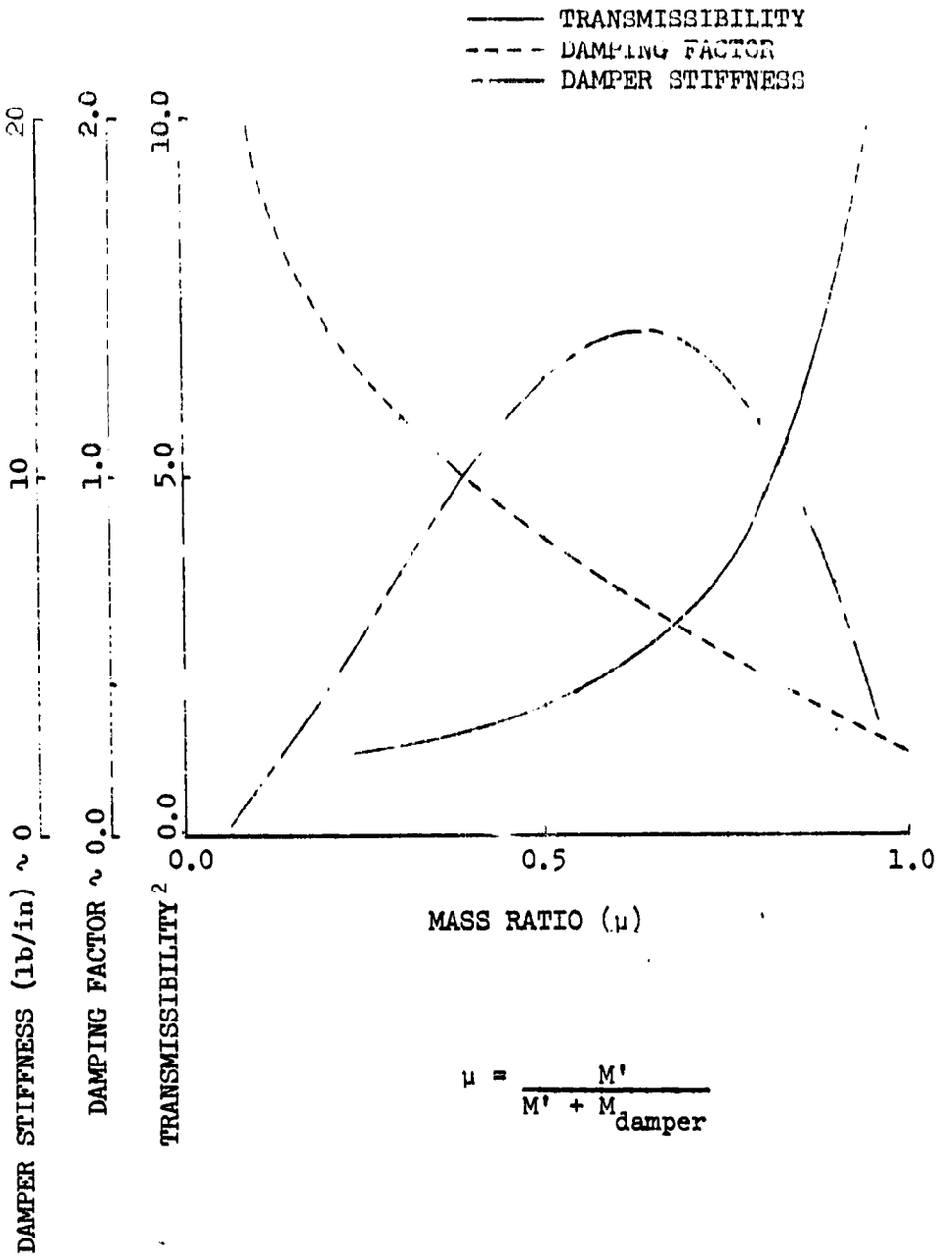

Figure 4.3 Optimum Theoretical Damping Parameters for an 18" x 18" x 0.032" Aluminum Panel

the panel equivalent stiffness may be given as

$$K' = \frac{F_p}{d_{fix}}$$

Substituting Equations (4.15) and (4.16) into the last equation, the equivalent panel stiffness is given by

$$K' = 76.9 \frac{Eh^3}{a^2} \tag{4.17}$$

The panel equivalent mass may be found by the equation for the panel natural frequency,

$$\omega_n = \left(\frac{K'}{M'}\right)^{1/2}$$

so:

$$M' = \frac{K'}{\omega_n^2} \tag{4.18}$$

The least noise reduction of the panel occurs at the first natural frequency of the panel. Therefore, the damper will be tuned to this frequency. The first natural frequency of a square panel under clamped edge conditions is given by References 7 and 10 as:

$$\omega_n = \frac{36}{a^2} \left[\frac{Eh^3}{12(1 - \nu^2)\bar{m}}\right]^{1/2} \text{ rad/s} \tag{4.19}$$

where:

$\bar{m}$ = mass of panel per unit area.

Equation (4.19) gives for an 18" x 18" x .032" aluminum panel a value of 218 rad/sec or 34.7 Hz. However, experimental tests on this panel indicated a fundamental resonance frequency of 60 Hz (see Figure 2.2). Reasons for this discrepancy are not fully known; but part of this is due to the cavity effect of the Beranek tube, which

will increase the stiffness and the fundamental resonance frequency of the panel. The experimental value of the natural frequency will be used in the calculation of the equivalent mass. Substituting Equation (4.17) and a value of 60 Hz into Equation (4.18), the equivalent panel mass is found to be

$$M' = \frac{K'}{[60(2\pi)]^{1/2}} = \frac{1}{1848}\frac{Eh^3}{a^2} \qquad (4.20)$$

4.3 DESCRIPTION OF THE TUNED DAMPER

Based on the equations derived in the first part of this chapter, optimum values for the damper's stiffnes, damping factor, and mass ratio were determined, as well as the corresponding value of the transmissibility. The designed damper was tuned to increase the noise reduction at the fundamental resonance frequency of a .032" aluminum panel (18" x 18" exposed area). Figure 4.3 showed these values as functions of the applied mass ratio. Table 4.1 presents numerical values for the computed values of the important tuning factors.

Optimum values for the damping factor as function of the applied mass ratio are given in Table 4.1. For viscoelastic materials these damping factors are relatively high. Only two materials have been found commercially available with damping factors this high. These materials are LD-400, manufactured by Lord Corporation, and Aquaplas, manufactured by H. L. Blachford Corporation. The properties of these two materials are shown in Figures 4.4 and 4.5. These figures show that the properties of these materials vary drastically with temperature. The temperatures at which the damper will be tested

TABLE 4.1 OPTIMUM TUNING PARAMETERS
FOR A .032" ALUMINUM PANEL

Panel mass (exposed area) = 1.04 lb

Equivalent mass, M' = .23 lb

Equivalent stiffness, K' = 84.7 lb/in

Ratio μ	Damper Mass (lb)	Spring Constant K2 (lb/in)	Damping Factor $\delta_{2E\omega}$	Transmissibility T
.9	.025	7.04	.289	3.124
.8	.057	11.48	.447	2.183
.7	.098	13.65	.562	1.763
.6	.150	13.92	.691	1.512
.5	.230	12.7	.826	1.342
.4	.340	10.33	.978	1.219

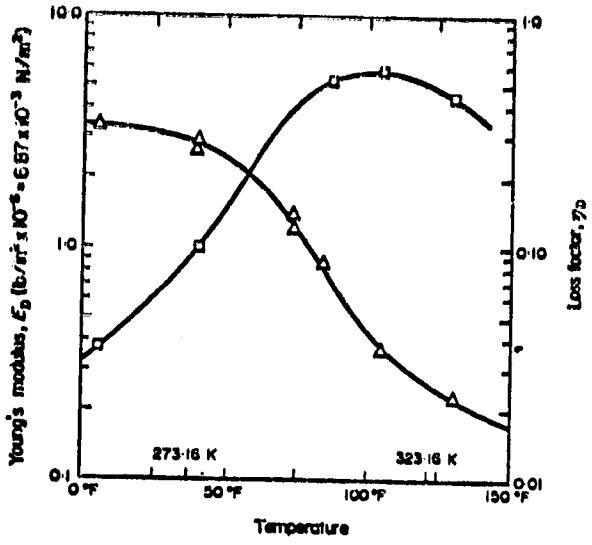

Figure 4.4 Young's Modulus (Δ-Δ) and Loss Factor (□-□) vs Temperature for "Aquaplas" (Reference 2)

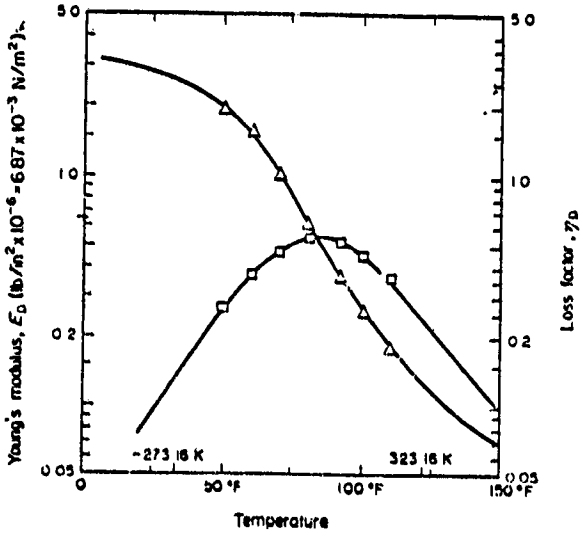

Figure 4.5 Young's Modulus (Δ-Δ) and Loss Factor (□-□) vs Temperature for "LD-400" (Reference 2)

range from 70 to 80°F. The frequencies on which the data from Figures 4.4 and 4.5 are based are approximately the same for the range of frequencies of interest.

When the optimum stiffness values, K2 = $k_2 E_{2\omega}$, from Table 4.1, are converted to any conventional solid (block) damper type, the required optimum damper modulus is far below that of any visco-elastic damping material available. To obtain the required stiffness, a ring damper of the type shown in Figure 4.6 will be used. By varying the diameter and the thickness, the required stiffness can be obtained. From Reference 2 the spring stiffness of a ring damper is given as:

$$K2 = 6.58 \frac{EI}{R^3} \tag{4.21}$$

where:

E = $E_{2\omega}$ = stiffness modulus of the damper material

I = cross section area moment of inertia

R = ring radius

The ring damper arrangement shown in Figure 4.6 consists of a cylindrical strip of damping material, mass, and two nylon screws and nuts. Because of the flexibility of the ring damper, a string was used to help support the damper mass. The arrangement used is obviously not very practical for commercial applications, but it does allow obtaining the required damping properties and testing the concept of the tuned damper. To verify that the string did not affect noticeably the experimental results, a special frame was used to clamp the panel to the speaker wall, allowing observation

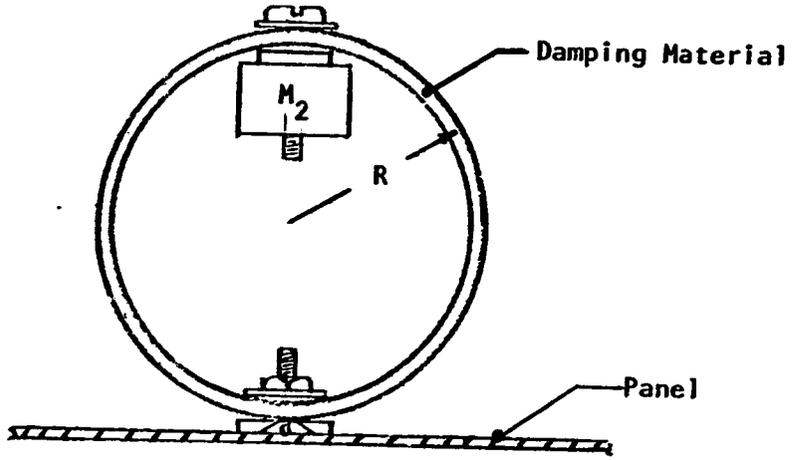

SECTION A-A

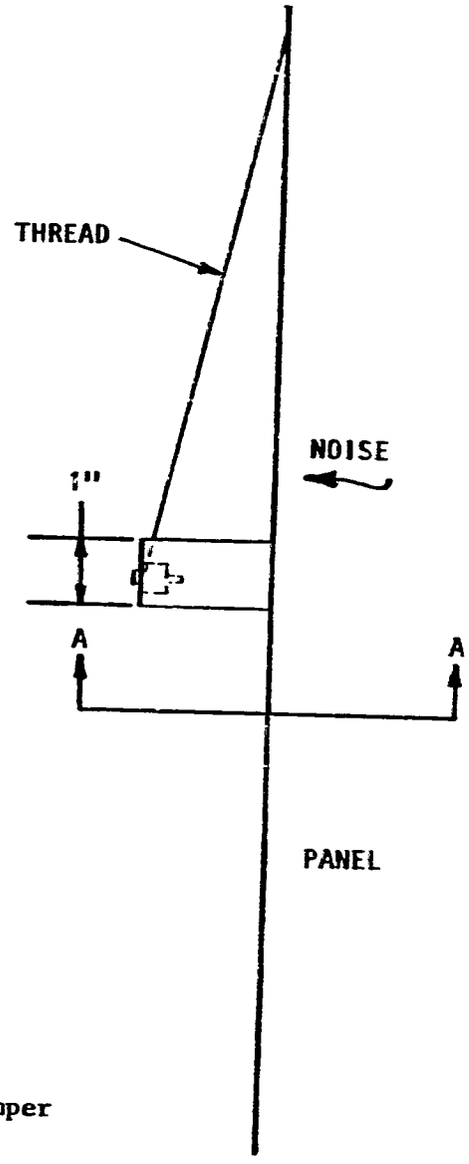

Figure 4.6 Schematic View of Tuned Damper

observation of the damper during the preliminary tests. Tests did not indicate a noticeable difference in vibration behavior. Nylon screws and nuts were used to connect the damper mass, M2, to the damper, as well as the damper to the panel. The screw used for the attachment of the damper to the panel was bonded to the panel and secured at the base by an aluminum washer to cover the head of the screw. Lead and steel washers of different mass were used for damper mass. Damper diameters varied from 1.5 to 2.5 inches, depending on the stiffness required. The width of the entire damper was one inch.

4.4 EXPERIMENTAL RESULTS

Tests were performed on a bare .032" thick aluminum panel. Two different damping materials were used; i.e., Aquaplas and LD-400, having an approximate value of .43 and .8, respectively, for the damping factor at room temperature. The dampers were tuned to increase the noise reduction of the panel around the undamental resonance frequency. The damper was placed at the center of the panel, where the maximum displacement of the panel at the fundamental resonance frequency is expected to be. According to the theoretical analysis, optimum values for the damper stiffness and mass ratio corresponding to these damping ratios are 12.8 lb/in and .8 for the Aquaplas damper, and 13 lb/in and .5 for the LD-400 damper. Test series were carried out to check the optimum value and its sensitivity to one tuning parameter, while the other parameter was held constant. Another objective was to find out the size of possible gain in noise reduction by using a tuned damper.

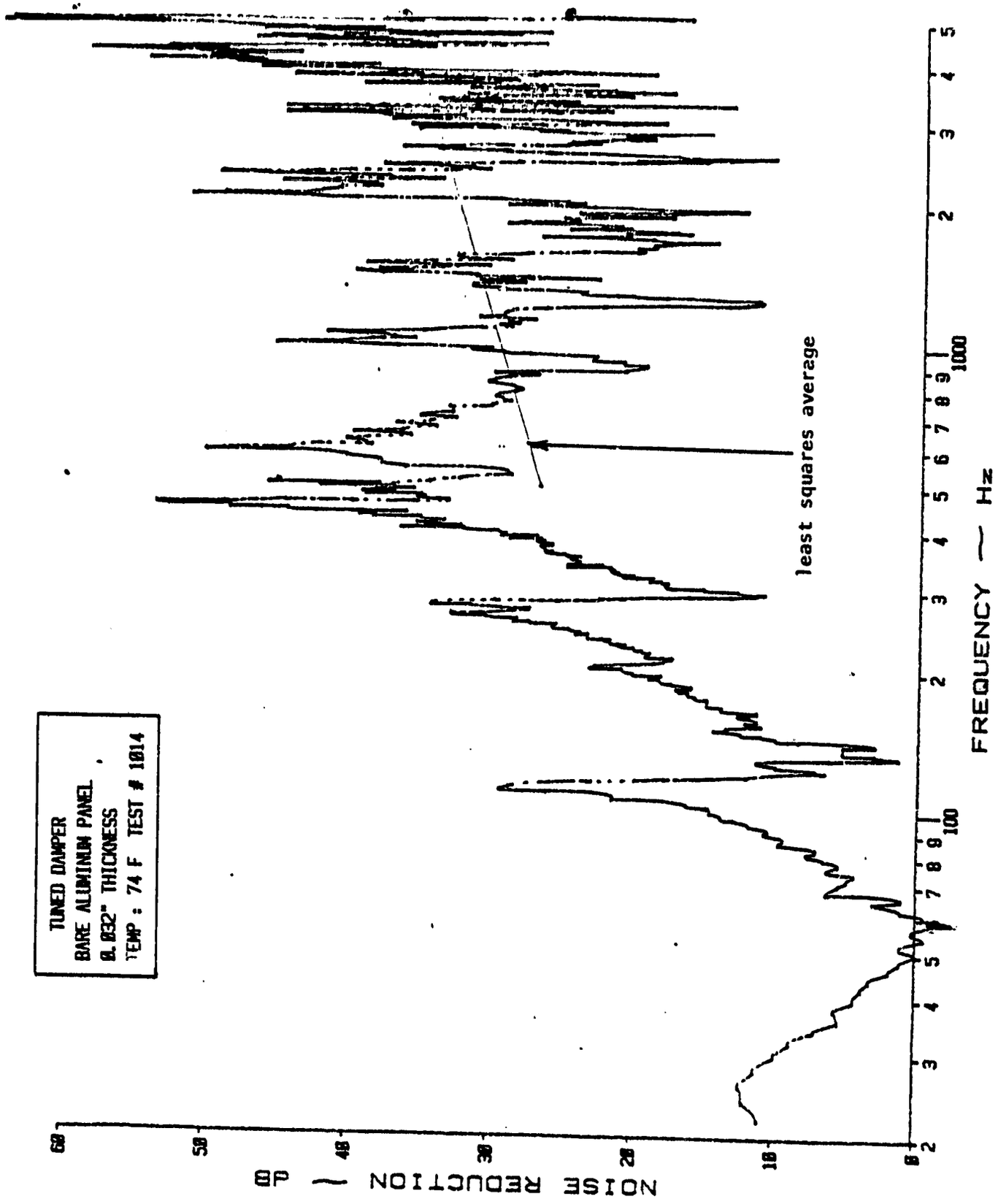

Figure 4.7 Noise Reduction Characteristics of a .032" Aluminum Panel without a Tuned Damper

Figure 4.7 shows the noise reduction as function of the frequency for the bare aluminum panel without the tuned damper. The fundamental resonance frequency is located at 58 Hz and has a noise reduction value of -3 dB. Appendix D presents the noise reduction curves for all the tests with the tuned damper. Figures 4.8 through 4.13 show the influence of a damper of LD-400, with a stiffness value of 13 lb/in, on the noise reduction characteristics of the panel for various values of the applied mass ratio. As might be expected, these figures indicate that the damper has its largest effect in the low frequency range (<150 Hz) and leave the high frequency region virtually unchanged. Therefore, measurements in the high frequency region (500-5000 Hz) were deleted in later tests.

As can be seen in Figure 4.9, application of a tuned damper with a mass ratio of .785 will dramatically change the low frequency characteristics. The first resonance frequency has decreased by 20 Hz to 38 Hz. In addition, two other resonance frequencies appeared at 65 and 95 Hz, respectively. When mass is added to the damper, i.e. mass ratio decreases, the following effects occur:

(1) The first fundamental resonance frequency shifts to a lower frequency, and the noise reduction at that frequency increases.

(2) The second dip or resonance frequency also moves to a lower frequency, but at a lower pace. The noise reduction at this frequency starts to decrease from a higher initial value than the two other minima.

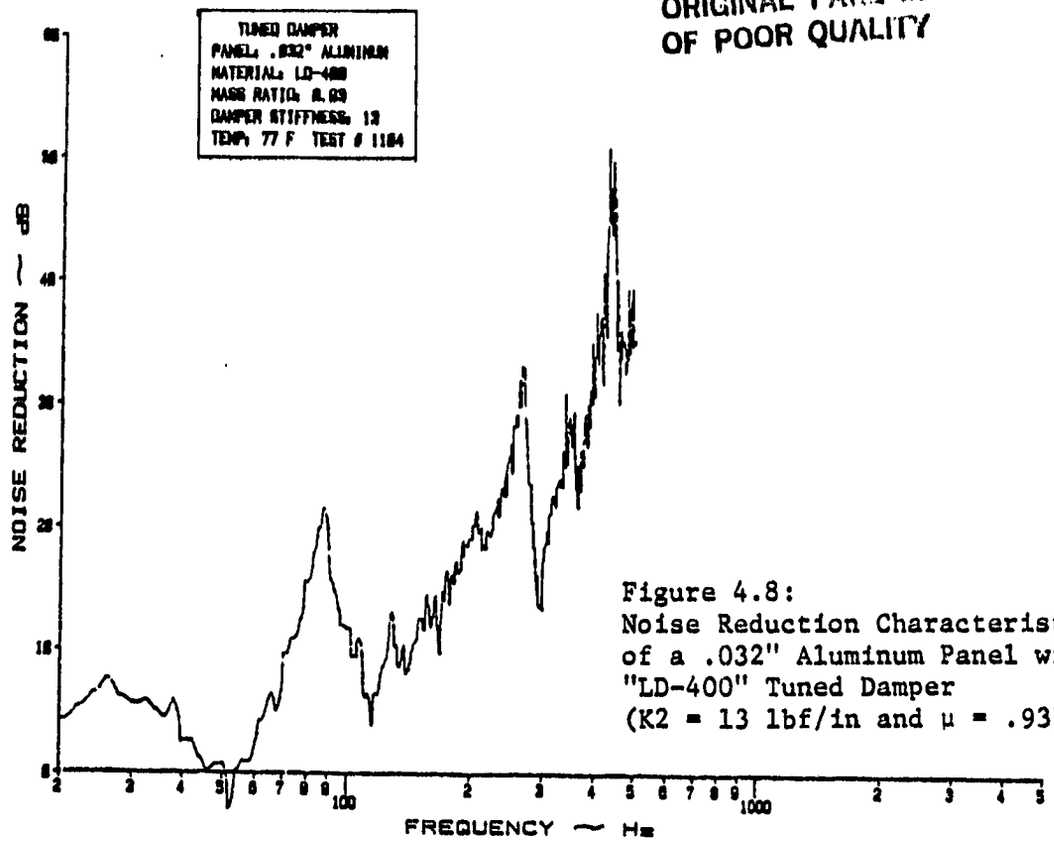

Figure 4.8:
Noise Reduction Characteristics of a .032" Aluminum Panel with an "LD-400" Tuned Damper
(K2 = 13 lbf/in and μ = .93)

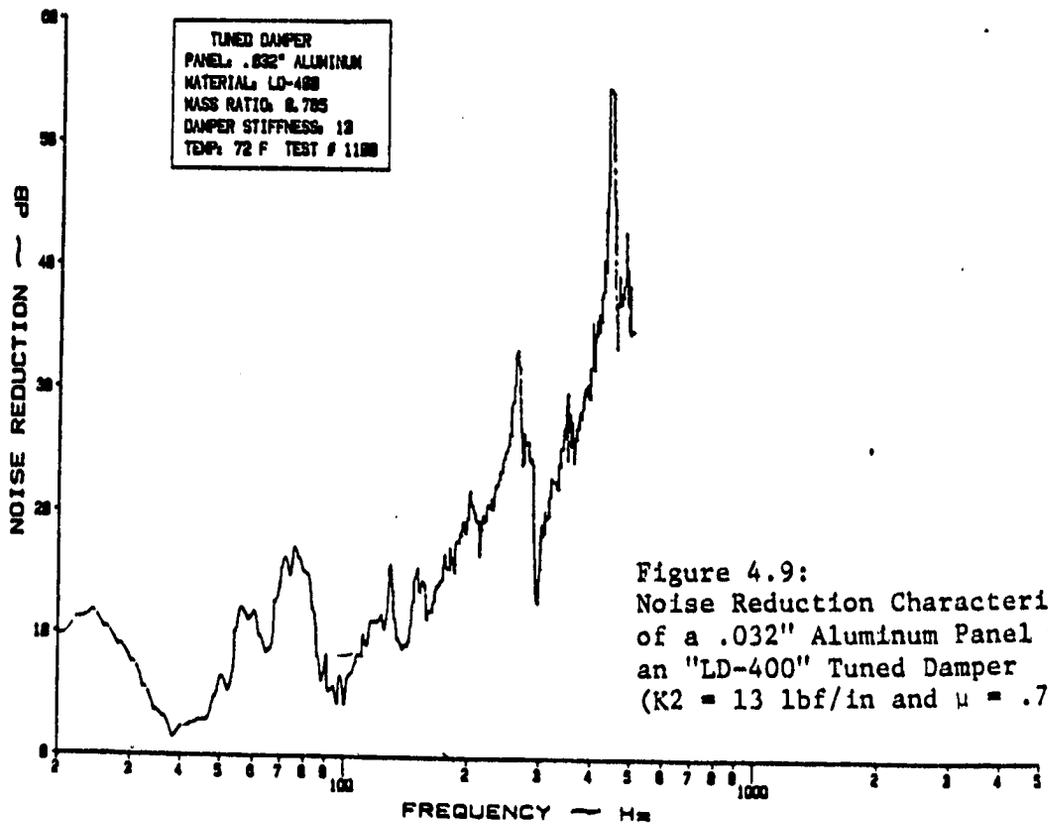

Figure 4.9:
Noise Reduction Characteristics of a .032" Aluminum Panel with an "LD-400" Tuned Damper
(K2 = 13 lbf/in and μ = .785)

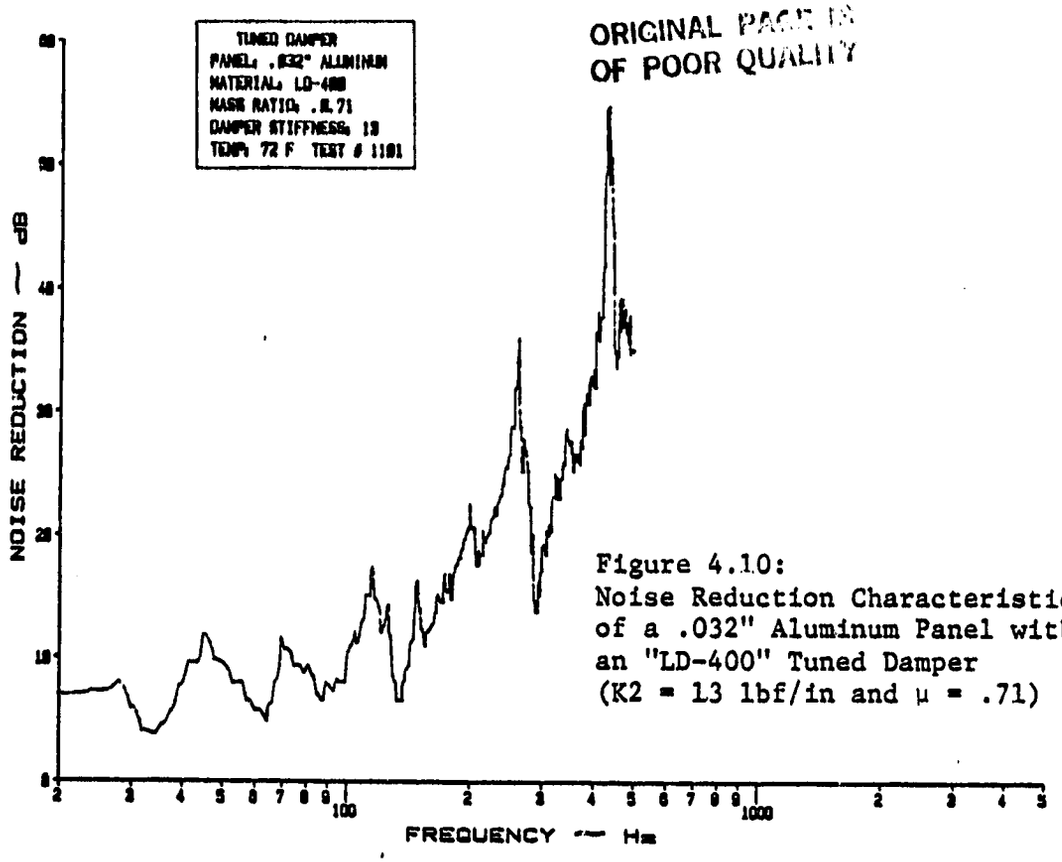

Figure 4.10:
Noise Reduction Characteristics of a .032" Aluminum Panel with an "LD-400" Tuned Damper ($K2 = 13$ lbf/in and $\mu = .71$)

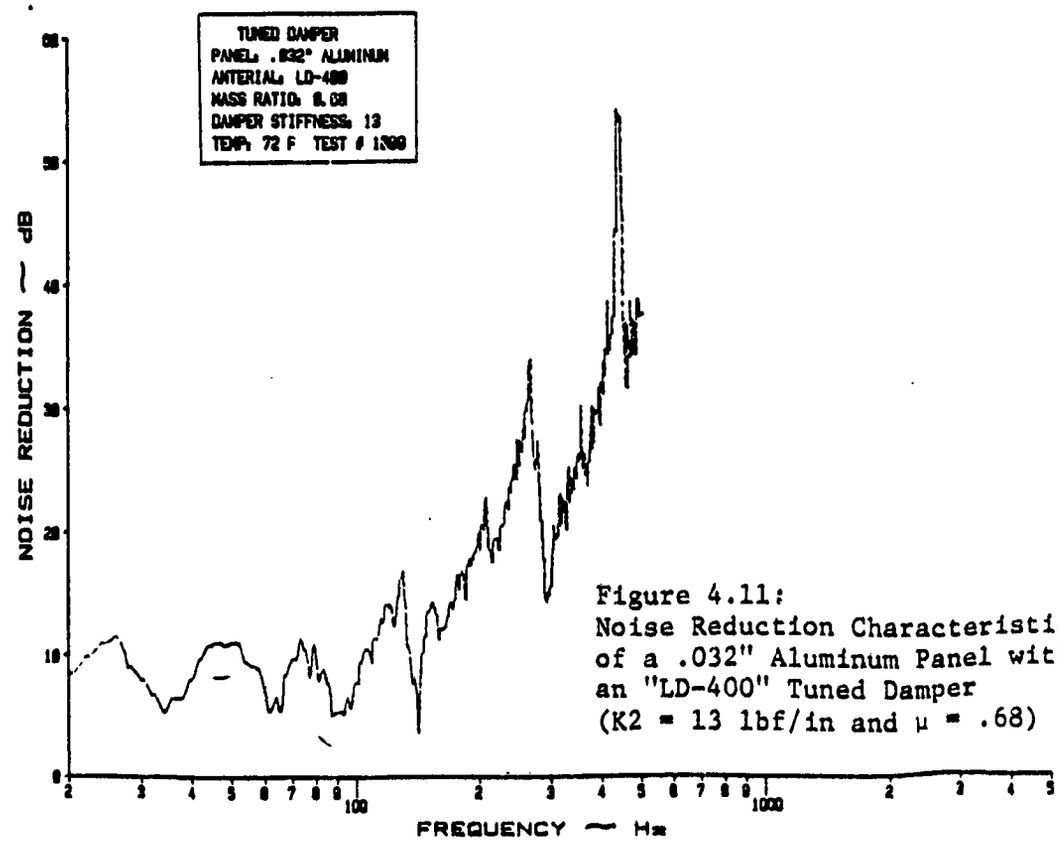

Figure 4.11:
Noise Reduction Characteristics of a .032" Aluminum Panel with an "LD-400" Tuned Damper ($K2 = 13$ lbf/in and $\mu = .68$)

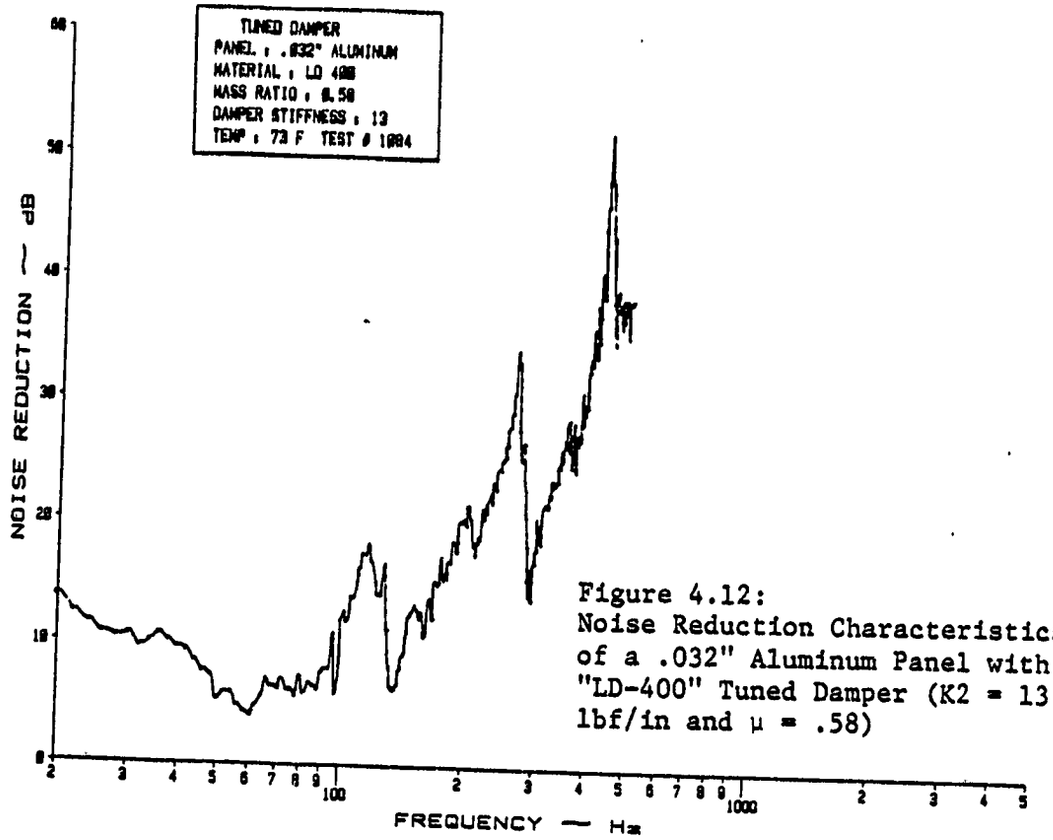

Figure 4.12:
Noise Reduction Characteristics of a .032" Aluminum Panel with an "LD-400" Tuned Damper (K2 = 13 lbf/in and μ = .58)

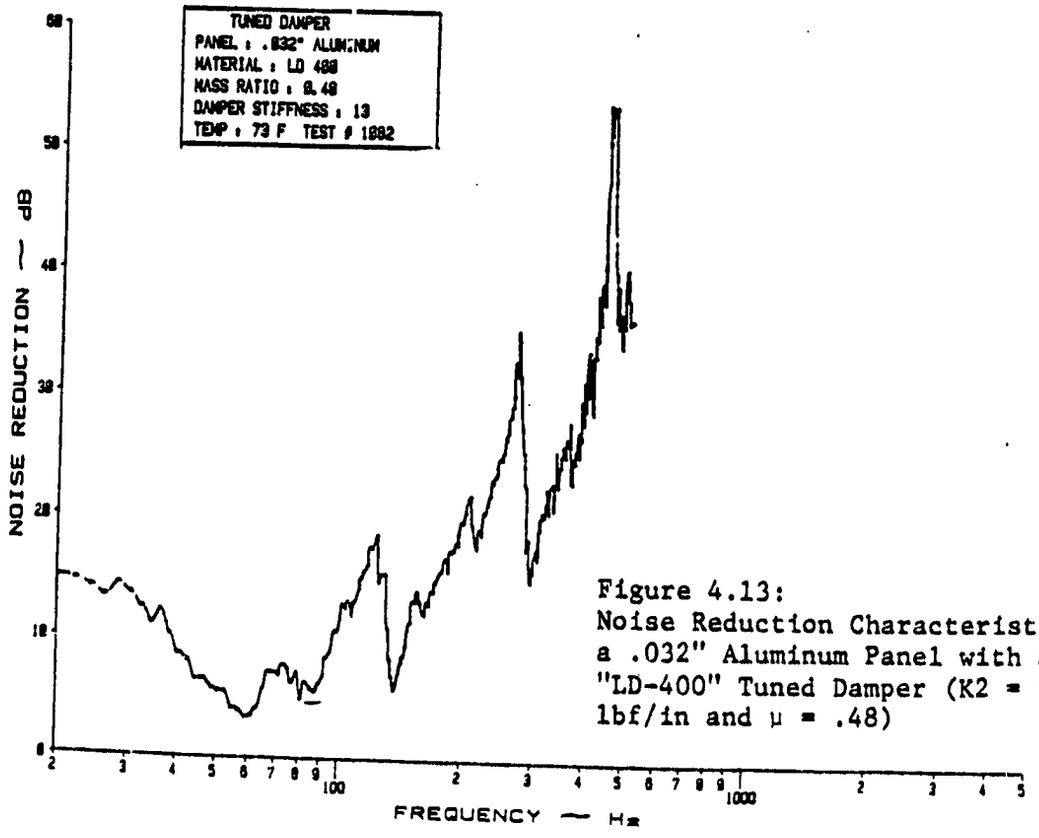

Figure 4.13:
Noise Reduction Characteristics of a .032" Aluminum Panel with an "LD-400" Tuned Damper (K2 = 13 lbf/in and μ = .48)

(3) The third resonance frequency decreases slightly when the mass ratio decreases but does not increase noticeably in noise reduction.

According to theory, optimum working of the damper will occur when the magnitudes of these resonances are equal. The influence of varying the mass ratio on the noise reduction characteristics of the panel/tuned damper combination is displayed more graphically in the upper part of Figure 4.14. Only the data points for the primary and secondary minima are given for a wide range of mass ratios. Some of the tests were repeated, and the variance between these tests was in general less than 2 dB. A value of one for the mass ratio corresponds with the bare panel without the damper. With decreasing mass ratio the noise reduction at the fundamental resonance frequency increases, while the secondary minimum decreases in value. An optimal value for μ is reached around .68 when the three minima are almost equal in value and the noise reduction over a wide range of frequencies is larger or equal to 5 dB (see also Figure 4.10). Compared to the bare panel, this is a gain of almost 8 dB over the minimum value of the original resonance frequency at 58 Hz. "Optimal" is used here in the context of a wide range of frequencies of interest. However, when the noise reduction of only a single frequency is important (e.g., the first propeller harmonic or, in this case, 58 Hz), only a slight increase in mass would be sufficient to get an increase in noise reduction at the desired frequency. It is recommended to conduct additional tests at a representative value of a first propeller harmonic to investigate this with the effects of the panel/cavity resonance frequency isolated.

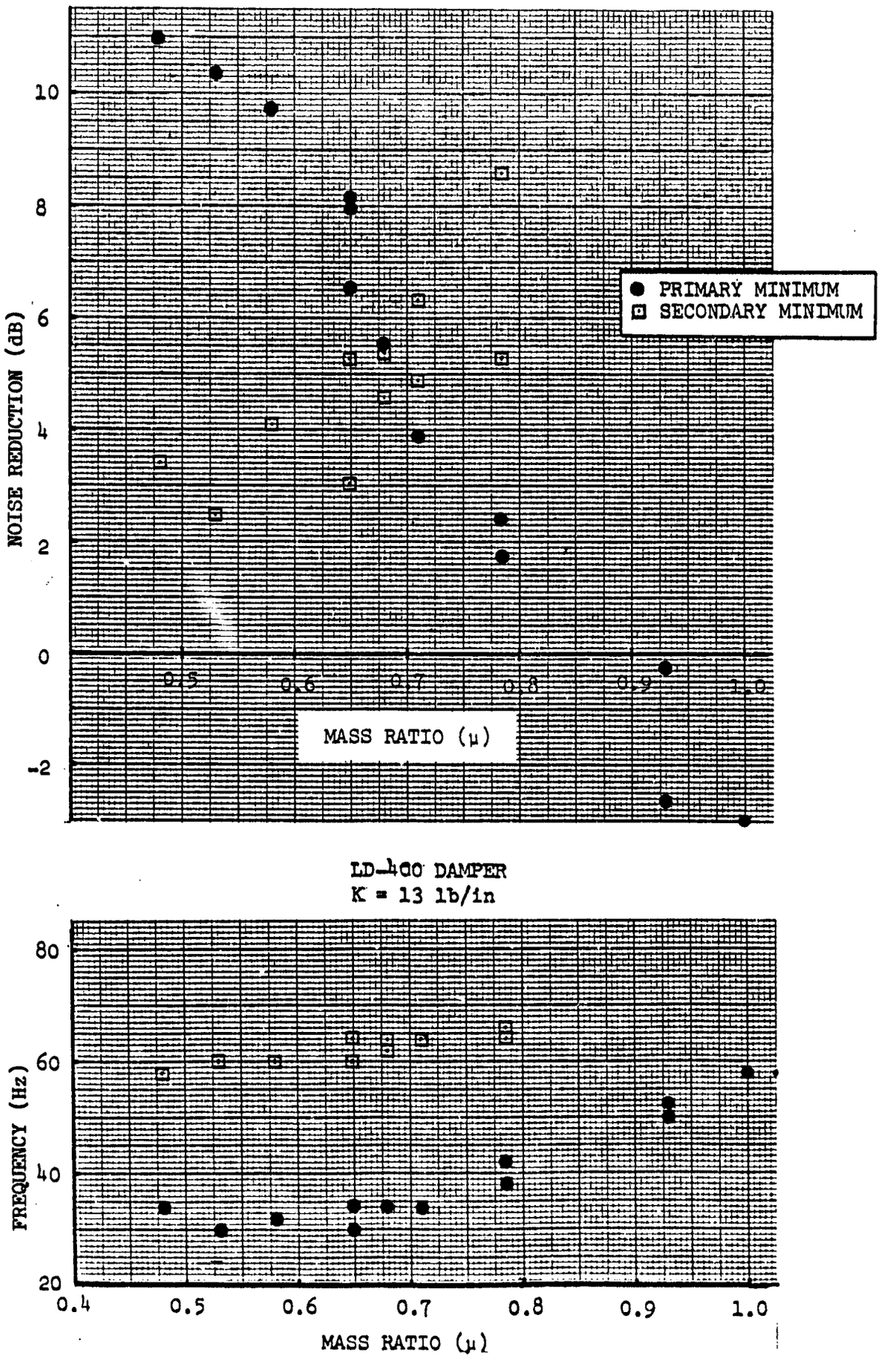

Figure 4.14 Influence of Mass Ratio on Noise Reduction Characteristics of a .032" Aluminum Panel with an "LD-400" Tuned Damper (K2 = 13 lbf/in)

It will then also be important to determine the optimum location of the damper at a tuned frequency other than the fundamental resonance frequency.

When the mass ratio decreases more, the value of the noise reduction at the first resonance increases, until it reaches a certain maximum equal at the surrounding values. The second dip at about 60 Hz decreases more in value and returns towards its original value (Figures 4-11-4.12). At these high values of the damper mass (low μ's), the effect of the bending of the mass on the effective form of the ring becomes more severe.

The lower graph of Figure 4.14 shows the influence of the applied mass ratio on the resonance frequencies. Because of the addition of mass, these frequencies decrease with decreasing mass ratio. The increase experienced in the noise reduction at the fundamental resonance frequency indicates that not the mass addition by the damper but the increased damping is the main driver behind the tuned damper concept.

Using the experimentally determined "optimum" value for the mass ratio, tests were conducted with varying values of the damper stiffness to determine the effect of the damper stiffness. Figure 4.15 presents the results of these series of tests. The damper stiffness varied between 8 through 32 lbf/in. It can be seen that over a relatively large range of K2, 13-21 lbf/in, the noise reduction values of the two resonances are within 2 dB. Below and above this range the first resonance decreases in value, while noise reduction at the second resonance around 60 Hz increases. The lower graph of

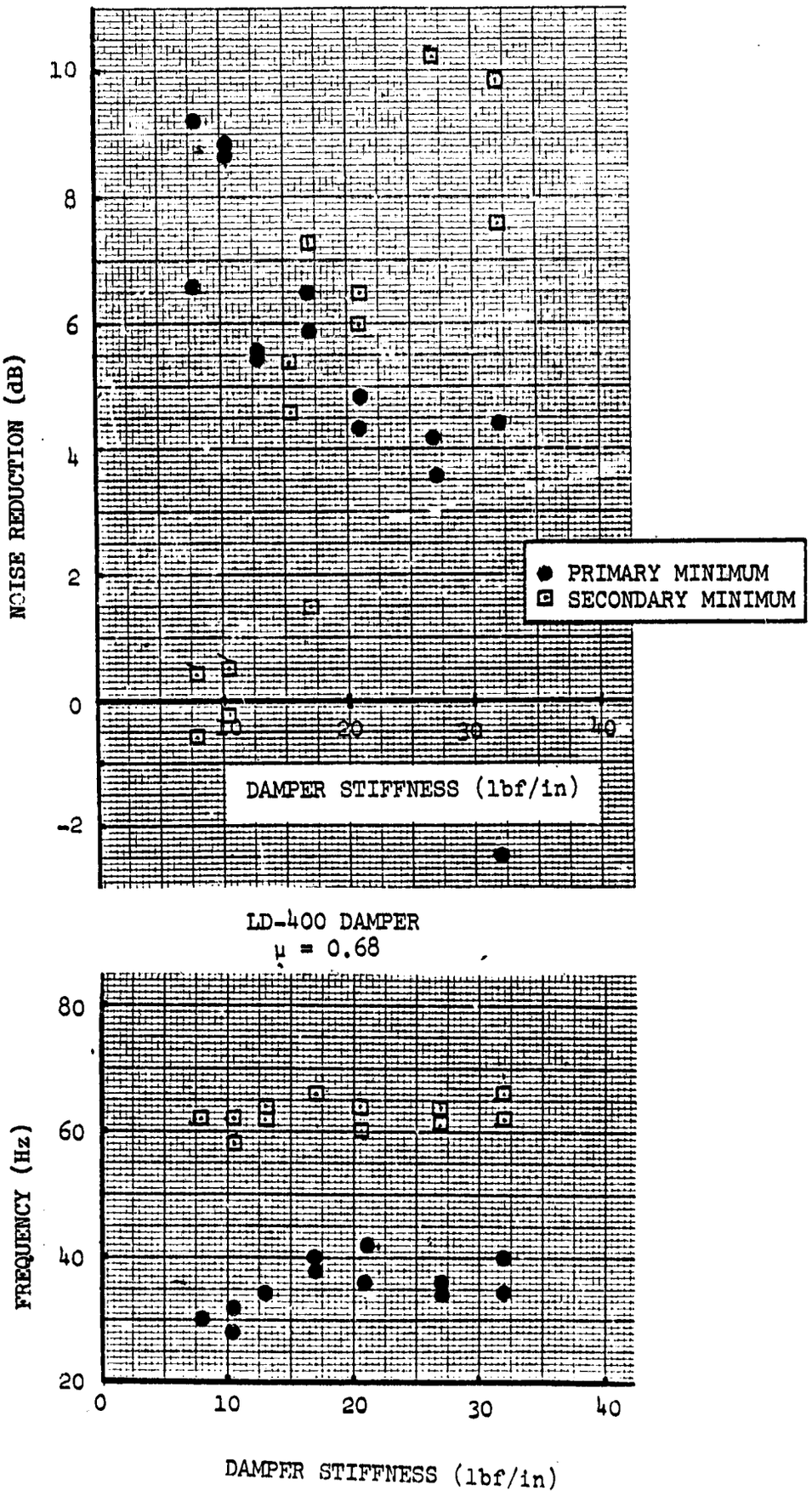

Figure 4.15 Influence of Damper Stiffness on Noise Reduction Characteristics of a .032" Aluminum Panel with an "LD-400" Tuned Damper (μ = .68)

Figure 4.14 represents the relationship of the position of both minima or resonances as function of the applied damper stiffness.

Aquaplas has, compared to LD-400, a higher E-modulus ($1.0x10^6$ vs. $.7x10^6$ at 75°F). As a result the required optimal ring diameter will be larger according to Equation 4.21 when other things are equal. A large ring diameter will, however, when combined with a large damper mass, influence detrimentally the optimum form and working of the damper due to the relatively large bending arm of the mass. A smaller ring diameter can also be obtained by a smaller inertia moment, i.e. a smaller thickness or width. Because Aquaplas is normally not available thinner than the .05" used, a ring width of .5" was used instead of the 1" used in the other tests.

In extended tests with the Aquaplas dampers, no noticeable influence of the damper was observed at the theoretical optimum value of the damper stiffness, K2 = 12.8 lbf/in; see also Figures 4.16-4.17. In particular with high damper mass values, the ring damper became noticeably deformed. When the ring damper stiffness was increased to a relatively high value, the behavior of the ring damper became more beneficial. Figure 4.18 shows this behavior of the Aquaplas damper at a value of 46 lbf/in for the stiffness as function of the applied mass ratio. The same effects which were described for the LD-400 damper were again observed with this high K2 value for the Aquaplas damper. With increasing application of damper mass, the first fundamental resonance frequency shifted to a lower frequency, and noise reduction increased. The second main minimum also shifted to a lower frequency, but the noise reduction corresponding to this resonance

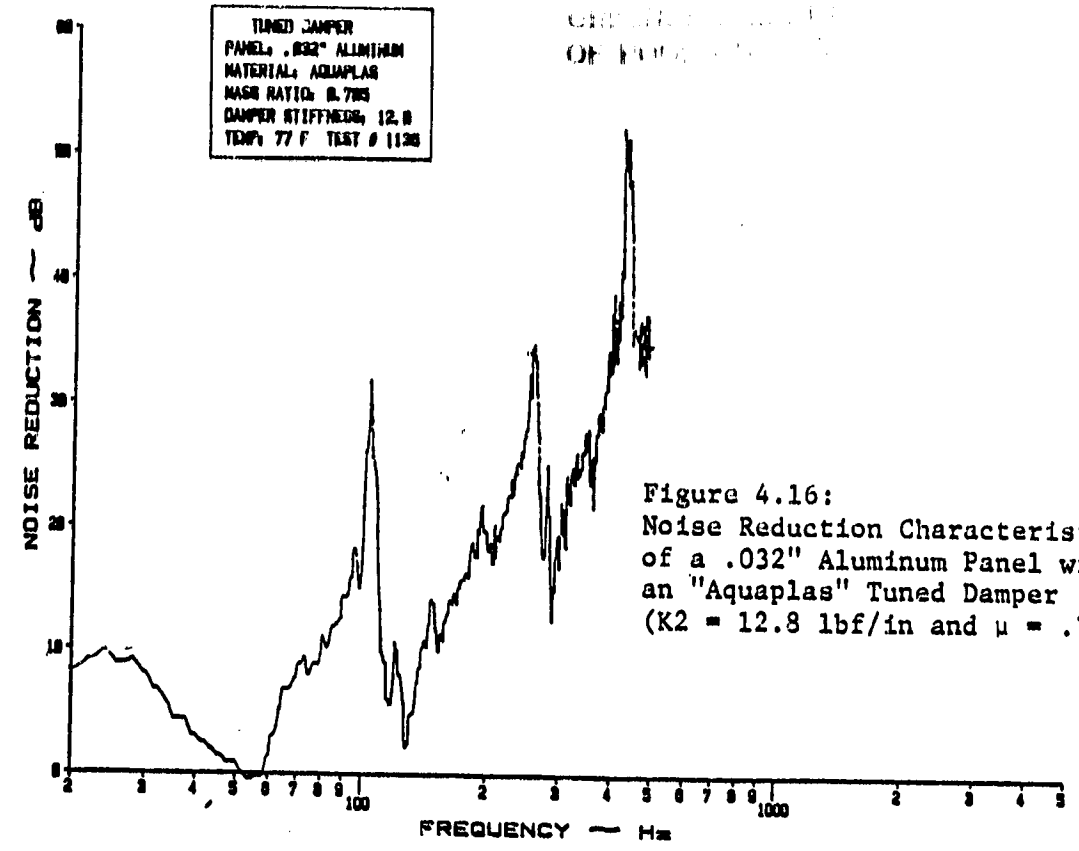

Figure 4.16:
Noise Reduction Characteristics of a .032" Aluminum Panel with an "Aquaplas" Tuned Damper (K2 = 12.8 lbf/in and μ = .785)

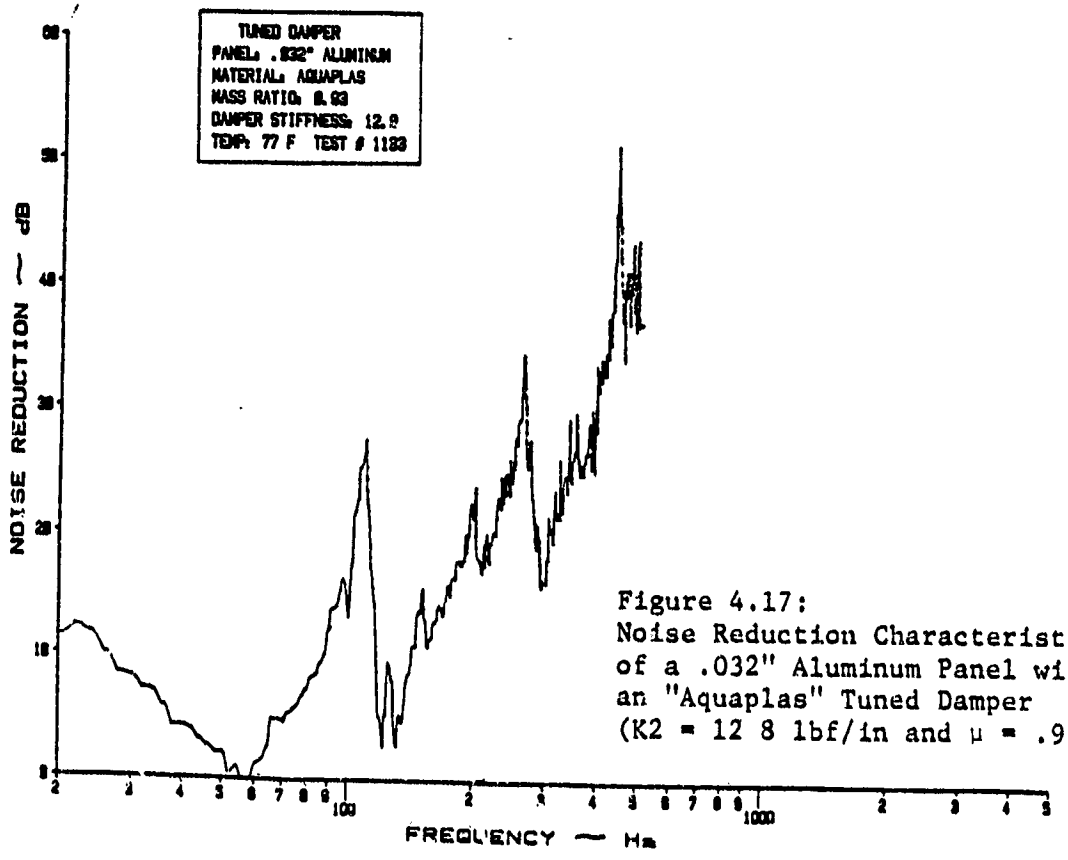

Figure 4.17:
Noise Reduction Characteristics of a .032" Aluminum Panel with an "Aquaplas" Tuned Damper (K2 = 12 8 lbf/in and μ = .93)

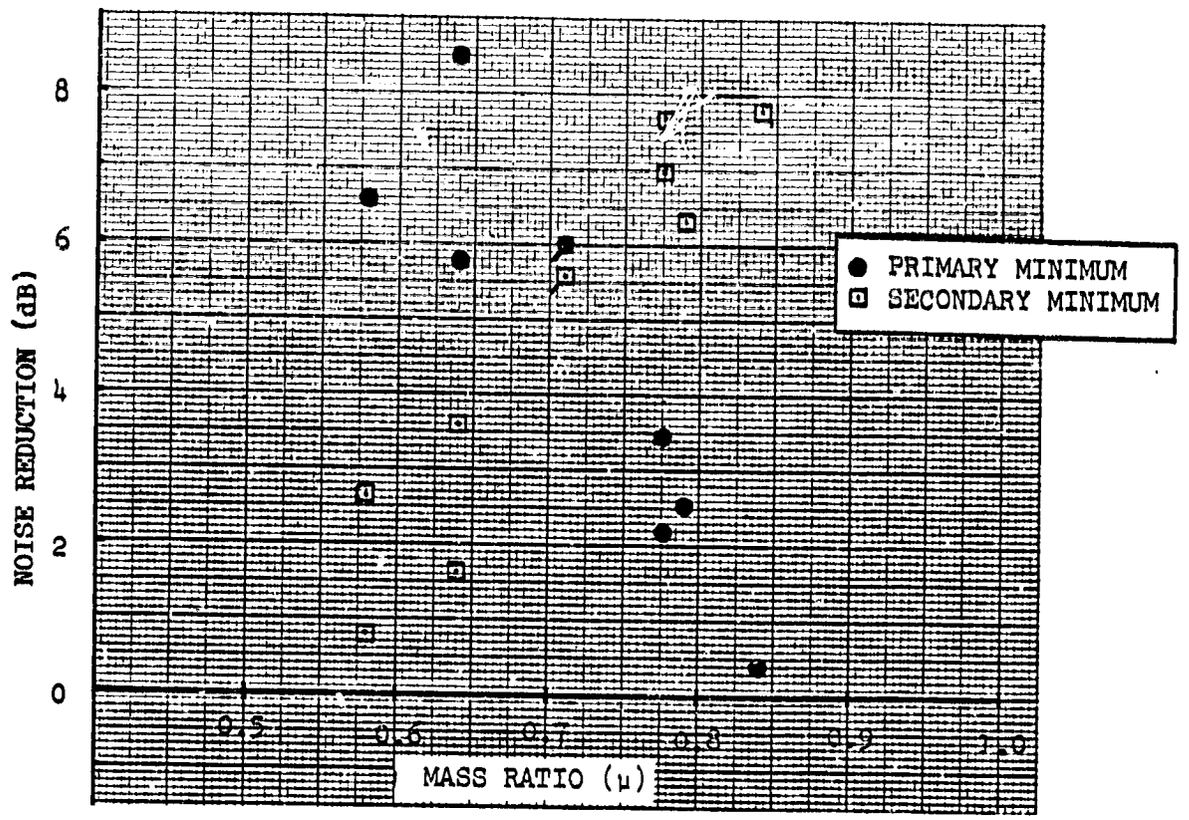

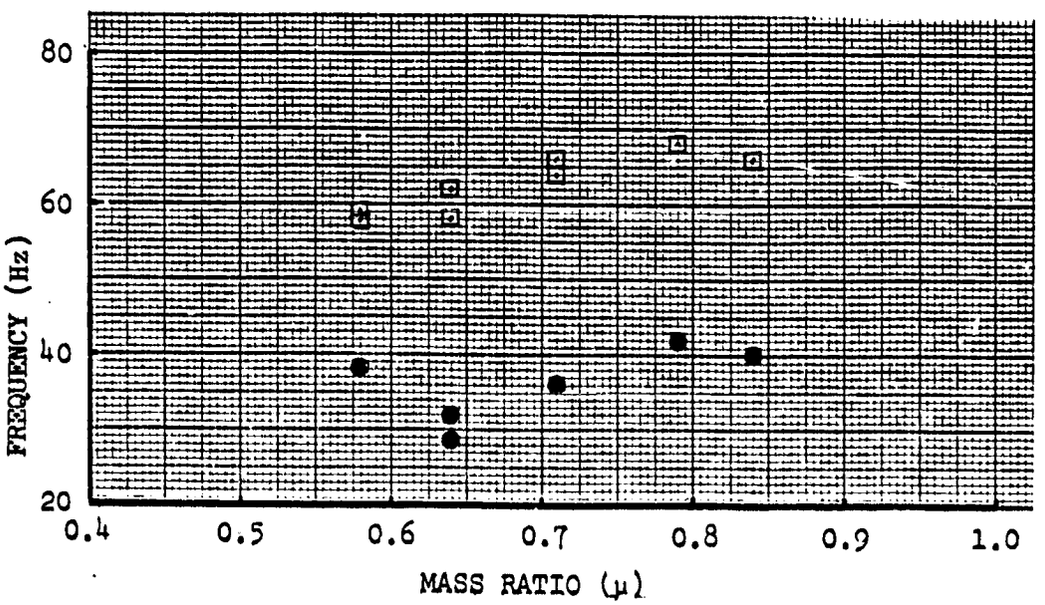

Figure 4.18 Influence of Mass Ratio on Noise Reduction Characteristics of a .032" Aluminum Panel with an "Aquaplas" Tuned Damper (K2 = 46 lbf/in)

now decreased in value. The value of the mass ratio, for which both minima have the same size, lies around .71 (& also Figure 4.19). The corresponding gain in noise reduction, compared to the bare panel, is 9 dB. The bottom graph of Figure 4.18 shows the relationship between applied mass ratio and the resonance frequencies. Figure 4.20 shows the relationship between the noise reduction at the two resonances with varying values of the applied damper stiffness, when the mass ratio is kept constant at a value of .71. This graph shows that only at relatively high damper stiffness values does noise reduction at the secondary minimum (around 58 Hz) increase in size and approach the magnitude of the primary resonance. Unlike the LD-400 dampers these results indicate no clear optimum range of values for the damper stiffness.

4.5 DISCUSSION, CONCLUSIONS AND RECOMMENDATIONS

In this chapter the application of dynamic absorber or tuned damper was investigated as a way to increase the damping properties of an aircraft panel in a certain frequency range. The scope of this investigation was limited to a standard .032" aluminum panel and to the first fundamental resonance frequency at 58 Hz. Using the theory developed by Snowdon in Reference 9 for a dynamic absorber, the parameters responsible for an optimal working of the damper were identified and computed for this panel and frequency (Figure 4.3). These parameters are the applied mass of the damper or the mass ratio, the stiffness of the damper and the damping factor of the

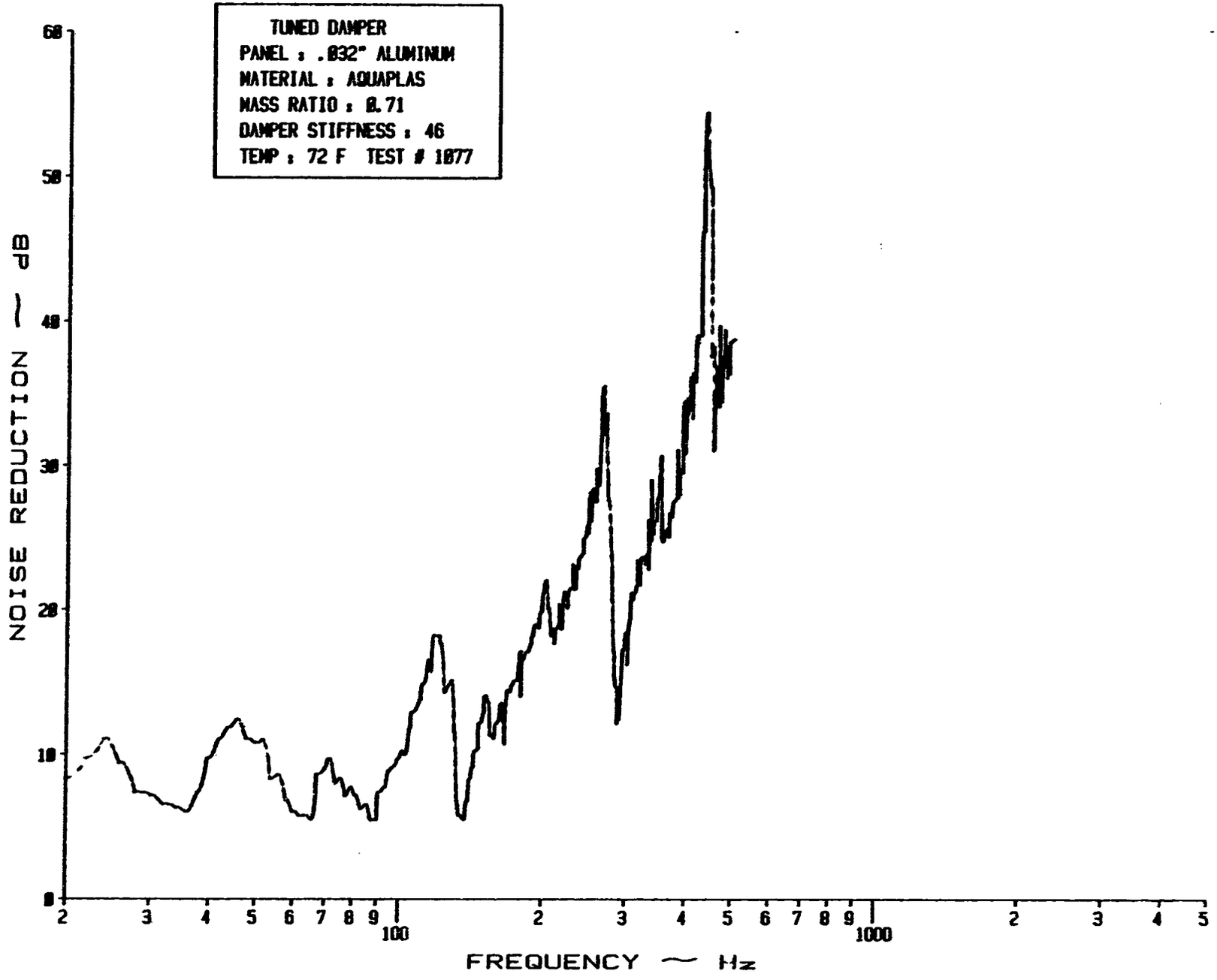

Figure 4.19 Noise Reduction Characteristics of a .032" Aluminum Panel with an "Aquaplas" Tuned Damper (K2 = 46 lbf/in and μ = .71)

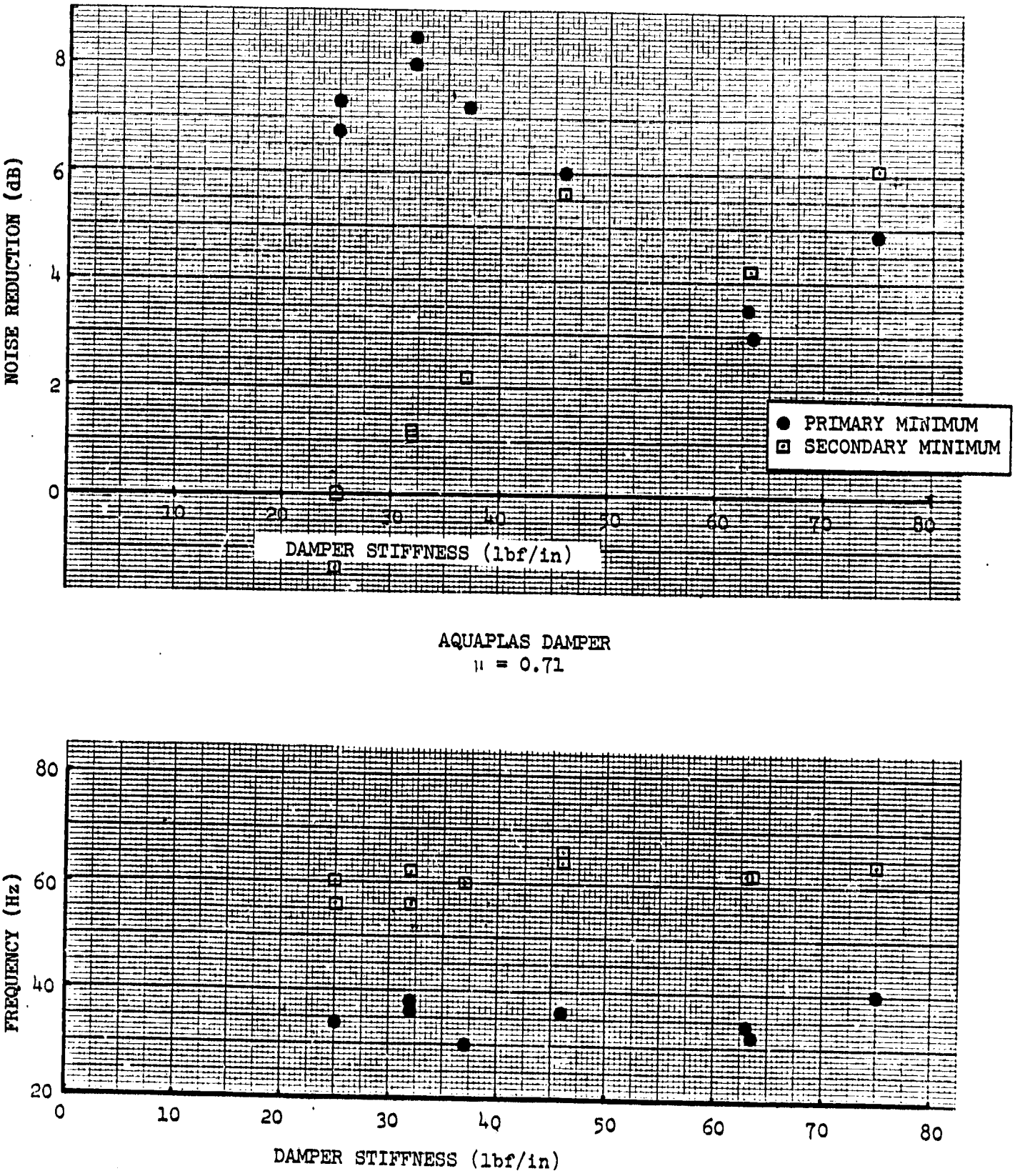

Figure 4.20 Influence of Damper Stiffness on Noise Reduction Characteristics of a .032" Aluminum Panel with an "Aquaplas" Tuned Damper (μ = .71)

damper material. No attempt was made to include the influence of the location of the damper and of higher modes.

Experimental tests were conducted to test the validity of the theory and to investigate the possible gain in noise reduction by the damper. The damper was made as a ring damper in order to achieve the required range of stiffnesses. The experiments were carried out for two different kinds of viscoelastic damping materials: LD-400 and Aquaplas.

Results of the tests with the LD-400 dampers indicated a positive influence by the damper, reflected in a shift of the fundamental resonance to a lower value and an increase of noise reduction over a wide range of frequencies due to the increase of damping. These tests confirmed the presence of two resonances, one at each side of the tuned frequency, predicted by the theory. Only one, however, was active and increased in size with decreasing damper mass applied. The other remained constant. Results indicated also that when all three resonances had equal magnitude, noise reduction was optimal over a wide range of frequencies around the tuned frequency. The corresponding value of the mass ratio (.68) did not, however, correspond with the value predicted by the theory: .5; and it was also not the optimum value of the noise reduction at 58 Hz, the original fundamental resonance frequency.

Results with the Aquaplas damper, having a lower damping factor than LD-400, did not show a beneficial effect of the damper at the predicted value of the damper stiffness. Only at much higher values of the damper stiffness did the beneficial influence appear. Again

the optimum experimental value of the mass ratio, at which according to theory the transmission T would be minimal--at equal magnitudes of the outside resonances--differed from the value of μ for which noise reduction at 58 Hz was optimal.

The large discrepancy between predicted and experimental values of the damper stiffness for the Aquaplas damper can partly be explained by the experienced behavior of these dampers at these low stiffness values--in particular, with high damper mass. Due to the larger required ring diameter, bending of the ring by the mass disturbed severely the effective form of the ring. The LD-400 dampers were smaller and thicker than the Aquaplas dampers, and less severe bending occurred. However, some tests conducted with an LD-400 damper and a stiffness of 46 lb/in did not result in an optimal noise reduction at normal values of the mass ratio.

In the theoretical analysis, average values of the damping factor and of the material stiffness were taken from Air Force and manufacturer's data at 75°F (Reference 2). Because it is not possible in the KU-FRL facility to conduct tests at other than the current room temperature, some variations in properties have occurred. During the tests, actual temperatures varied between 72 and 78 degrees Fahrenheit. The results should be judged in this context because actual temperatures in the flight condition will also be different. Figure 4.21 shows essentially the same relationship between noise reduction at the first two resonances for both kinds of dampers as do Figures 4.13 and 4.18, but now as function of the applied damper mass as well as of percentage of panel weight. "Optimum" values are, for both dampers, about 9% of the panel mass.

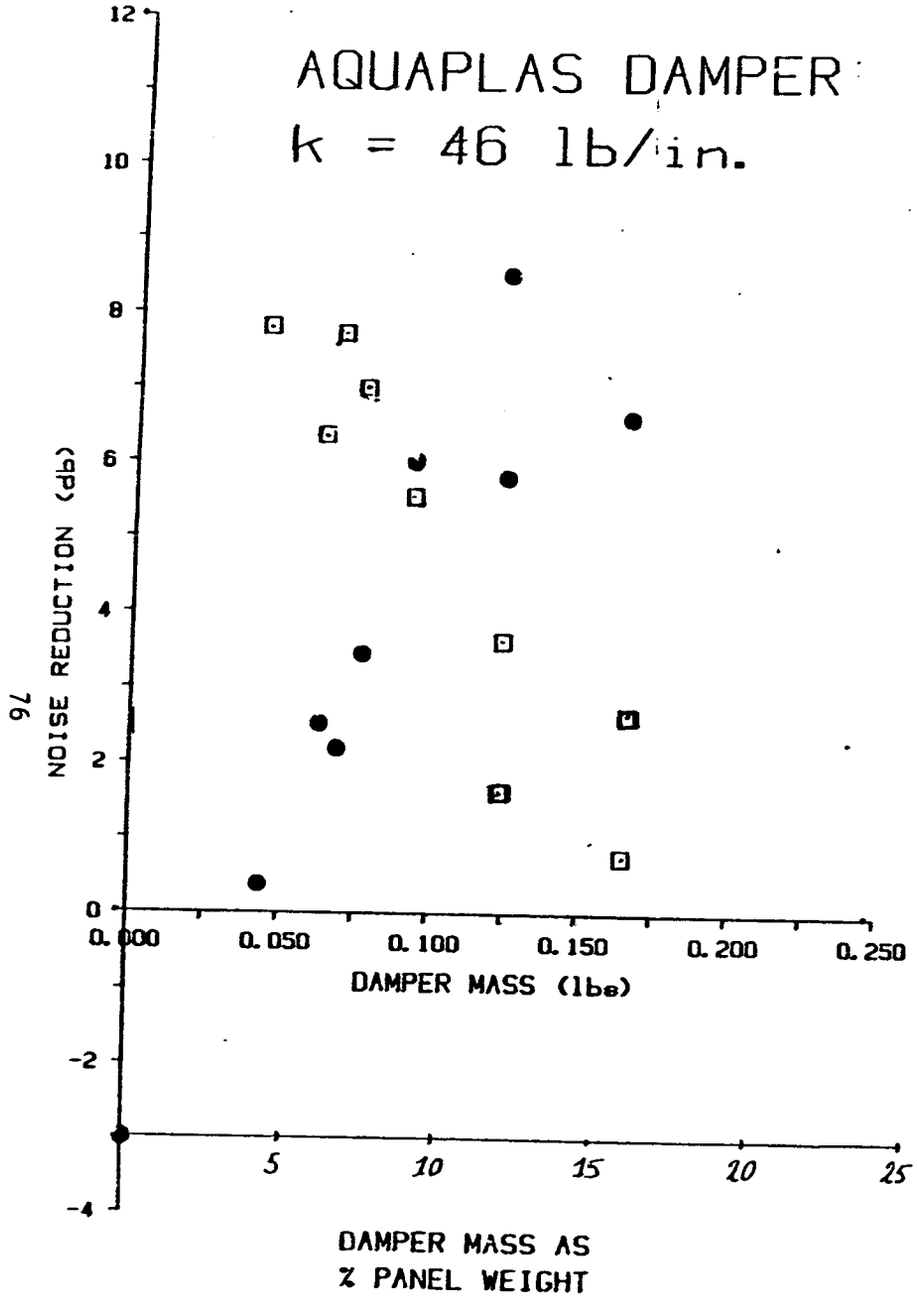

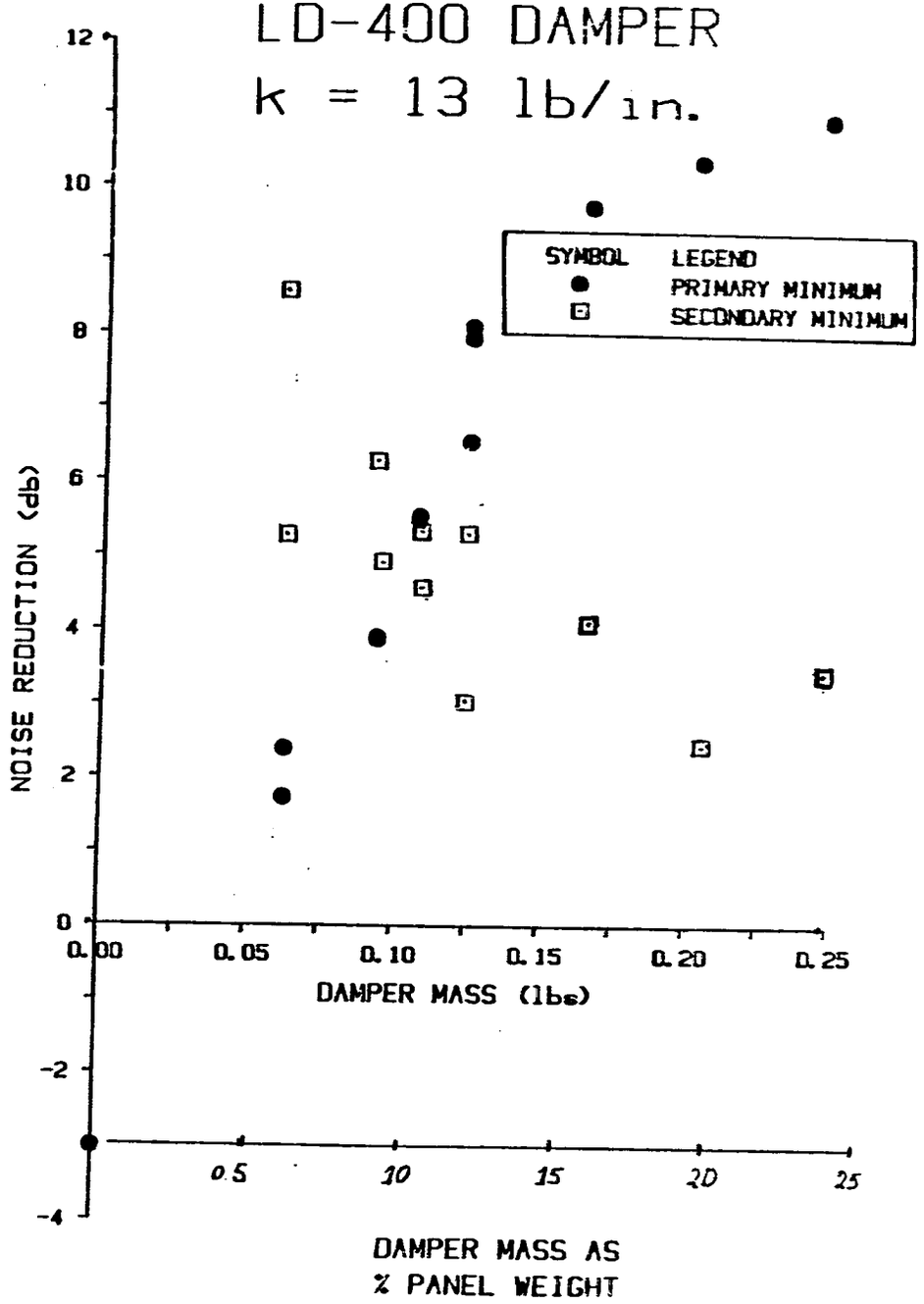

Figure 4.21 Influence of Damper Mass on Noise Reduction Characteristics of a .032" Aluminum Panel with an "Aquaplas" or "LD-400" Tuned Damper

Based on the results and the experiences during the tests, the following conclusions can be drawn:

- It is possible to increase the total damping and noise reduction of a panel over a wide range of frequencies by the use of a tuned damper.

- Dependent on the definition of optimal performan e by a tuned damper, application of a damper will increase noise reduction at the frequency of interest by at least 8 dB in the case of an LD-400 damper and 9 dB for an Aquaplas damper. When only a particular frequency is of interest, the results suggest a higher possible gain at a lower damper mass than when an increase in a wide range is desired.

- The developed theory did not clearly predict the effect of the tuning parameters on the optimal performance of a tuned ring damper.

- The ring damper itself, despite its simple form, is not very suitable for application in an aircraft environment. Bending of the ring by the damper mass will cause deformation of the effective form of the ring damper.

It is recommended that in future research, the use of other types of dampers--better suited in handling bending and creep of the material--be studied. To understand better the behavior of a tuned damper, it is also recommended to expand experimental tests with measurements of the effective damping of the panel with the help of accelerometers at the location of the damper. To study the effect of the damper at a particular frequency of interest, the

influence of higher modes and the location of the damper(s) have to be studied. The results of this limited program also indicate that more theoretical analysis is needed and that the influence of temperature and material stiffness have to be included.

REFERENCES

1. Navaneethan, R.; Streeter, B.; Koontz, S.; "Influence of Depressurization and Damping Material on the Noise Reduction Characteristics of Flat and Curved Stiffened Panels," KU-FRL-417-17, Flight Research Laboratory, University of Kansas, Lawrence, Kansas 66045, October 1981.

2. Jones, D. I. G.; Nashif, A. D.; Adkins, R. L.; "Effect of Tuned Dampers on Vibrations of Simple Structures," AIAA Journal, Vol. 5, No. 2, Feb. 1967, pp. 310-315.

3. Jones, D. I. G.; "Effect of Isolated Tuned Dampers on Response of Multispan Structures," Journal of Aircraft, Vol. 4, No. 4, July-August 1967.

4a. Product Data Sheets, Hexel Corporation.

4b. Structural Handbook, U.S. Polymeric, 1977.

5. Ashton, J. E.; Halpin, J. C.; Petit, P. H.; Primer on Composite Materials: Analysis; Technomic Publishing Co., Inc., Stamford, Conn., 1969.

6. Ashton, J. E.; Whitney, J. M.; Theory of Laminated Plates; Technomic Publishing Co., Inc., Stamford, Conn., 1970.

7. Grosveld, F. M. W. A.; "Study of Typical Parameters that Affect Sound Transmission through General Aviation Aircraft Structures,"

KU-FRL-417-13, Flight Research Laboratory, University of Kansas, Lawrence, Kansas, August 1980.

8. Beranek, L. L.; Noise and Vibration Control,; McGraw Hill Book Company, New York, 1971.

9. Snowdon, J. C.; Vibration and Shock in Damped Mechanical Systems; John Wiley & Sons, Inc., New York, 1968.

10. Szilard, R.; Theory and Analysis of Plates; Prentice Hall, Inc., Englewood Cliffs, New Jersey, 1974.

11. Gent, A. N.; Lindley, P. B.; "The Compression of Bonded Rubber Blocks," Procurements of Institution of Mechanical Engineers, Vol. 173, No. 3, 1959.

APPENDIX A

LISTING OF COMPUTER PROGRAM COMP

This program calculates the flexural rigidity matrix elements Dij and the natural frequency of a 3-layer laminated panel.

```
      PROGRAM COMP
C
    2 TYPE *,'COMPOSITE NATURAL FREQUENCY PROGRAM'
      TYPE *,' '
      TYPE *,'PANEL CONSISTS OF 3 LAYERS OF THE SAME THICKNESS'
C
CC    INPUT DATA IN ENGLISH UNITS, ( PSI,IN,DEGREES )
CC    OUTPUT IN METRIC UNITS
C
      TYPE *,'ENTER PANEL NUMBER'
      ACCEPT *,IN
      PRINT 1,IN
    1 FORMAT(5X,15HPANEL NUMBER = ,I3)
      PRINT 21
   21 FORMAT(T11,3HE11,T24,3HE22,T35,3HG12,T48,3HV12,T56,3HTHE)
C
CC    INPUT MATERIAL PROPERTIES OF TOP LAYER
C
      TYPE *,'  '
      TYPE *,'TOP LAYER'
      CALL ENTER(Q11N,Q22N,Q12N,Q66N,Q16N,Q26N,S)
      QA11=Q11N
      QA22=Q22N
      QA12=Q12N
      QA66=Q66N
      QA16=Q16N
      QA26=Q26N
C
CC    INPUT MATERIAL PROPERTIES MIDDLE LAYER
C
      TYPE *,' '
      TYPE *,'MIDDLE LAYER'
      CALL ENTER(Q11N,Q22N,Q12N,Q66N,Q16N,Q26N,S)
      QB11=Q11N
      QB22=Q22N
      QB12=Q12N
      QB66=Q66N
      QB16=Q16N
      QB26=Q26N
C
CC    INPUT MATERIAL PROPERTIES BOTTOM LAYER
C
      TYPE *,' '
      TYPE *,'BOTTOM LAYER'
      CALL ENTER(Q11N,Q22N,Q12N,Q66N,Q16N,Q26N,S)
      QC11=Q11N
      QC22=Q22N
      QC12=Q12N
      QC66=Q66N
      QC16=Q16N
      QC26=Q26N
C
CC    INPUT CHARACTERISTIC PROPERTIES OF PANEL
C
      TYPE *,'ENTER THICKNESS OF PANEL'
      ACCEPT *,TH
      TH=TH*.0254
      TYPE *,'ENTER SURFACE DENSITY OF PANEL'
      ACCEPT *,RHO
      RHO=RHO*.4536/(.0254)**2
```

```
C
C       COMPUTATION OF ELEMENTS OF 'D' MATRIX
C
        A=.040123
        B=.003086
        C= A
C
        D11=A*TH**3*QA11+B*TH**3*QB11+C*TH**3*QC11
        D22=A*TH**3*QA22+B*TH**3*QD22+C*TH**3*QC22
        D12=A*TH**3*QA12+B*TH**3*QB12+C*TH**3*QC12
        D66=A*TH**3*QA66+B*TH**3*QD66+C*TH**3*QC66
        D16=A*TH**3*QA16+B*TH**3*QB16+C*TH**3*QC16
        D26=A*TH**3*QA26+B*TH**3*QB26+C*TH**3*QC26
C
C
    6   TYPE *,' '
        TYPE *,'ENTER DIMENSIONS OF EXPOSED AREA,a AND b'
        ACCEPT *,A,B
        A=A*.0254
        B=B*.0254
C
C       CALCULATION OF NATURAL FREQUENCY
C
C
C       SIMPLY SUPPORTED BOUNDARY CONDITION
C
        TYPE 5
    5   FORMAT(5X,44HNATURAL FREQUENCY FOR SIMPLY SUPPORTED EDGES)
        PRINT 5
C
        DO 20 M=1,5
        DO 20 N=1,5
C
C
        PI=3.141592654
C
C       Ai BOUNDARY COEFFICIENTS
C
        A1=M*PI
        A2=(M*N*PI*PI)**2
        A3=N*PI
C
        FREQ = FEQ(D11,D22,D12,D66,M,N,RHO,A,B,A1,A2,A3)
C
        PRINT 10,M,N,FREQ
   10   FORMAT(5X,4HM = ,I1,5X,4HN = ,I1,5X,17HNAT  FREQUENCY = ,F10.2
        TYPE 10,M,N,FREQ
   20   CONTINUE
C
C       CLAMPED BOUNDARY CONDITION
C
        TYPE *,' '
        TYPE 77
   77   FORMAT(5X,36HNATURAL FREQUENCY FOR CLAMPED EDGES )
        PRINT 77
C
        DO 50 M=1,5
        DO 50 N=1,5
C
        IF(N.NE.1) GO TO 25
```

```
      IF(M.NE.1) GO TO 30
      A1=4.730
      A2=151.3
      A3=A1
      GO TO 40
   30 A1=(M+.5)*PI
      A3=4.730
      A2=12.30*A1*(A1-2.)
      GO TO 40
   25 IF(M.NE.1) GO TO 35
      A1=4.730
      A3=(N+.5)*PI
      A2=12.30*A3*(A3-2.)
      GO TO 40
   35 A1=(M+.5)*PI
      A3=(N+.5)*PI
      A2=A1*A3*(A1-2.)*(A3-2.)
   40 FREQ=FEQ(D11,D22,D12,D66,M,N,RHO,A,B,A1,A2,A3)
C
      PRINT 10,M,N,FREQ
      TYPE  10,M,N,FREQ
   50 CONTINUE
C
C     PRINT ELEMENTS OF 'D' MATRIX
  300 PRINT 15
   15 FORMAT(/T7,3HD11,T17,3HD22,T27,3HD12,T37,3HD26,T47,3HD16,
     1T57,3HD66)
      PRINT 16,D11,D12,D16
      PRINT 17,D22,D26,D66
   16 FORMAT(/4X,3(F7.2,10X))
   17 FORMAT(15X,3(F7.2,10X))
C
      TYPE *,'MORE PANELS? YES=1'
      ACCEPT *,J
      IF(J.EQ.1) GO TO 2
      STOP
      END

      FUNCTION FEQ(W,X,Y,Z,I,J,R,F,G,B1,B2,B3,E)
C
C     COMPUTATION OF Fm,n
C
      PI=3.141592654
      FEQ=SQRT((W*(B1/F)**4+2*(Y+2*Z)*B2/(F*F*G*G) + (B3/G)**4*X)/R)
      FEQ=FEQ/(2*PI)
C
      END

      SUBROUTINE ENTER(W,X,Y,Z,U,V,S)
C
C     INPUT MATERIAL PROPERTIES OF LAYER
C
      TYPE *,'ENTER E11'
      ACCEPT *,E11
      TYPE *,'ENTER E22'
      ACCEPT *,E22
      TYPE *,'ENTER G12'
      ACCEPT *,G12
      TYPE *,'ENTER V12'
      ACCEPT *,V12
```

C-2

```
      TYPE *,'ENTER ANGLE'
      ACCEPT *,THE
C
      E11=E11*6894.
      E22=E22*6894.
      G12=G12*6894.
C
      S=(E11+E22)/2.
C
      PI=3.141592654
      PHI= THE*2*PI/360.
      V21=V12*E22/E11
      A=1-V12*V21
C
C     STIFFNESS MATRIX Q
C
      Q11=E11/A
      Q22=E22/A
      Q12=V12*Q22
      Q66=G12
C
C     TRANSFORM Q MATRIX TO NEW AXES SYSTEM ALONG PLATE-AXES
C
      U1=(3*Q11+3*Q22+2*Q12+4*Q66)/8.
      U2=(Q11-Q22)/2.
      U3=(Q11+Q22-2*Q12-4*Q66)/8.
      U4=(Q11+Q22+6*Q12-4*Q66)/8.
      U5=(Q11+Q22-2*Q12+4*Q66)/8.
C
      W=U1+U2*COS(2*PHI)+U3*COS(4*PHI)
      X=U1-U2*COS(2*PHI)+U3*COS(4*PHI)
      Y=U4-U3*COS(4*PHI)
      Z=U5-U3*COS(4*PHI)
      U=-(U2/2.)*SIN(2*PHI)-U3*SIN(4*PHI)
      V=-(U2/2.)*SIN(2*PHI)+U3*SIN(4*PHI)
C
C     PRINT MATERIAL PROPERTIES OF LAYER (METRIC UNITS)
C
      PRINT 22,E11,E22,G12,V12,THE
   22 FORMAT(5X,3(3X,E10.3),4X,F4.2,4X,F6.2)
      RETURN
      END
```

APPENDIX B

EXPERIMENTAL NOISE REDUCTION DATA FOR FIBER-REINFORCED COMPOSITE PANELS

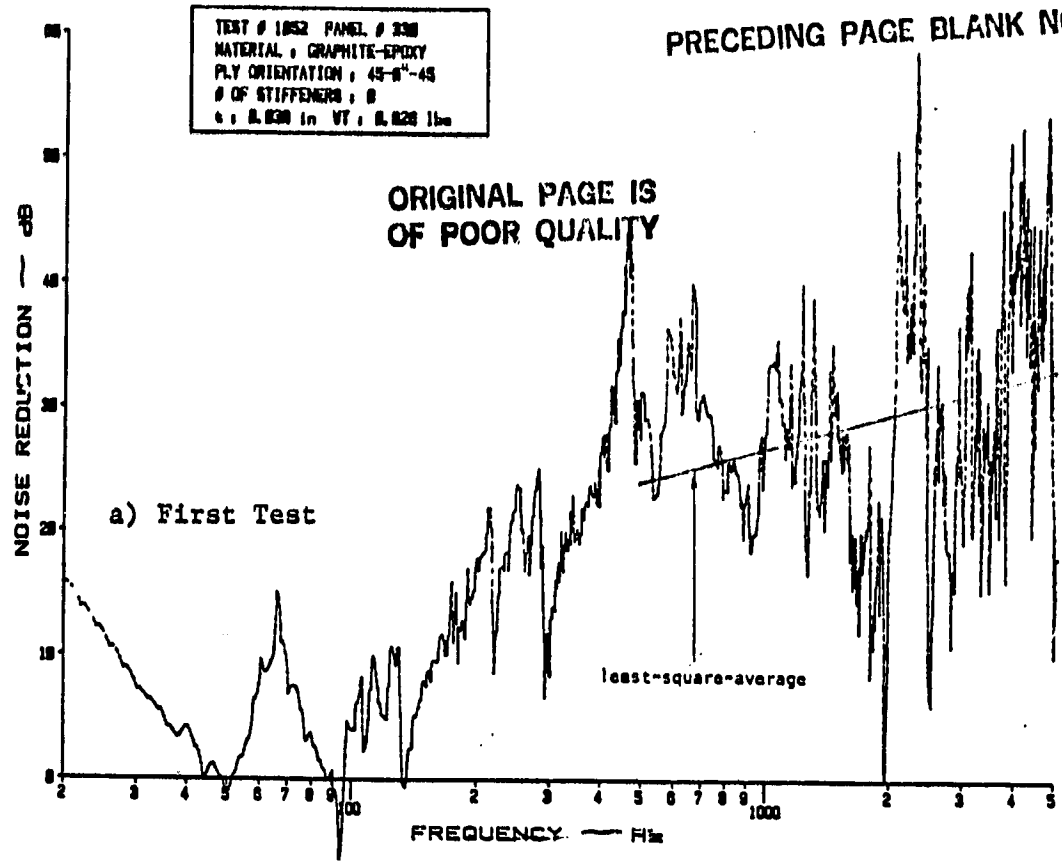

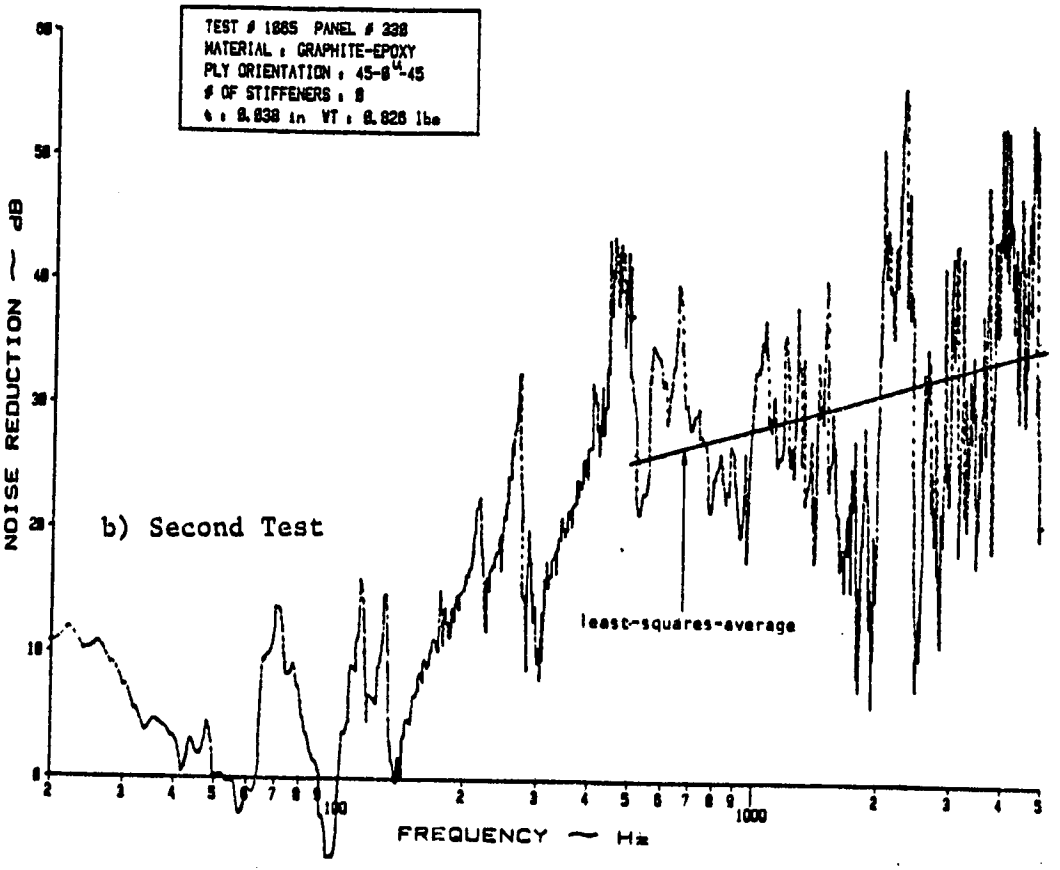

Figure B.1 Noise Reduction Characteristics of a Graphite-Epoxy Panel with Ply-Orientation $45\text{-}0^{u}\text{-}45$

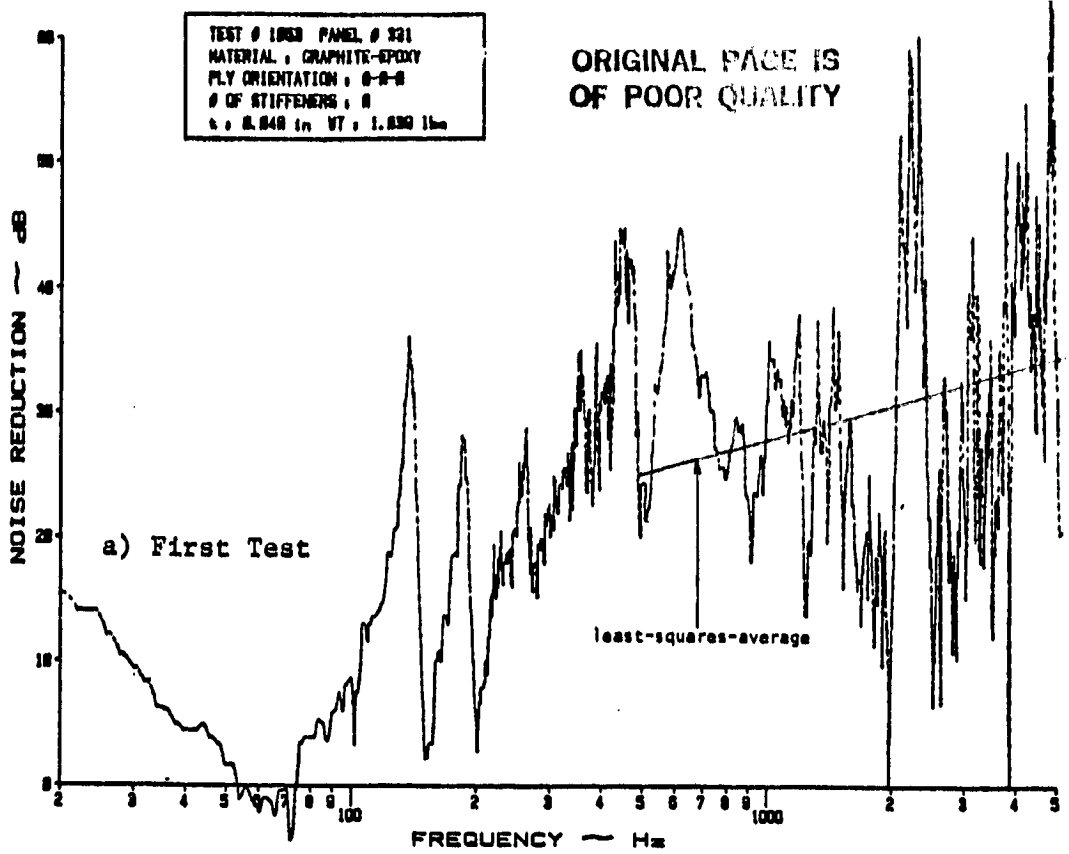

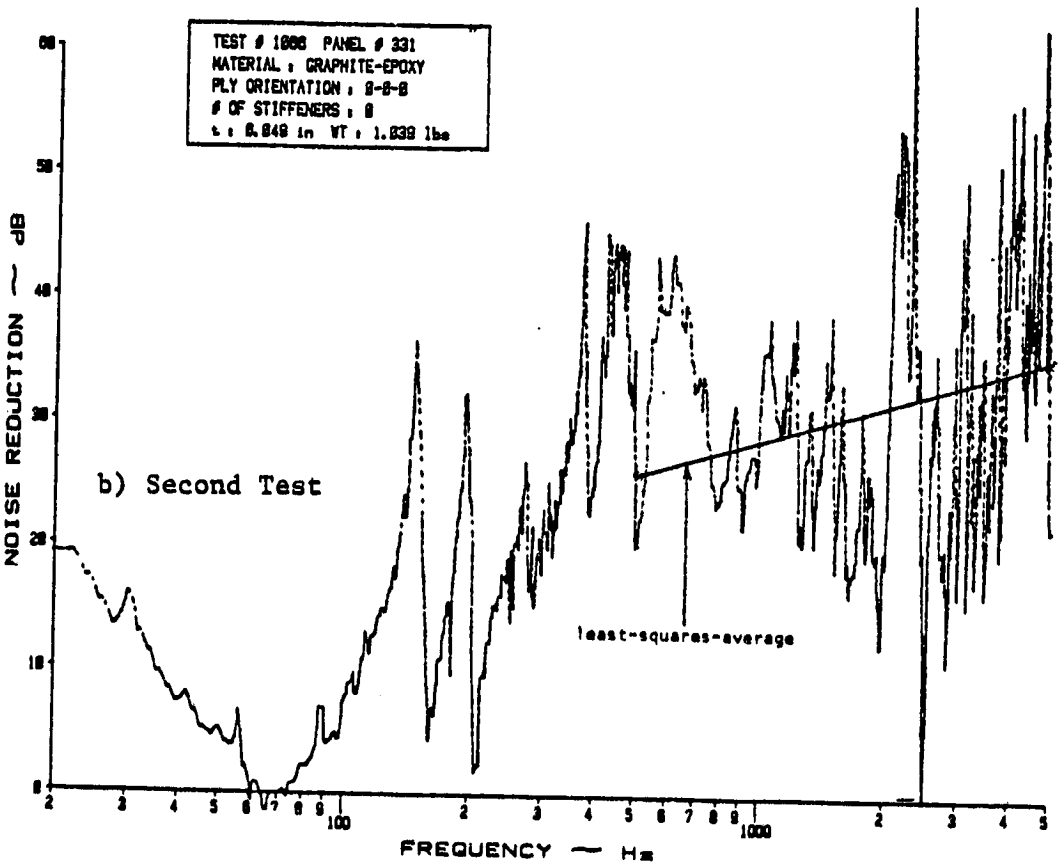

Figure B.2 Noise Reduction Characteristics of a Graphite-Epoxy Panel with Ply-Orientation 0-0-0

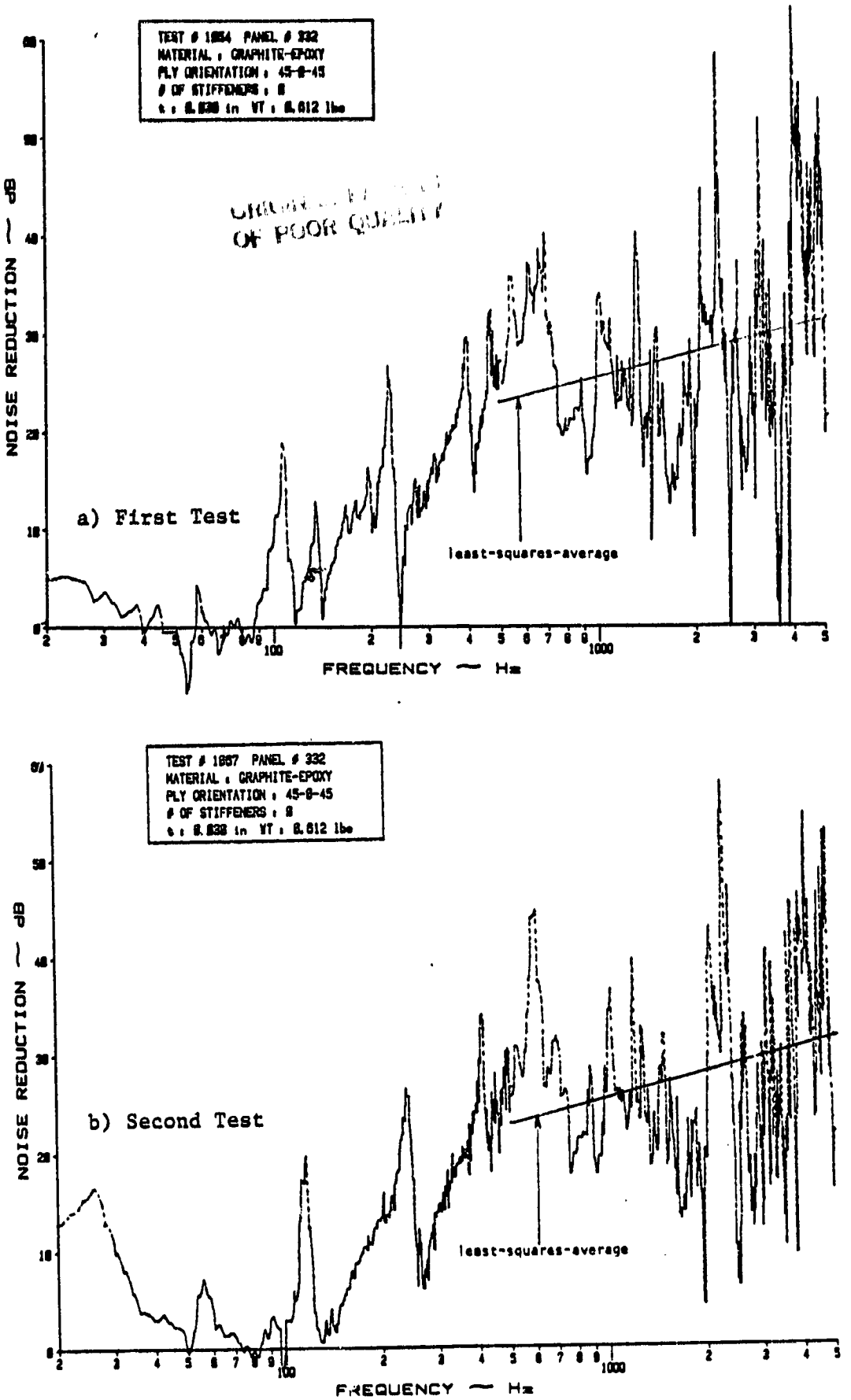

Figure B.3 Noise Reduction Characteristics of a Graphite-Epoxy Panel with Ply Orientation 45-0-45

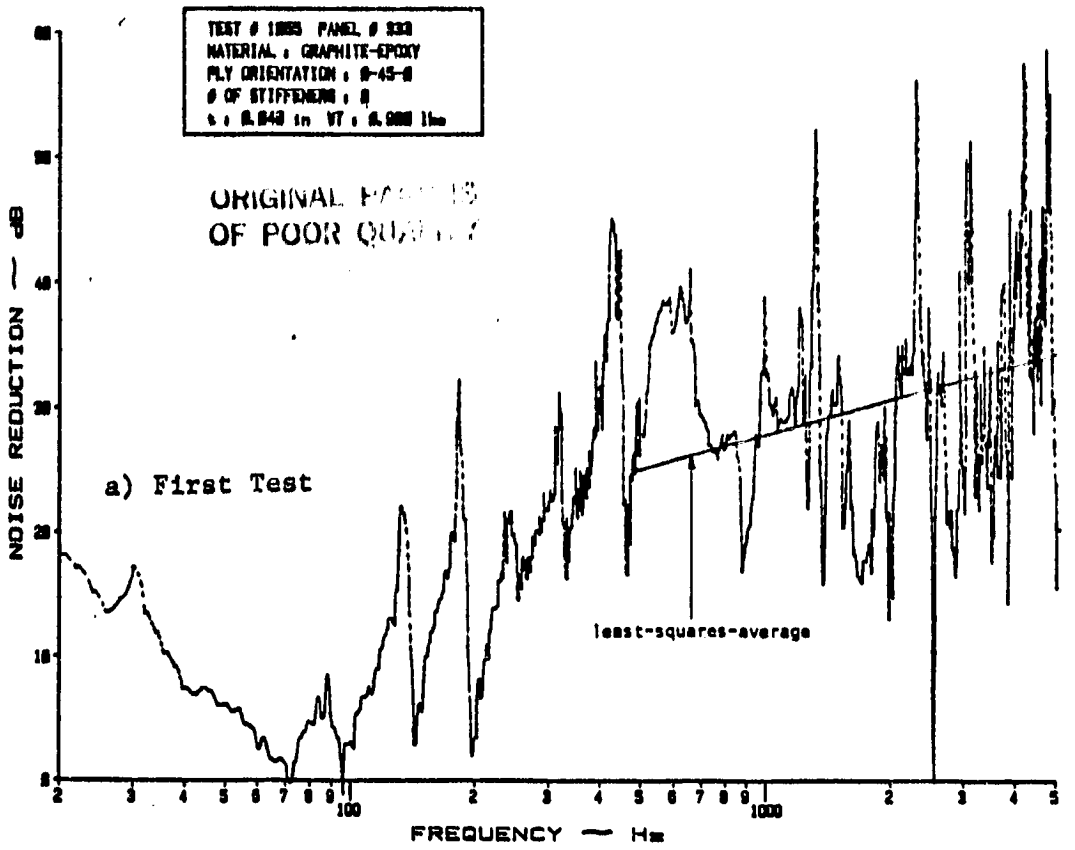

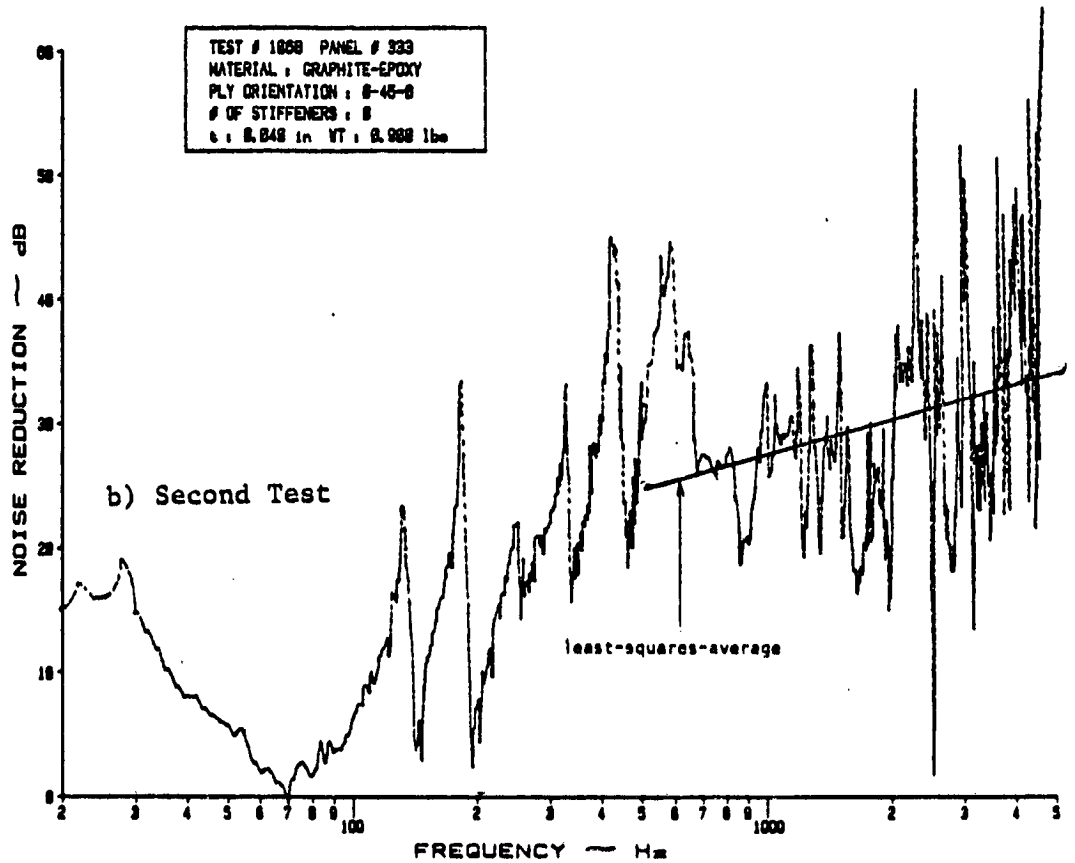

Figure B.4 Noise Reduction Characteristics of a Graphite-Epoxy Panel with Ply Orientation 0-45-0

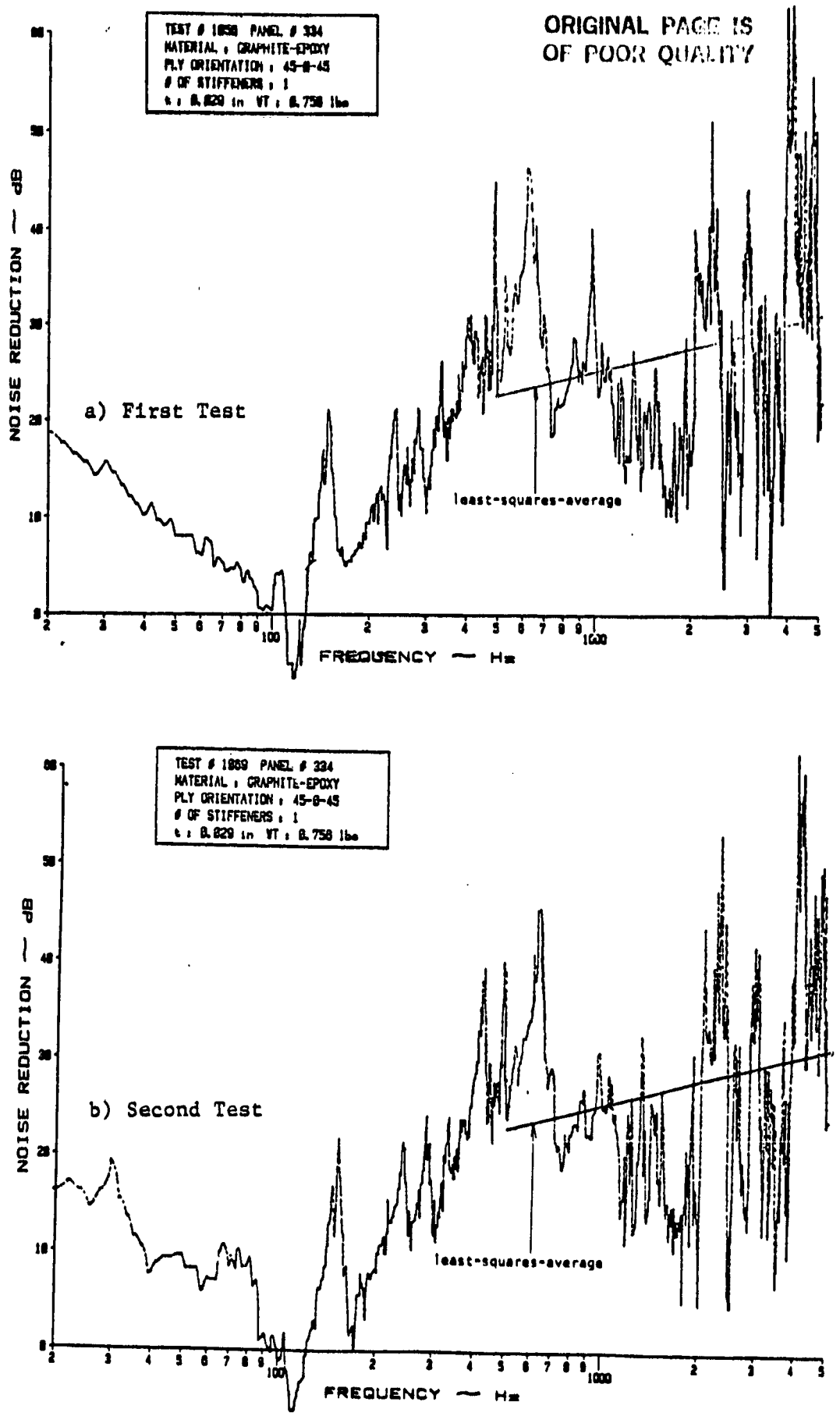

Figure B.5 Noise Reduction Characteristics of a Graphite-Epoxy Panel with Ply Orientation 45-0-45 and 1 Stiffener

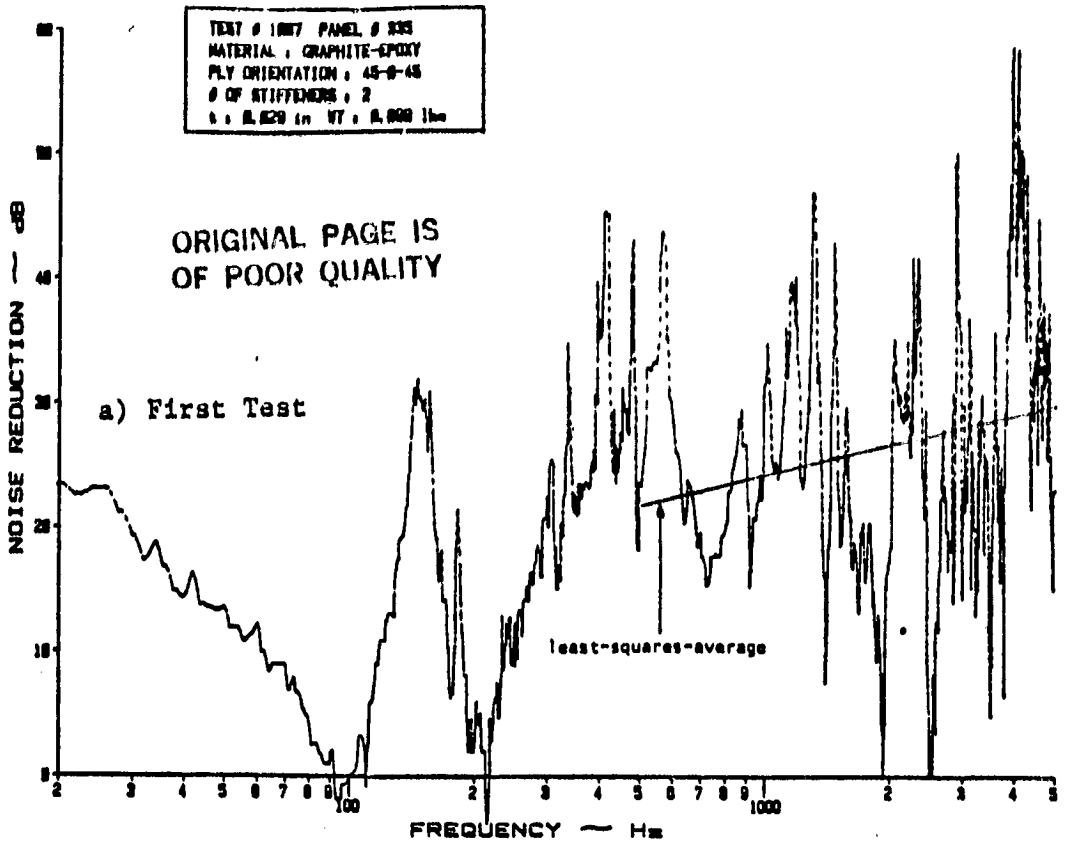

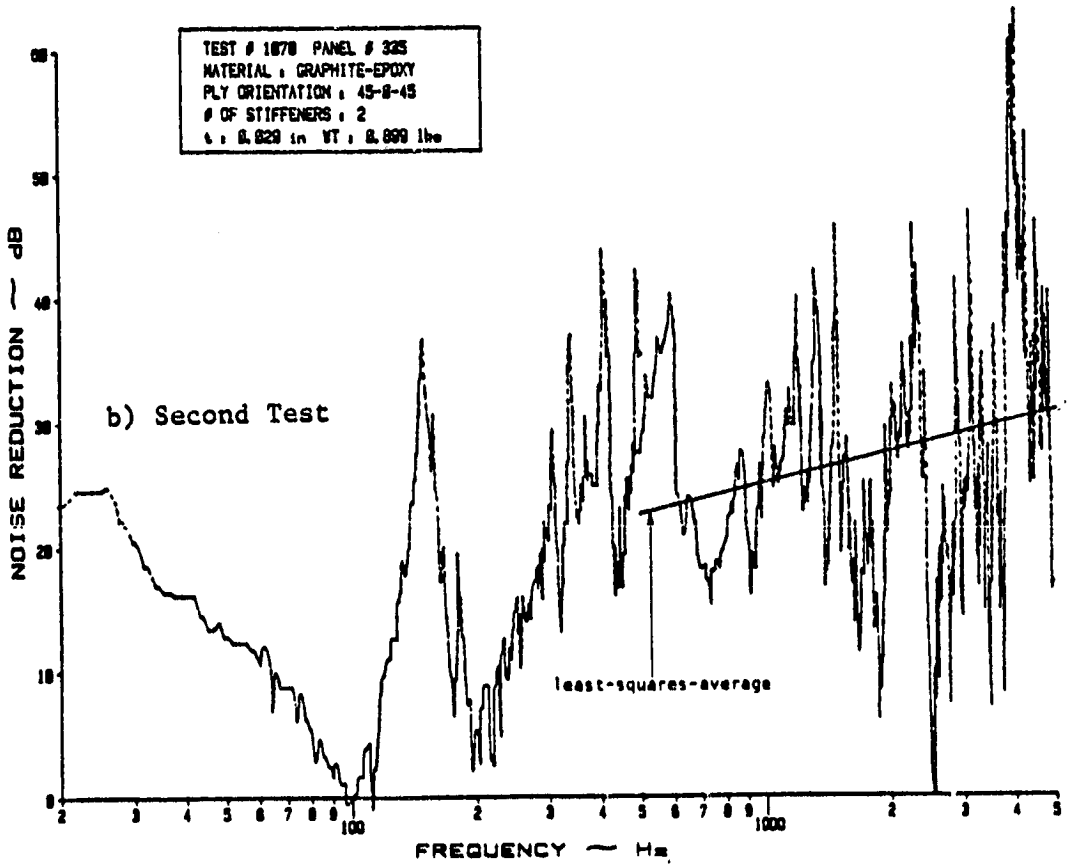

Figure B.6 Noise Reduction Characteristics of a Graphite-Epoxy Panel with Ply Orientation 45-0-45 and 2 Stiffeners

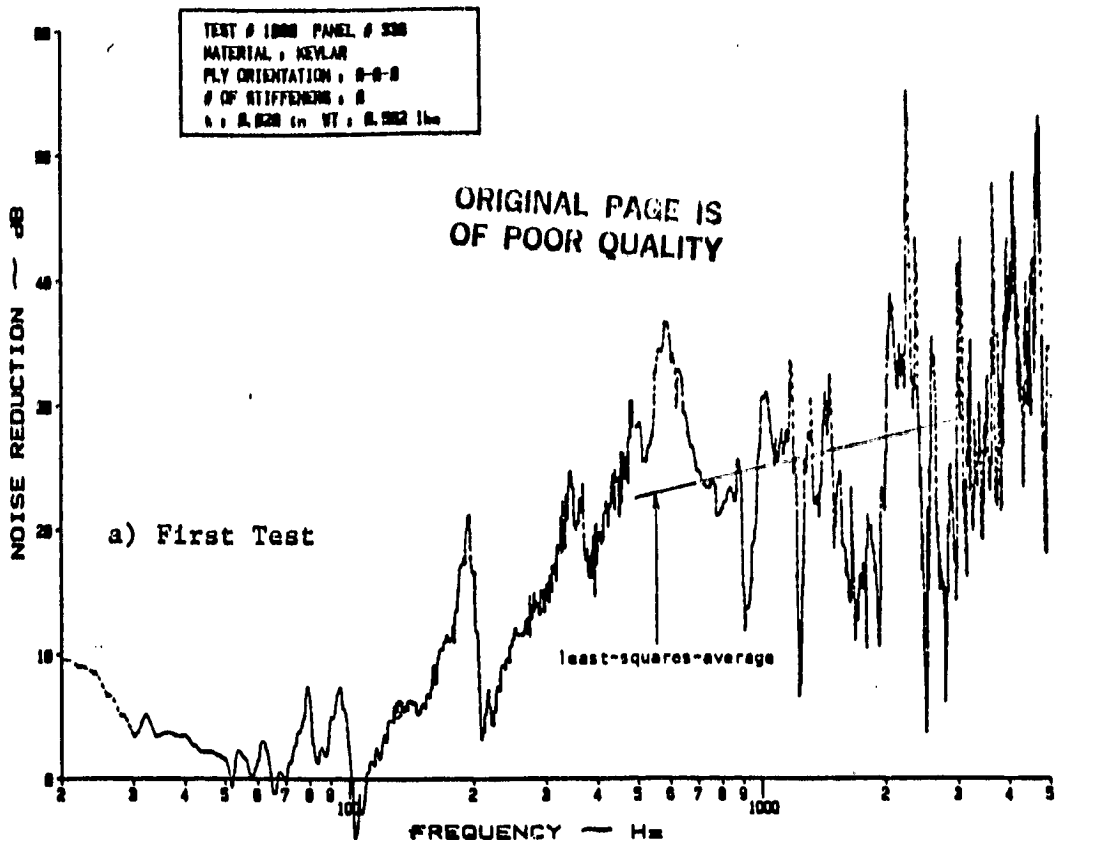

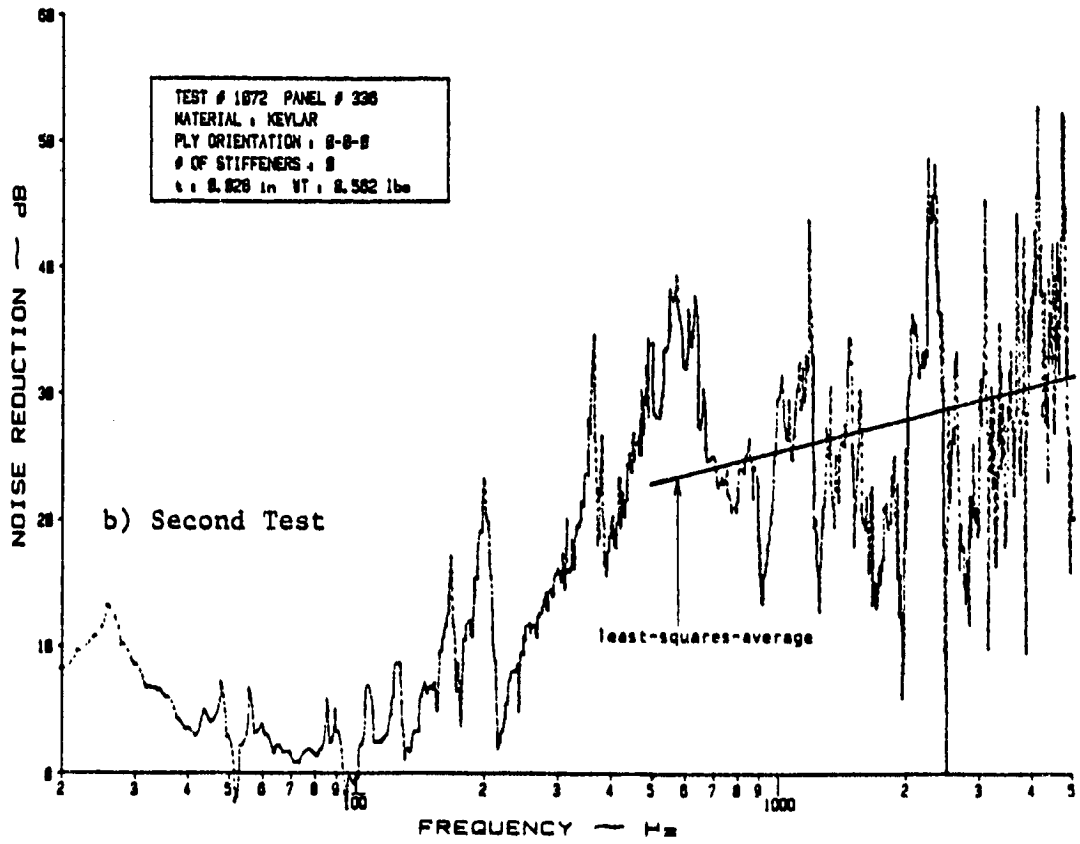

Figure B.7 Noise Reduction Characteristics of a Kevlar Panel with Ply Orientation 0-0-0

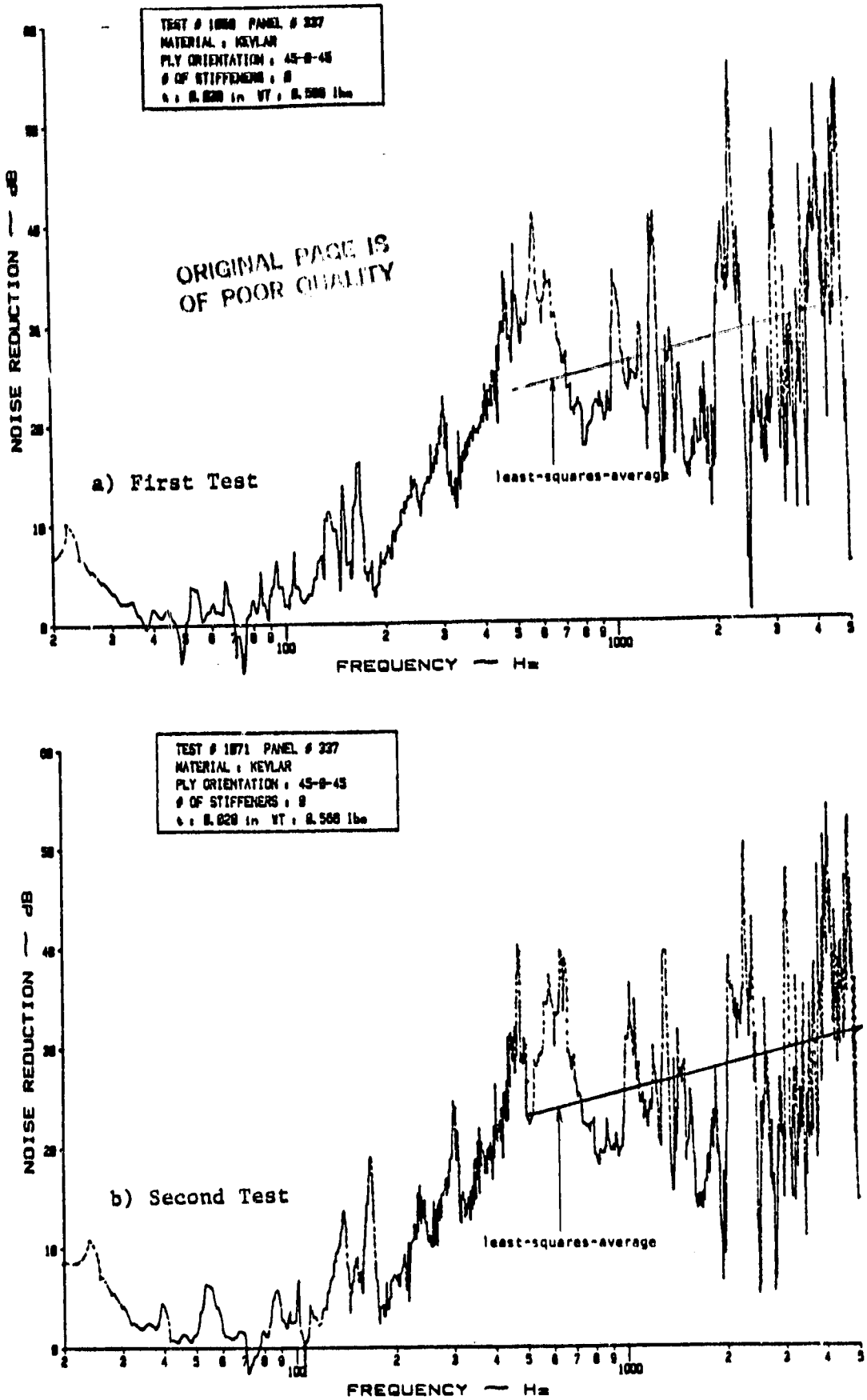

Figure B.8 Noise Reduction Characteristics of a Kevlar Panel with Ply Orientation 45-0-45

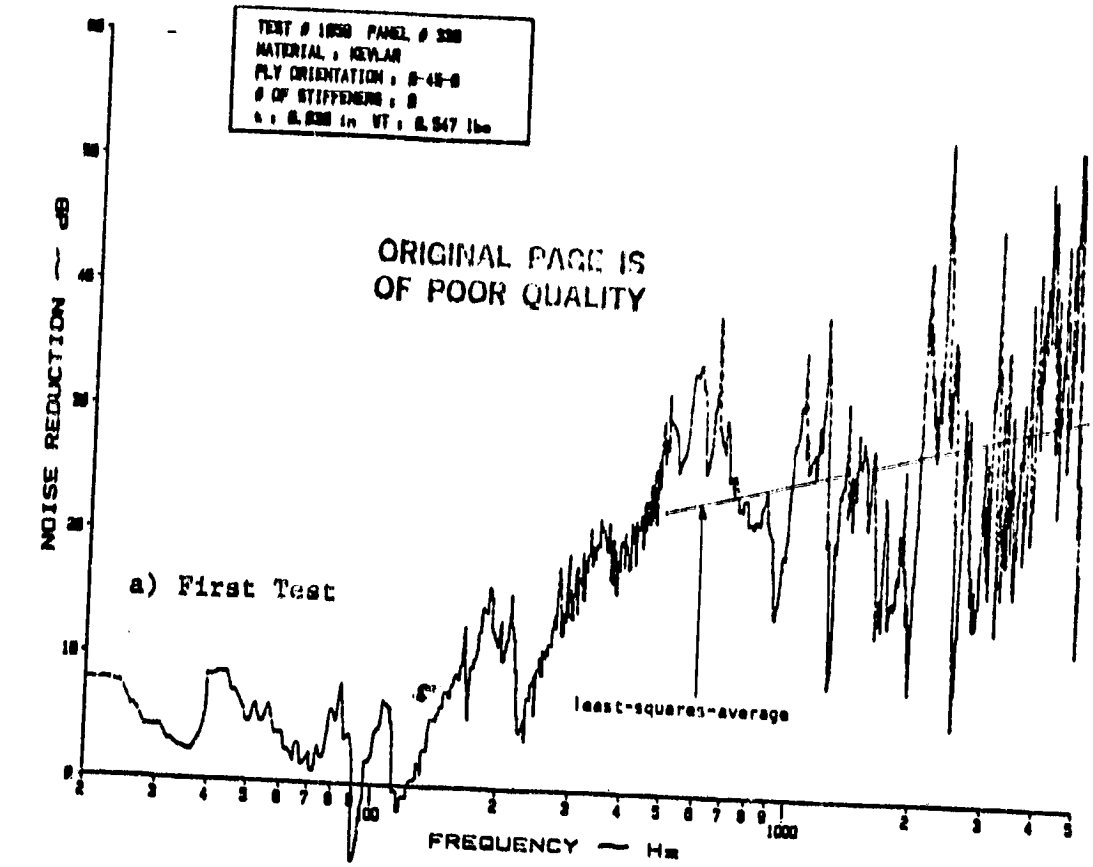

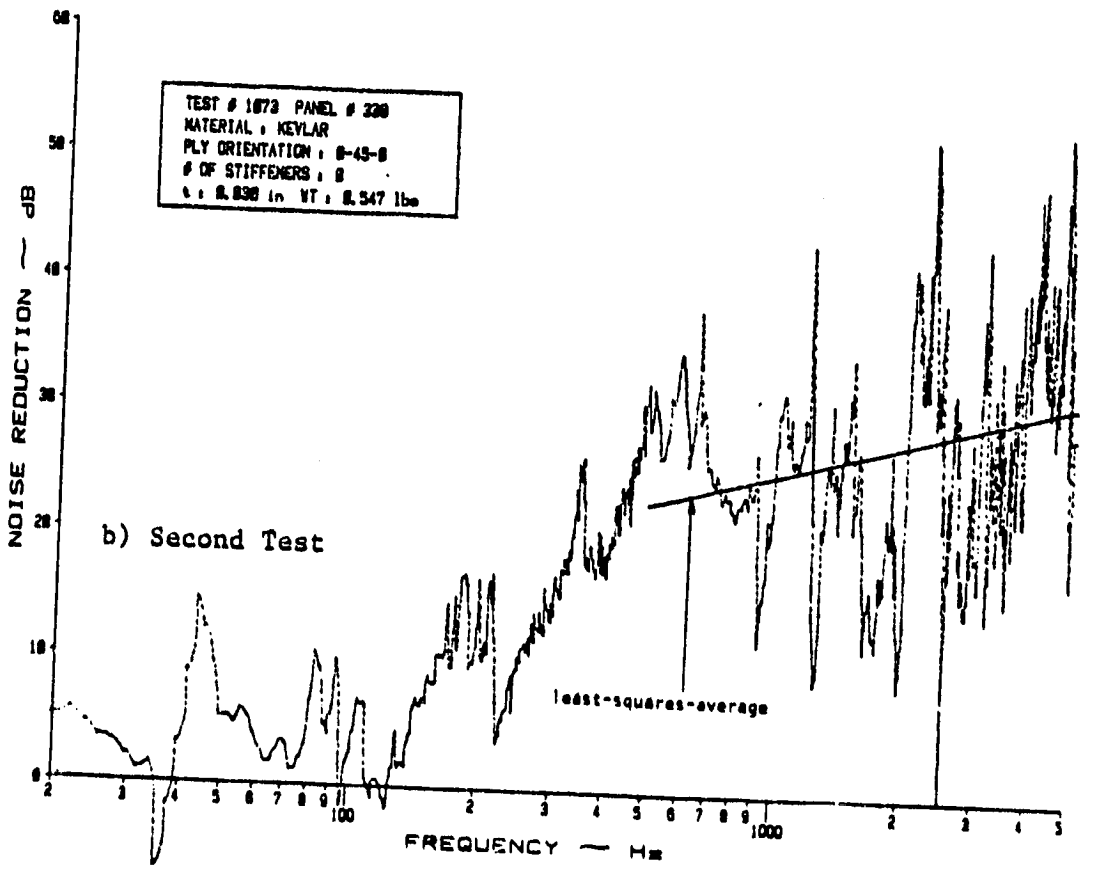

Figure B.9 Noise Reduction Characteristics of a Kevlar Panel with Ply-Orientation 0-45-0

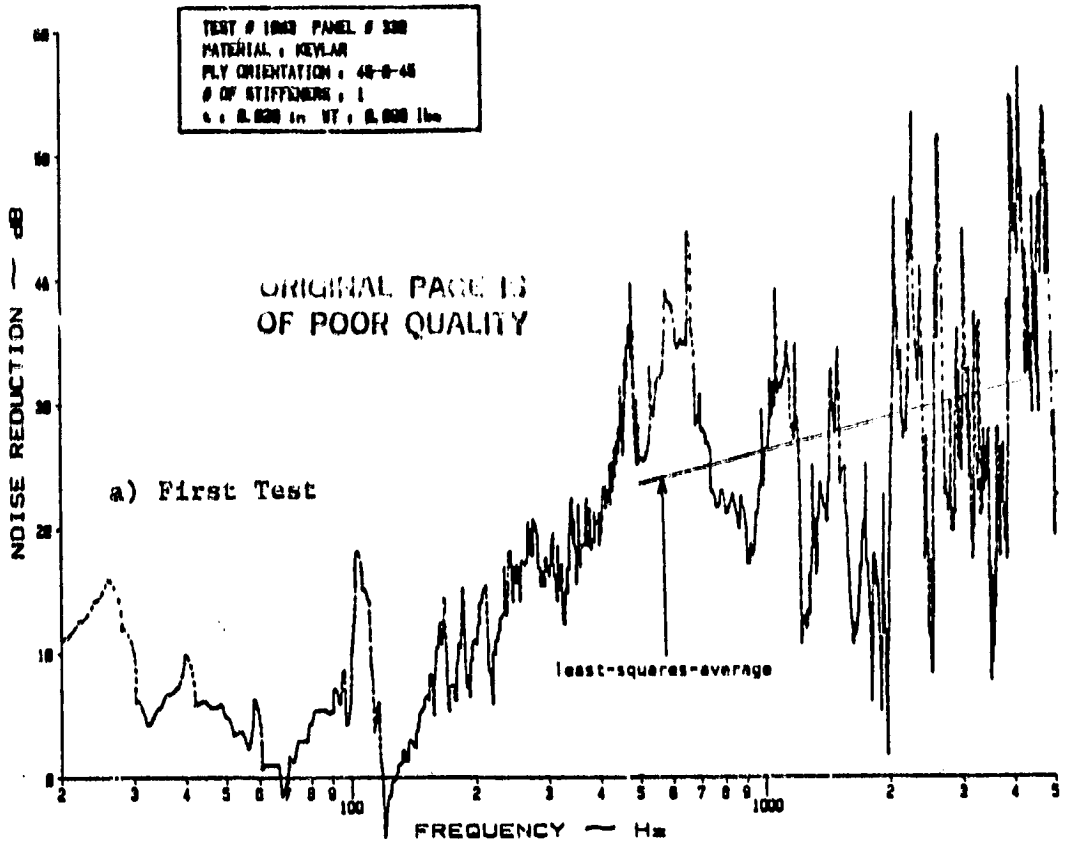

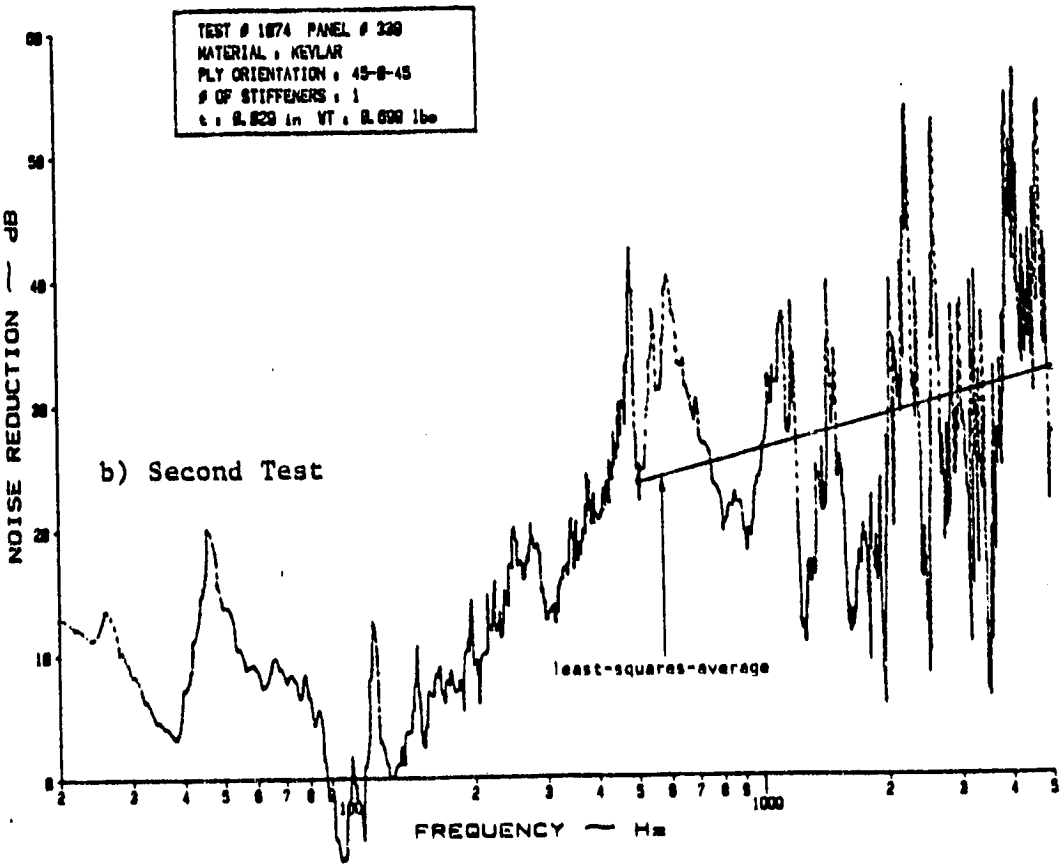

Figure B.10 Noise Reduction Characteristics of a Kevlar Panel with Ply Orientation 45-0-45 and 1 Stiffener

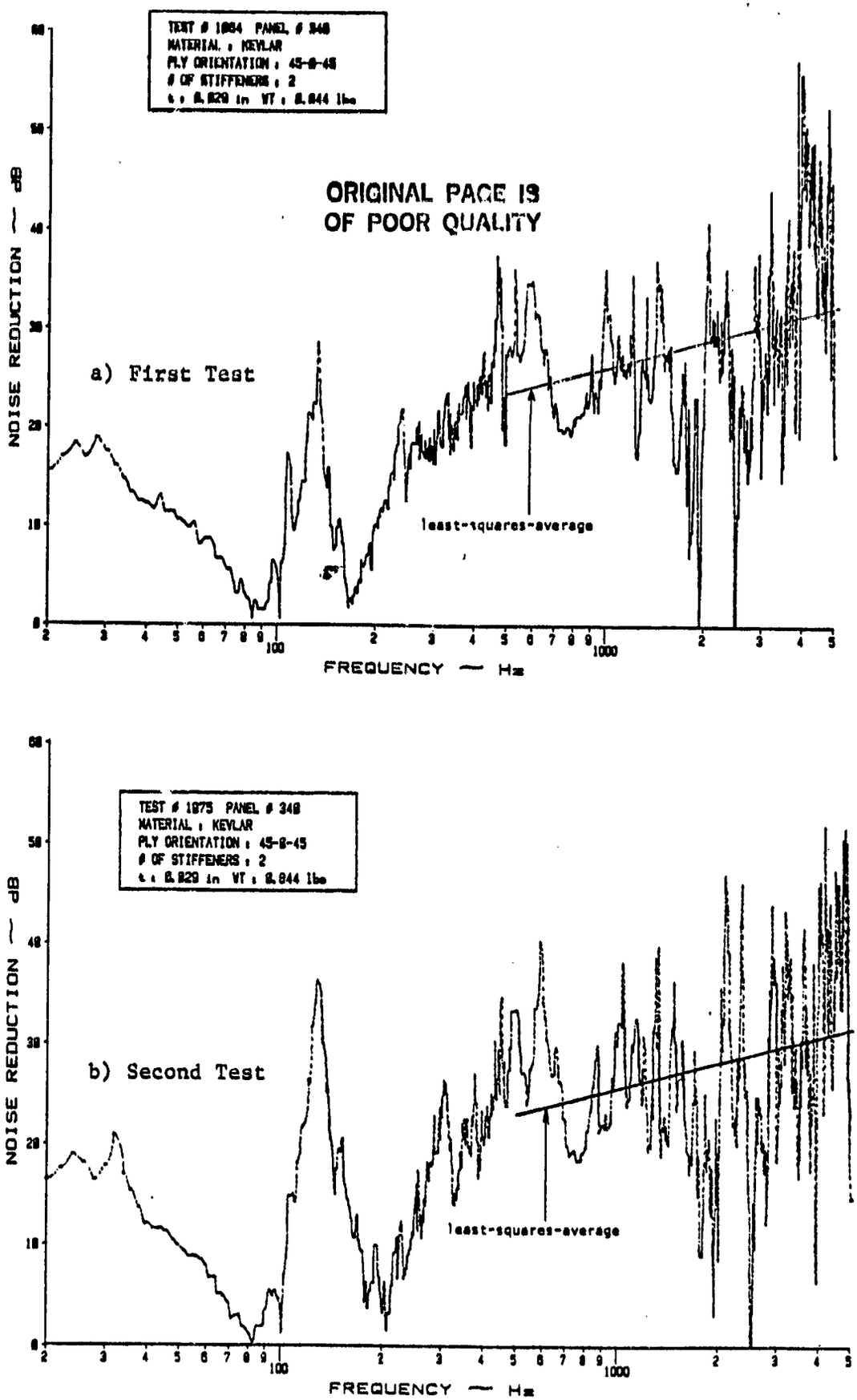

Figure B.11 Noise Reduction Characteristics of a Kevlar Panel with Ply Orientation 45-0-45 and 2 Stiffeners

APPENDIX C

EXPERIMENTAL NOISE REDUCTION DATA FOR INTERNAL PANEL CONFIGURATIONS

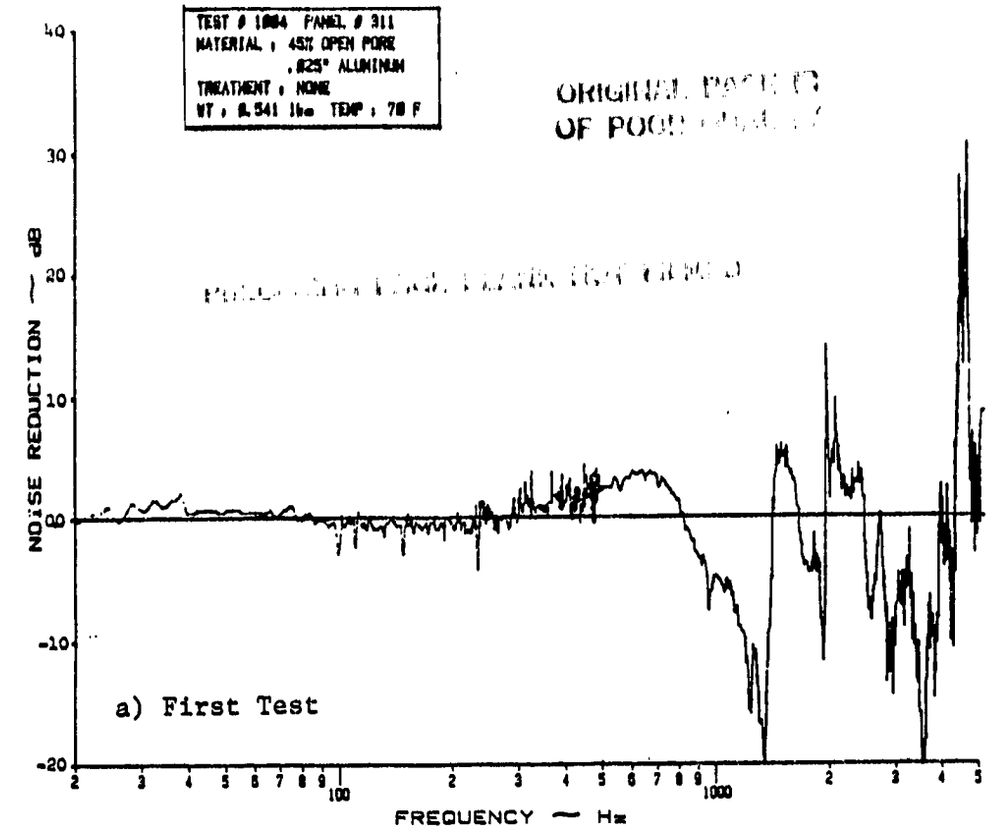

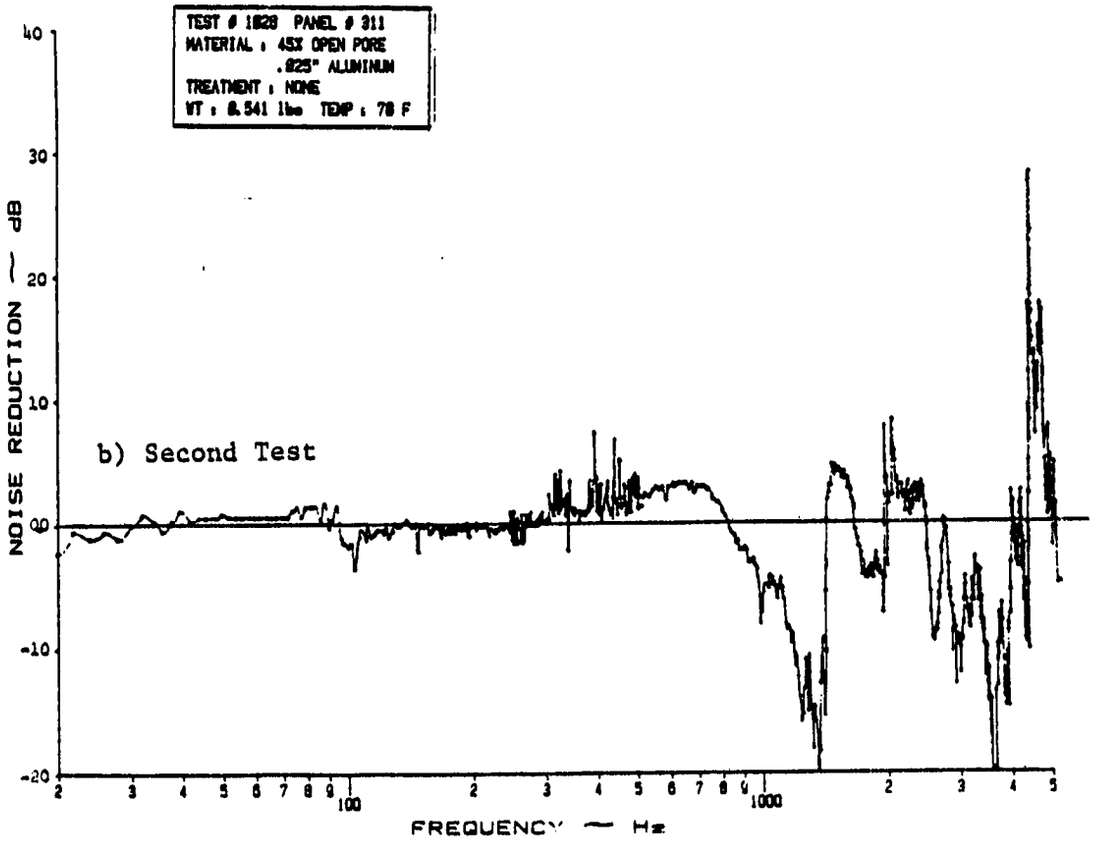

Figure C.1 Noise Reduction Characteristics of a Perforated (45%) Aluminum Panel with .025" Thickness and No Treatment

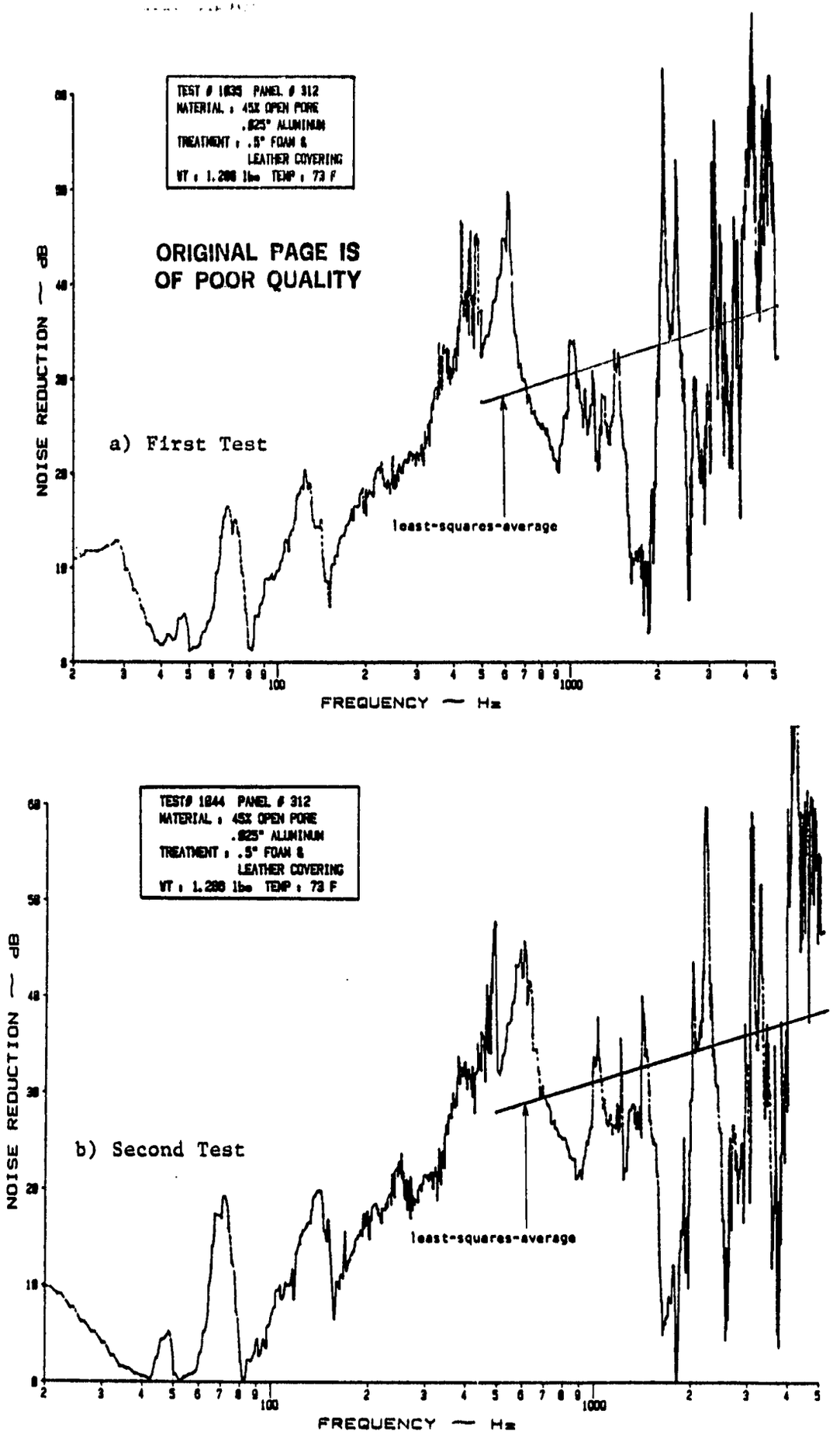

Figure C.2 Noise Reduction Characteristics of a Perforated (45%) Aluminum Panel with .025" Thickness and a .05" Foam and Leather Covering as Treatment

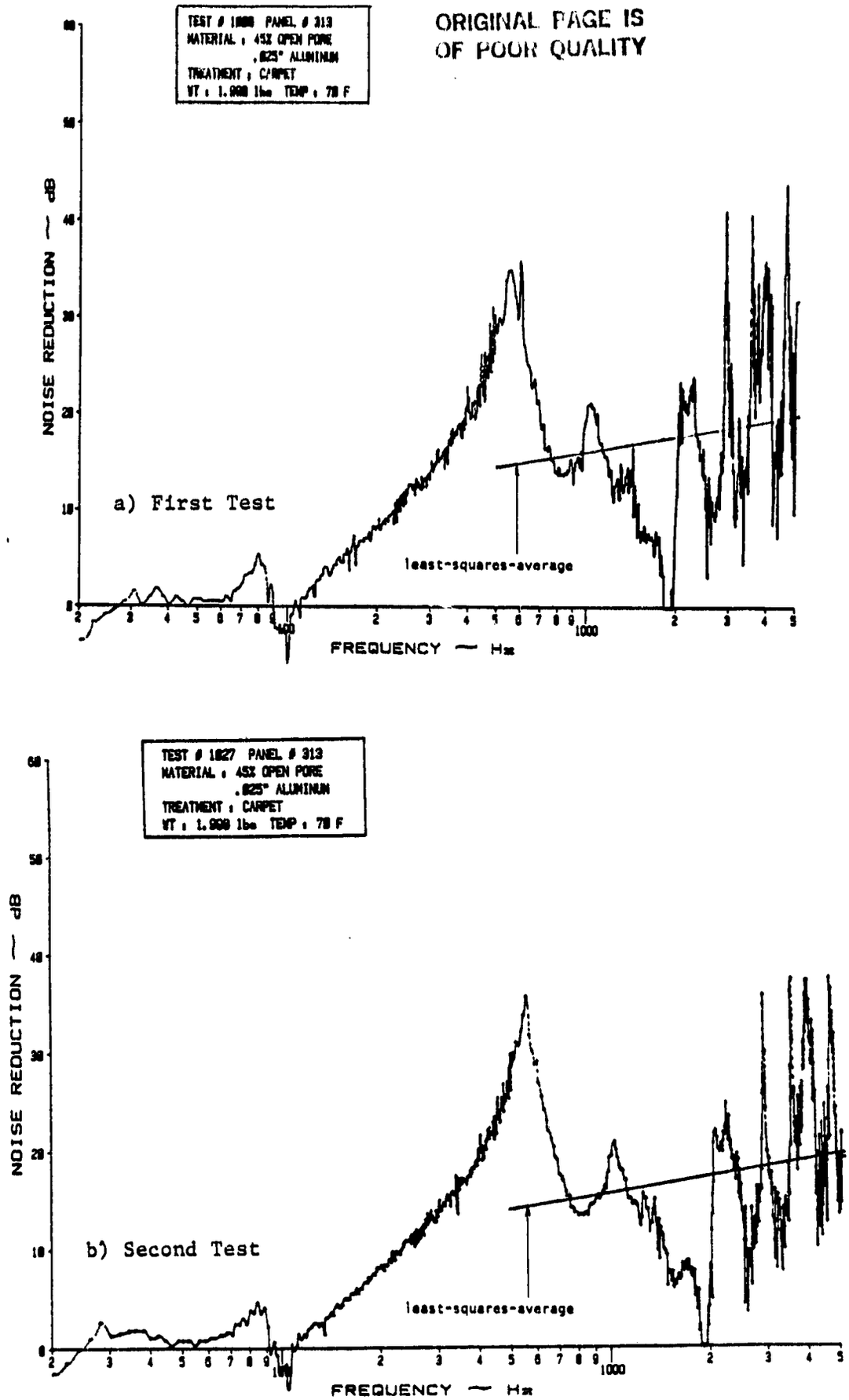

Figure C.3 Noise Reduction Characteristics of a Perforated (45%) Aluminum Panel with .025" Thickness and Carpet as Treatment

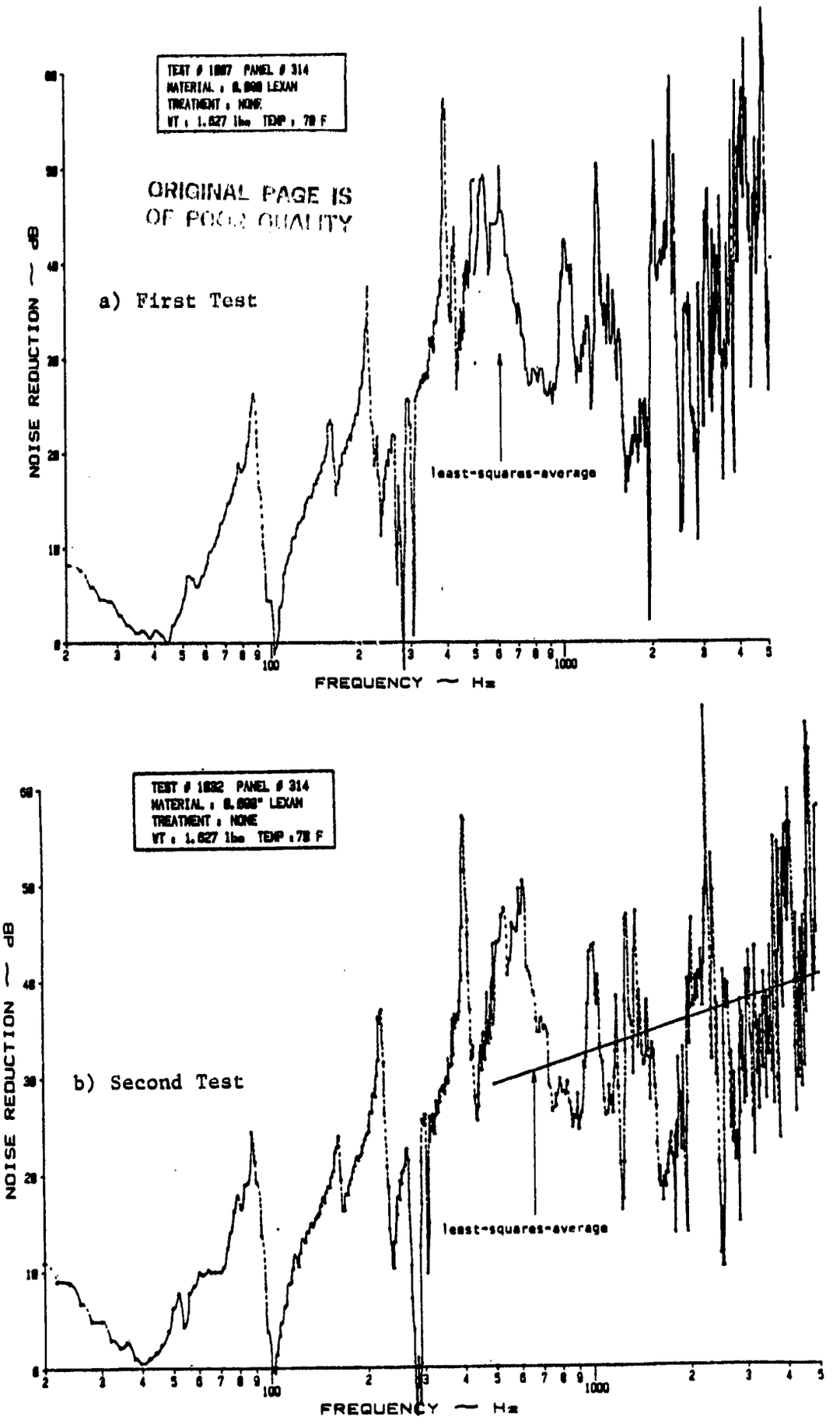

Figure C.4 Noise Reduction Characteristics of a .09" Lexan Panel with No Treatment

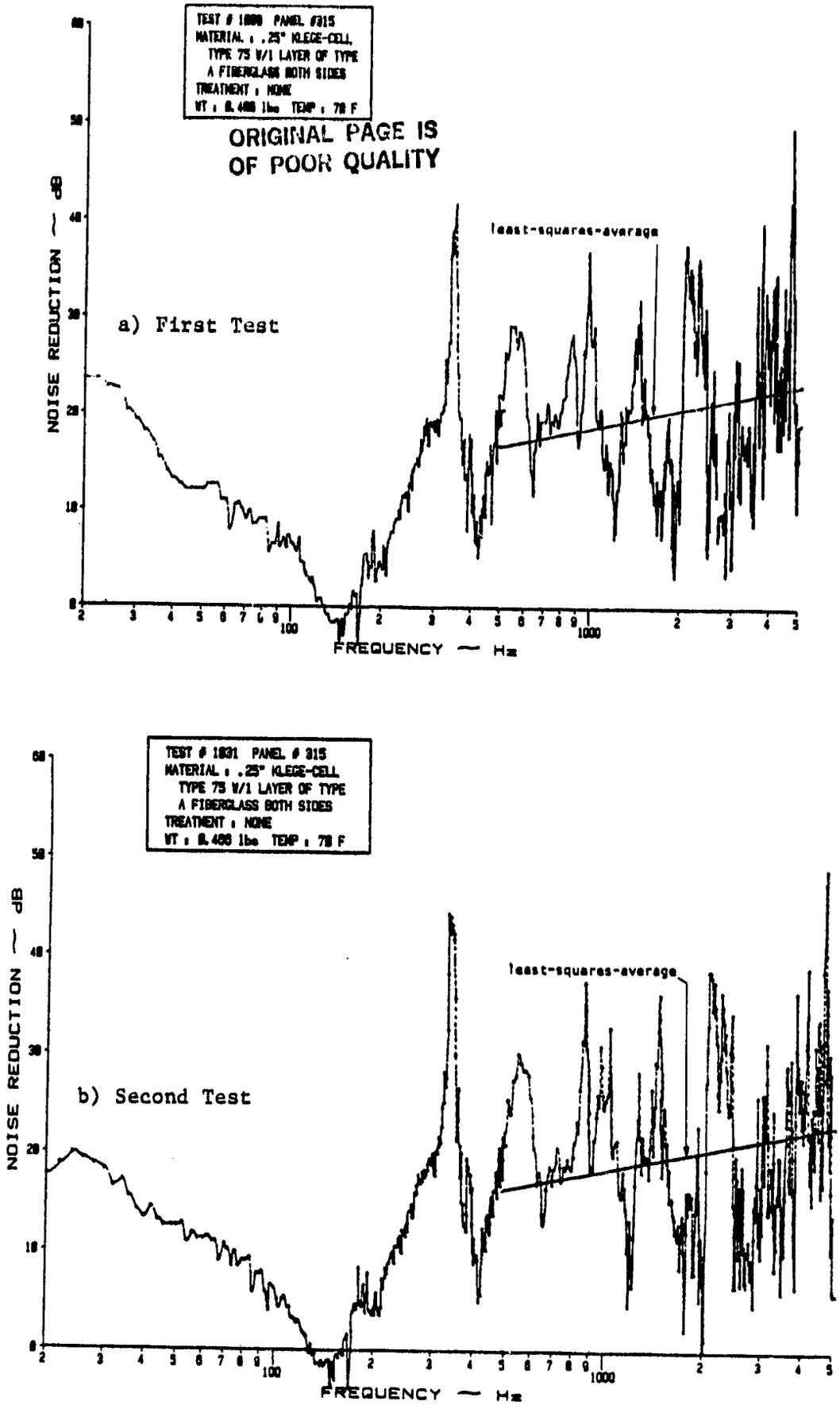

Figure C.5 Noise Reduction Characteristics of a Sandwich Panel with a .25" Klege-Cell Type 75 Core and 1 Layer of Type A Fiberglass on Both Sides with No Treatment

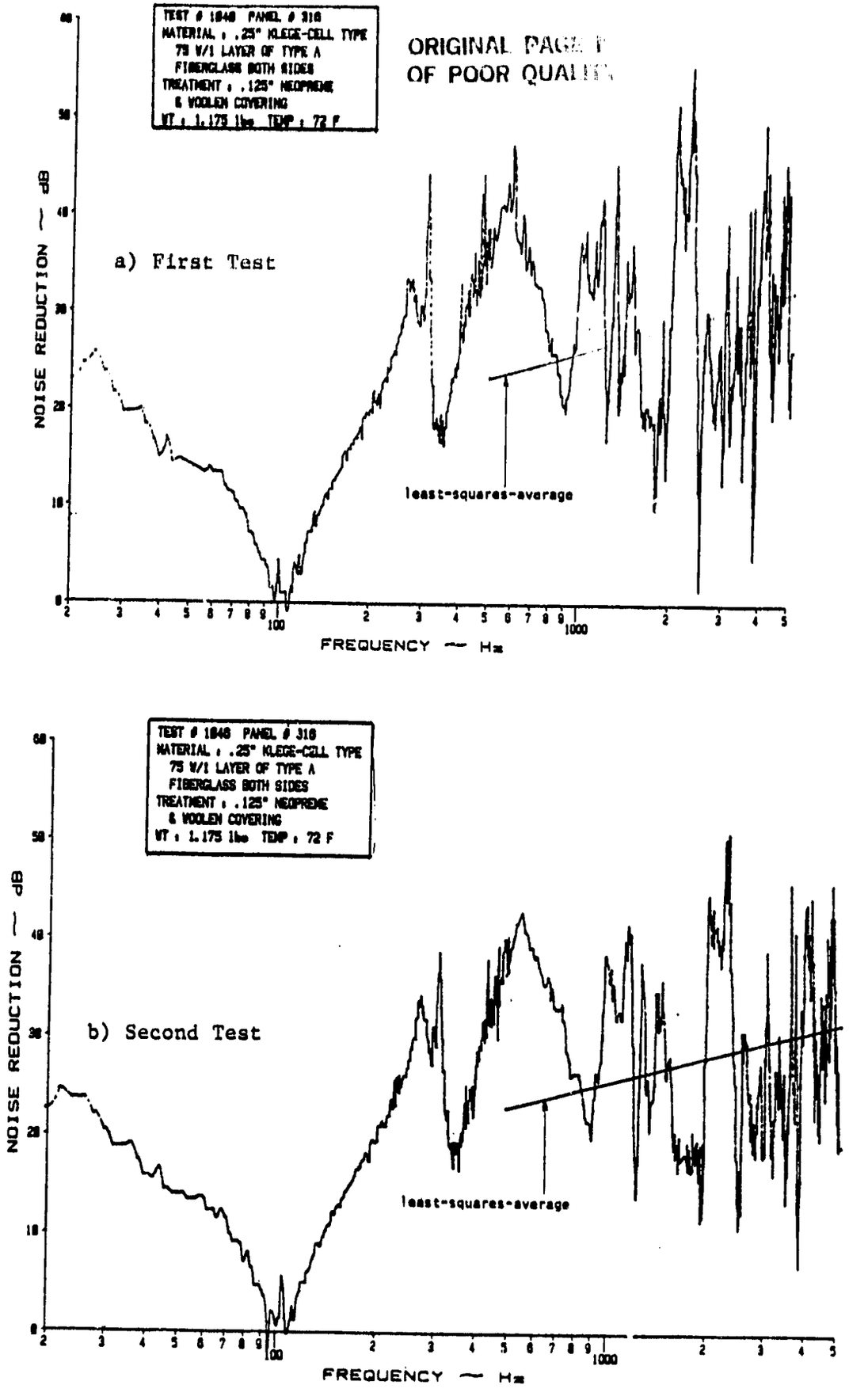

Figure C.6 Noise Reduction Characteristics of a Sandwich Panel with a .25" Klege-Cell Type 75 Core and 1 Layer of Type A Fiberglass on Both Sides and a .125" Neoprene and Woolen Covering as Treatment

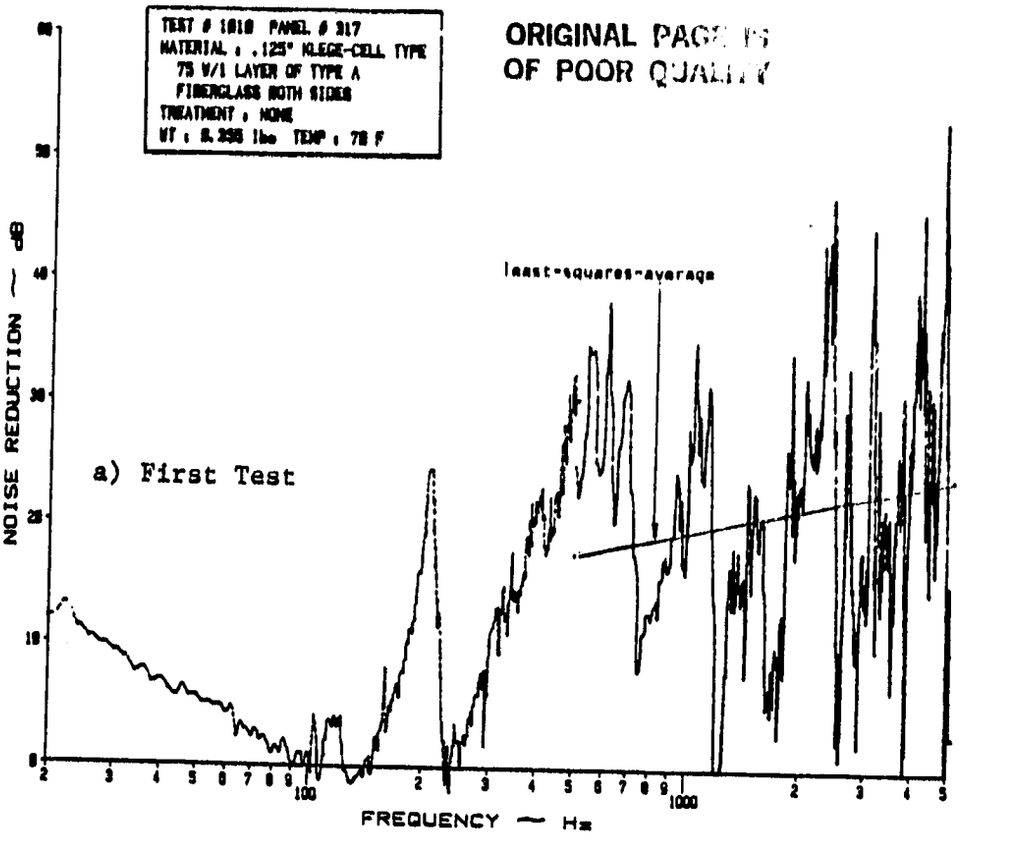

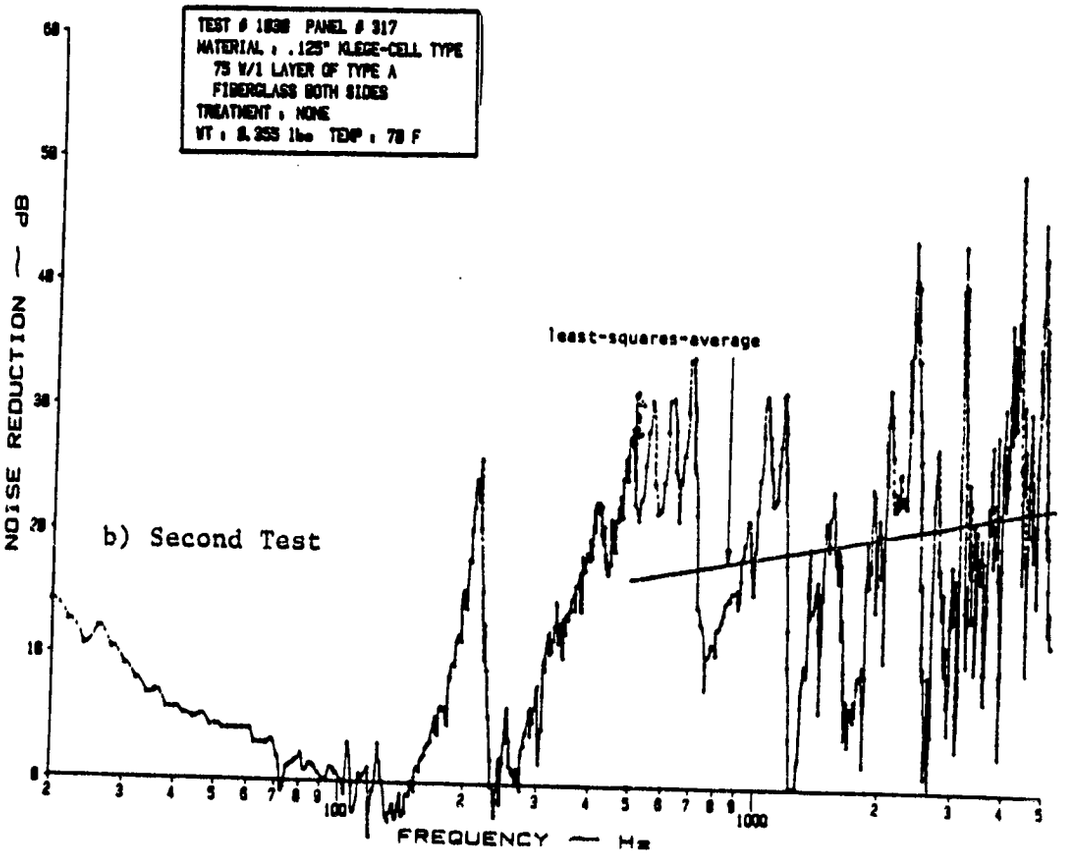

Figure C.7 Noise Reduction Characteristics of a Sandwich Panel with a .125" Klege-Cell Type 75 Core and 1 Layer of Type A Fiberglass on Both Sides and with No Treatment

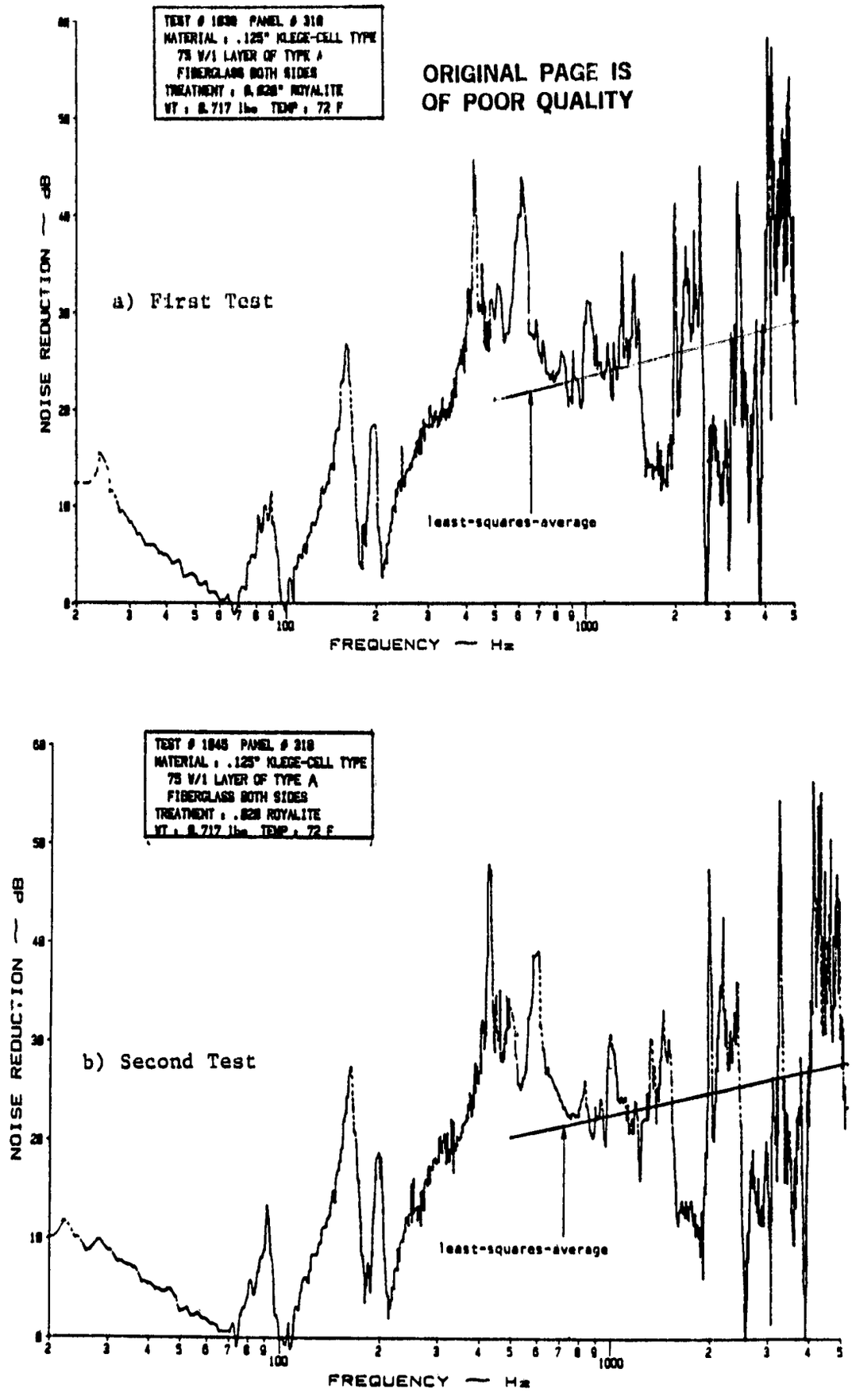

Figure C.8 Noise Reduction Characteristics of a Sandwich Panel with a .125" Klege-Cell Type 75 Core and 1 Layer of Type A Fiberglass on Both Sides and a .020" Royalite Cover as Treatment

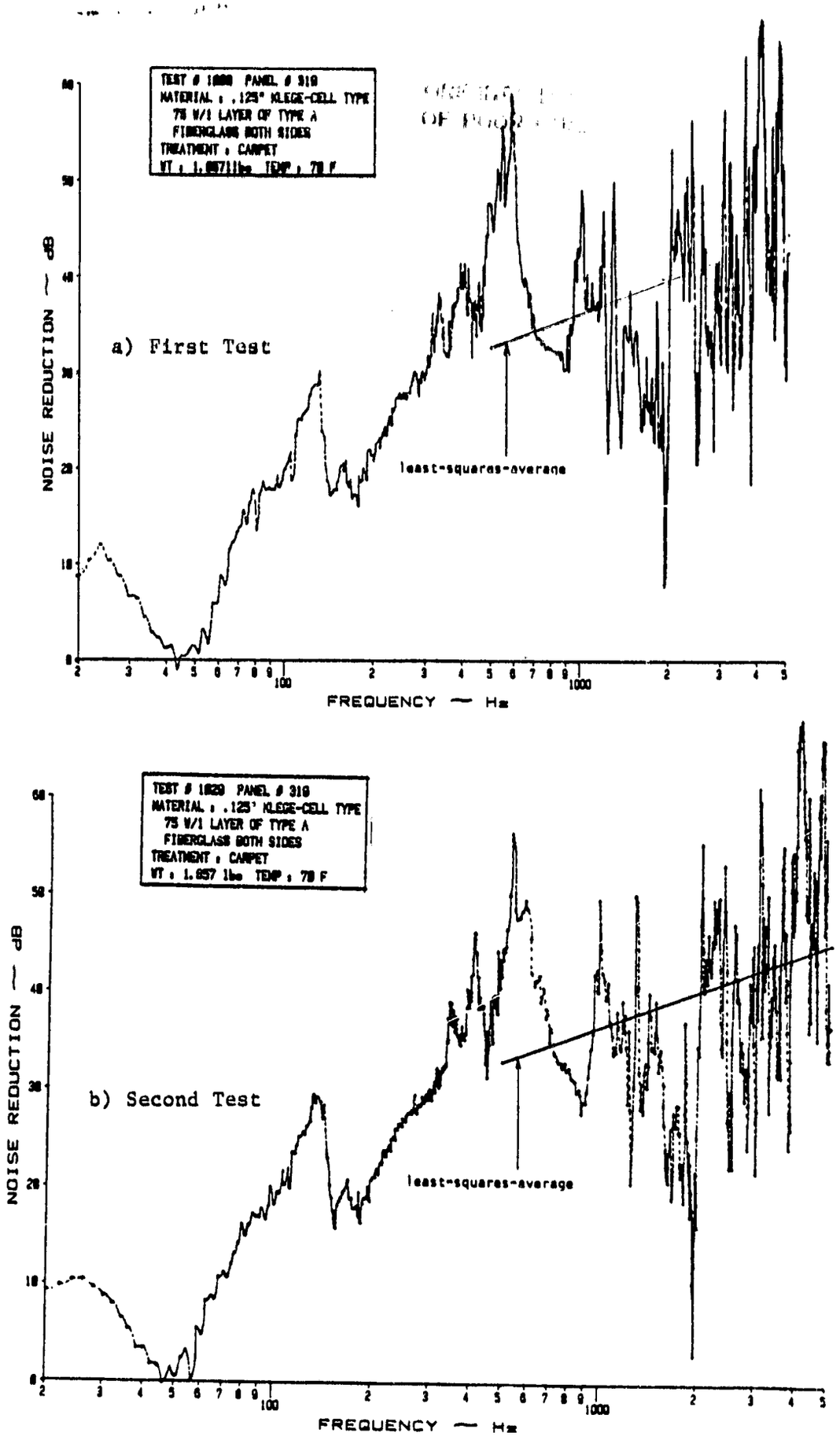

Figure C.9 Noise Reduction Characteristics of a Sandwich Panel with a .125" Klege-Cell Type 75 Core and 1 Layer of Type A Fiberglass on Both Sides and Carpet as Treatment

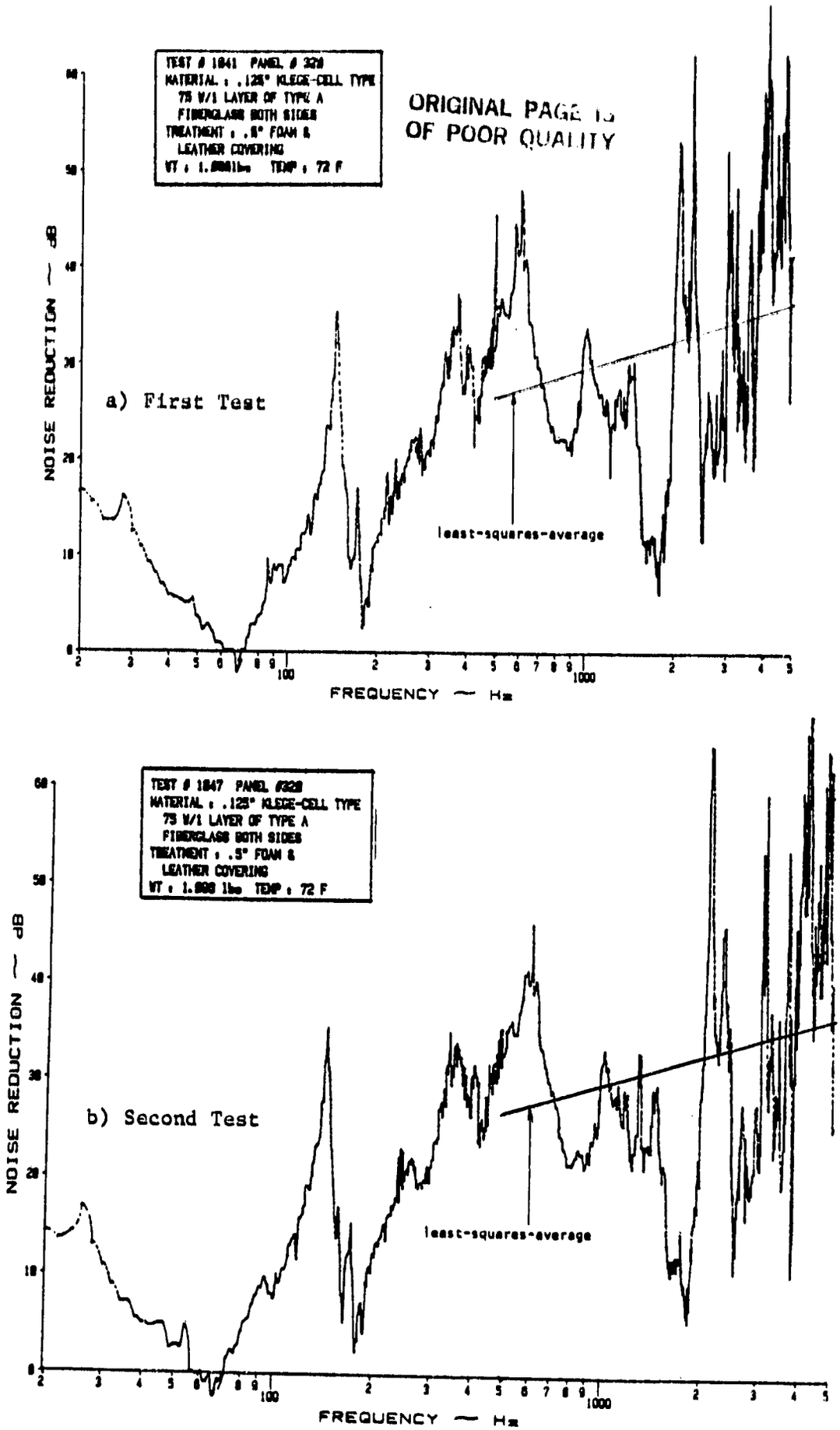

Figure C.10 Noise Reduction Characteristics of a Sandwich Panel with a .125" Klege-Cell Type 75 Core and 1 Layer of Type A Fiberglass on Both Sides and .5" Foam and Leather Covering

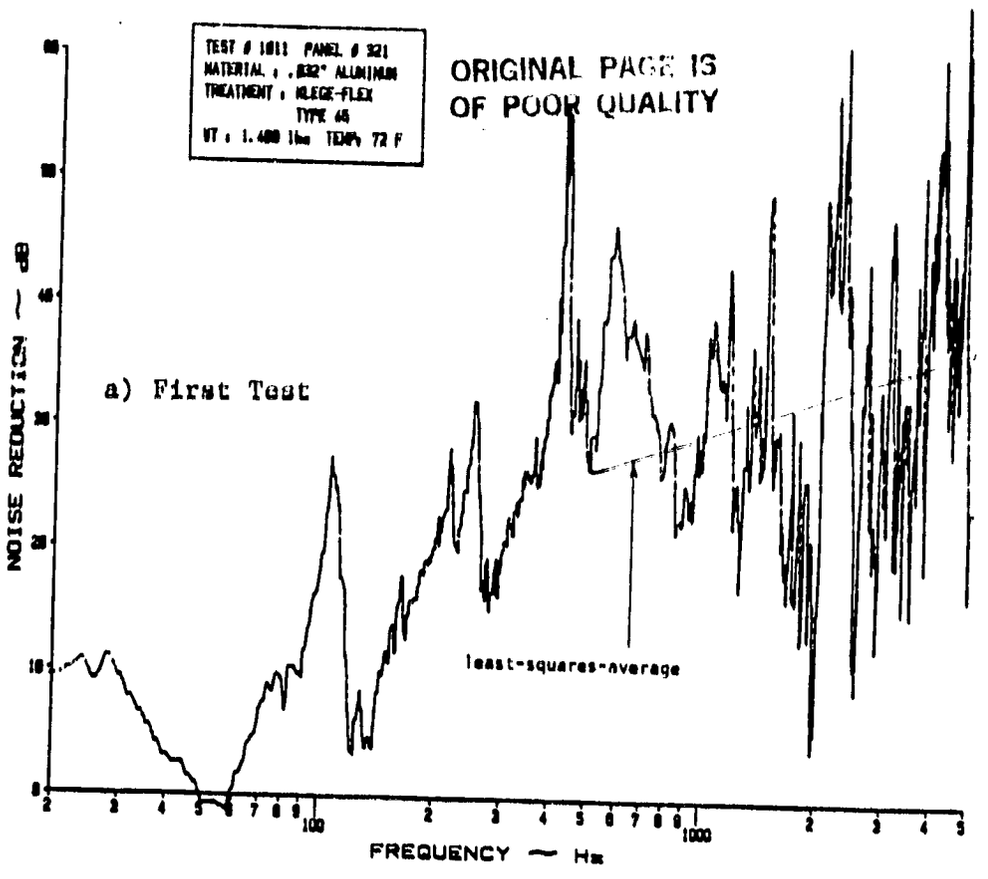

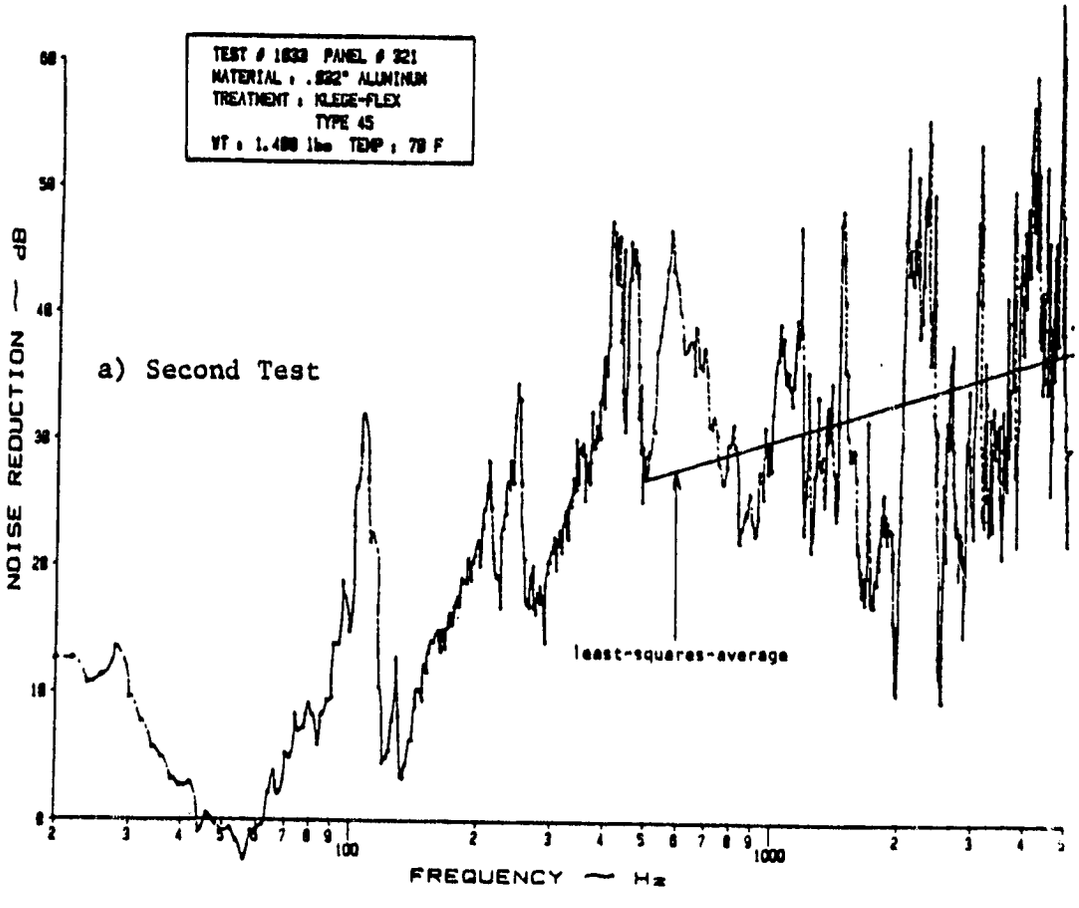

Figure C.11 Noise Reduction Characteristics of a .032" Aluminum Panel with Klege-Flex Type 45 as Treatment

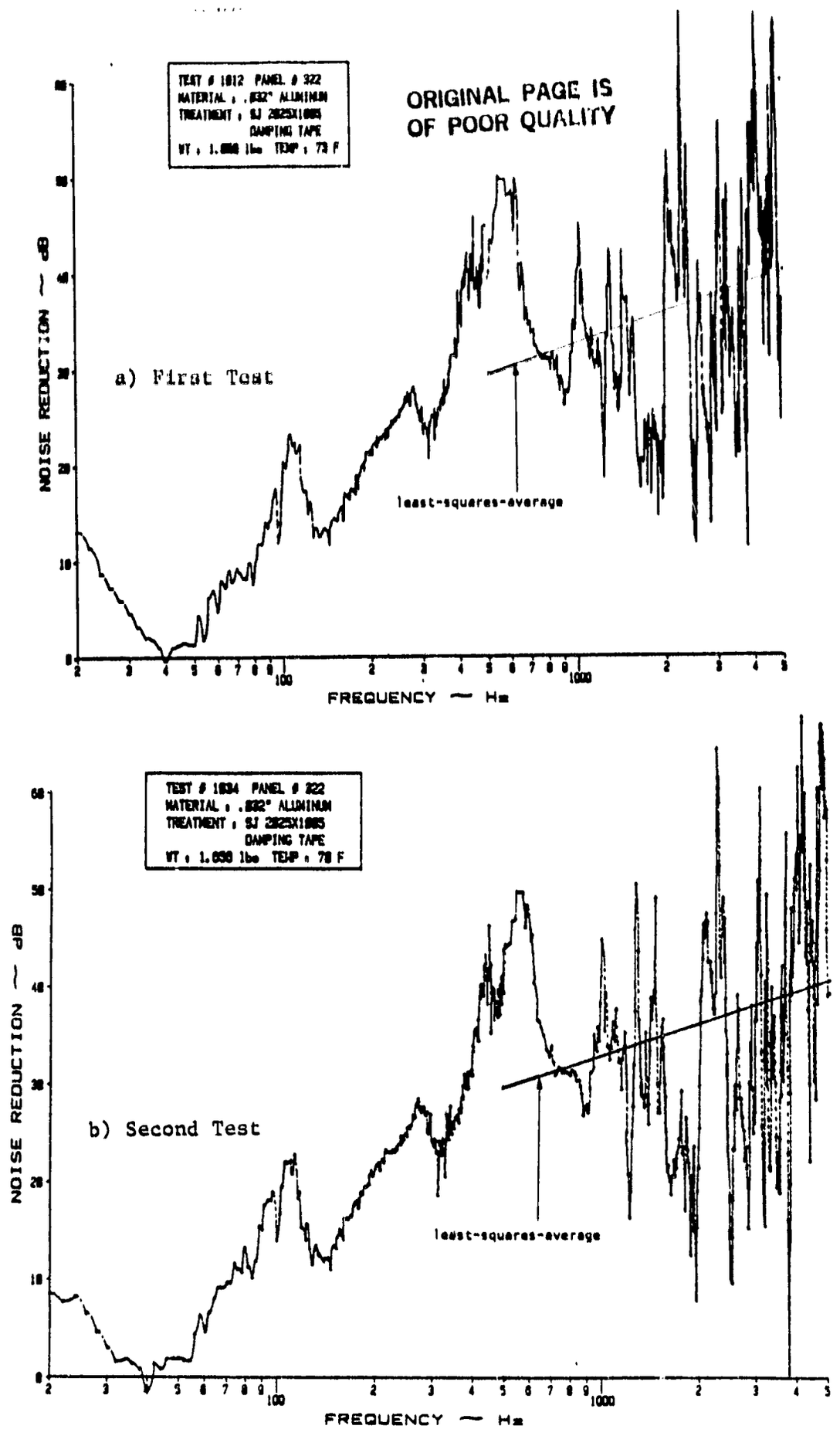

Figure C.12 Noise Reduction Characteristics of a .032" Aluminum Panel with SJ2025x1005 Damping Tape as Treatment

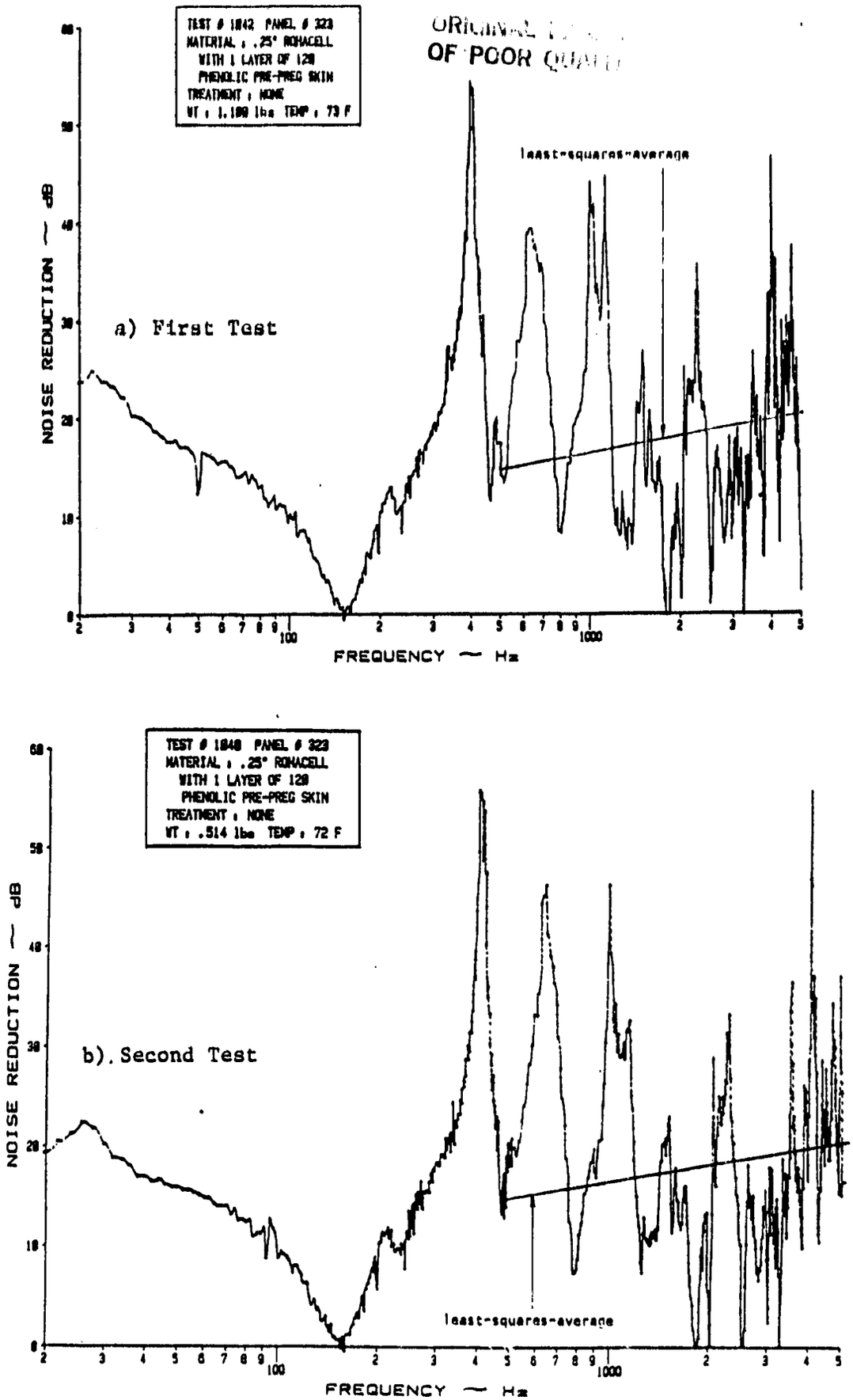

Figure C.13 Noise Reduction Characteristics of a Sandwich Panel with a .25" Rohacell Core and 1 Layer of 120 Phenolic Pre-Preg Skin on Both Sides and No Treatment

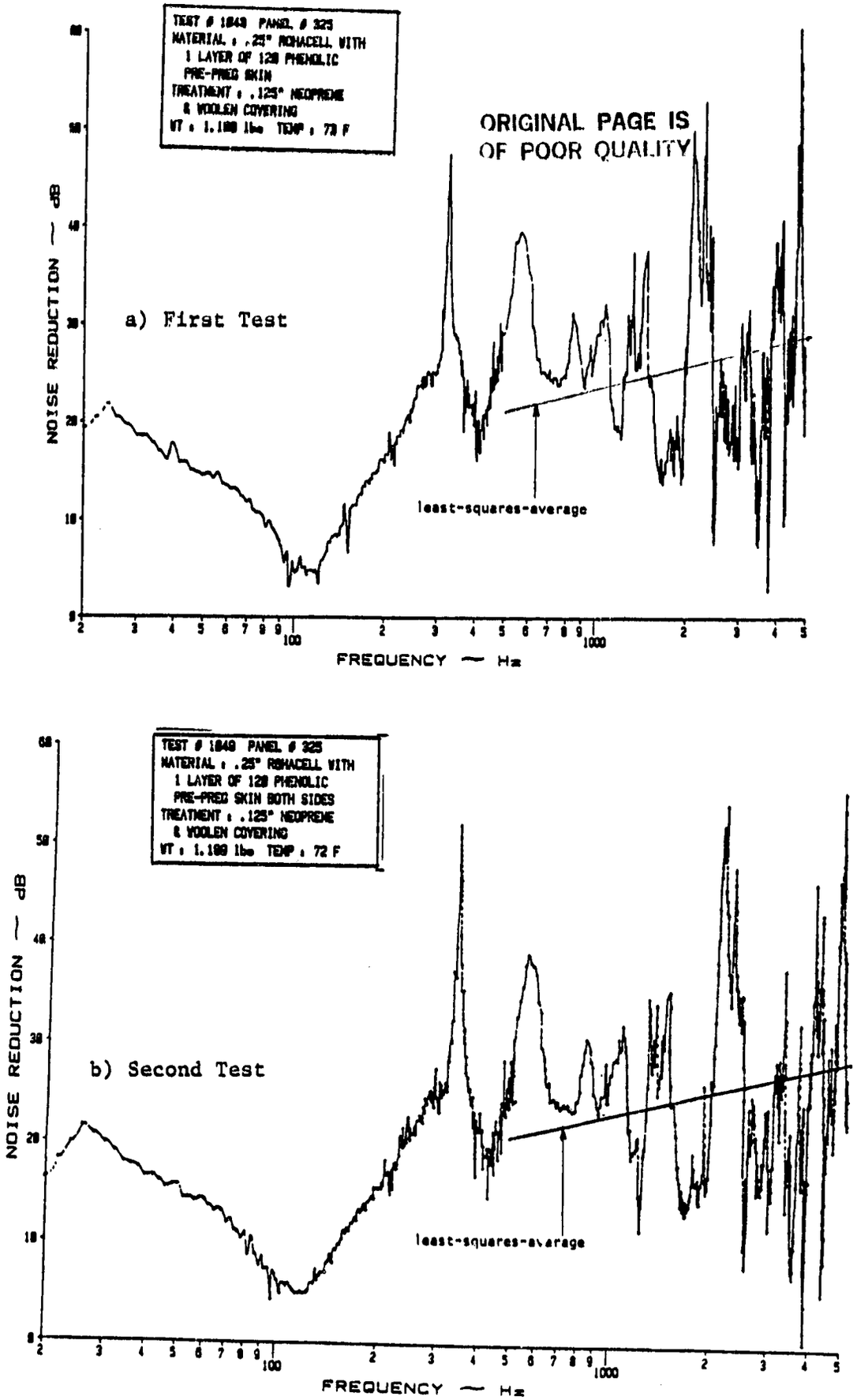

Figure C.14 Noise Reduction Characteristics of a Sandwich Panel with a .25" Rohacell Core and 1 Layer of 120 Phenolic Pre-Preg Skin on Both Sides and a .125" Neoprene and Woolen Covering as Treatment

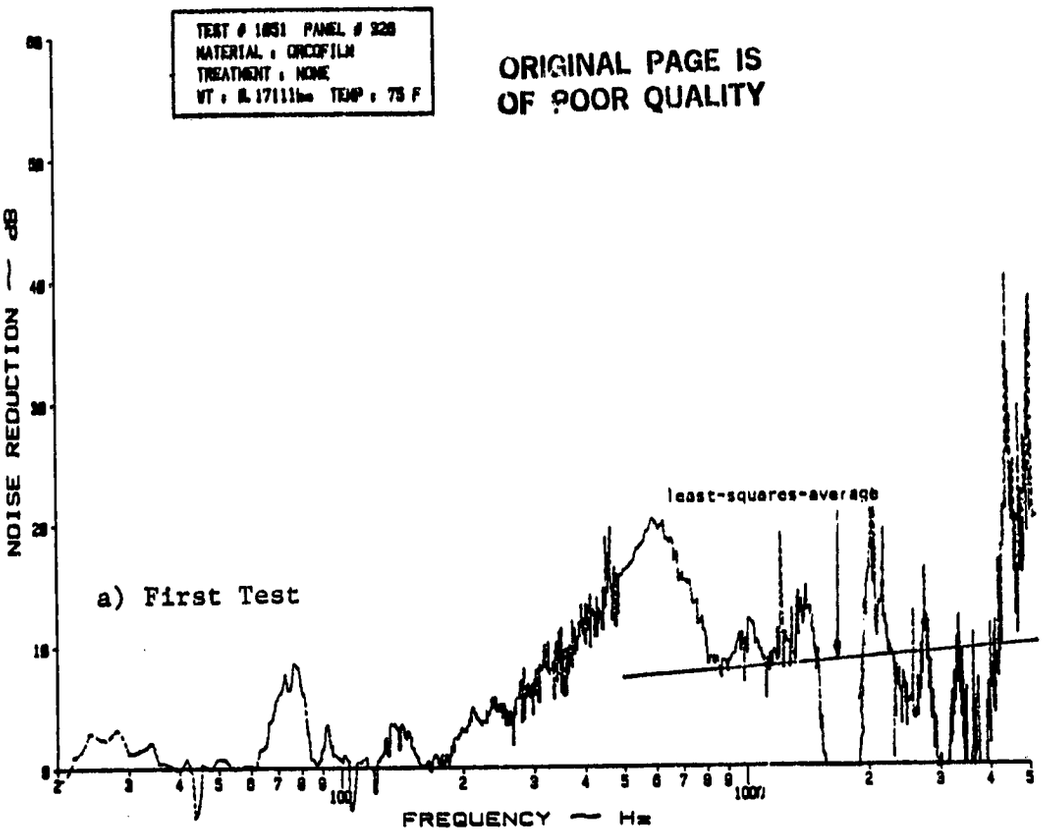

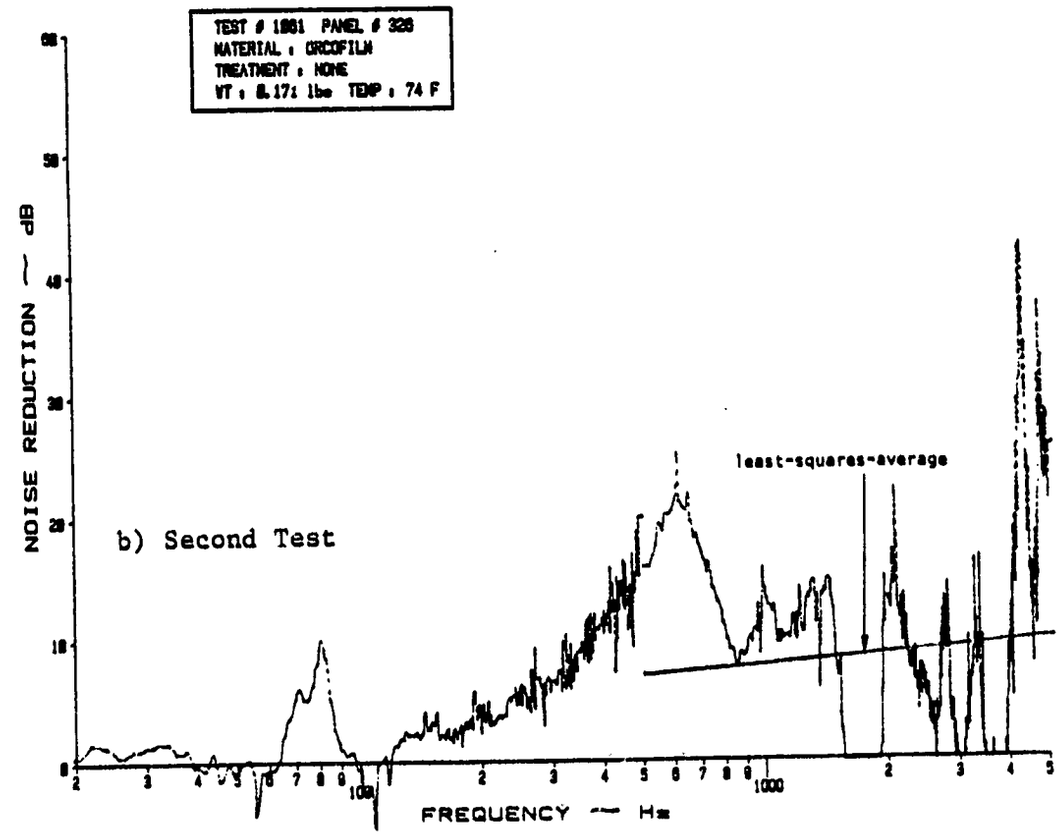

Figure C.15 Noise Reduction Characteristics of a .5" Thermal Blanket Contained in a Bag of Orcofilm

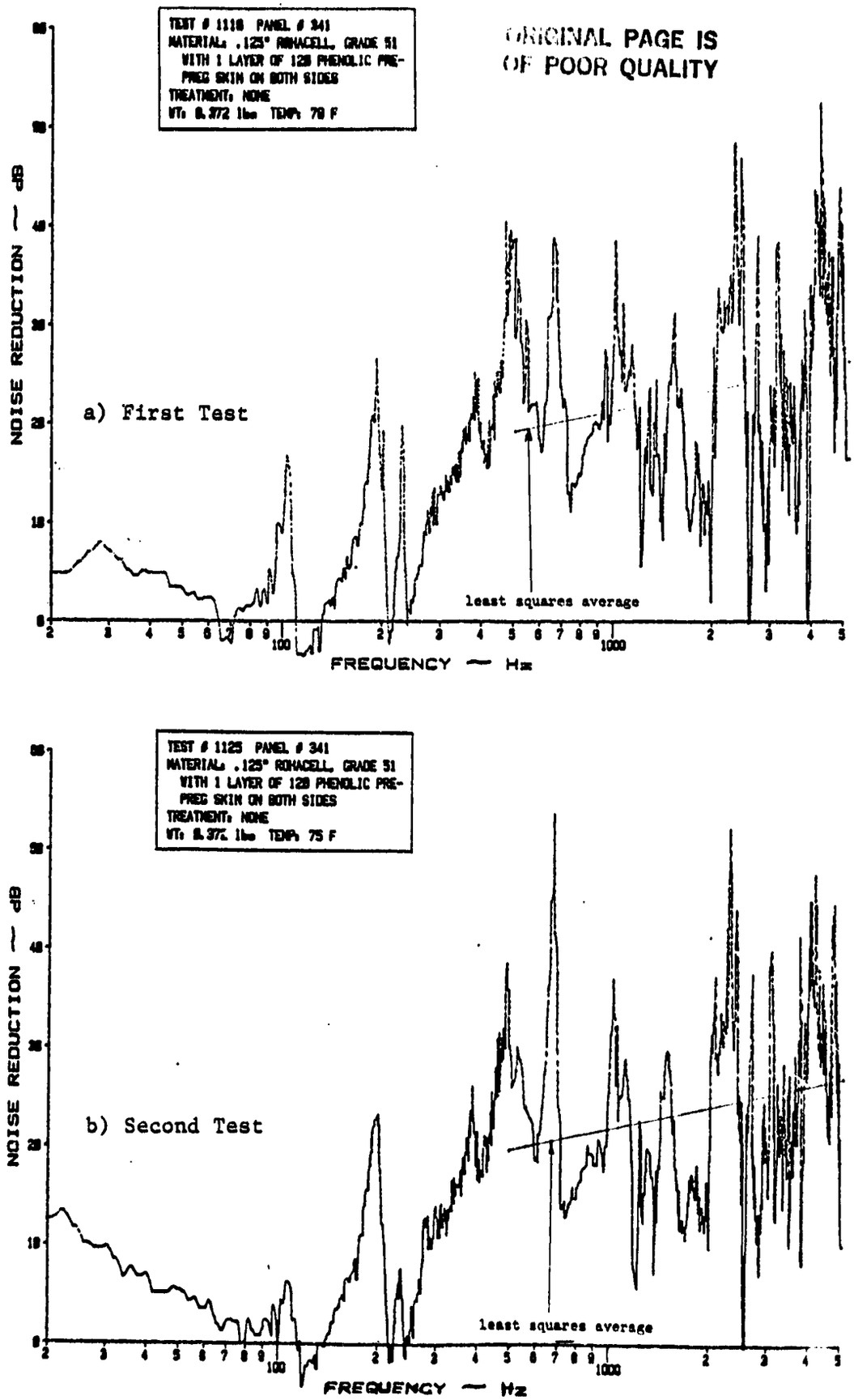

Figure C.16 Noise Reduction Characteristics of a Sandwich Panel with a .125" Rohacell Core and 1 Layer of 120 Phenolic Pre-Preg Skin on Both Sides with No Treatment

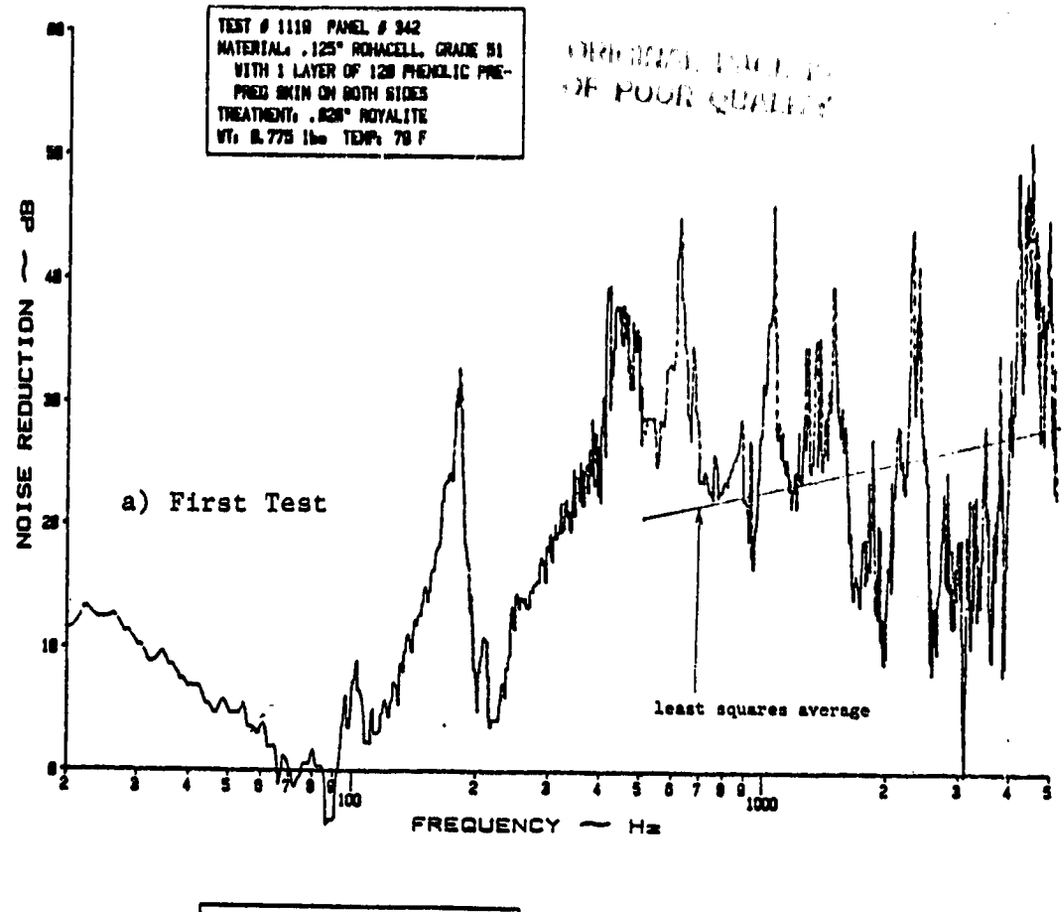

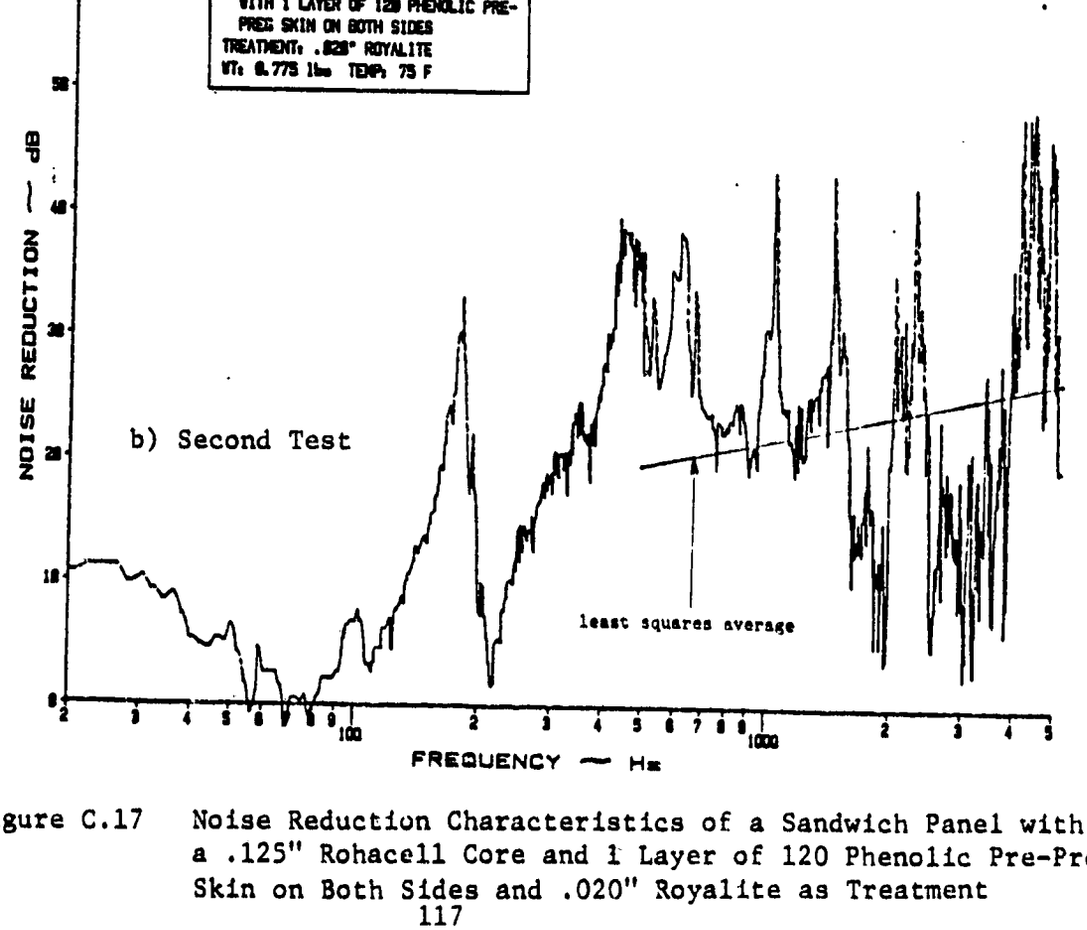

Figure C.17 Noise Reduction Characteristics of a Sandwich Panel with a .125" Rohacell Core and 1 Layer of 120 Phenolic Pre-Preg Skin on Both Sides and .020" Royalite as Treatment

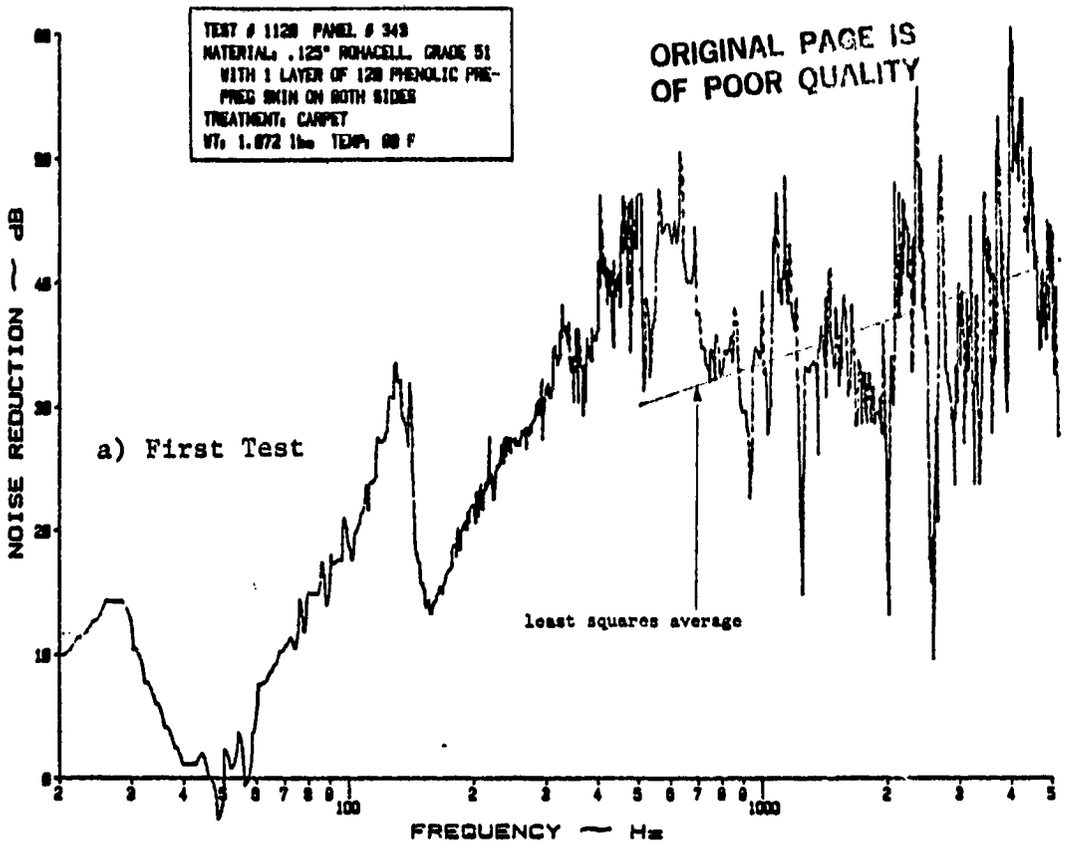

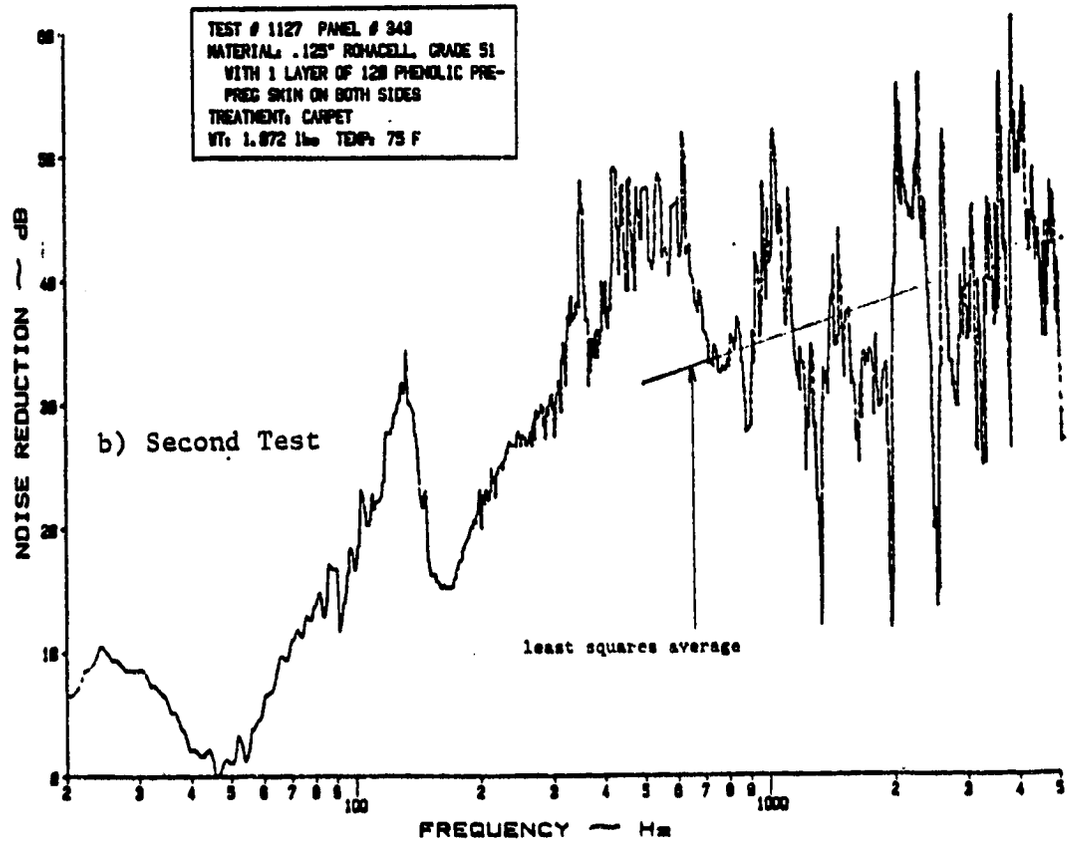

Figure C.18 Noise Reduction Characteristics of a Sandwich Panel with a .125" Rohacell Core with 1 Layer of 120 Phenolic Pre-Preg Skin on Both Sides and Carpet as Treatment

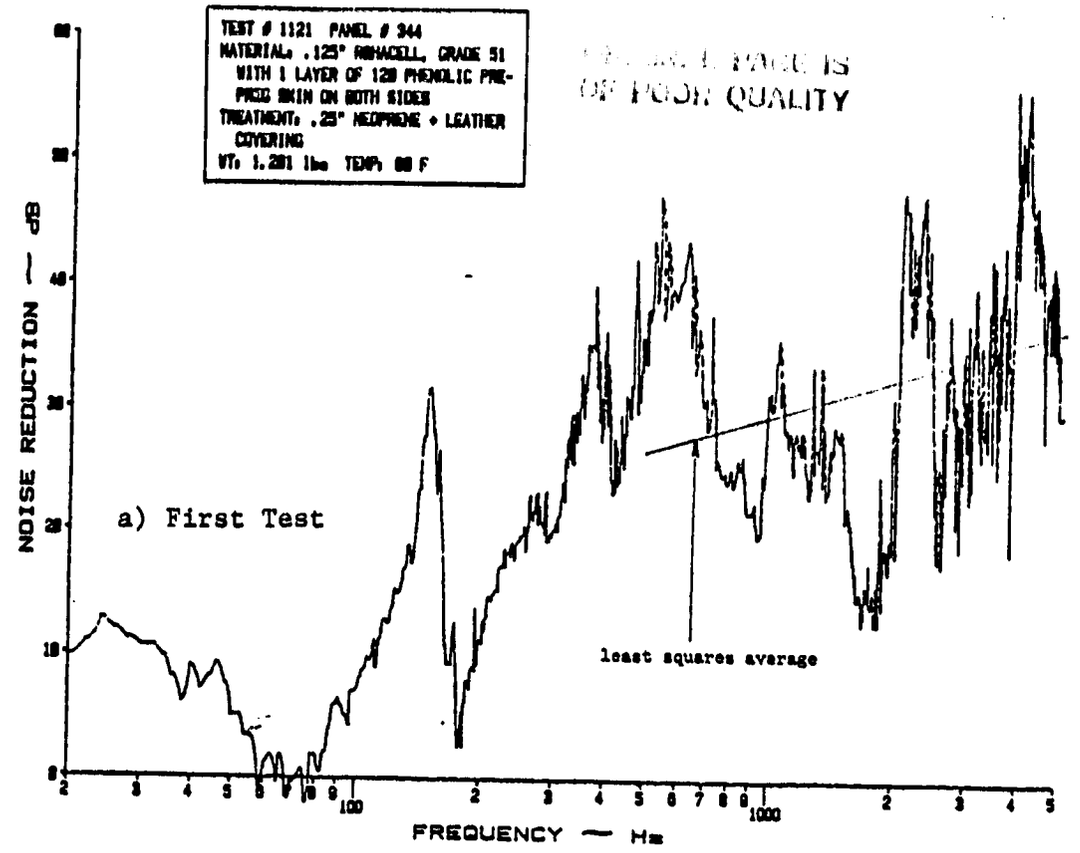

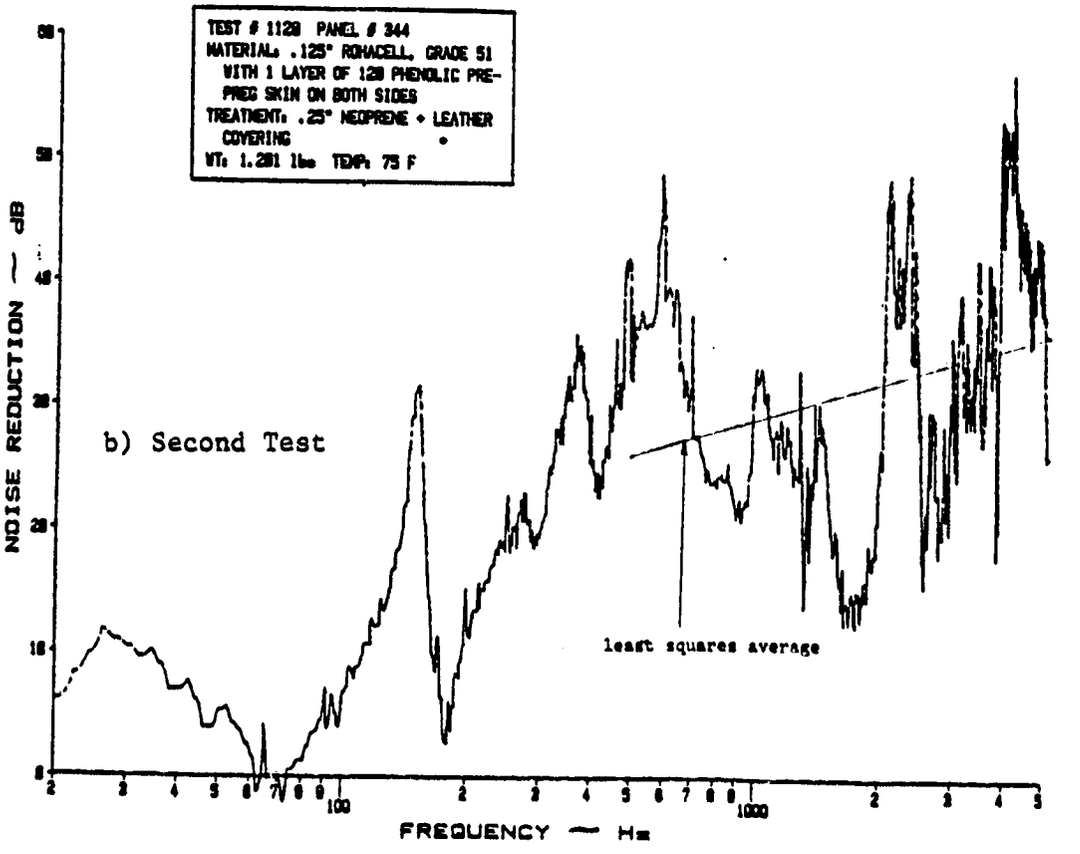

Figure C.19 Noise Reduction Characteristics of a Sandwich Panel with a .125" Rohacell Core with 1 Layer of 120 Phenolic Pre-Preg Skin on Both Sides and .25" Neoprene + Leather Covering as Treatment

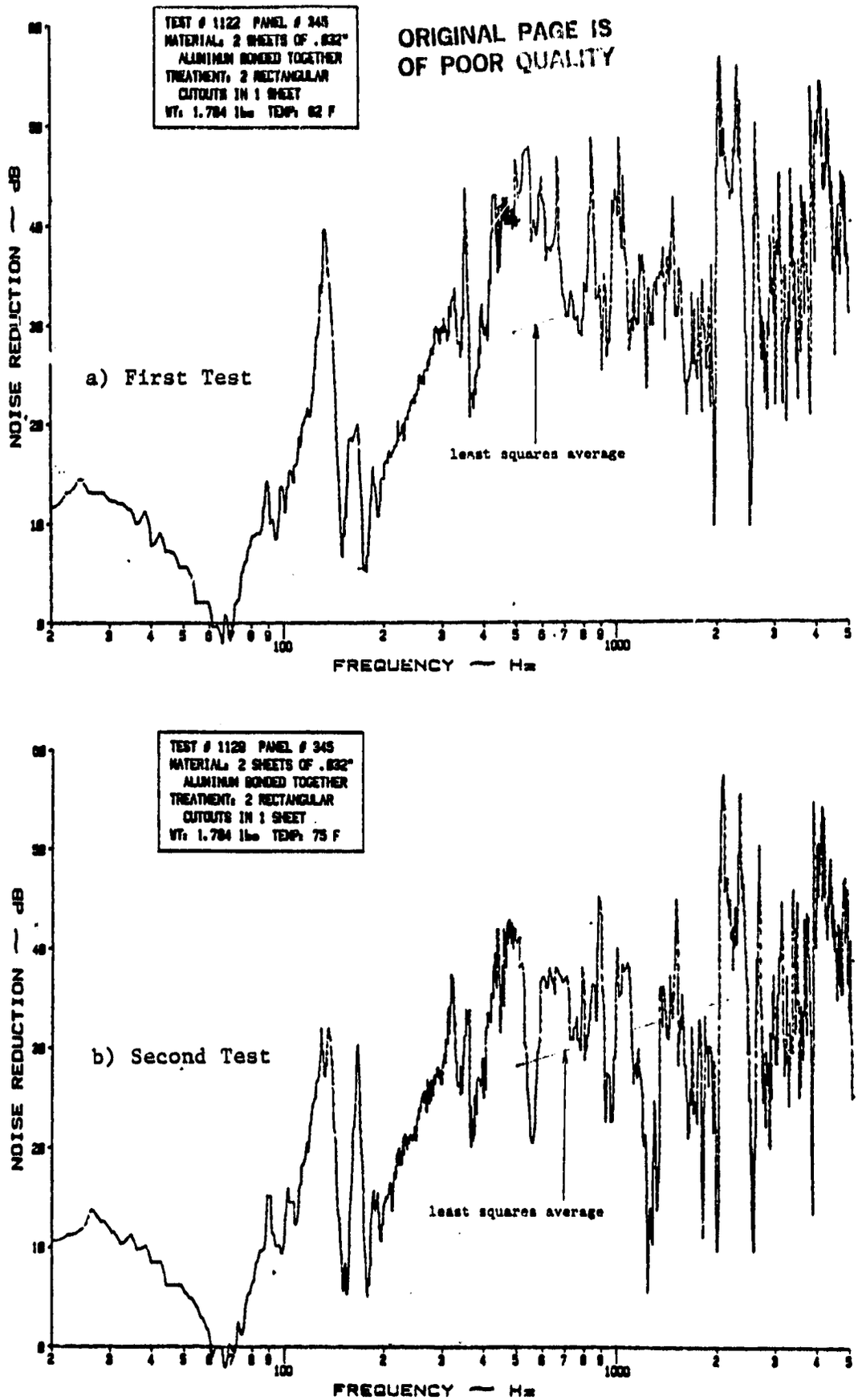

Figure C.20 Noise Reduction Characteristics of Two Sheets of Aluminum Bonded Together with Two Rectangular Cutouts in one Sheet

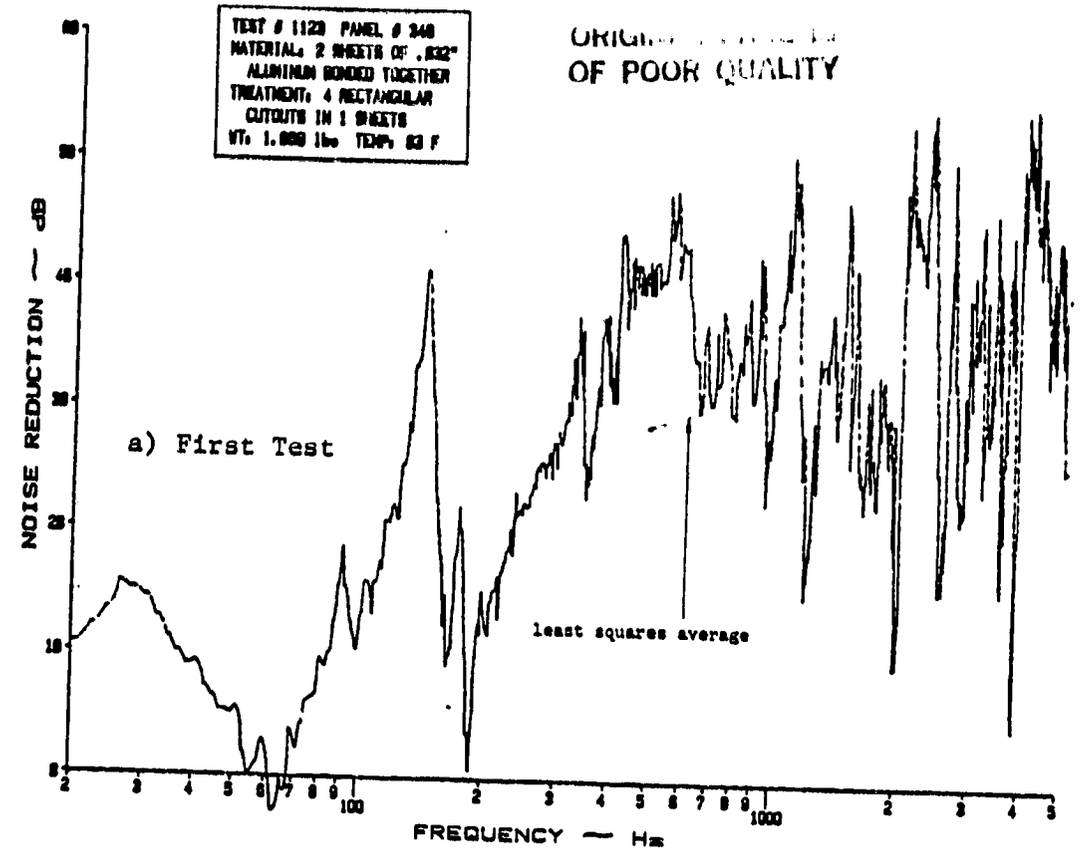

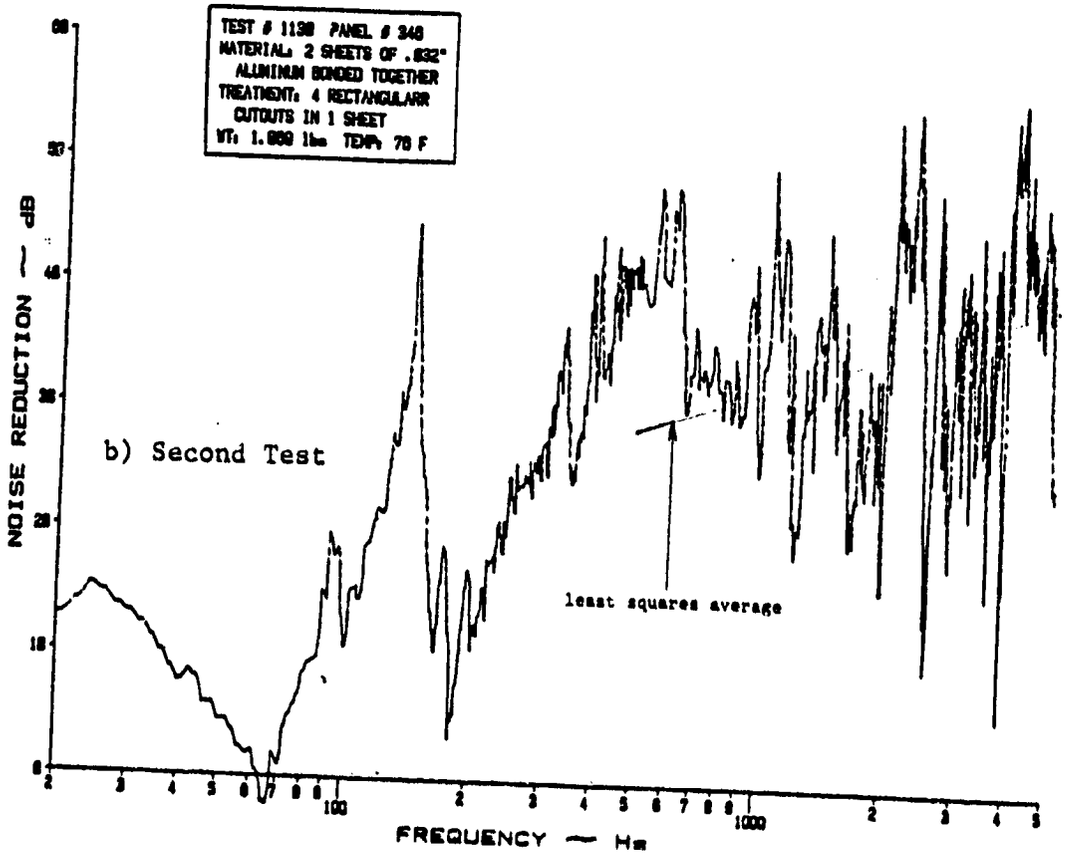

Figure C.21 Noise Reduction Characteristics of Two Sheets of Aluminum Bonded Together with Four Rectangular Cutouts in One Sheet

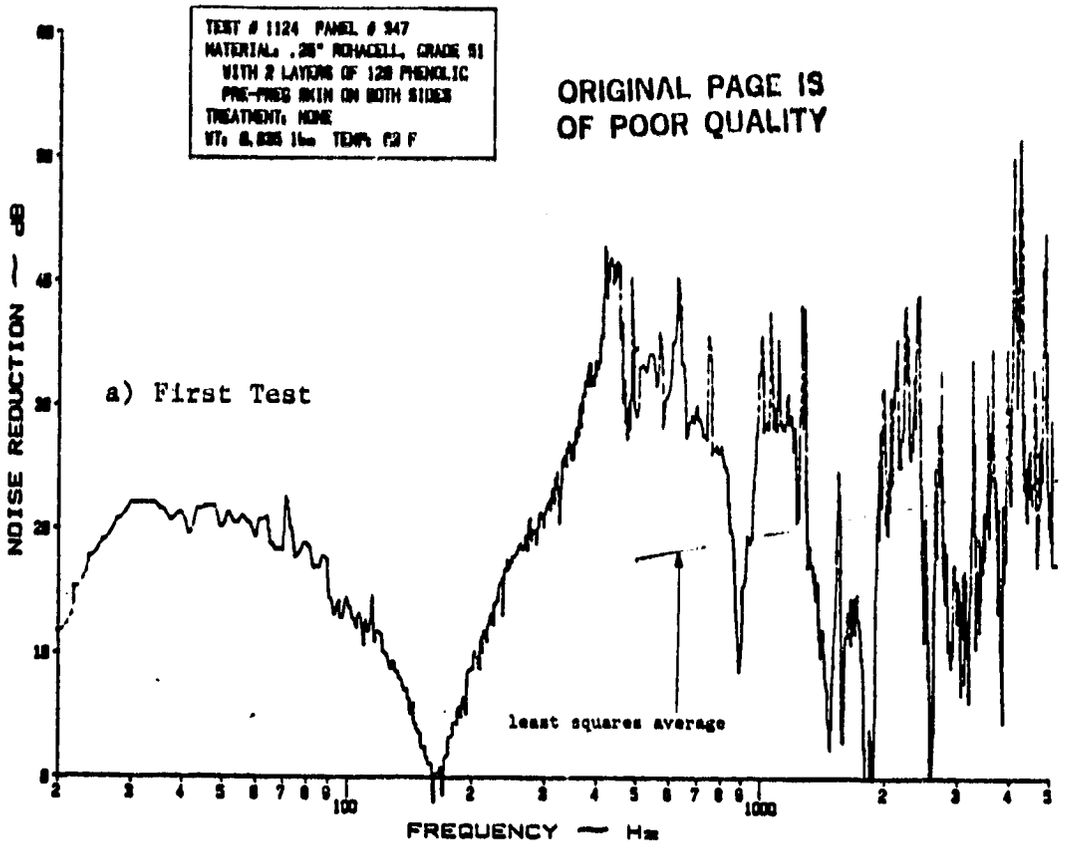

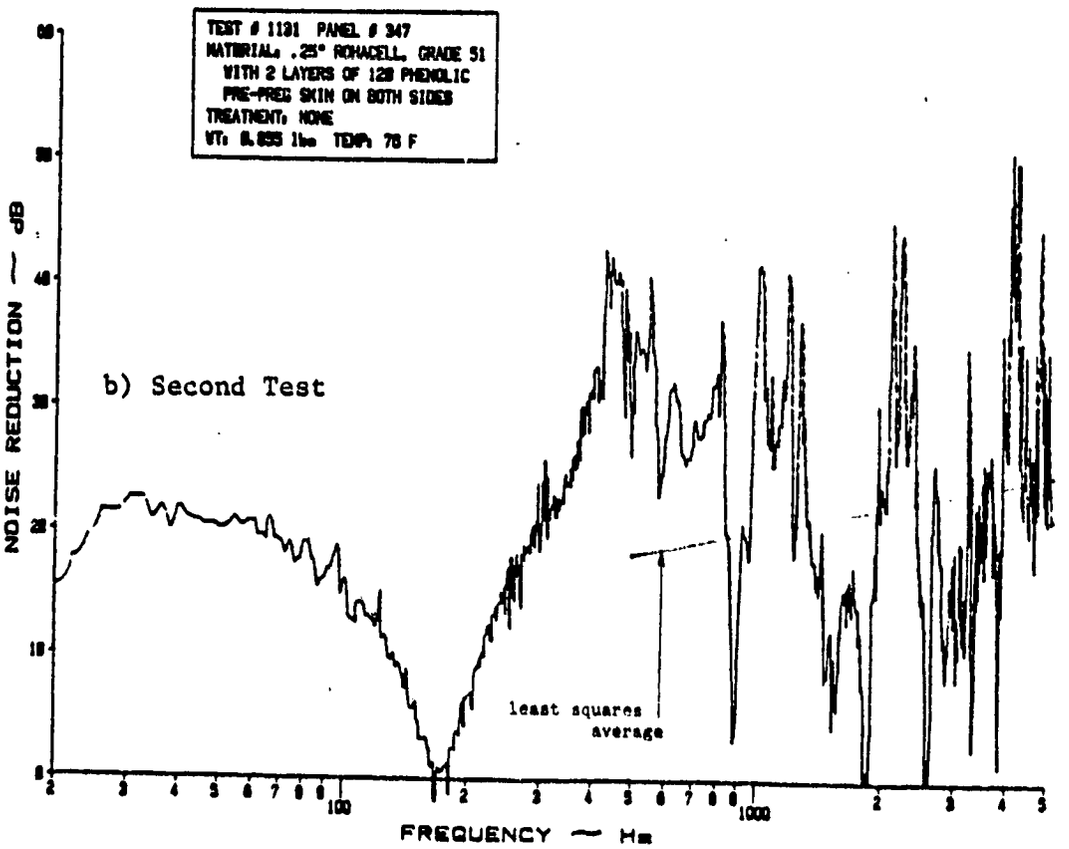

Figure C.22 Noise Reduction Characteristics of a Sandwich Panel with a .25" Rohacell Core and 2 Layers of 120 Phenolic Pre-Preg Skin on Both Sides and No Treatment

APPENDIX D

EXPERIMENTAL NOISE REDUCTION DATA

FOR TUNED DAMPER TESTS

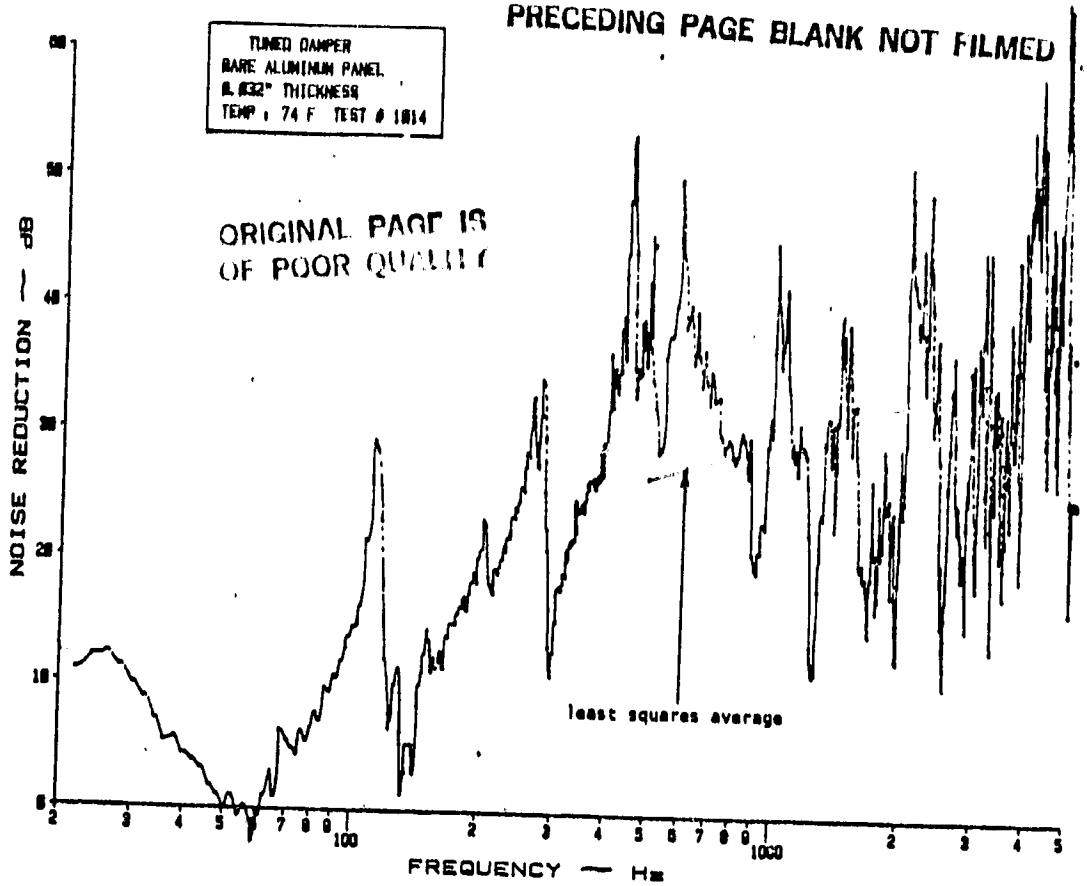

Figure D.1 Noise Reduction Characteristics of a .032" Aluminum Panel without a Tuned Damper.

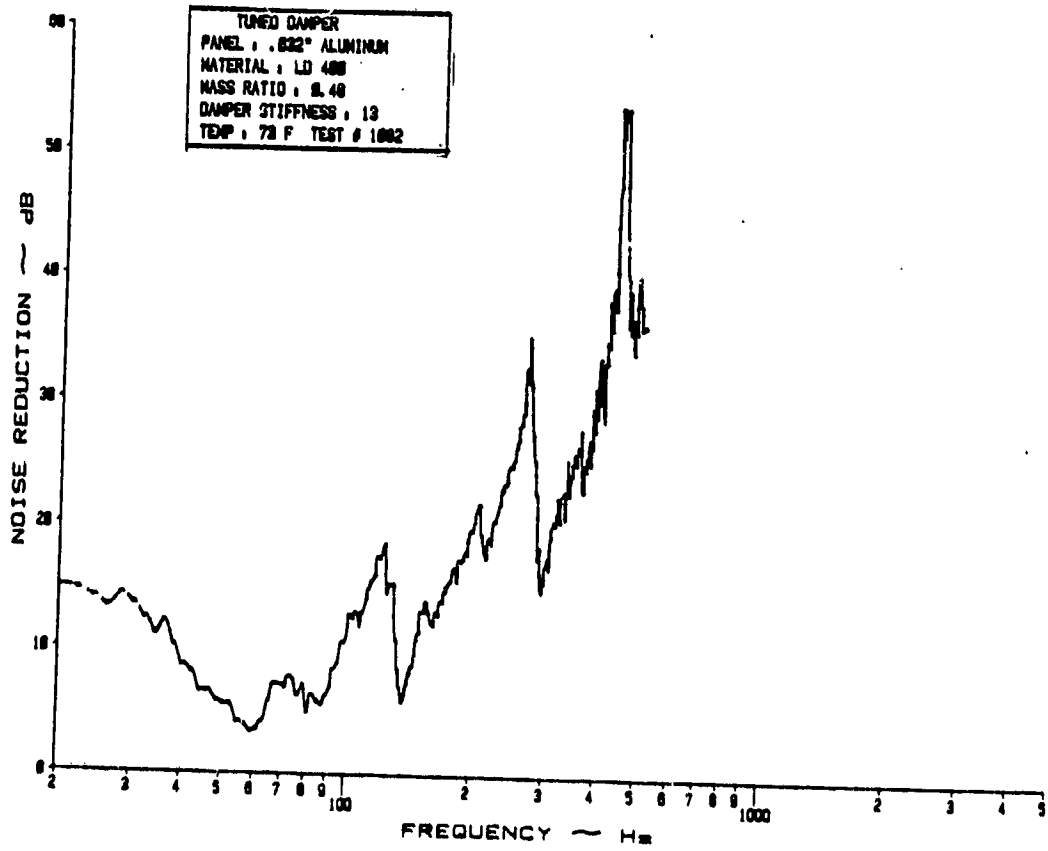

Figure D.2 Noise Reduction Characteristics of a .032" Aluminum Panel with an "LD-400" Tuned Damper; μ = .48 and K-2 = 13 lbf/in.

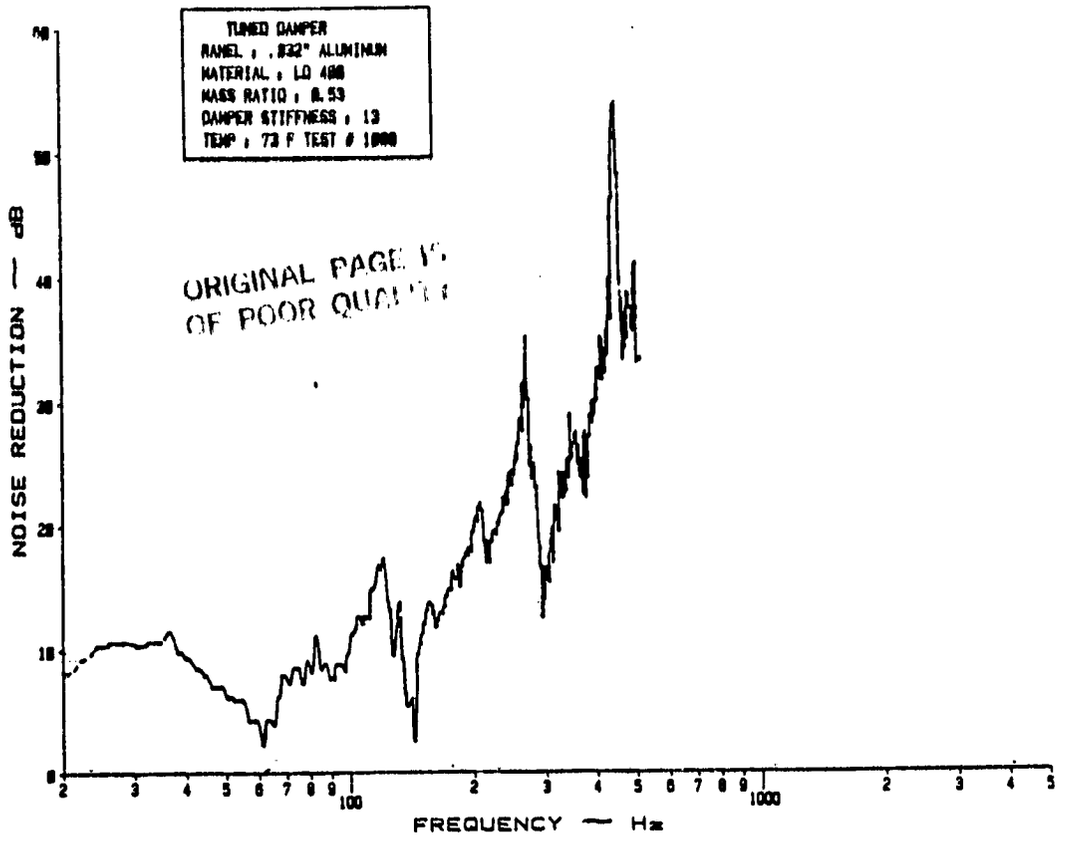

Figure D.3 Noise Reduction Characteristics of a .032" Aluminum Panel with an "LD-400" Tuned Damper; μ = .53 and K2 = 13 lbf/in.

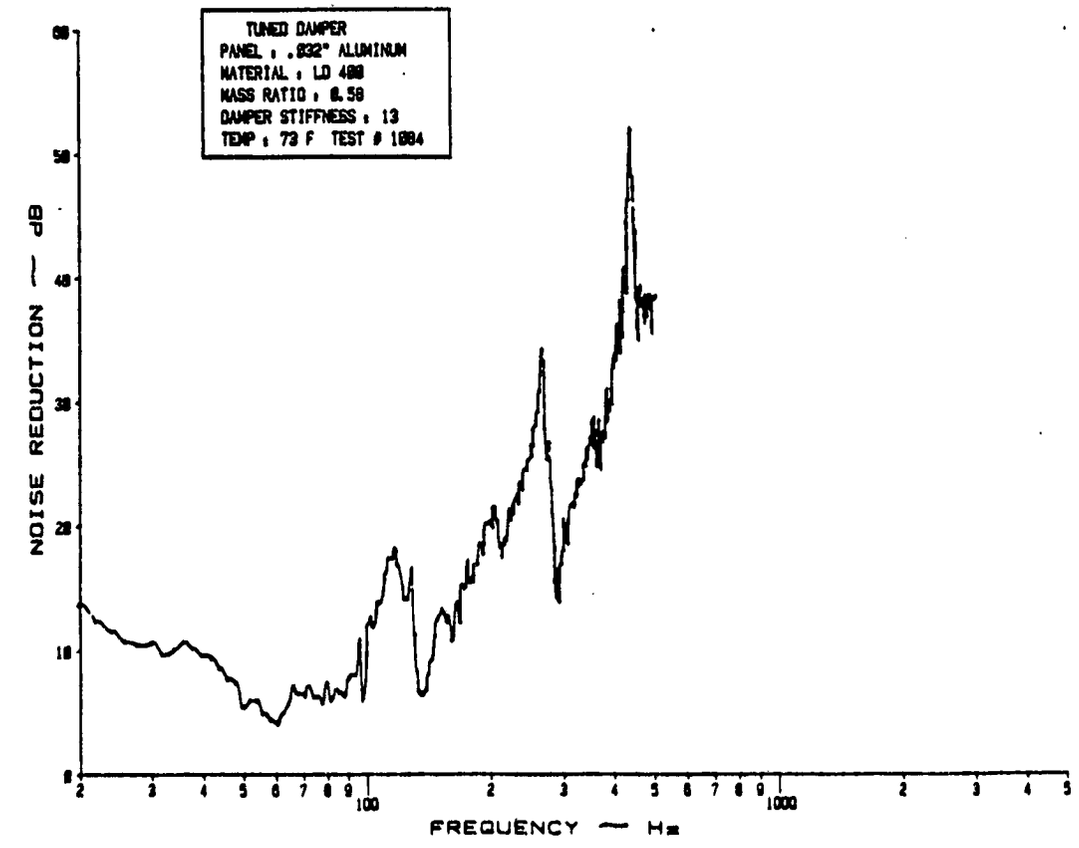

Figure D.4 Noise Reduction Characteristics of a .032" Aluminum Panel with an "LD-400" Tuned Damper; μ = .58 and K2 = 13 lbf/in.

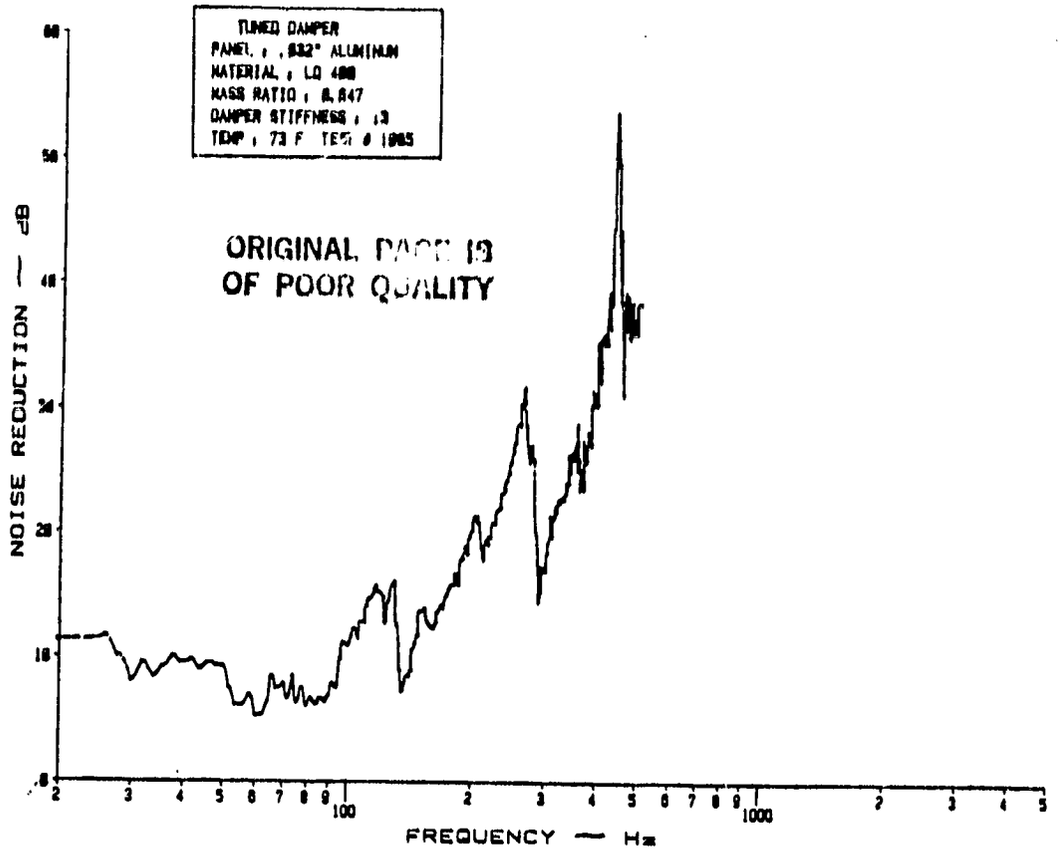

Figure D.5 Noise Reduction Characteristics of a .032" Aluminum Panel with an "LD-400" Tuned Damper; μ = .647 and K2 = 13 lbf/in.

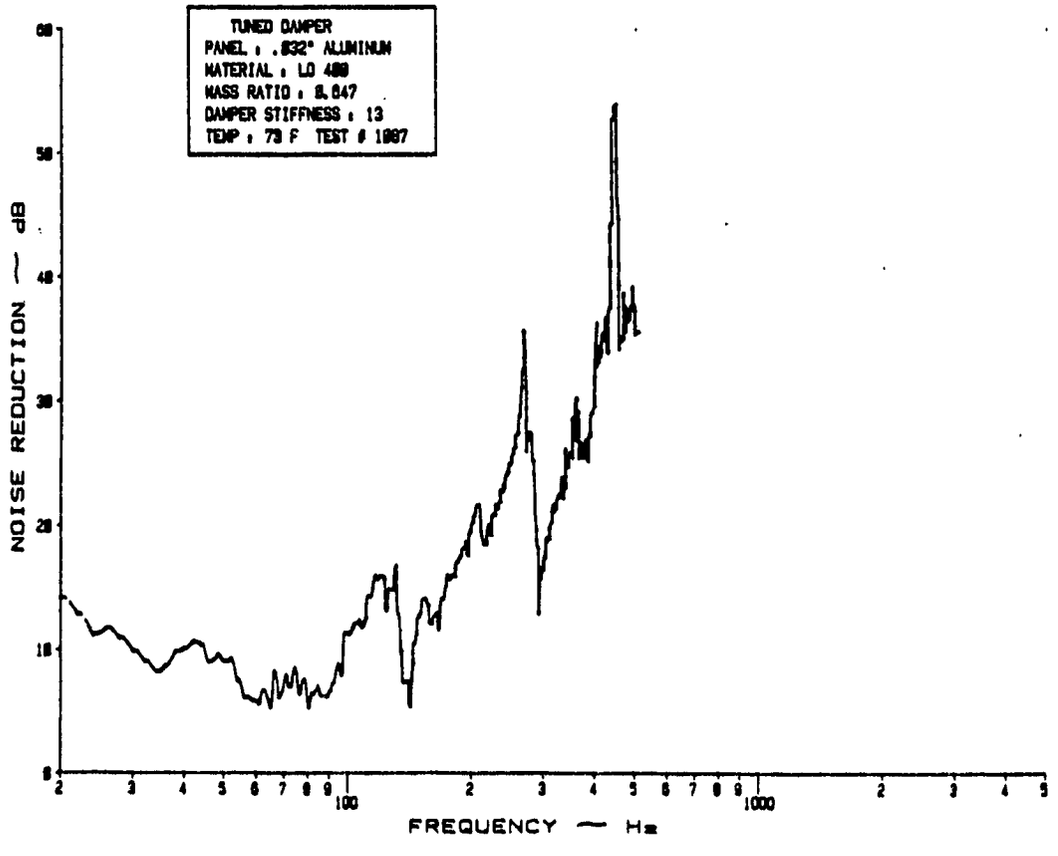

Figure D.6 Noise Reduction Characteristics of a .032" Aluminum Panel with an "LD-400" Tuned Damper; μ = .647 and K2 = 13 lbf/in.

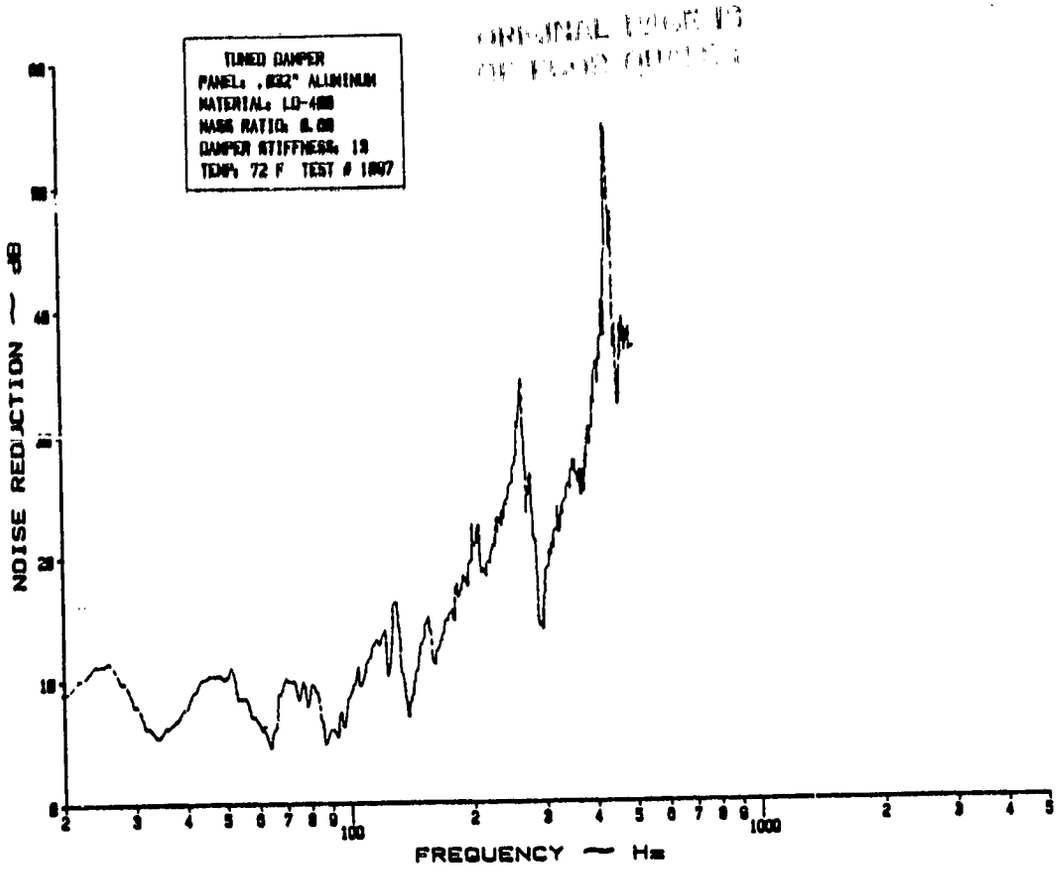

Figure D.7 Noise Reduction Characteristics of a .032" Aluminum Panel with an "LD-400" Tuned Damper; μ = .68 and K2 = 13 lbf/in.

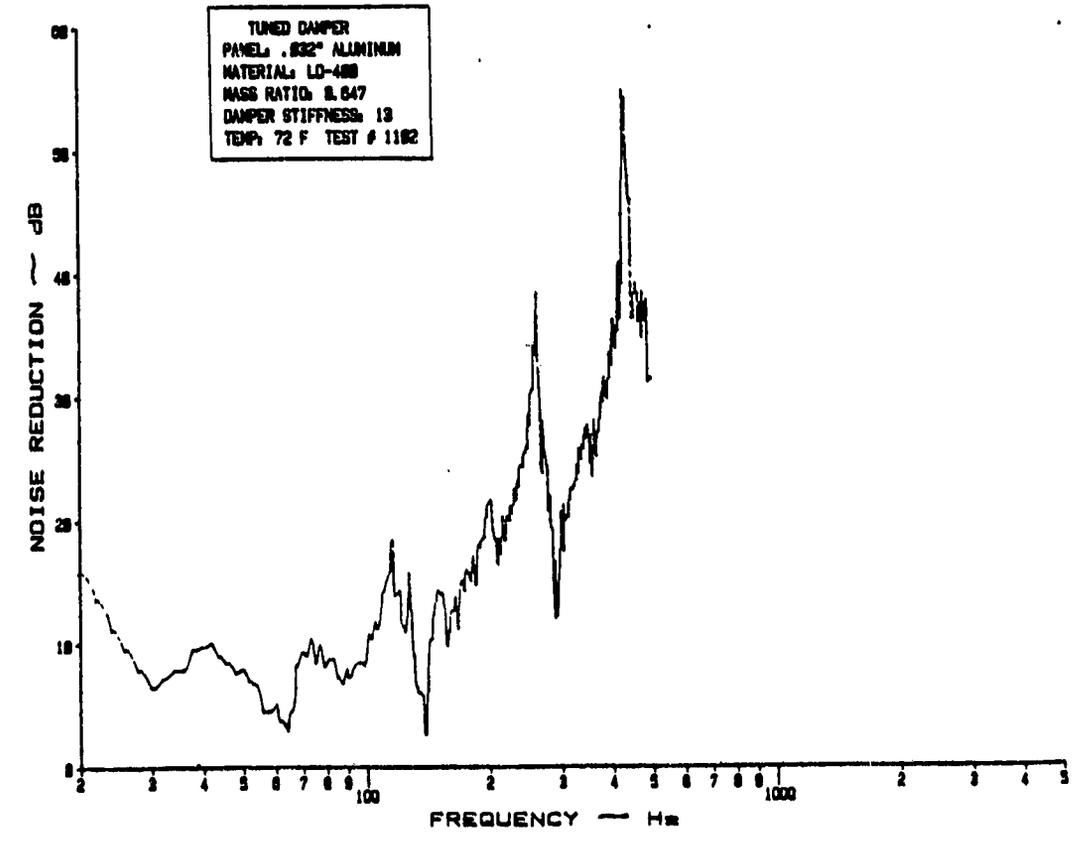

Figure D.8 Noise Reduction Characteristics of a .032" Aluminum Panel with an "LD-400" Tuned Damper; μ = .647 and K2 = 13 lbf/in.

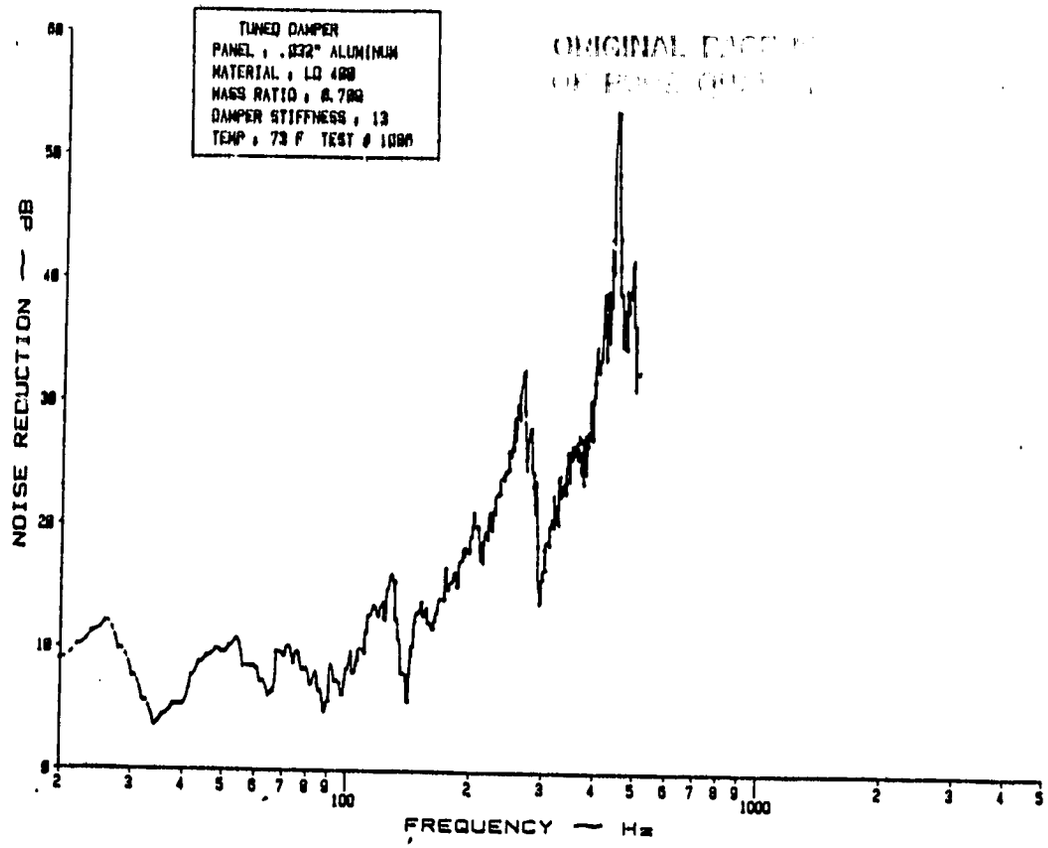

Figure D.9 Noise Reduction Characteristics of a .032" Aluminum Panel with an "LD-400" Tuned Damper; μ = .709 and K2 = 13 lbf/in.

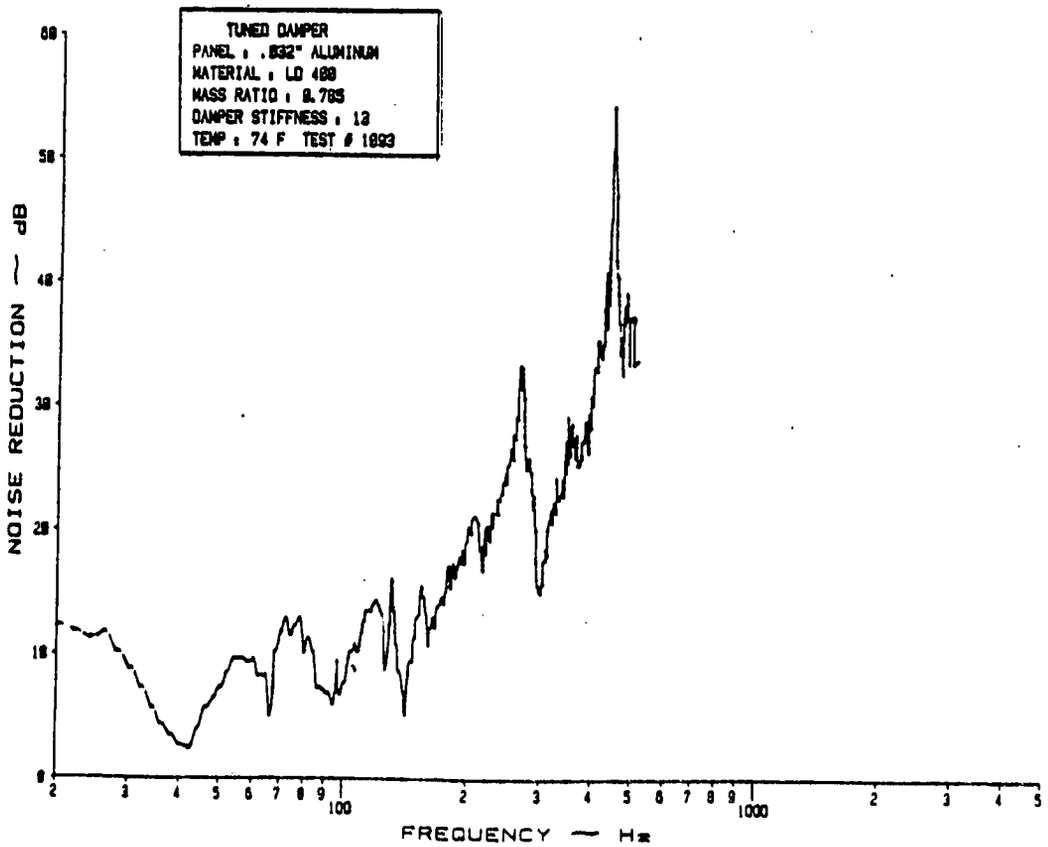

Figure D.10 Noise Reduction Characteristics of a .032" Aluminum Panel with an "LD-400" Tuned Damper; μ = .785 and K2 = 13 lbf/in.

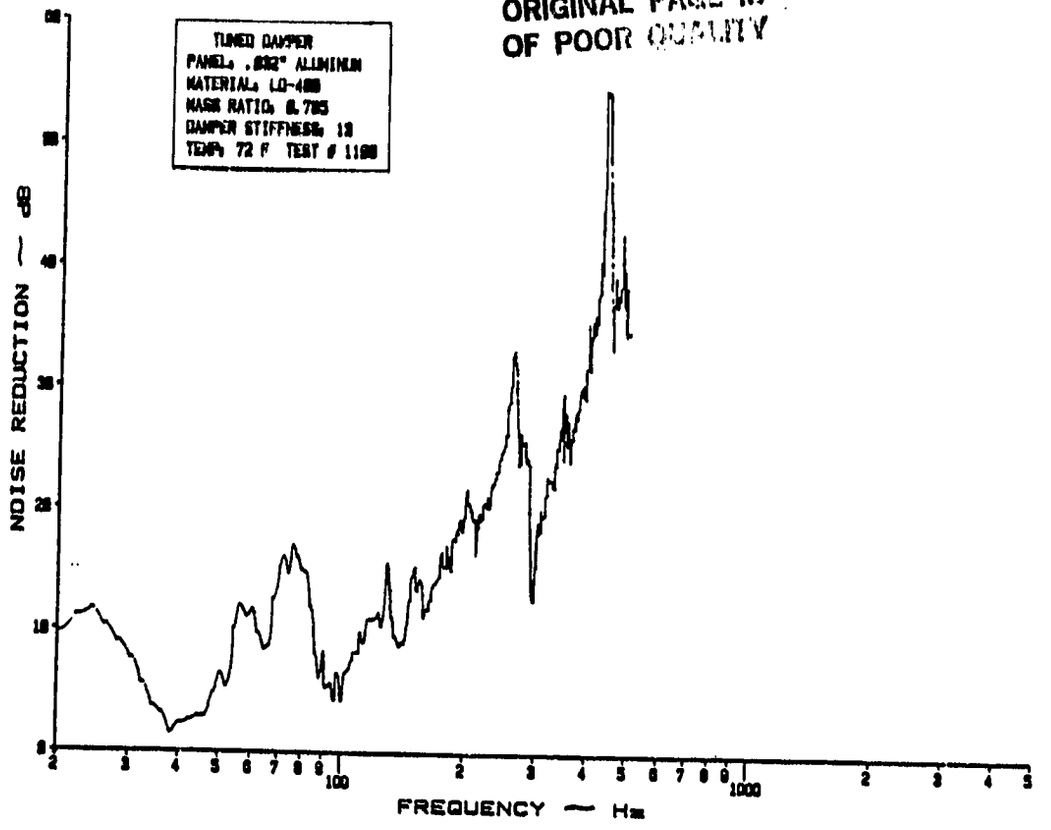

Figure D.11 Noise Reduction Characteristics of a .032" Aluminum Panel with an "LD-400" Tuned Damper; μ = .785 and K2 = 13 lbf/in.

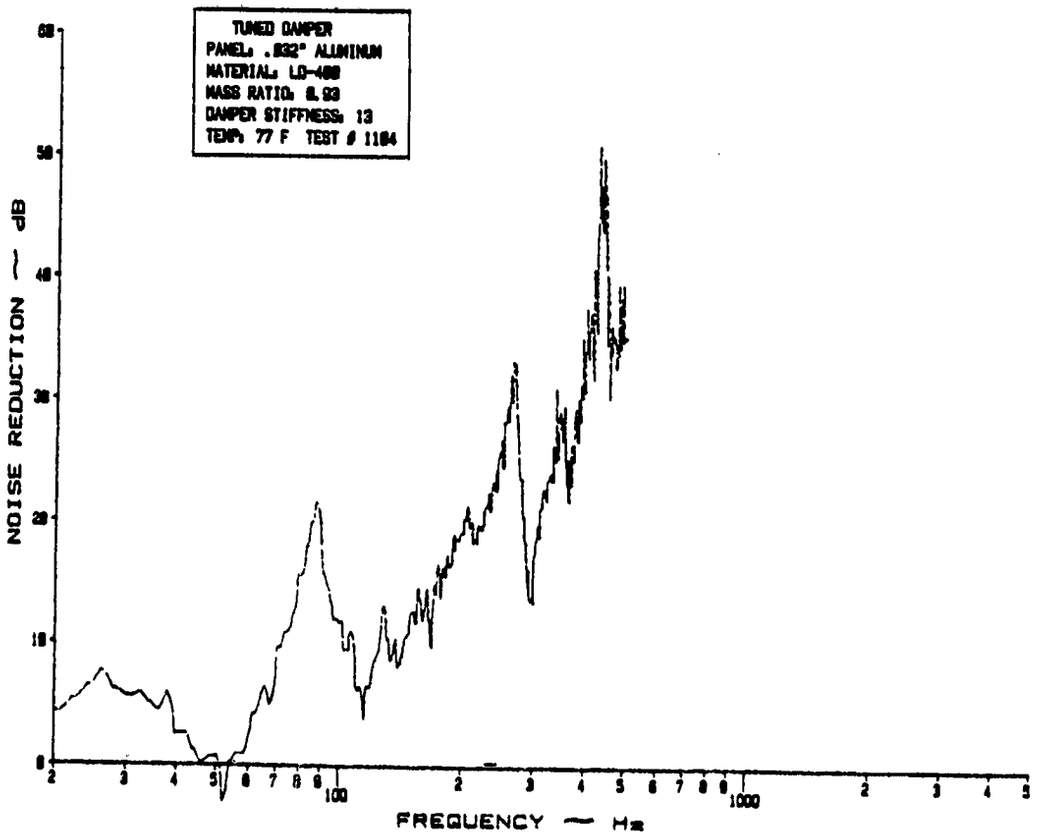

Figure D.12 Noise Reduction Characteristics of a .032" Aluminum Panel with an "LD-400" Tuned Damper; μ = .93 and K2 = 13 lbf/in.

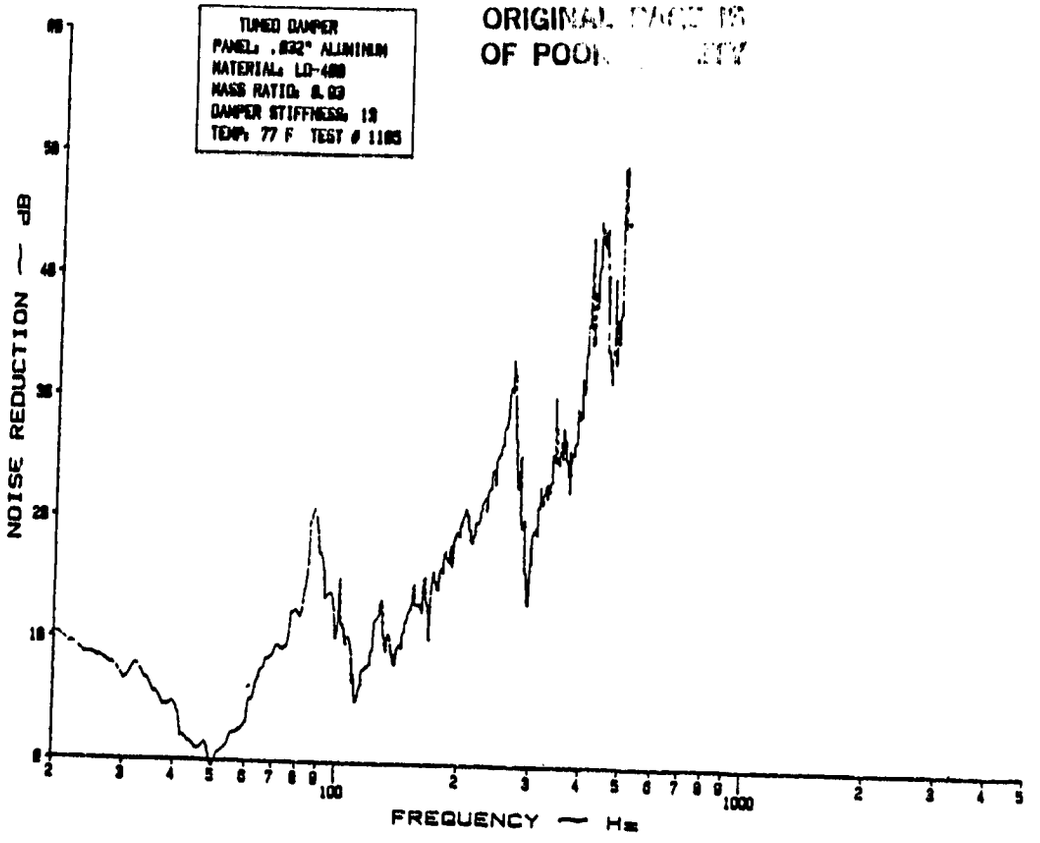

Figure D.13 Noise Reduction Characteristics of a .032" Aluminum Panel with an "LD-400" Tuned Damper; μ = .93 and K2 = 13 lbf/in.

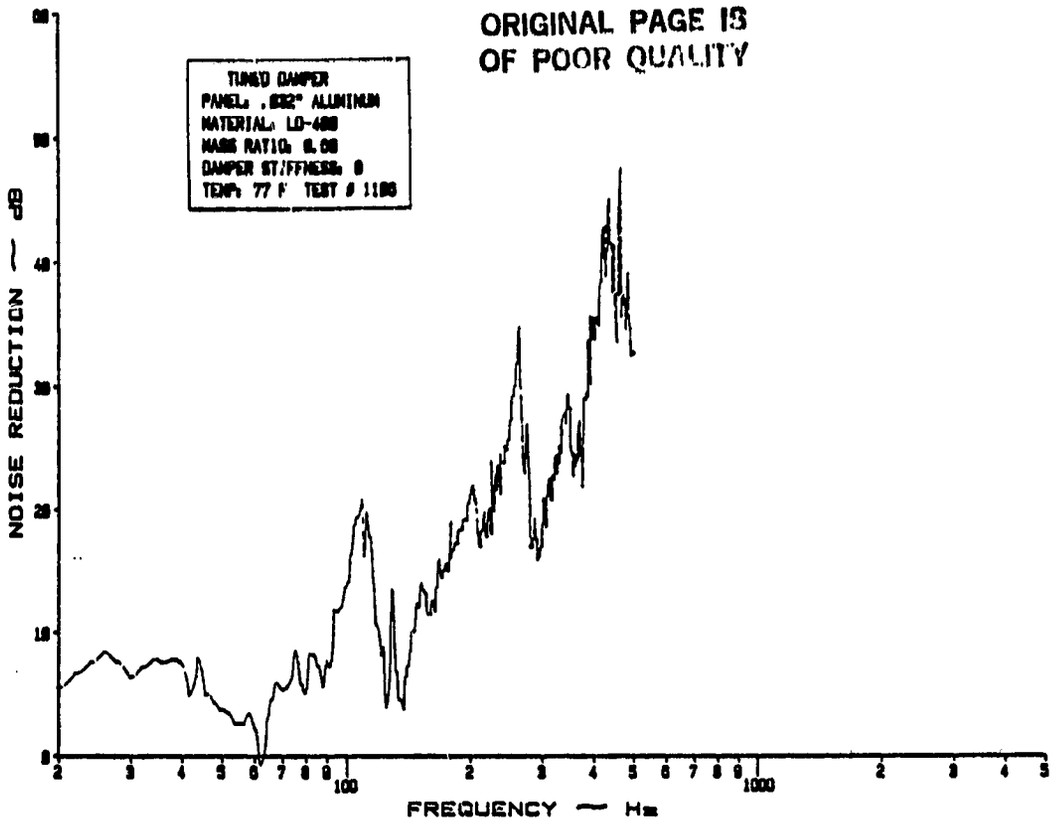

Figure D.14 Noise Reduction Characteristics of a .032" Aluminum Panel with an "LD-400" Tuned Damper; μ = .68 and K2 = 8 lbf/in.

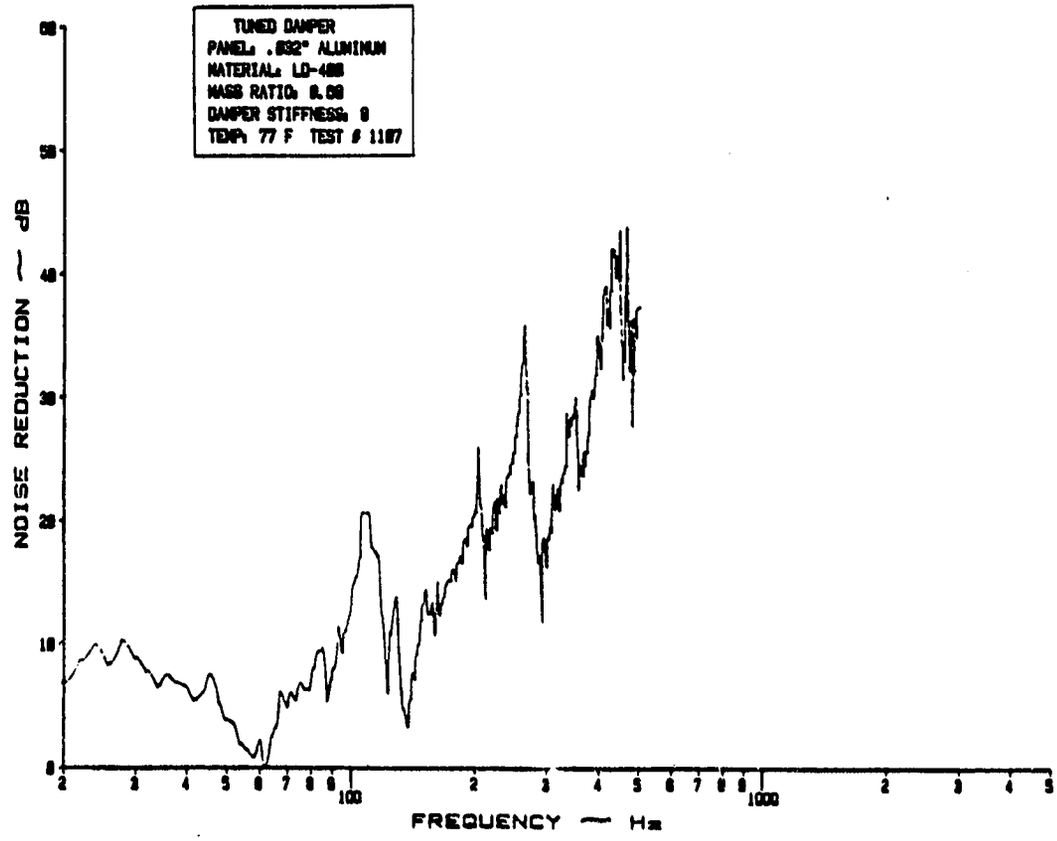

Figure D.15 Noise Reduction Characteristics of a .032" Aluminum Panel with an "LD-400" Tuned Damper; μ = .68 and K2 = 8 lbf/in.

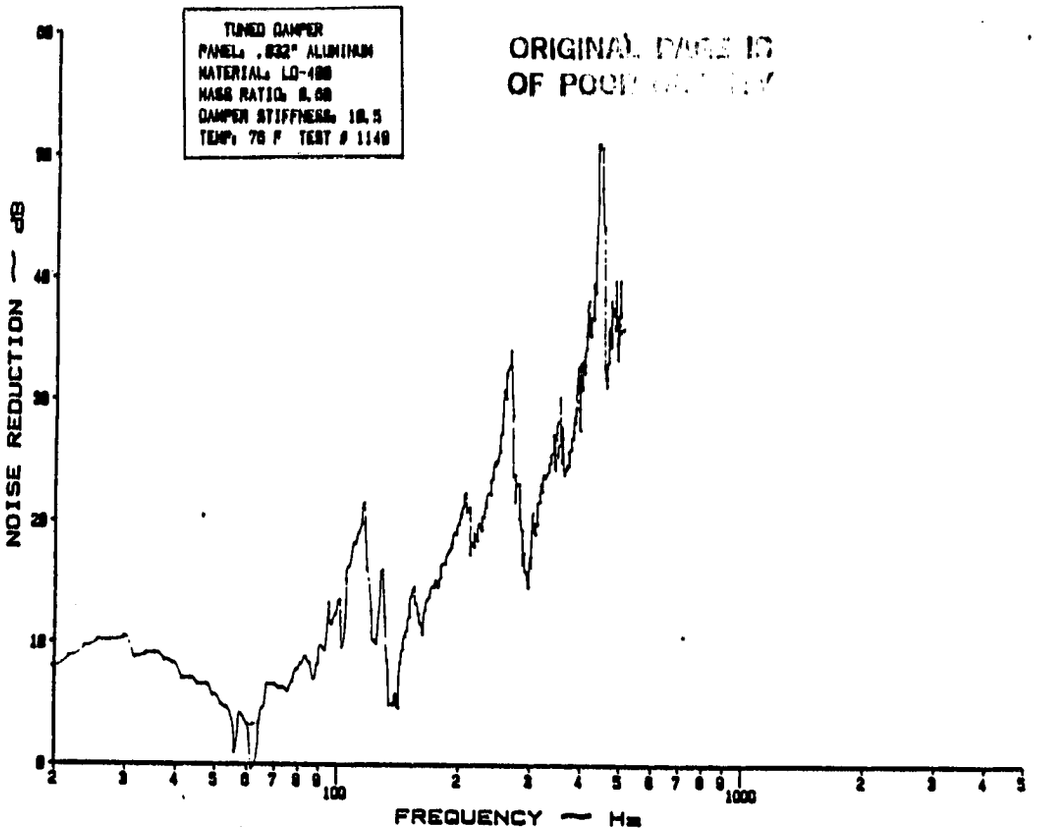

Figure D.16 Noise Reduction Characteristics of a .032" Aluminum Panel with an "LD-400" Tuned Damper; μ = .68 and K2 = 10.5 lbf/in.

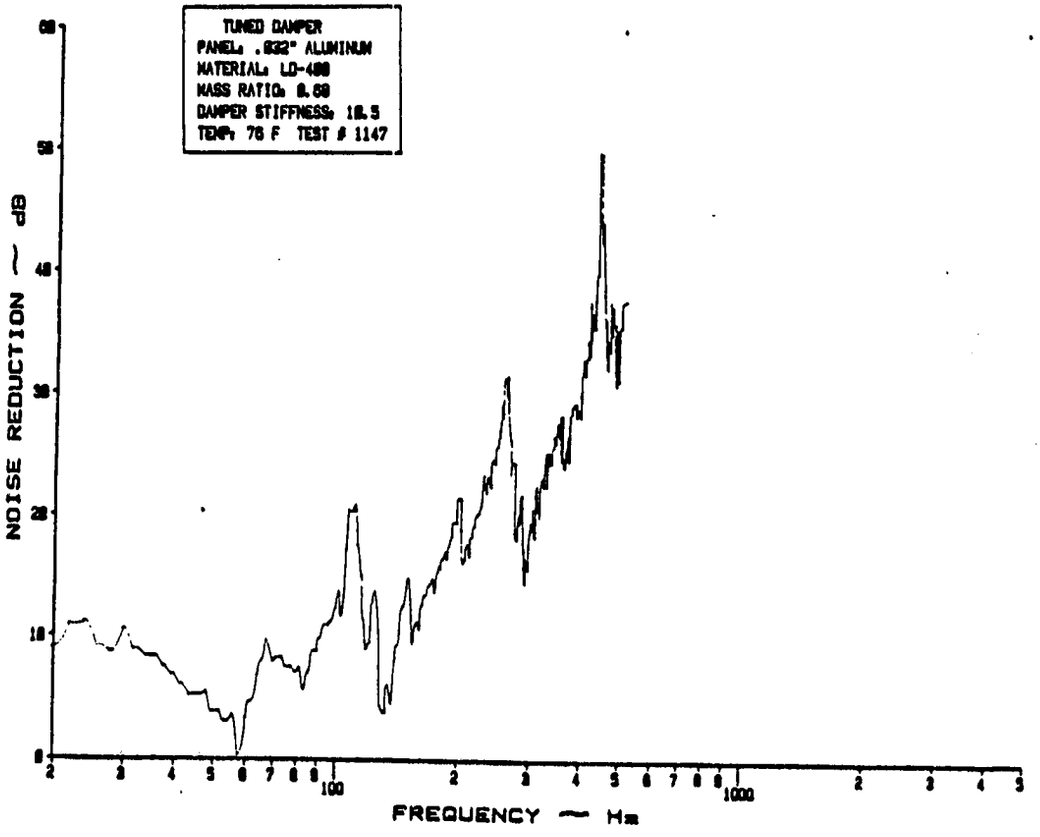

Figure D.17 Noise Reduction Characteristics of a .032" Aluminum Panel with an "LD-400" Tuned Damper; μ = .68 and K2 = 10.5 lbf/in.

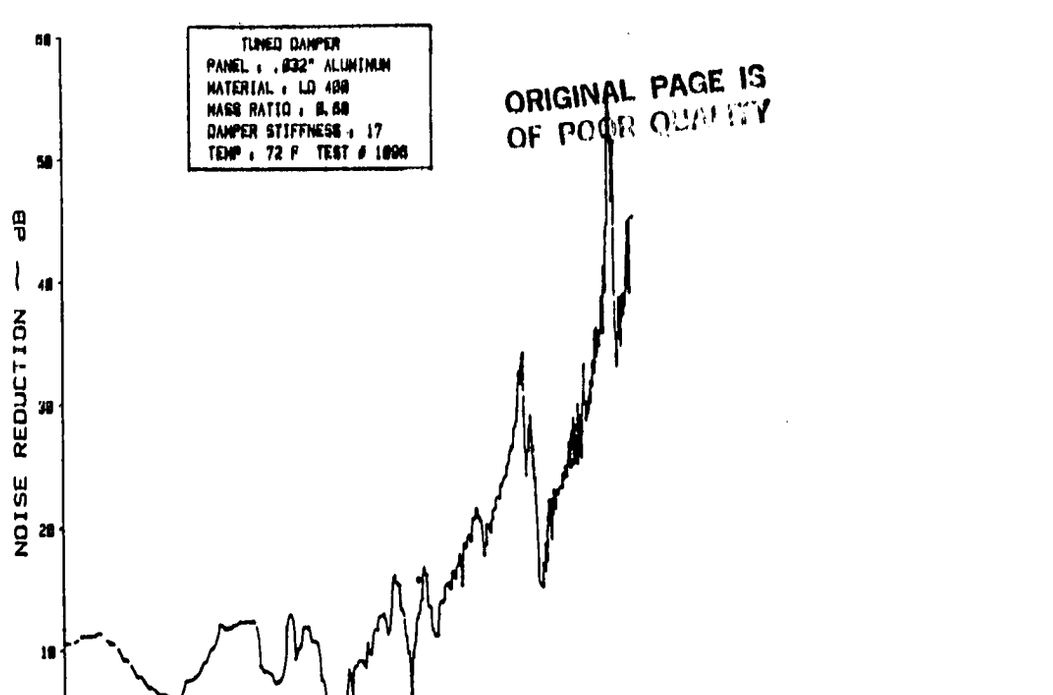

Figure D.18 Noise Reduction Characteristics of a .032" Aluminum Panel with an "LD-400" Tuned Damper; μ = .68 and K2 = 17 lbf/in.

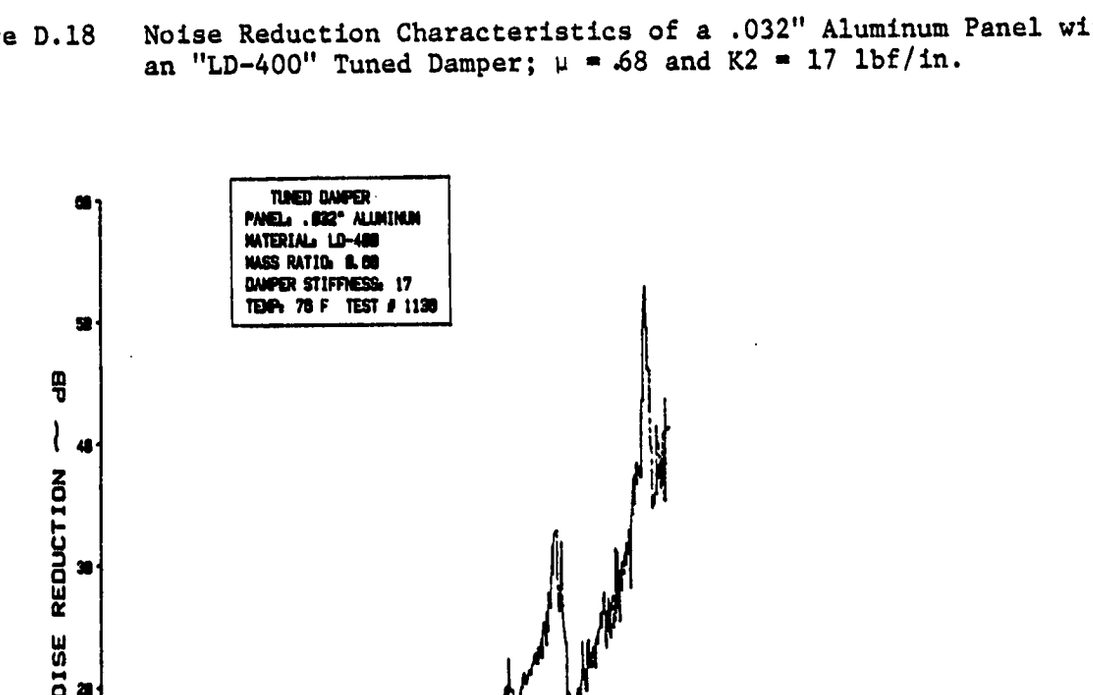

Figure D.19 Noise Reduction Characteristics of a .032" Aluminum Panel with an "LD-400" Tuned Damper; μ = .68 and K2 = 17 lbf/in.

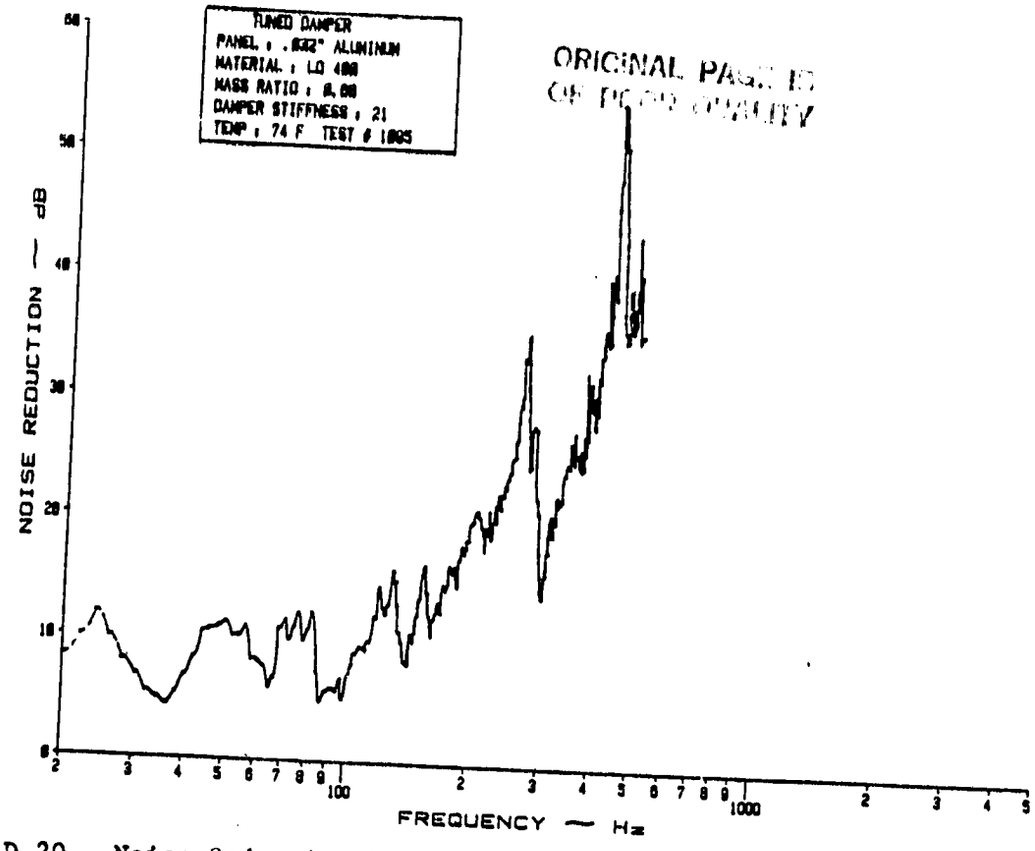

Figure D.20 Noise Reduction Characteristics of a .032" Aluminum Panel with an "LD-400" Tuned Damper; μ = .68 and K2 = 21 lbf/in.

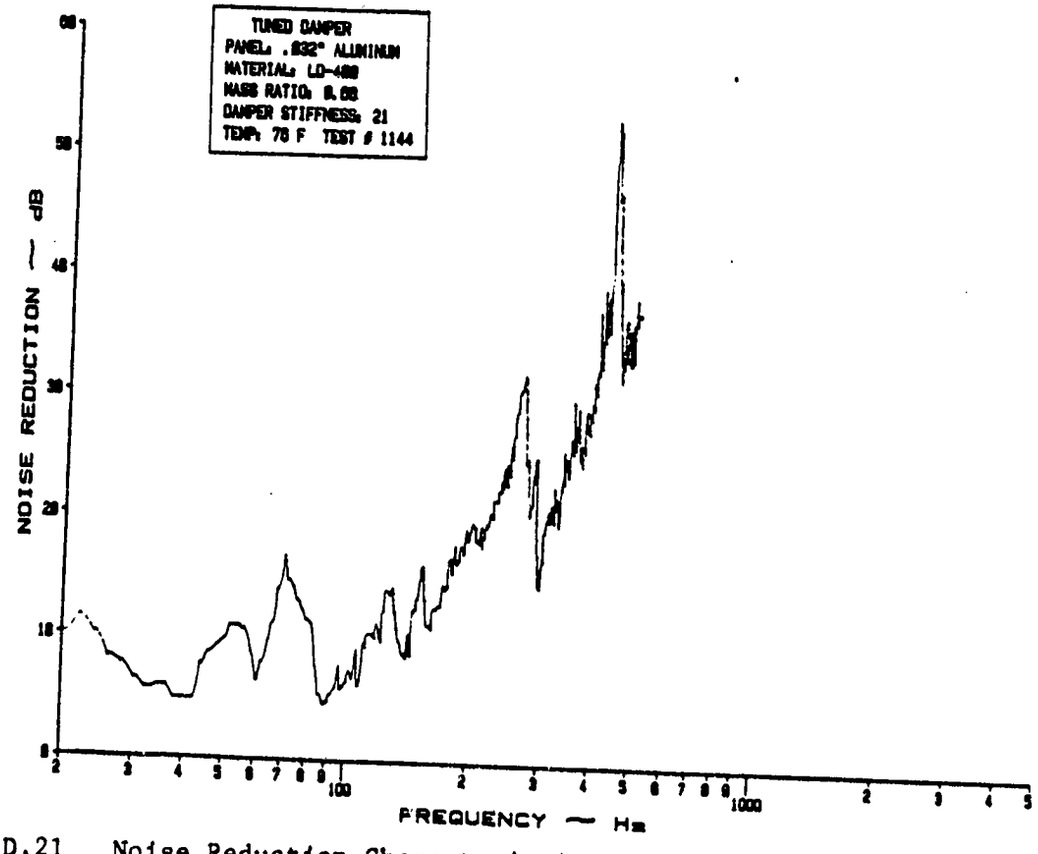

Figure D.21 Noise Reduction Characteristics of a .032" Aluminum Panel with an "LD-400" Tuned Damper; μ = .68 and K2 = 21 lbf/in.

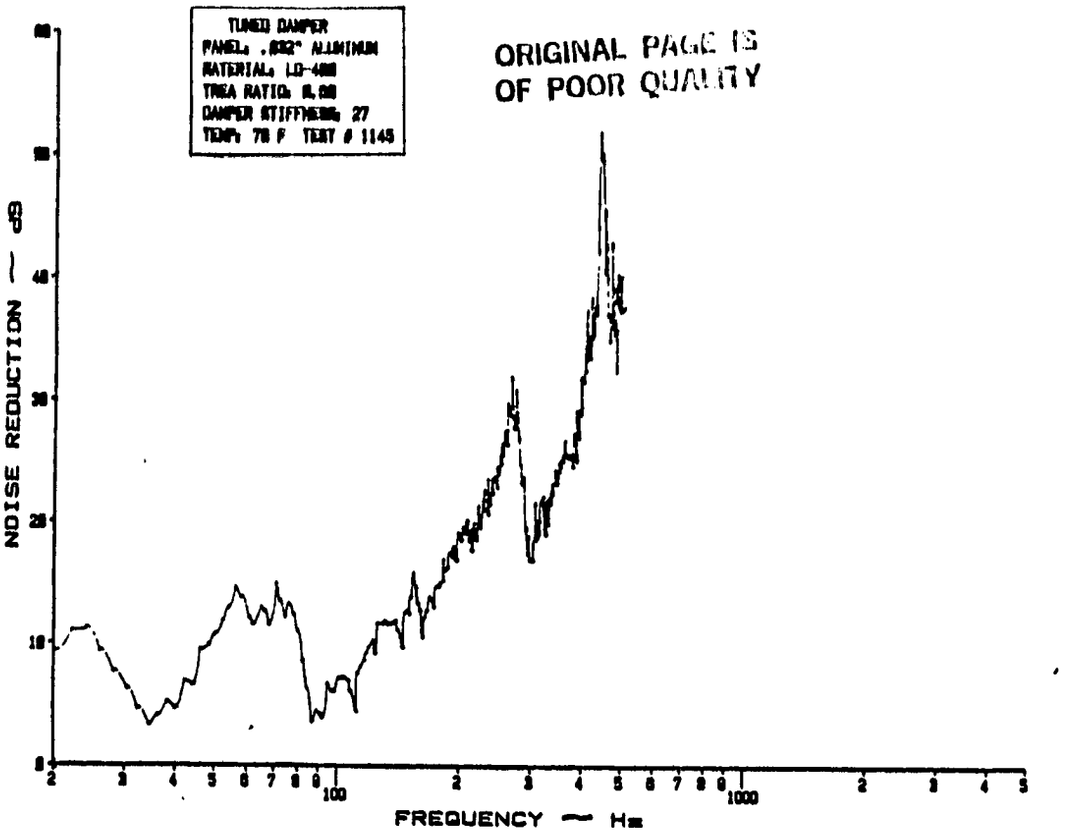

Figure D.22 Noise Reduction Characteristics of a .032" Aluminum Panel with an "LD-400" Tuned Damper; μ = .68 and K2 = 27 lbf/in.

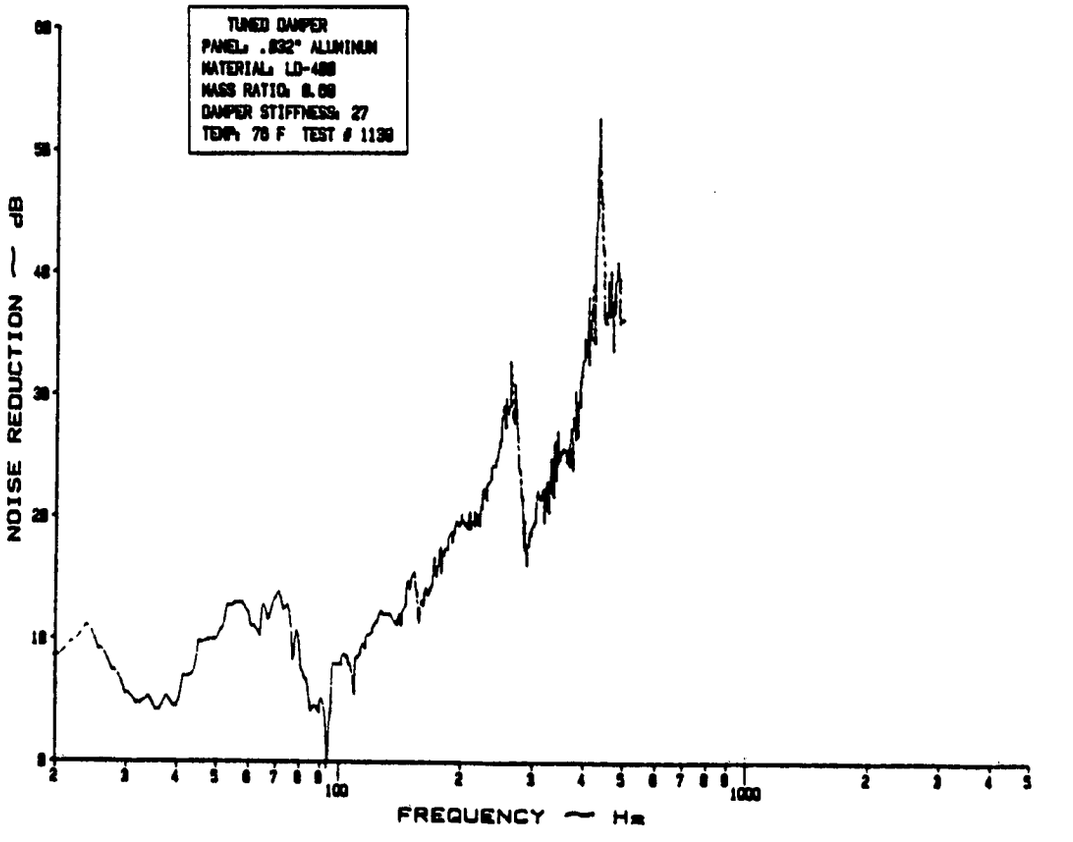

Figure D.23 Noise Reduction Characteristics of a .032" Aluminum Panel with an "LD-400" Tuned Damper; μ = .68 and K2 = 27 lbf/in.

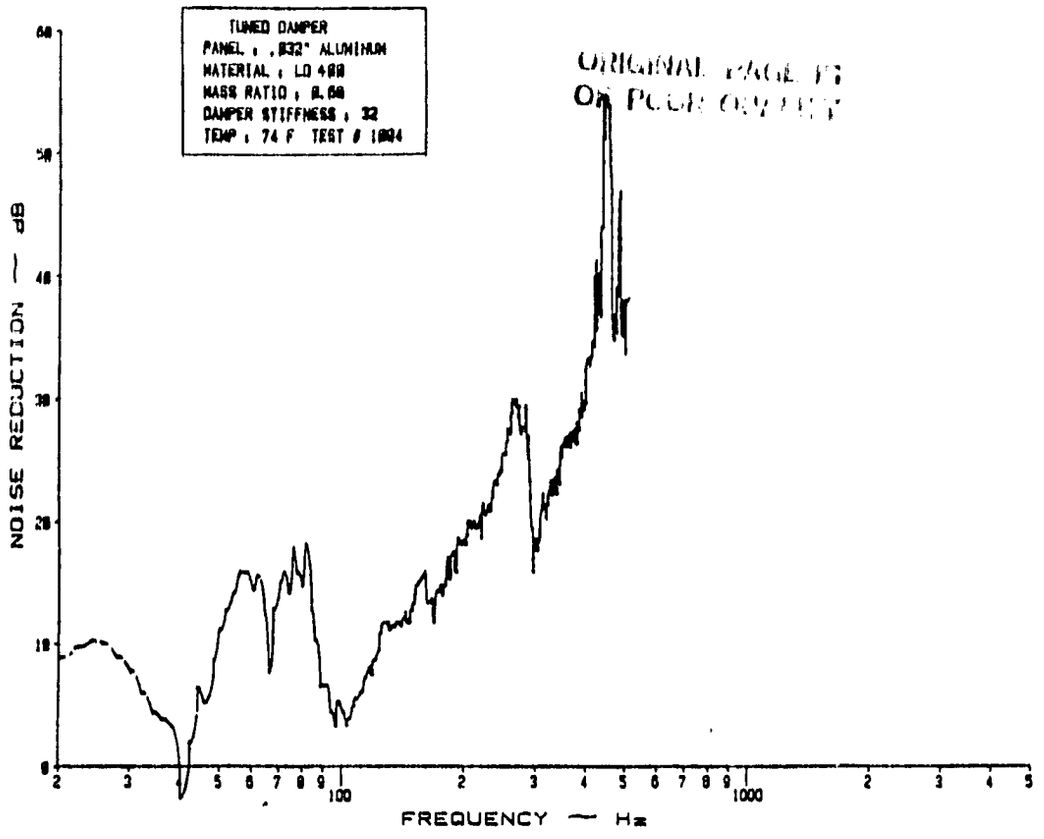

Figure D.24 Noise Reduction Characteristics of a .032" Aluminum Panel with an "LD-400" Tuned Damper; μ = .68 and K2 = 32 lbf/in.

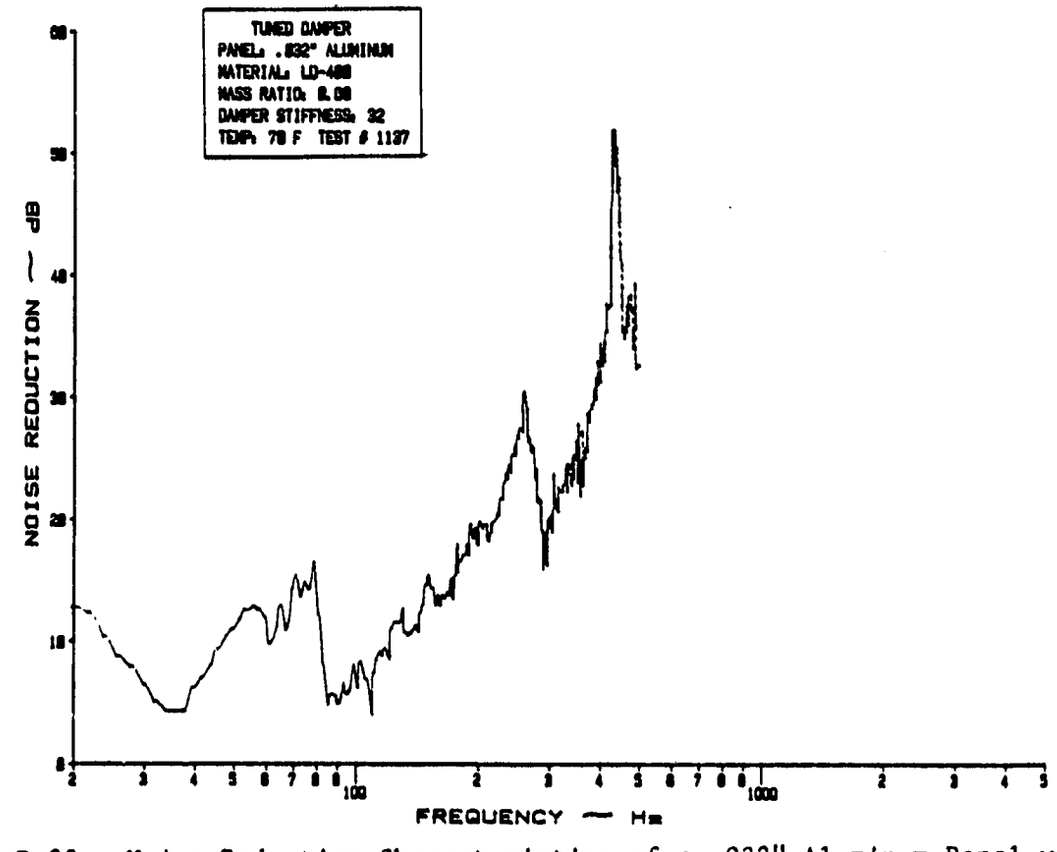

Figure D.25 Noise Reduction Characteristics of a .032" Aluminum Panel with an "LD-400" Tuned Damper; μ = .68 and K2 = 32 lbf/in.

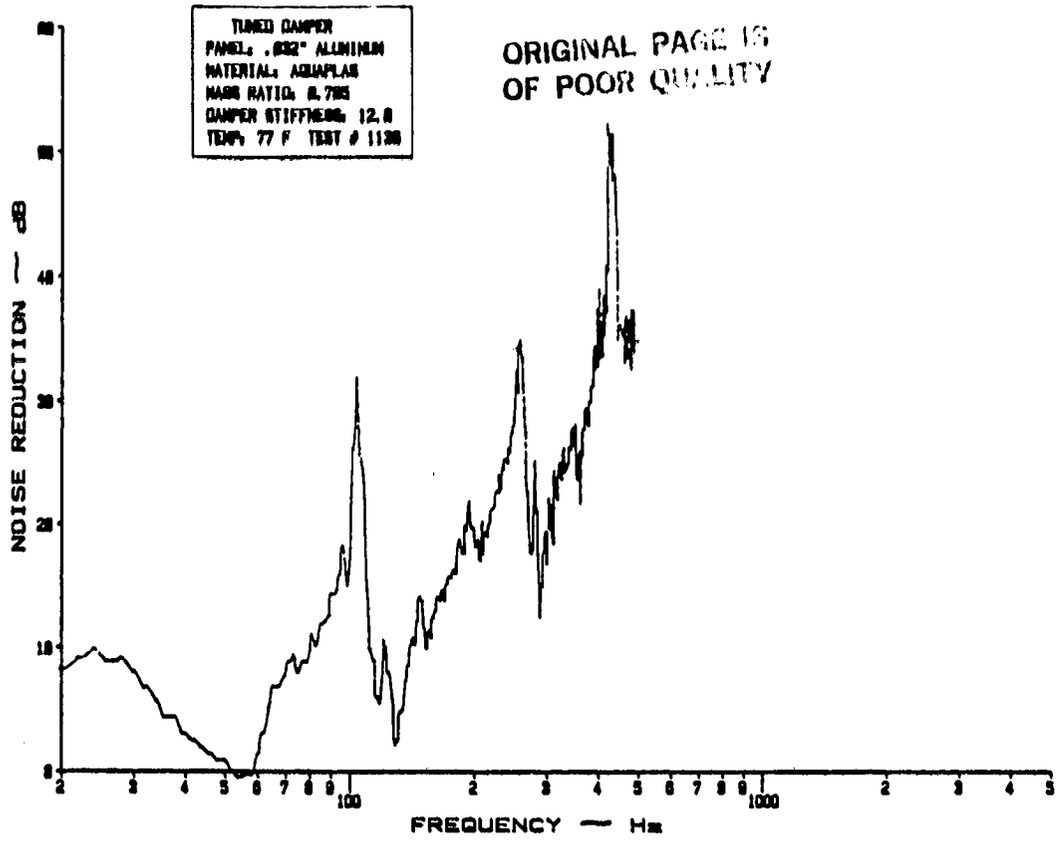

Figure D.26 Noise Reduction Characteristics of a .032" Aluminum Panel with an "Aquaplas" Tuned Damper; μ = .785 and K2 = 12.8 lbf/in.

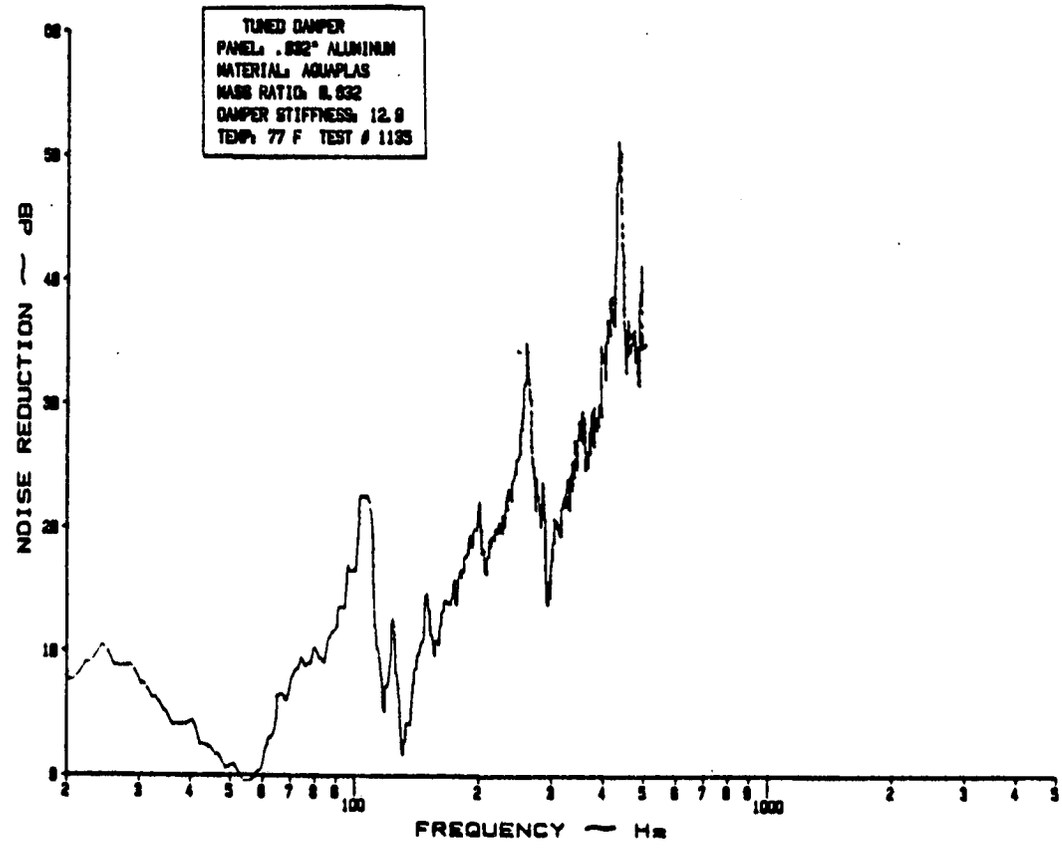

Figure D.27 Noise Reduction Characteristics of a .032" Aluminum Panel with an "Aquaplas" Tuned Damper; μ = .832 and K2 = 12.8 lbf/in.

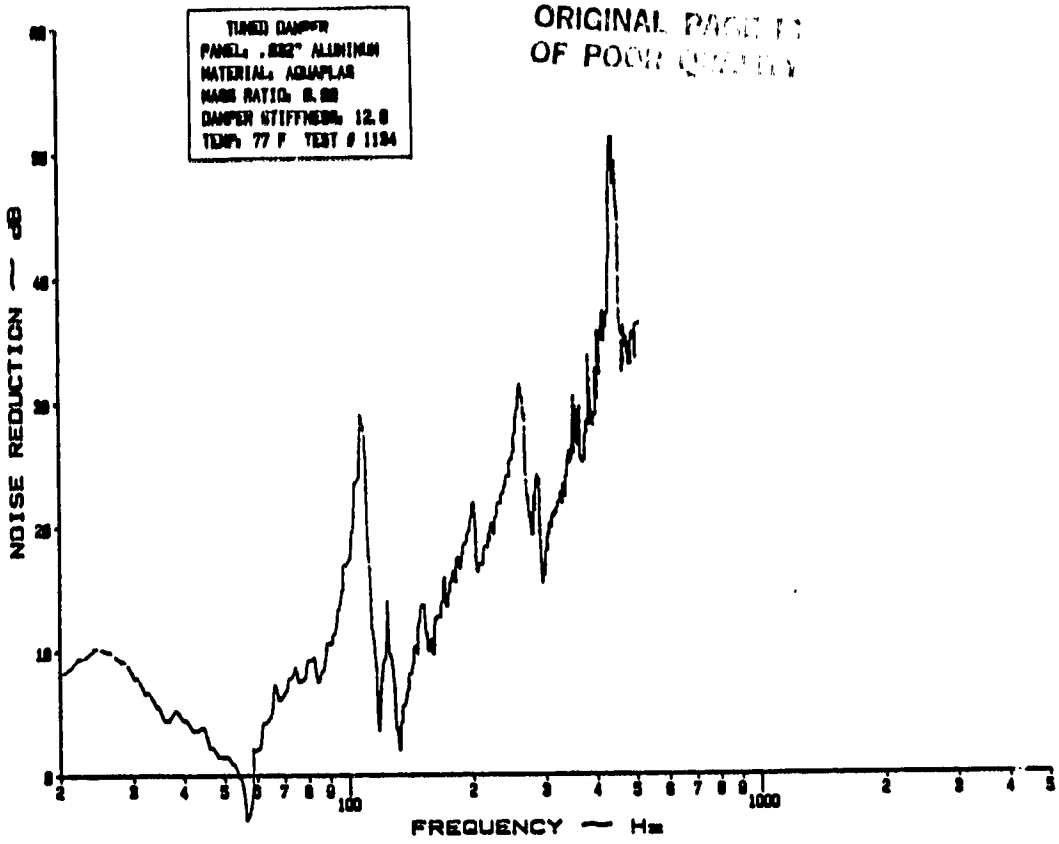

Figure D.28 Noise Reduction Characteristics of a .032" Aluminum Panel with an "Aquaplas" Tuned Damper; μ = .88 and K2 = 12.8 lbf/in.

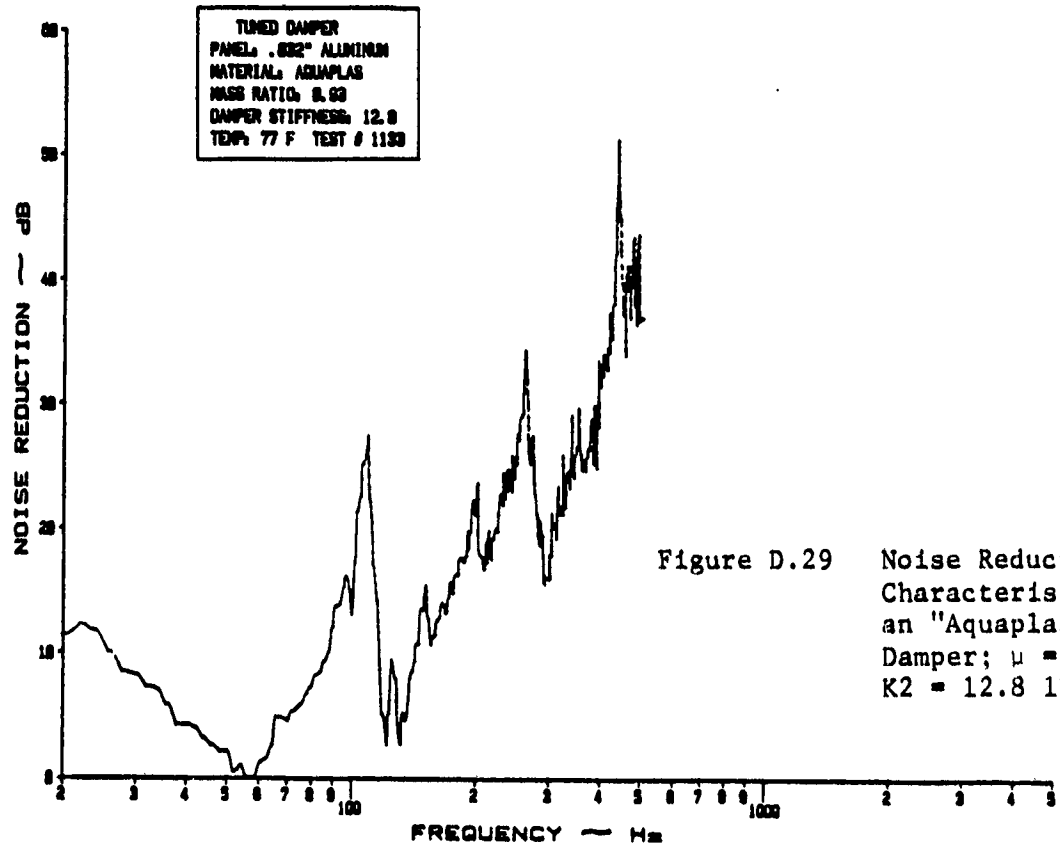

Figure D.29 Noise Reduction Characteristics of an "Aquaplas" Tuned Damper; μ = .93 and K2 = 12.8 lbf/in.

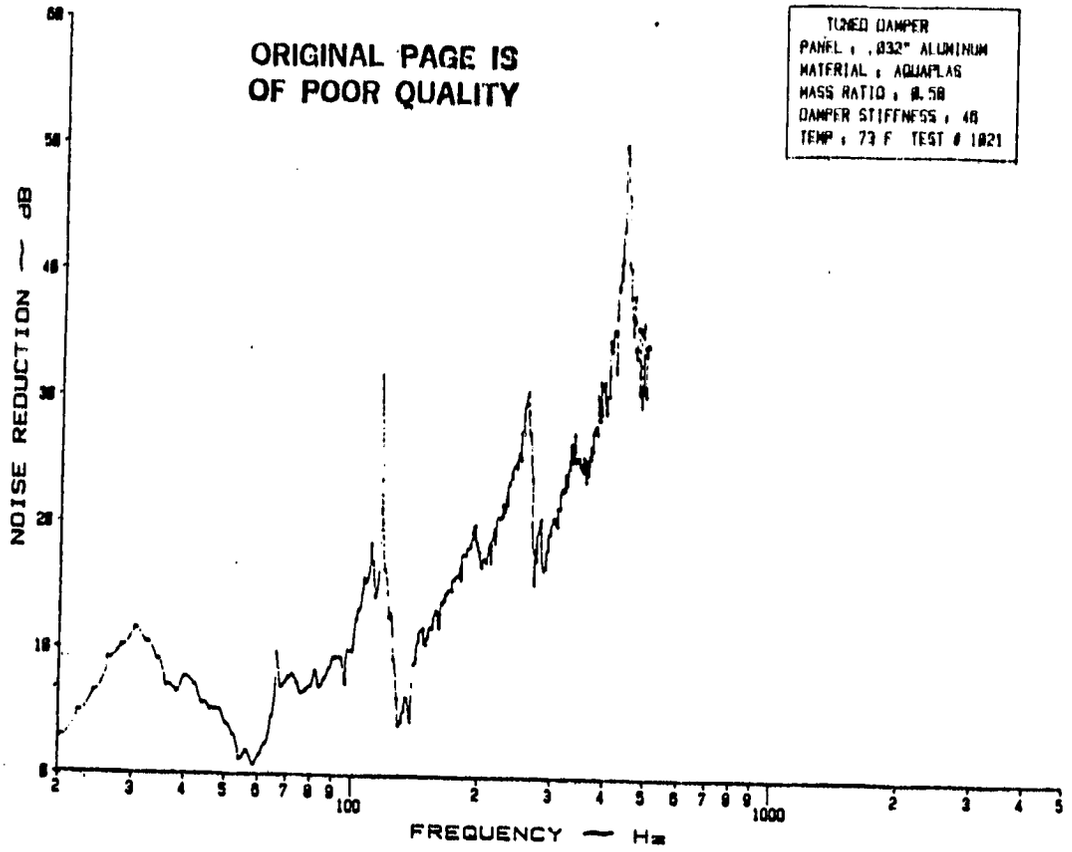

Figure D.30 Noise Reduction Characteristics of a .032" Aluminum Panel with an "Aquaplas" Tuned Damper; μ = .58 and K2 = 46 lbf/in.

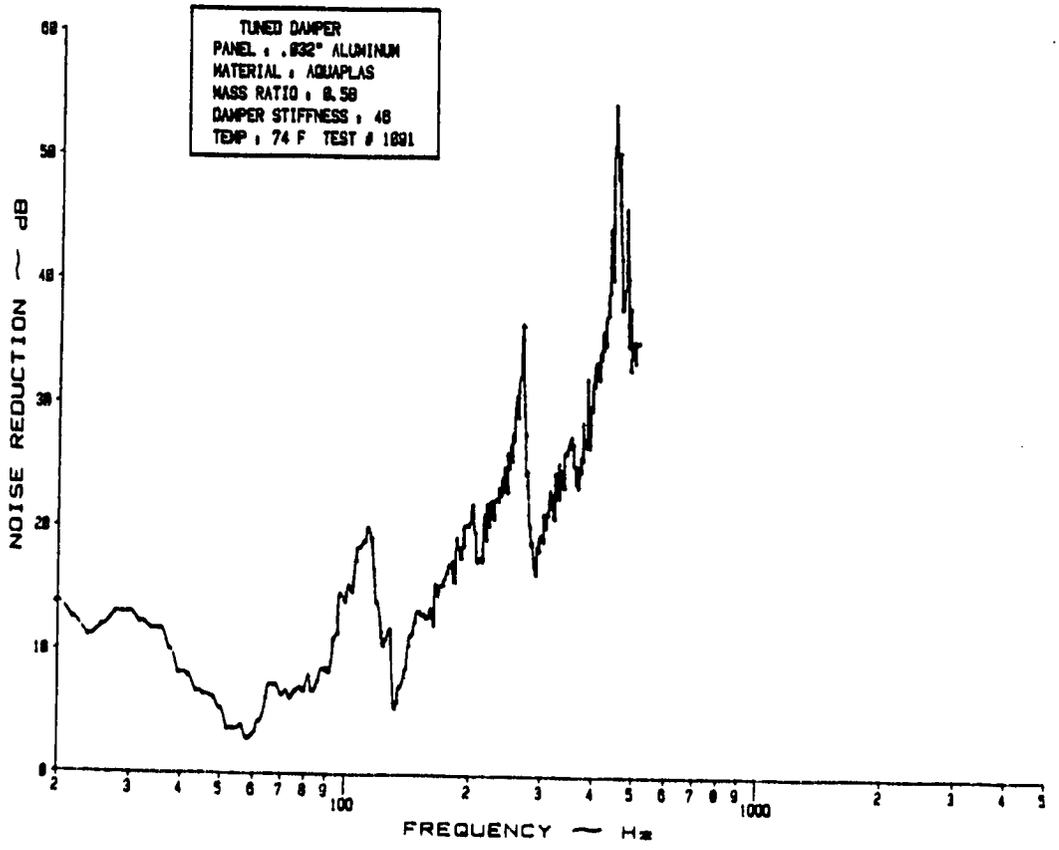

Figure D.31 Noise Reduction Characteristics of a .032" Aluminum Panel with an "Aquaplas" Tuned Damper; μ = .58 and K2 = 46 lbf/in.

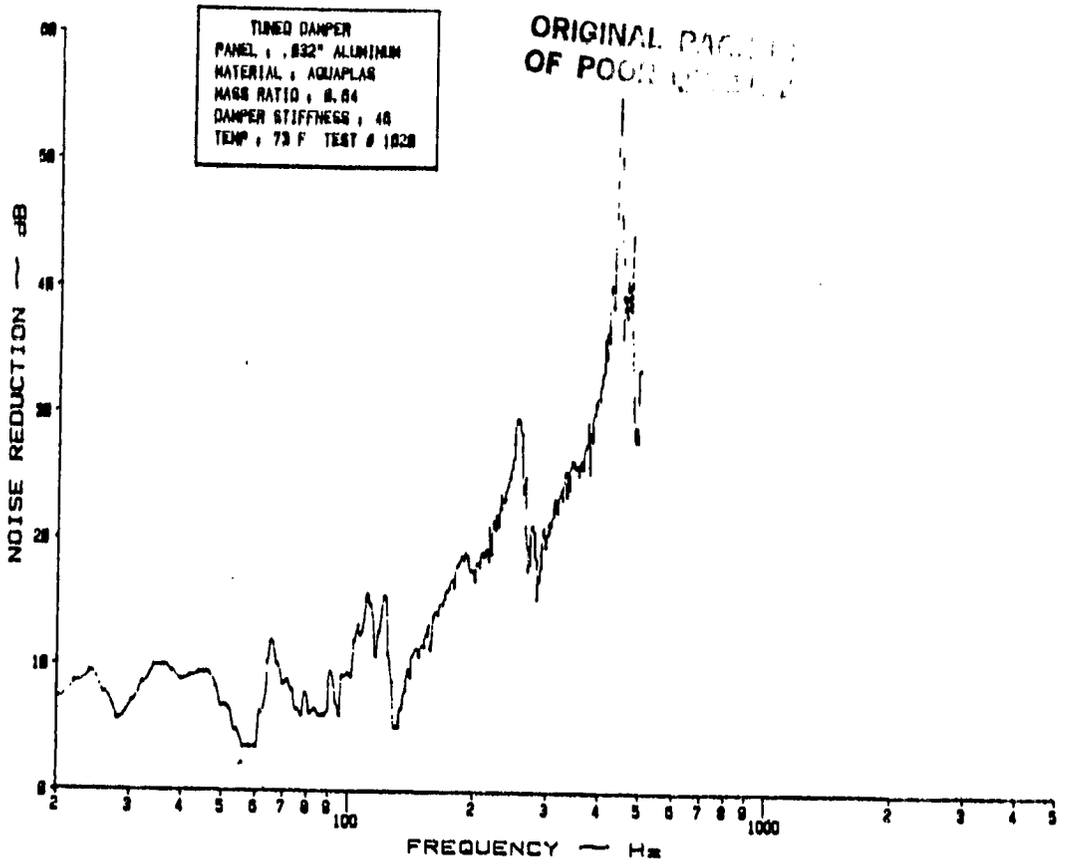

Figure D.32 Noisc Reduction Characteristics of a .032" Aluminum Panel with an "Aquaplas" Tuned Damper; μ = .64 and K2 = 46 lbf/in.

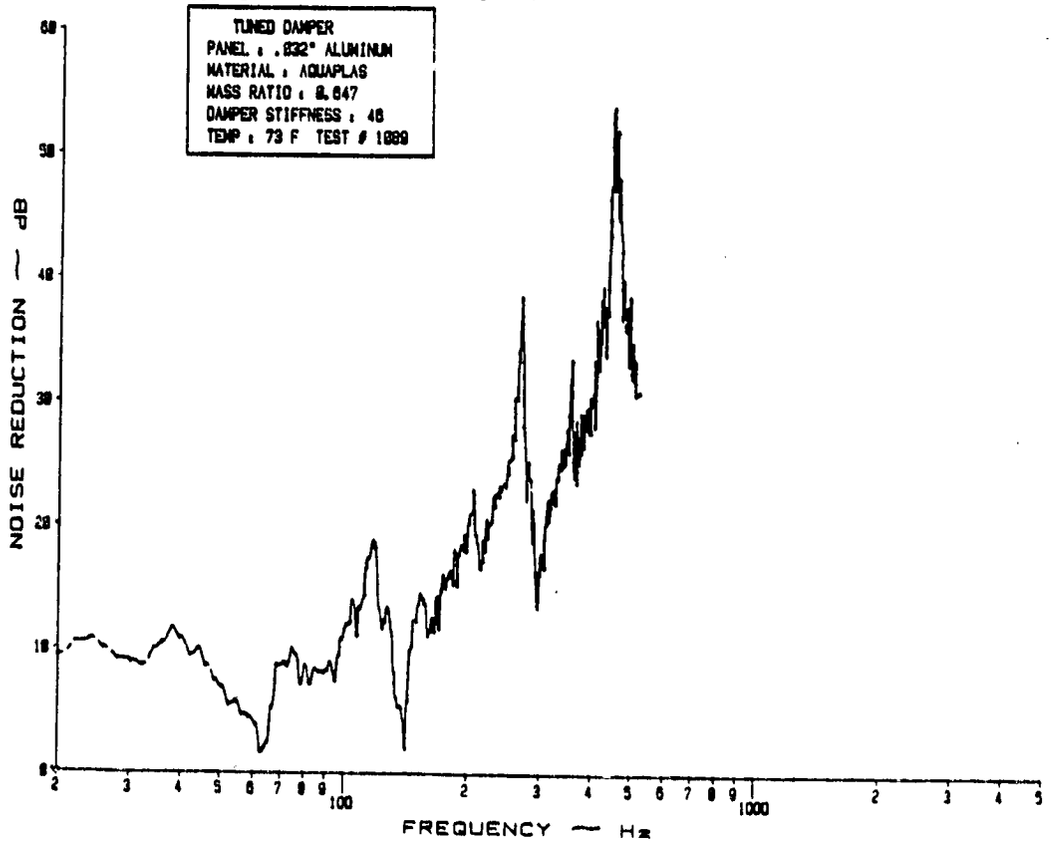

Figure D.33 Noise Reduction Characteristics of a .032" Aluminum Panel with an "Aquaplas" Tuned Damper; μ = .647 and K2 = 46 lbf/in.

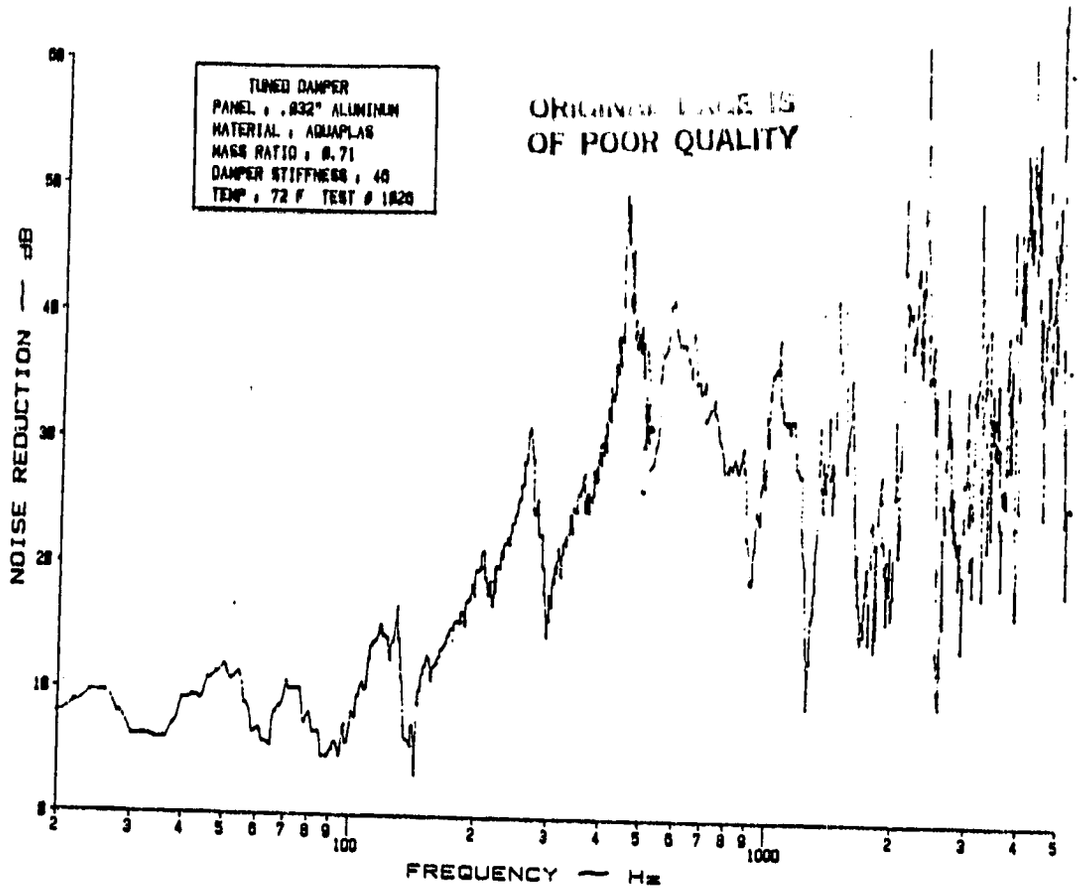

Figure D.34 Noise Reduction Characteristics of a .032" Aluminim Panel with an "Aquaplas" Tuned Damper; μ = .71 and K2 = 46 lbf/in.

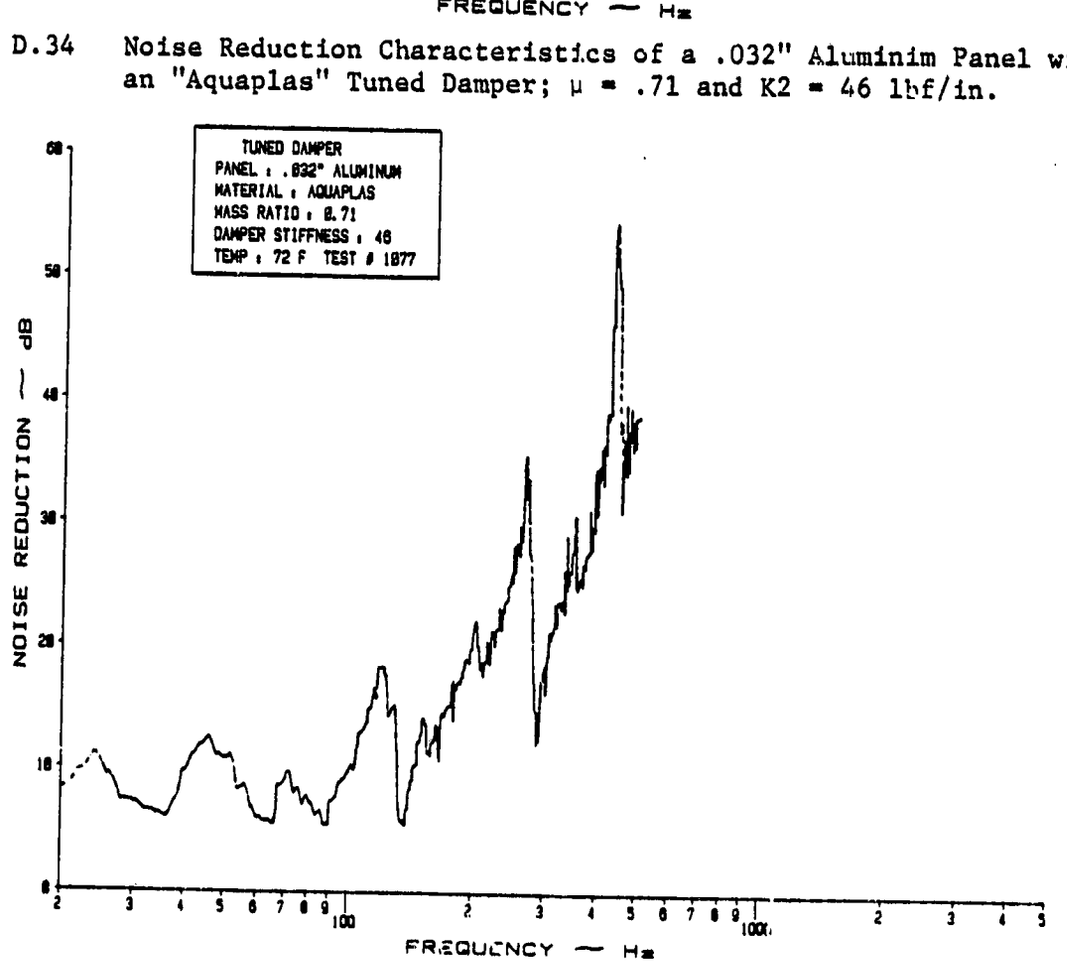

Figure D.35 Noise Reduction Characteristics of a .032" Aluminum Panel with an "Aquaplas" Tuned Damper; μ = .71 and K2 = 46 lbf/in.

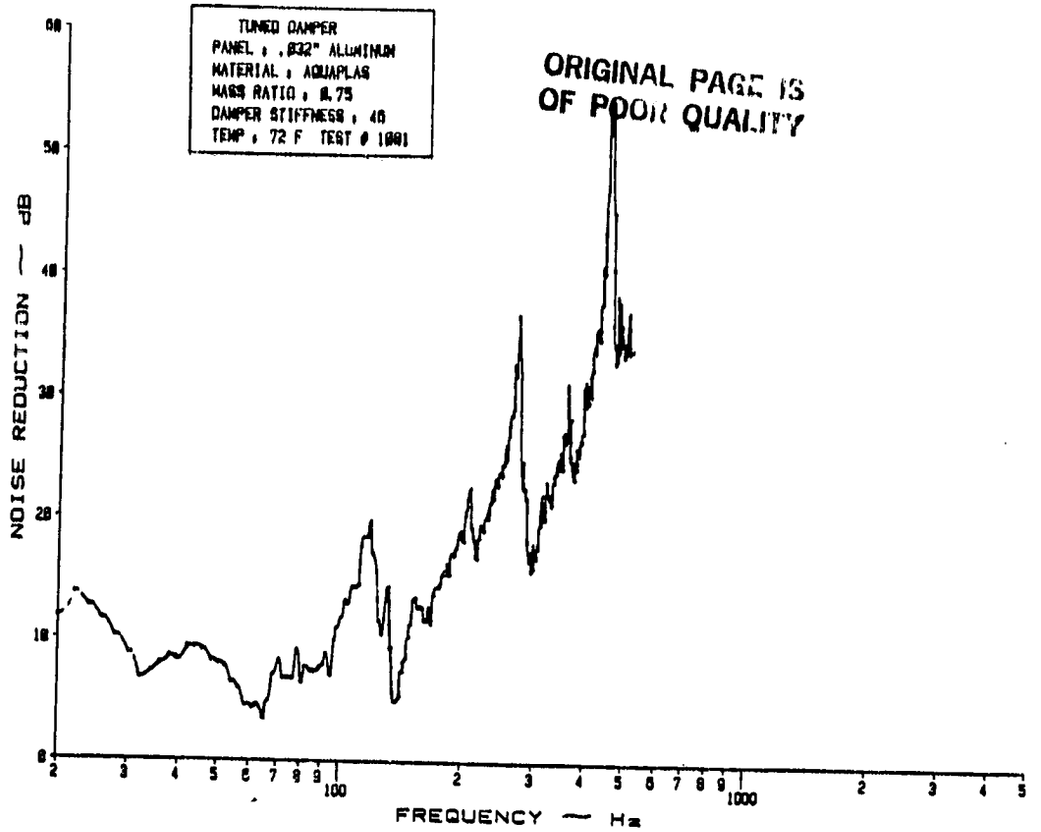

Figure D.36 Noise Reduction Characteristics of a .032" Aluminum Panel with an "Aquaplas" Tuned Damper; μ = .75 and K2 = 46 lbf/in.

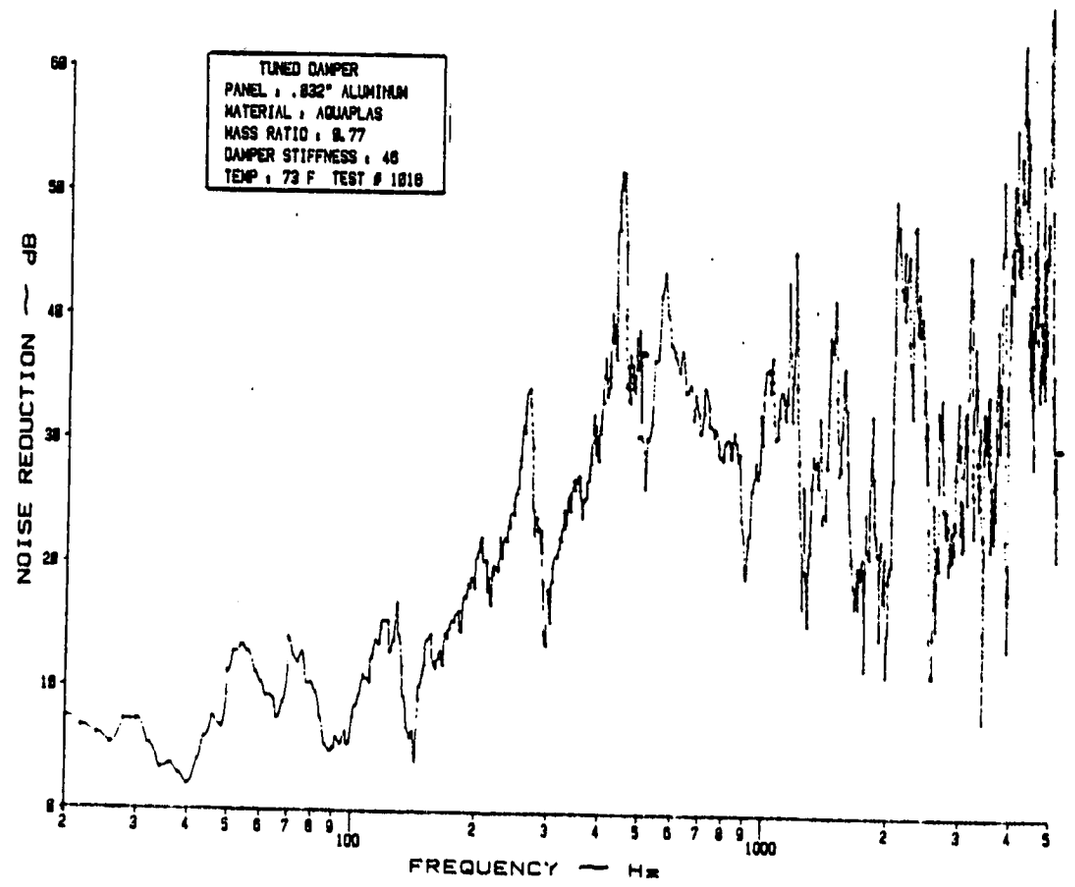

Figure D.37 Noise Reduction Characteristics of a .032" Aluminum Panel with an "Aquaplas" Tuned Damper; μ = .77 and K2 = 46 lbf/in.

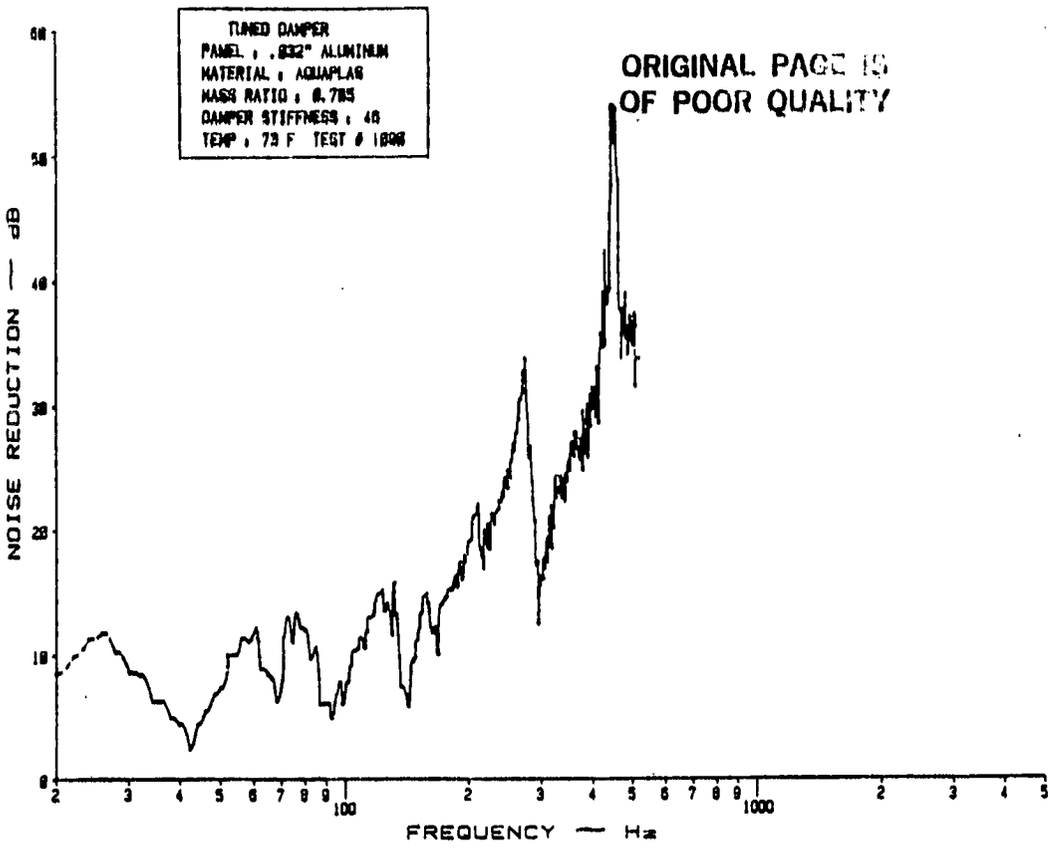

Figure D.38 Noise Reduction Characteristics of a .032" Aluminum Panel with an "Aquaplas" Tuned Damper; μ = .785 and K2 = 46 lbf/in.

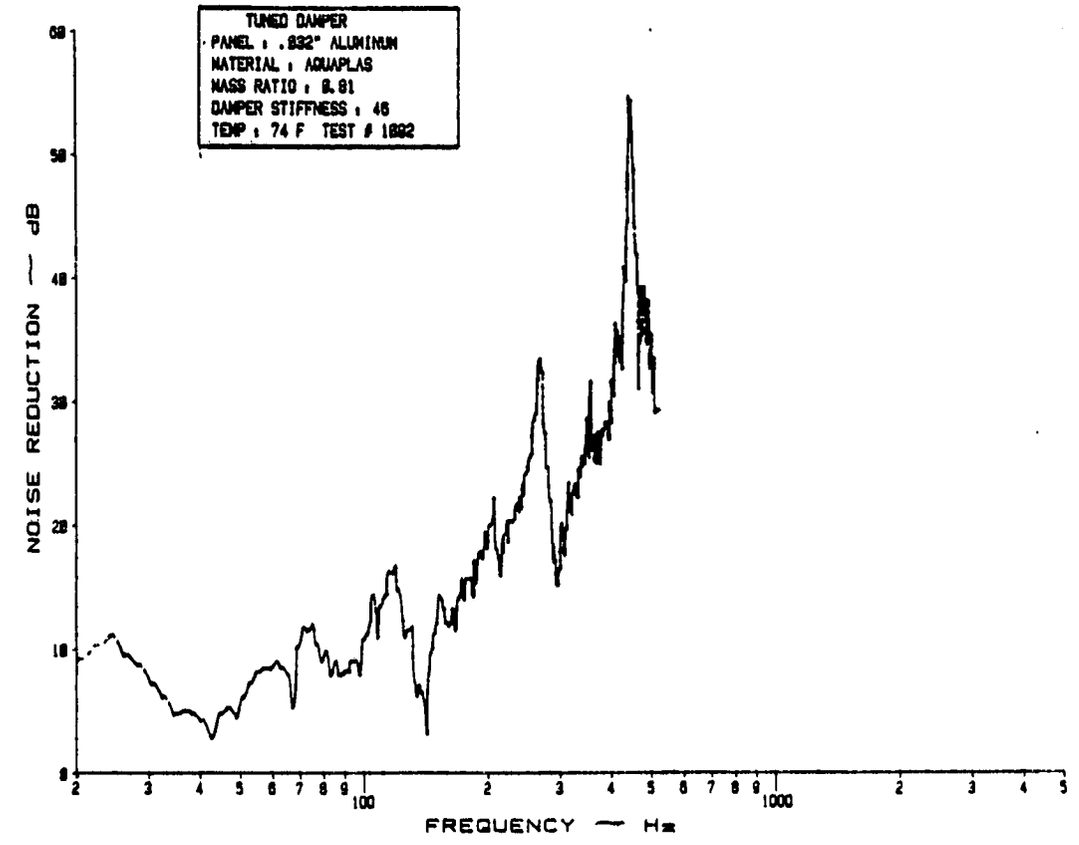

Figure D.39 Noise Reduction Characteristics of a .032" Aluminum Panel with an "Aquaplas" Tuned Damper; μ = .81 and K2 = 46 lbf/in.

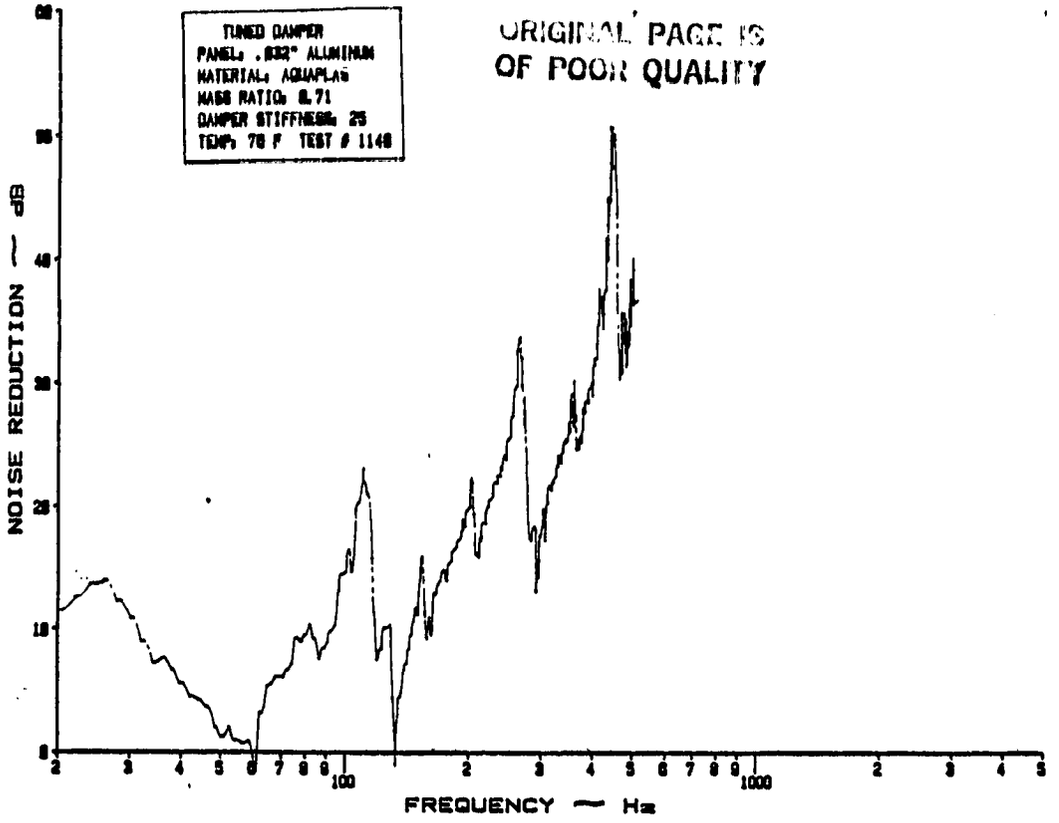

Figure D.40 Noise Reduction Characteristics of a .032" Aluminum Panel with an "Aquaplas" Tuned Damper; μ = .71 and K2 = 25 lbf/in.

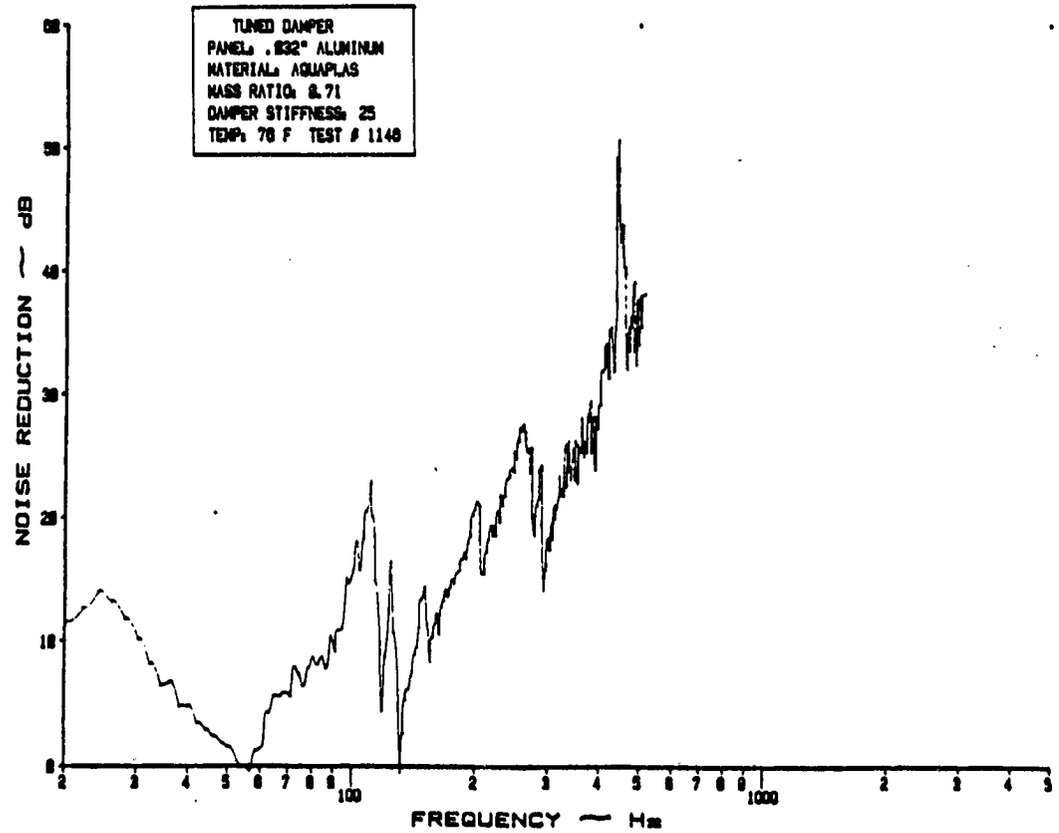

Figure D.41 Noise Reduction Characteristics of a .032" Aluminum Panel with an "Aquaplas" Tuned Damper; μ = .71 and K2 = 25 lbf/in.

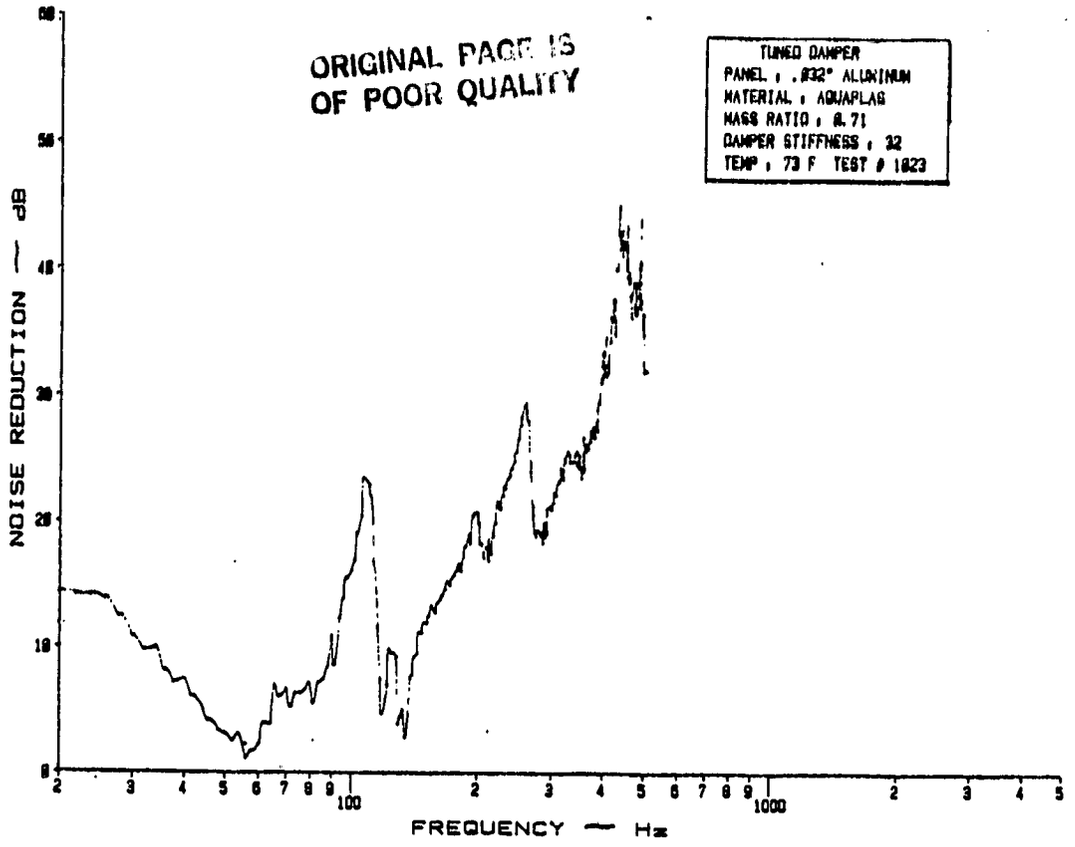

Figure D.42 Noise Reduction Characteristics of a .032" Aluminum Panel with an "Aquaplas" Tuned Damper; μ = .71 and K2 = 32 lbf/in.

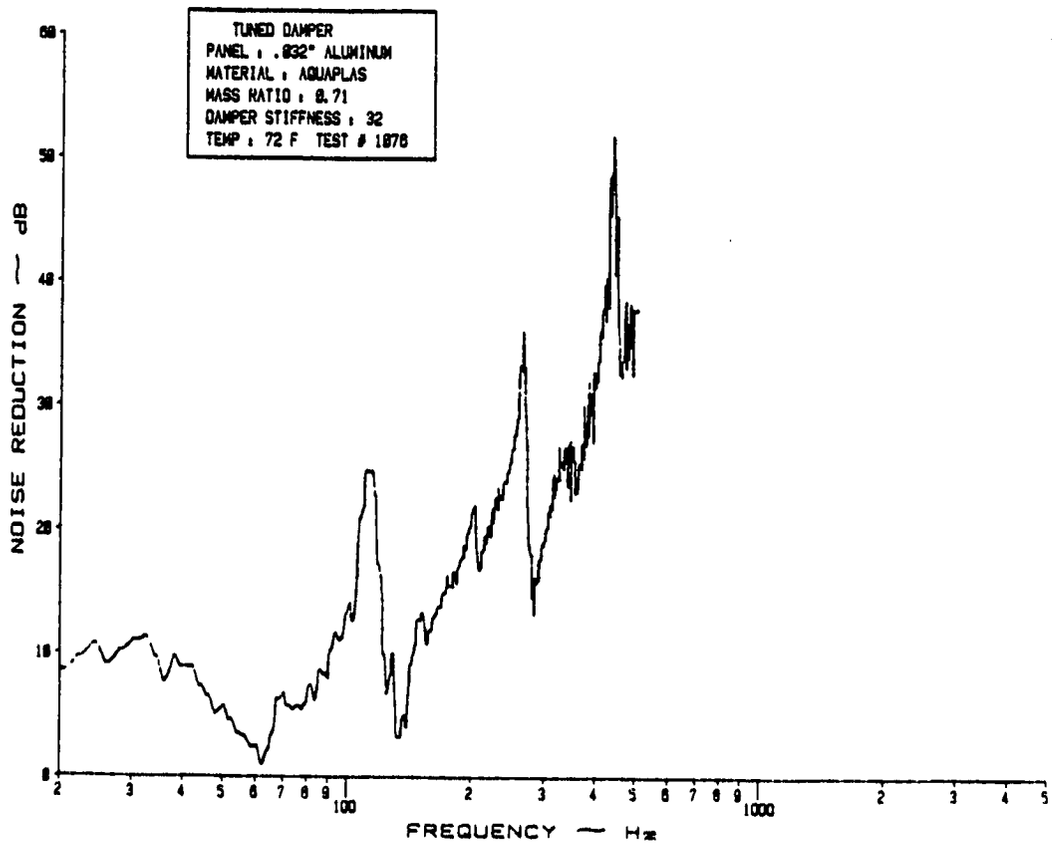

Figure D.43 Noise Reduction Characteristics of a .032" Aluminim Panel with an "Aquaplas" Tuned Damper; μ = .71 and K2 = 32 lbf/in.

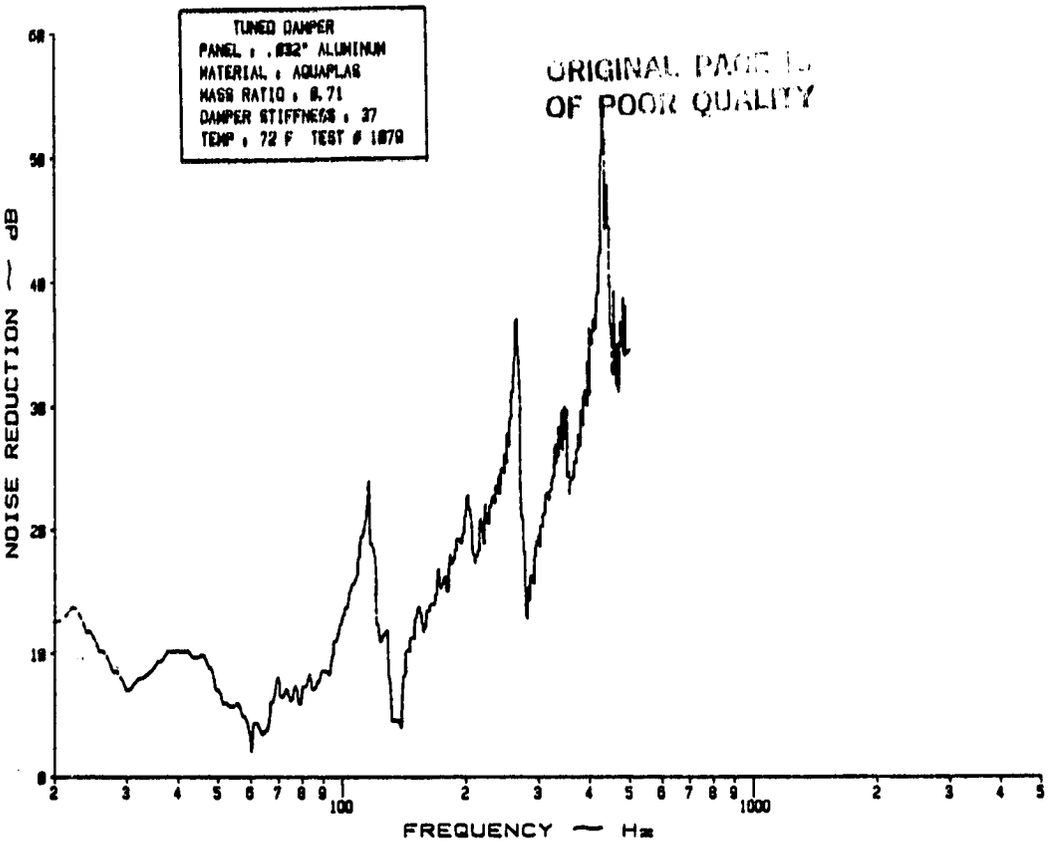

Figure D.44 Noise Reduction Characteristics of a .032" Aluminum Panel with an "Aquaplas" Tuned Damper; μ = .71 and K2 = 37 lbf/in.

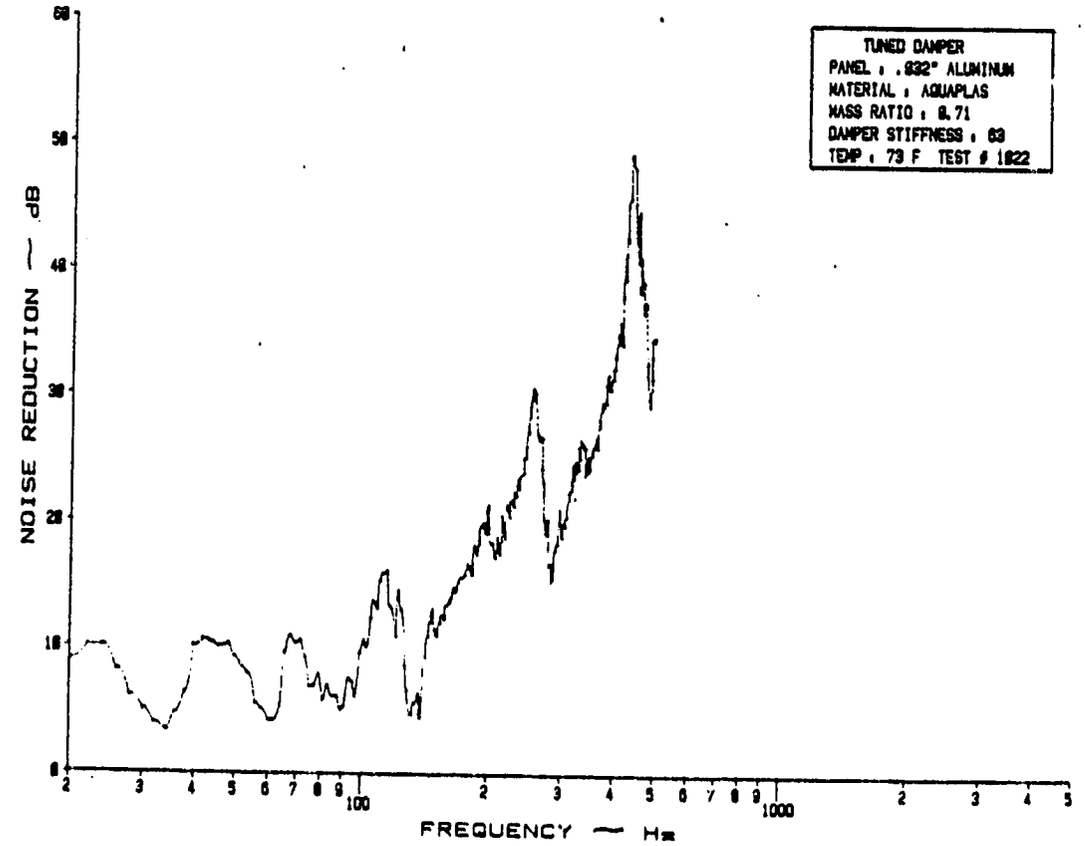

Figure D.45 Noise Reduction Characteristics of a .032" Aluminum Panel with an "Aquaplas" Tuned Damper; μ = .71 and K2 = 63 lbf/in.

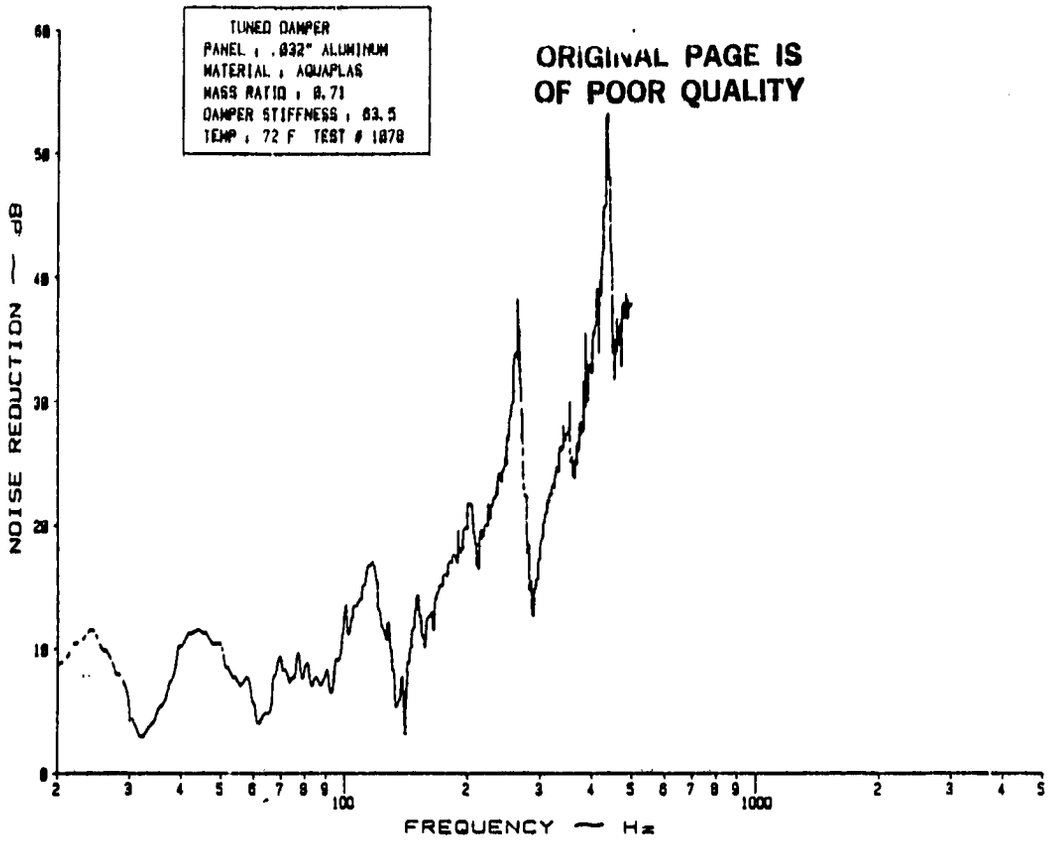

Figure D.46 Noise Reduction Characteristics of a .032" Aluminum Panel with an "Aquaplas" Tuned Damper; μ = .71 and K2 = 63.5 lbf/in.

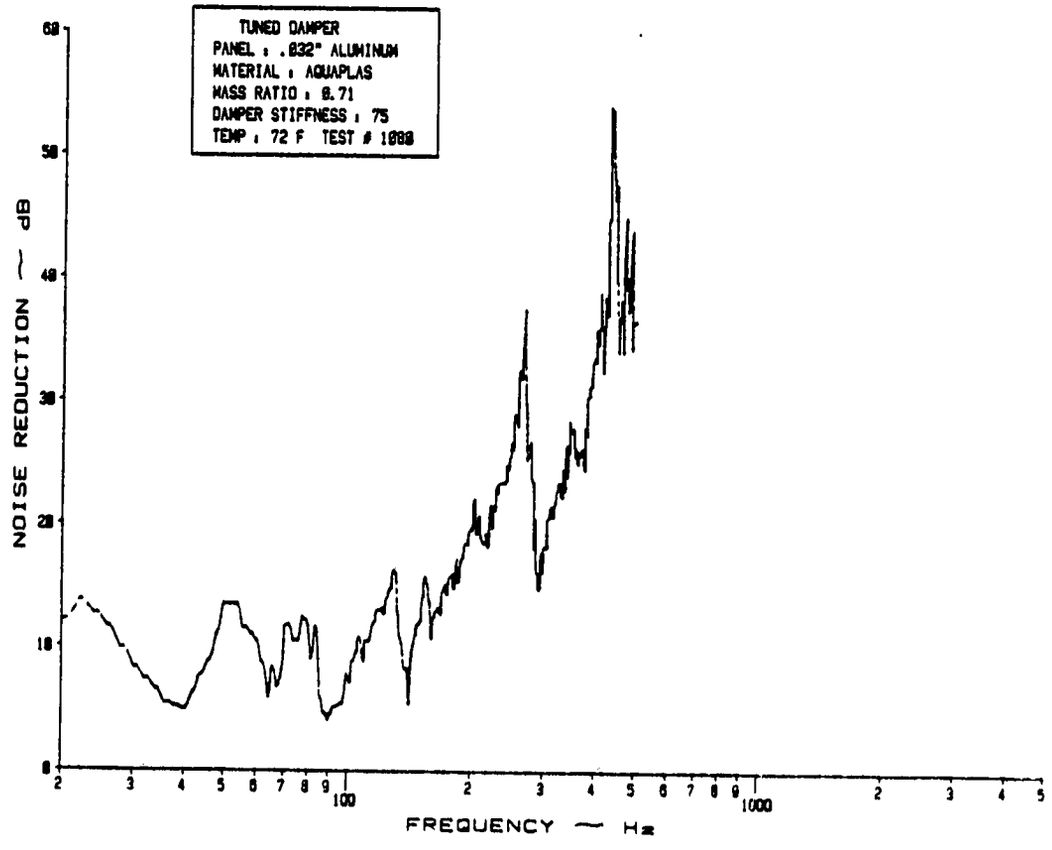

Figure D.47 Noise Reduction Characteristics of a .032" Aluminum Panel with an "Aquaplas" Tuned Damper; μ = .71 and K2 = 75 lbf/in.